

Synthesis of porphyrin-phthalocyanine triple-decker arrays around a triphenylene core

Sultanah Mohammed N Alhunayhin



Supervised by Prof Andrew N. Cammidge.

School of Chemistry
University of East Anglia, Norwich, United Kingdom

February 2024

©This copy of the thesis has been supplied on the condition that anyone who consults it, is understood to recognise that its copyright rests with the author and that no quotation from the thesis, nor any information derived therefrom, may be published without the author's prior written consent.

Declaration

The research described in this thesis is, to the best of my knowledge, original except where due reference has been made.

Sultanah Mohammed N Alhunayhin

This thesis is dedicated to my beloved parents Dr.Mohammed N
Alhunayhin & Shamma Alhamad, as well as to my dear husband, Fahad
Alsaif.

Acknowledgements

I am sincerely grateful for the chance of being supervised by Prof Andrew N. Cammidge during my project, where his faith in my abilities and his heartfelt mentorship have been instrumental in seeing this project into fruition. The significant influence of his guidance, patience, and advice extends beyond the academic domain, shaping my personal and professional development. I will always be grateful to him for supporting and helping me each and every day, especially providing guidance and proofreading during my writing and for all the tools he provided to expand my knowledge of chemistry which motivated me to continuously develop my Ph.D. journey.

I would also like to express my appreciation to my second supervisor, Dr. Isabelle Chambrier, for her continuous support. My special thanks go to her for the valuable advice and suggestions she has consistently offered. Dr. Isabelle has always given helpful advice during my laboratory work and when designing my introduction.

I also would like to convey my gratitude to Dr. Saeed Samman and Muteb Alshammari for their valuable contributions and collaboration on our recent publications. Thanks to all involved for the exceptionally fruitful collaboration that has greatly enhanced the quality of our joint efforts. I would like to extend my gratitude to all members of Cammidge's group for supporting a positive work environment and offering helpful guidance. I would particularly like to thank Ibtesam Mashnoy for her generous assistance, which has been greatly appreciated.

I would like to thank, from the bottom of my heart, my beloved parents, Dr. Mohammad N Alhunayhin and Mrs. Shamma Alhamad, who have given me so much help during my academic journey. I extend my heartfelt thanks to my dear husband, Mr. Fahad Alsaif, for his love, support, and help during this period. I am particularly grateful for my wonderful children (Shouq, Rand, Saif, Raghad, and Aljazi Alsaif), who have adapted so well to their lives in the UK and never complained when I was busy. My heartfelt thanks also go out to my best brother, Mr. Abdulrahman Alhunayhin, who moved with me during my first year in the UK to assist me in finding a suitable house and ensure everything was in order before he left. His support has been a source of strength for me. I am grateful to all my brothers and sisters for their support and love. My special thanks also go out to our family's friend Hamad Almana for his support, and he never hesitated to help us. I extend my gratitude to all the friends I've met in the UK for the unforgettable moments we shared throughout the years, especially in Norwich city.

Finally, I would also like to acknowledge my great debt to my University, Majmaah University, who encouraged me to study abroad and provided all the necessary financial support.

Abstract

Controlling the assembly of multiply functional components is important for both development of fundamental supramolecular chemistry and in the application of complex materials. Double and triple-decker complexes of the porphyrinoid macrocycles display electronic absorption across the whole visible range and into the near IR. When the linking metal(s) are lanthanides, some examples offer further potential as molecular magnets and therefore as high-density information storage components of the future. This project focuses on synthetic strategies to assemble examples of such structures, particularly the synthesis and assembly of new multi-decker systems of porphyrins and phthalocyanines and controlling the synthesis of high-order macrocycle–lanthanide complexes. The chosen core in this project was a triphenylene molecule, where our lab has much experience in producing triphenylenes due to its use as a liquid crystal.

The synthesis of isomeric di-substituted triphenylenes is first described, where link points are introduced at 2,3- and 3,6 positions. Links from these positions to porphyrins through a 5-atom linker then provided the model di-porphyrins with different spacings. The separation between porphyrins was hoped to influence *single* triple-decker formation when using phthalocyanine as the central core with different ionic radii of lanthanide M^{3+} salts ($La^{3+} = 103\text{ pm}$, $Pr^{3+} = 99\text{ pm}$, $Nd^{3+} = 98\text{ pm}$, $Sm^{3+} = 96\text{ pm}$, $Eu^{3+} = 95\text{ pm}$, $Dy^{3+} = 90\text{ pm}$). The synthesis and investigation the two series of novel *single* triple-deckers is reported. They have comparable spectroscopic properties and no apparent difference in stability between two distinct isomeric TD complexes was noted. As expected, stable triple deckers were not formed when the small Dy ions were employed.

The selectivity of *single* triple-decker formation was investigated for 2,3 versus 3,6-*bis* (porphyrin)triphenylene triple-deckers through competition experiments. No selectivity was observed in competition experiments with different La metals in either model. However, the competition experiment using the two isomeric model di-porphyrins demonstrated significant kinetic selectivity, and in this case the 3,6-isomer was preferentially formed. This result indicated that the corresponding *hexa*-porphyrin based on fully (beta) substituted triphenylene would selectively form a single-isomer *tris* triple-decker system. The *hexa*-porphyrin was successfully constructed and subjected to triple-decker assembly. New TD complexes formed it is observed that the insertion of the final metal ion is difficult and slow, indicating significant congestion in the final complex. The reaction is further complicated by competitive formation if a structure presumed to be a *bis*-TD, and separation of the reaction components could not be achieved. Finally, the synthesis of alternative *bis*-TD structures was investigated.

Access Condition and Agreement

Each deposit in UEA Digital Repository is protected by copyright and other intellectual property rights, and duplication or sale of all or part of any of the Data Collections is not permitted, except that material may be duplicated by you for your research use or for educational purposes in electronic or print form. You must obtain permission from the copyright holder, usually the author, for any other use. Exceptions only apply where a deposit may be explicitly provided under a stated licence, such as a Creative Commons licence or Open Government licence.

Electronic or print copies may not be offered, whether for sale or otherwise to anyone, unless explicitly stated under a Creative Commons or Open Government license. Unauthorised reproduction, editing or reformatting for resale purposes is explicitly prohibited (except where approved by the copyright holder themselves) and UEA reserves the right to take immediate 'take down' action on behalf of the copyright and/or rights holder if this Access condition of the UEA Digital Repository is breached. Any material in this database has been supplied on the understanding that it is copyright material and that no quotation from the material may be published without proper acknowledgement.

Publications

1. Scramble-free synthesis of lightly substituted trans-A₂B₂-*meso*aryl porphyrins via bromophenyl dipyrromethanes.

Muteb H. Alshammari, [Sultanah M. N. Alhunayhin](#), David L. Hughes, Isabelle Chambrier and Andrew N. Cammidge*

Organic Letters **2024** DOI: 10.1021/acs.orglett.3c04215.

2. Triphenylene discotic liquid crystals: biphenyls, synthesis, and the search for nematic systems

[Sultanah M. N. Alhunayhin](#), Richard J. Bushby, Andrew N. Cammidge & Saeed S. Samman

Liquid Crystals **2023**, DOI: 10.1080/02678292.2023.2259856.

Qualification

1. Associate Fellow (AFHEA)

Higher Education Academy, UK

16th of August **2022**

Presentations

1. Macrocyclic and Supramolecular Chemistry Conference (MASC)

School of Chemistry at the University of Nottingham, UK

19-20th December **2022**

2. 16th International conference on materials chemistry (MC16)

University College Dublin, Dublin, Ireland

3-6 July **2023**

Contents

Acknowledgements	IV
Abstract.....	V
List of Abbreviations.....	XI
List of figures.....	XIII
List of schemes.....	XVII
List of tables.....	XIX
1. Introduction.....	2
1.1 Molecular building blocks.....	2
1.2 Tetrapyrrolic aromatic system.....	2
1.2.1 Porphyrins and phthalocyanines aromatic characteristics.....	3
1.2.2 The nomenclature and structure of porphyrins and phthalocyanines.....	4
1.3 Natural and synthetic porphyrins	6
1.3.1 Early development in naturally occurring porphyrins.....	6
1.3.2 The synthesis of porphyrins.....	8
1.3.2.1 Synthesising symmetrical porphyrins.....	9
1.3.2.2 Synthesising unsymmetrically substituted porphyrins.....	13
1.4 Phthalocyanine chemistry.....	17
1.4.1 Symmetrical and unsymmetrical phthalocyanines.....	17
1.4.2 General synthetic procedure for formation of phthalocyanines.....	18
1.5 Spectral properties of porphyrins and phthalocyanines.....	21
1.5.1 UV-vis spectroscopy.....	21
1.5.2 NMR-spectroscopy.....	23
1.6 General metalation of porphyrin and phthalocyanines.....	24
1.7 Porphyrin and phthalocyanine arrays.....	25
1.7.1 Linear arrays.....	26
1.7.2 Cyclic arrays.....	28
1.7.3 Nanoparticles arrays.....	30
1.7.4 Rare-earth complexes (double- and triple-decker arrays).....	35
1.7.4.1 The reaction of porphyrins and phthalocyanines with lanthanide metals.....	35
1.7.4.2 Synthesis of porphyrins and phthalocyanines double-and triple-decker arrays.....	38
1.7.4.2.1 Homoleptic complex arrays.....	39
1.7.4.2.2 Heteroleptic complex arrays.....	43

1.8 Rare-earth complexes (double- and triple-decker arrays) applications.....	48
2. <u>Aim of this project</u>	55
3. <u>Results and discussion</u>	60
3.1 Synthesis of 2,3 triphenylene-linked <i>bis</i>(porphyrin) model 89	60
3.1.1 Preparation of unsymmetrical porphyrin 94	61
3.1.2 The triphenylene core.....	63
3.1.2.1 Preparation of triphenylene core (2,3- <i>bis</i> (hydroxy)triphenylene 92).....	63
3.1.2.2 Synthesis of 2,3- <i>bis</i> (3-bromoproxy)triphenylene 99 (linker 1 st attempt).....	65
3.1.2.3 Synthesis of bromoalkoxyprophyrin 93 (linker 2 nd attempt).....	67
3.1.3 Preparation of 2,3- <i>bis</i> (porphyrin) triphenylene model 89.....	72
3.2 Synthesis of 3,6-triphenylene-linked <i>bis</i>(porphyrin) model 90	76
3.2.1 Preparation of triphenylene core (3,6- <i>bis</i> (hydroxy)triphenylene) 106	77
3.2.2 Synthesis of 3,6- <i>bis</i> (porphyrin)triphenylene model 90.....	79
3.3 Synthesis of 2,3- and 3,6-novel <i>single</i> triple-decker (LnTD)	82
3.3.1 Synthesis of metal-free phthalocyanine 2 (central unit-Pc).....	82
3.3.2 Synthesis of closed triple-decker complex of porphyrin and phthalocyanine 111	83
3.3.2.1 Triple-decker formation from TPP 9 and Pc 2	85
3.3.2.2 New attempts of synthesis 2,3-LaTD 112 from 2,3-isomer 89	88
3.3.3 Successful synthesis of 2,3- <i>bis</i> (porphyrin)triphenylene triple-decker (2,3-LnTD).....	92
3.3.3.1 Lanthanum triple-decker (2,3-LaTD) 112	94
3.3.3.2 Praseodymium triple-decker (2,3-PrTD) 119	99
3.3.3.3 Europium triple-decker (2,3-EuTD) 120	101
3.3.3.4 Dysprosium triple-decker (2,3-DyTD) 121	103
3.3.3.5 Comparison of 2,3 triple-deckers 112 , 119 and 120	104
3.3.4 Synthesis of 3,6- <i>bis</i> -(porphyrin)triphenylene triple-decker (3,6-LnTD).....	104
3.3.4.1 Lanthanum triple-decker (3,6-LaTD) 122	106
3.3.4.2 Neodymium, Samarium and Europium triple-decker ((3,6-NdTD) 123 , (3,6-SmTD) 124 and (3,6-EuTD) 125 , respectively).....	108
3.3.4.3 Dysprosium triple-decker (3,6-DyTD) 126	110
3.3.5 The spectroscopy characterization comparison.....	110
3.3.5.1 Comparing between (2,3-LaTD) 112 with (3,6-LaTD) 122	110
3.3.5.2 Comparing between (2,3-EuTD) 120 with (3,6-EuTD) 125	111
3.3.6 Conclusion	113
3.4 TD formation study	113
3.4.1 Transmetallation using a different lanthanide ions.....	114
3.4.2 Metalation using a mixture of lanthanide ions.....	117
3.4.2.1 Distribution study (using 2,3- and 3,6-TD system).....	117
3.4.3 Mixed isomers experiment.....	118
3.4.4 Conclusion	119

3.5 Synthesis of <i>hexa</i>-(porphyrin) triphenylene system 127	120
3.5.1 Preparation of triphenylene core	121
3.5.1.1 Synthesis of <i>hexa</i> -(hydroxy)triphenylene 129	121
3.5.1.2 Synthesis of 2,3,6,7,10,11- <i>hexa</i> -(3-chloropropoxy)triphenylene 130	122
3.5.2 Synthesis of <i>hexa</i> -(porphyrin)triphenylene 127	124
3.5.2.1 Optimisation procedure for the formation of target compound 127	125
3.5.2.1.1 Attempted synthesis of compound 133 (test reaction)	125
3.6 Synthesis of <i>tris</i> triple-decker system 135	130
3.7 Synthesis of open <i>bis</i> triple-decker system 144	140
3.7.1 Comparing between open <i>bis</i> triple-decker 144 with <i>bis</i> triple-decker for Cammdge's group	144
3.8 Conclusion	147
4. Experimental	150
4.1 General methods	150
4.1.1 Physical methods	150
4.1.2 Reagents, solvents and reaction conditions	151
4.2 Synthesis	152
4.2.1 Synthesis (unsymmetrical tetraphenyl-porphyrin) TPP-OH 94	152
4.2.2 Synthesis 1,2-dihexyloxy benzene 96	153
4.2.3 Synthesis of 2,3,6,7,10,11- <i>hexa</i> -hexyloxytriphenylene [HAT6] 98 (iron(III) chloride route)	154
4.2.4 Synthesis of 2,3-dimethoxy-6,7,10,11- <i>tetra</i> -hexyloxytriphenylene 91	155
4.2.5 Deprotection of 2,3- <i>bis</i> (hydroxy)triphenylene 92	156
4.2.6 3,4-dihydro-2H-[b][1,4]dioxepine 101 (Side Product)	157
4.2.7 Synthesis of 2,3- <i>bis</i> (hydroxypropanyloxy)triphenylene 102	158
4.2.8 Synthesis of bromoalkoxyporphyrin 93	159
4.2.9 Synthesis of 2,3- <i>bis</i> (porphyrin)triphenylene first model 98	160
4.2.10 Synthesis 4-bromo-1-hexyloxy-2-methoxybenzene 108	161
4.2.11 Synthesis di(hexyloxy)di(methoxy)biphenyl 109	162
4.2.12 Synthesis of 3,6- <i>bis</i> (methoxy)triphenylene 105	163
4.2.13 Deprotection of 3,6- <i>bis</i> (hydroxy)triphenylene 106	164
4.2.14 Synthesis of 3,6- <i>bis</i> (porphyrin)triphenylene second model 90	165
4.2.15 Metal free phthalocyanine 2	166
4.2.16 Lnathanum triple-decker from 2,3- <i>bis</i> (porphyrin)triphenylene 112	167
4.2.17 Praseodymium triple-decker from 2,3- <i>bis</i> (porphyrin)triphenylene 119	168
4.2.18 Europium triple-decker from 2,3- <i>bis</i> (porphyrin)triphenylene 120	169
4.2.19 Lnathanum triple-decker from 3,6- <i>bis</i> (porphyrin)triphenylene 122	170
4.2.20 Neodymium triple-decker from 3,6- <i>bis</i> (porphyrin)triphenylene 123	171
4.2.21 Samarium triple-decker from 3,6- <i>bis</i> (porphyrin)triphenylene 124	172
4.2.22 Europium triple-decker from 3,6- <i>bis</i> (porphyrin)triphenylene 125	173
4.2.23 Synthesis of <i>hexa</i> (methoxy)triphenylene 128	174
4.2.24 Deprotection of <i>hexa</i> (methoxy)triphenylene 129	174
4.2.25 Synthesis of <i>o-bis</i> -((3-hydroxypropyl)oxy)benzene 131	175

4.2.26	Synthesis of 1,2- <i>bis</i> -(3-chloropropoxy)benzene 132.....	175
4.2.27	Synthesis of 2,3,6,7,10,11- <i>hexa</i> -(3-chloropropoxy)triphenylene 130.....	176
4.2.28	Synthesis test reaction with phenol 133.....	177
4.2.29	Synthesis of <i>hexa</i> -(porphyrin) triphenylene 127.....	178
4.2.30	Synthesis of <i>tris</i> triple-decker system 135.....	179
4.2.31	Synthesis of 3,6-open <i>bis</i> triple-decker system 144.....	181
5.	<u>Appendix</u>	184
5.1	Selected NMR-spectra	184
5.2	Publications from side projects not covered by this thesis	198
5.2.1	Published paper 1: Scramble-free synthesis of lightly substituted trans-A₂B₂-<i>meso</i>aryl porphyrins via bromophenyl dipyrromethanes. Organic Letters 2024	198
5.2.2	Published paper 2: Triphenylene discotic liquid crystals: biphenyls, synthesis, and the search for nematic systems. Liquid Crystals 2023, ...	203
6.	<u>References</u>	215

List of Abbreviations

acac	acetylacetonate
Ar	aryl
BINAP	2,2'-bis(diphenylphosphino)-1,1'-binaphthyl
b.p	Boiling point
C10	decane
C12	dodecane
°C	Degrees Centigrade
cm	Centimetre
COSY	Correlation spectroscopy
δ	NMR Chemical Shift
DABCO	1,4-diazabicyclo [2.2.2] octane
DBU	1.8-diazabicyclo [5.4.0] undec-7-ene
d	Doublet
d-	Deuterated
dd	Doublet of doublets
DCM	dichloromethane
DCB	dichlorobenzene
TCB	trichlorobenzene
DDQ	2,3-Dichloro-5,6-dicyano-1,4-benzoquinone
DMF	dimethyl formamide
DMSO	dimethyl sulfoxide
TCE-d ₂ D	1,1,2,2-tetrachloroethane
dt	Doublet of triplets
Et ₂ O	diethyl ether
EtOAc	ethyl acetate
ϵ	Extinction coefficient
eq	Equivalent
g	grams
h or hrs	Hours
min	minutes
HOMO	Highest Occupied Molecular Orbital
Hz	Hertz
IR	Infrared
<i>J</i>	Coupling constant
K	Kelvin

L	Ligand
Ln	Lanthanide
TD(La)	Lanthanum linked Triple deckers
LUMO	Lowest unoccupied molecular orbital
m	Multiplet
M (in structures)	Metal (any)
M	Molarity
MALDI-TOF-MS	Matrix-assisted laser desorption/ionization (time of flight)
Me	Methyl
MHz	MegaHertz
min	Minutes
mg	Milligrams
ml	Millilitres
mm	Millimetres
mmol	Millimol
M.P.	Melting point
MS	Mass spectrometry
Mwt	Molecular weight
nm	Nanometres
NMR	Nuclear Magnetic Resonance
OMe	methoxy
oi	<i>Ortho</i> -inside
oo	<i>Ortho</i> -outside
Pc	Phthalocyanine
PDT	Photodynamic therapy
PET	petroleum ether (40-60 °C)
MgSO ₄	Magnesium sulphate
Ph	phenyl
pm	Picometre
Por	Porphyrin
H ₂ (Oep)	Octaethylporphyrin
ppm	Parts per million
py	pyridine
pyr	pyrrole

q	Quadruplet
r.t.	Room temperature
λ	wavelength
s	Singlet
S	Solvent
SMM	Single-Molecule Magnets
t	Triplet
^t Bu	<i>tert</i> -butyl
TD	Triple decker
THF	Tetrahydrofuran
TLC	Thin Layer Chromatography
TPP	Tetraphenyl porphyrin
TPPOH	5,10,15-tris-phenyl-20-(<i>p</i> -hydroxyphenyl) porphyrin
tt	Triplet of triplets
UV-Vis	Ultraviolet-Visible

List of Figures

Figure 1.1. The basic structure of porphyrins **1** and phthalocyanines **2**.

Figure 1.2. General tetrapyrrolic aromatic structure for both porphyrin and phthalocyanine.

Figure 1.3. Six porphyrin cores illustrating the different possible delocalisation of 18 π electrons.

Figure 1.4. The preferred π -electron delocalization pathway.

Figure 1.5. Porphyrins Nomenclature: Fischer and *IUPAC* nomenclature.

Figure 1.6. Phthalocyanine Nomenclature: Common and *IUPAC* nomenclature.

Figure 1.7. Several examples of natural compounds that resemble porphyrins.

Figure 1.8. The structure of linear tetrapyrroles and tripyrrans.

Figure 1.9. Various substitution structures for phthalocyanines.

Figure 1.10. Illustration some examples of substituted phthalocyanines-like molecules **23**, **24**, **25**, **26** and **27**.

Figure 1.11. UV-Vis spectra for metal-free porphyrins (*a*), and for metalloporphyrins (*b*).

Figure 1.12. UV-vis spectra of phthalocyanine as (*a*) a metal-free and (*b*) a metallated-Pc.

Figure 1.13. The NMR spectrum of porphyrin TPP **9**.

Figure 1.14. The structures of [M(Por)] and [M(Pc)] complexes where the metal fits inside the cavity.

Figure 1.15. Some types for porphyrin wires conjugated.

Figure 1.16. Ethene-bridged diporphyrins as single linkages.

Figure 1.17. Some examples of fused-porphyrin structure.

Figure 1.18. Diphenylethyne linker between diporphyrin units, resulting in a weak conjugation between the porphyrin units.

Figure 1.19. Linear arrays example using metalated phthalocyanine.

Figure 1.20. An example of multi-porphyrins by ethyne-bridged **45** (left), and cyclic porphyrin trimers **46** (right).

Figure 1.21. *Meso-meso*-linked diporphyrin.

Figure 1.22. Example structures of cyclic studies using metallo-porphyrin **48** and metallo-phthalocyanine **49**.

Figure 1.23. Example of gold nanoparticles, connected with porphyrin units.

Figure 1.24. Example of gold nanoparticles coated with phthalocyanine cores.

Figure 1.25. The structure of gold nanoparticle **52**, using PR-SH porphyrins and thiolated polyethylene glycol (PEG), which induces the production of singlet oxygen, resulting in increased effectiveness of the photosensitizer.

Figure 1.26. Molecular structures for self-assembling nanoparticles using amphiphilic porphyrins or metallo-porphyrins **53-58**.

Figure 1.27. The direction of electron spanning.

Figure 1.28. The sites of lanthanide metals of the double-and multi-decker complexes and their magnetic structure system.

Figure 1.29. Schematic structures for both homoleptic and heteroleptic complexes.

Figure 1.30. An example of (STM) image using rare-earth metal complexes.

Figure 1.31. Providing an example of the application of MRI imaging technique through the utilisation of Ln-SMMs design of multi-decker complexes.

Figure 1.32. An ambipolar OFET device was assembled using a triple-decker complex.

Figure 1.33. Applying tetrapyrrole complex for developing quantum technology.

Figure 1.34. An example of using porphyrin and phthalocyanine in layering Solar Cells.

Figure 2.1. Connecting 3×triple-decker for making *tris*-triple-decker system.

Figure 2.2. The structure of *hexa*-system and the numbering system of triphenylene.

Figure 3.1. The ^1H NMR spectra of symmetrical porphyrin TPP (A) and unsymmetrical tetraphenylporphyrin TPP-OH **94** (B), (500 MHz, CDCl_3).

Figure 3.2. The ^1H NMR-spectrum for unwanted cyclized product **101**.

Figure 3.3. Comparison of ^1H NMR spectra for TPP-OH **94** A) and compound **93** B), (500 MHz, CDCl_3), zoom of the 9.0-7.0 ppm area.

Figure 3.4. ^1H NMR spectrum of forming bromoalkoxy porphyrin **93** compound, (500 MHz, CDCl_3).

Figure 3.5. The MALDI-TOF-MS for bromoalkoxy porphyrin **93**. The inset shows (B) obtained and (A) theoretical isotopic patterns.

Figure 3.6. The UV-vis spectrum of bromoalkoxy porphyrin **93** compound, zoom of the 450-750 nm area.

Figure 3.7. The full ^1H NMR spectrum of 2,3-bis(porphyrin)triphenylene **89**, (500 MHz, CD_2Cl_2), expansion of the 8.9-7.3 ppm aromatic area and of the 4.8-2.5 ppm aliphatic area.

Figure 3.8. MALDI-MS spectrum of 2,3-bis(porphyrin)triphenylene **89**. The inset shows (B) obtained and (A) theoretical isotopic patterns.

Figure 3.9. The UV-vis spectrum of 2,3-bis(porphyrin)triphenylene **89**, expansion of the 450-750 nm area.

Figure 3.10. The ^1H NMR spectrum of synthesizing 3,6-bis(porphyrin)triphenylene **90** compound, (500 MHz, CDCl_3), expansion of the 9.0-7.2 ppm aromatic area and of the 4.7-2.49 ppm aliphatic area.

Figure 3.11. 2D COSY-NMR spectrum of second model **90**, zoom of the 8.25-1.89 ppm area.

Figure 3.12. UV-vis spectra for metal-free phthalocyanine **2**.

Figure 3.13. MALDI-TOF-MS result for one porphyrin linked to Pc central unit, product **113**.

Figure 3.14. MALDI-TOF-MS results for test reactions 1-5.

Figure 3.15. MALDI-TOF-MS result for double-decker **118** by testing first model with 'one-pot' reaction.

Figure 3.16. Comparison between UV-vis spectra of starting material **89** (A), double-decker complex **118** (B) and double-decker from literature (C).

Figure 3.17. Comparison of ^1H NMR-spectrum between (starting materials **89** and double-decker complex **118**).

Figure 3.18. ^1H NMR-spectrum of a porphyrin starting material and double-decker from literature.

Figure 3.19. The MALDI-TOF-MS for a green solid for lanthanum triple-decker of 2,3-bis(porphyrin)triphenylene **112**. The inset shows (B) obtained and (A) theoretical isotopic patterns.

Figure 3.20. UV-vis spectrum obtained for the lanthanum triple-decker **89** compared to 2,3-model **112**, expansion of the 450-750 nm area.

Figure 3.21. The ^1H NMR-spectrum of the lanthanum triple-decker **112** (500 MHz, CD_2Cl_2), expansion of 10.5-6.5 ppm aromatic area.

Figure 3.22. 2D Cosy NMR-spectra of 2,3-bis(porphyrin)triphenylene triple-decker **112**.

Figure 3.23. MALDI-TOF-MS obtained for a green solid for Praseodymium triple-decker **119**. The inset shows (B) obtained and (A) theoretical isotopic patterns.

Figure 3.24. The ^1H NMR-spectrum obtained for 2,3-PrTD **119** (*b*) with comparing ^1H NMR-spectra to 2,3-LaTD **112** (*a*) and PrTD for Cammidge's group (*c*).

Figure 3.25. MALDI-TOF-MS obtained for a green solid for Europium triple-decker complex **120**. The inset shows (**B**) obtained and (**A**) theoretical isotopic patterns.

Figure 3.26. UV-vis spectra for 2,3-LnTD complexes for all three metals (La, Pr and Eu), expansion of the 450-750 nm area.

Figure 3.27. The spacing for 3,6-isomer **90**.

Figure 3.28. The ^1H NMR-spectrum of synthesizing complex **122** (500 MHz, CD_2Cl_2), expansion of 10.74-6.51 ppm aromatic area.

Figure 3.29. 2D COSY NMR 3,6-*bis*(porphyrin)triphenylene closed triple decker **122**.

Figure 3.30. MALDI-TOF-MS obtained for 3,6-Nd, Sm and Eu- triple-decker **123**, **124** and **125**. The inset shows (**B**) obtained and (**A**) theoretical isotopic patterns.

Figure 3.31. ^1H NMR-spectroscopy comparison between (2,3-LaTD) **112** with (3,6-LaTD) **122**.

Figure 3.32. ^1H NMR-spectroscopy comparison between (2,3-EuTD) **120** with (3,6-EuTD) **125**.

Figure 3.33. ^1H NMR-spectra for 3,6-LaTD (*a*) and 3,6-EuTD (*b*).

Figure 3.34. Comparing ^1H NMR-spectra for 3,6-EuTD **125** down, and 3,6-LaTD **120** up with an aliquot from the exchange experiment middle after reflux for 24 hrs (500 MHz, CD_2Cl_2), expansion of 14.5-6.00 ppm aromatic area.

Figure 3.35. Comparing ^1H NMR spectra for 2,3 triple-decker complex above, and 3,6 triple-decker complex down with the mixed isomers experiment result middle (500 MHz, CD_2Cl_2), expansion of 10.45-6.55 ppm aromatic area.

Figure 3.36. ^1H NMR-spectra for both triphenylenes **128** and **129**.

Figure 3.37. ^1H NMR spectra for test compound **133**.

Figure 3.38. MALDI-TOF-MS of *hexa*-(porphyrin) triphenylene **127**. The inset shows (**B**) obtained and (**A**) theoretical isotopic patterns.

Figure 3.39. ^1H NMR-spectroscopy for *hexa*-(porphyrin) triphenylene system **127**, (500 MHz, CD_2Cl_2), expansion of 8.9-7.0 ppm aromatic area.

Figure 3.40. HSQC NMR-spectroscopy for *hexa*-(porphyrin) triphenylene system **127**.

Figure 3.41. MALDI-TOF-MS results for by-products of *tris* triple-decker reaction attempts.

Figure 3.42. MALDI-TOF-MS for first attempt of synthesising *tris* triple-decker system.

Figure 3.43. MALDI-TOF results.

Figure 3.44. illustrating further MALDI-TOF-MS results.

Figure 3.45. MALDI-TOF-MS for final attempt.

Figure 3.46. Illustrating similar peaks characteristic of both *single* and *tris* system.

Figure 3.47. Additional MALDI-TOF-MS investigation results.

Figure 3.48. UV-vis spectra for *tris* triple-decker system **135** with starting material **127** and 3,6-La *single* triple-decker complex.

Figure 3.49. MALDI-TOF-MS of compound **144**. The inset shows (B) obtained and (A) theoretical isotopic patterns.

Figure 3.50. ¹H NMR of *bis*-triple-decker system **144** (500 MHz, CD₂Cl₂), expansion of 10.0-7.51 ppm aromatic area.

Figure 3.51. ¹H NMR-spectroscopy comparison between **144** system open *bis* complex of Cambridge's group.

Figure 3.52. 2D COSY NMR-spectroscopy for *bis*-triple-decker system **144**.

Figure 3.53. UV-vis spectroscopy for *bis* triple-decker system **144**, *single* triple-decker and 3,6-model.

List of Schemes

Scheme 1.1. The fundamental structure of *meso*-arylporphyrin and various possibilities for modifying the macroheterocycle.

Scheme 1.2. The mechanism of *meso*-arylporphyrins.

Scheme 1.3. The main procedures for synthesis of *meso*-arylporphyrins with symmetric substitution.

Scheme 1.4. Synthesis of 5,10,15,20-tetrakis(3-hydroxyphenyl)porphyrin **12** by Rocha Gonsalves and colleagues.

Scheme 1.5. The synthesis of porphyrins, using the two-step, one flask method.

Scheme 1.6. Synthesis of ABCD-type porphyrin.

Scheme 1.7. Illustration example of the synthesis of dipyrromethanes **15**.

Scheme 1.8. Another route for making ABCD- porphyrins.

Scheme 1.9. Synthesis of trans-porphyrin **20**.

Scheme 1.10. Scrambling cyclization mechanism.

Scheme 1.11. Examples of the synthesis of unsymmetrical porphyrins, using mixed condensation.

Scheme 1.12. General starting materials for forming phthalocyanines.

Scheme 1.13. The synthesis of the first metal-free phthalocyanine.

Scheme 1.14. Synthesis of iron phthalocyanine **33**.

Scheme 1.15. Cyclization mechanism of phthalocyanine **2**.

Scheme 1.16. Preparation method for homoleptic complexes.

Scheme 1.17. The synthesise of homoleptic double-decker complexes **53**.

Scheme 1.18. Synthesis of homoleptic porphyrin double-decker complex.

Scheme 1.19. A general method for producing mono-decker complexes of porphyrins or phthalocyanines.

Scheme 1.20. The synthesis of phthalocyanine double-decker complex **56**.

- Scheme 1.21.** Another example of homoleptic complex, pentakis(phthalocyaninato)-M^{III}-Cd^{II} **59**.
- Scheme 1.22.** Synthesising heteroleptic double and triple-decker complexes, using a “**one-pot**” reaction.
- Scheme 1.23.** Synthesis of heteroleptic complexes.
- Scheme 1.24.** Synthesis of double- and triple- decker complexes.
- Scheme 1.25.** Synthesis of heteroleptic triple-decker complexes **79** and **80**.
- Scheme 1.26.** A recent synthesis of double-decker complexes **82-84**.
- Scheme 1.27.** Previous triple-decker by Cammidge group, using a “**one-pot**” reaction.
- Scheme 2.1.** The structure design of *tris*-triple decker system and how can be controlled.
- Scheme 2.2.** The structure design of *single* 2,3 and 3,6 triple-decker complex.
- Scheme 3.1.** Proposed synthesis of 2,3-linked *bis*(porphyrin)triphenylene **89**.
- Scheme 3.2.** The synthesis of **TPP-OH 94**.
- Scheme 3.3.** Stepwise synthesis of triphenylene core **92**.
- Scheme 3.4.** The reaction conditions for forming 2,3-*bis*(hydroxy)triphenylene **92**.
- Scheme 3.5.** General synthesis plan for 2,3-*bis*(3-bromopropoxy)triphenylene **99**.
- Scheme 3.6.** Forming side product **101** by reacting with dibromopropane.
- Scheme 3.7.** Converting compound **92** into compound **102**.
- Scheme 3.8.** Converting **102** to the required compound **103**.
- Scheme 3.9.** The formation of bromoalkoxy porphyrin **93**.
- Scheme 3.10.** The possible side products that can be presented in a mixture in synthesising the desired compound **93**.
- Scheme 3.11.** Synthesizing of the first model **89**.
- Scheme 3.12.** Dimethylformamide degradation.
- Scheme 3.13.** Proposed synthesis of 3,6-linked *bis*(porphyrin)triphenylene **90**.
- Scheme 3.14.** The steps for formation 3,6-*bis*(hydroxy)triphenylene **106**.
- Scheme 3.15.** Ullman coupling catalytic cycle with copper and with nickel.
- Scheme 3.16.** The formation of di(hexyloxy)di(methoxy)biphenyl **109**.
- Scheme 3.17.** Synthesizing the second model **90**.
- Scheme 3.18.** Formation of metal-free phthalocyanine **2**.
- Scheme 3.19.** Reaction process for closed triple-decker **111**.
- Scheme 3.20.** Proposed structure of 2,3 and 3,6 *single* triple-decker complex.
- Scheme 3.21.** Synthesis of 2,3-*bis*(porphyrin)triphenylene triple-decker **112**.
- Scheme 3.22.** General synthesis of test reaction by using TPP **9**.

Scheme 3.23. Double-decker formation **118**.

Scheme 3.24. The reaction process for synthesizing a *single* triple-decker complex **2,3-LnTD**.

Scheme 3.25. 2,3-La triple-decker **112**.

Scheme 3.26. Triple-decker with Praseodymium ions **119**.

Scheme 3.27. Triple-decker via Europium ion **120**.

Scheme 3.28. The reaction process for synthesizing a *single* triple-deckers **3,6-LnTD**.

Scheme. 3.29. 3,6-La triple-decker **122**.

Scheme 3.30. Exchange reaction of Europium to Lanthanum in 3,6-EuTD.

Scheme 3.31 General procedure for the combination metals experiment, to assess selective synthesis of one metal triple-decker.

Scheme 3.32. Selective reaction of mixed isomers.

Scheme 3.33. Proposed synthesis of *hexa*-(porphyrin) triphenylene system **127**.

Scheme 3.34. General synthesis of *hexa*-(hydroxy)triphenylene **129**.

Scheme 3.35. Synthesis of the final triphenylene core **130** via stepwise process.

Scheme 3.36. Using oxalyl or thionyl chlorides to produce acyl chlorides.

Scheme 3.37. Converting compound **131** to compound **132**.

Scheme 3.38. New route for synthesis *hexa*-(porphyrin) triphenylene system **127**.

Scheme 3.39. Examples of side products which can be formed.

Scheme 3.40. Synthesis of compound **133** as tester.

Scheme 3.41. Using dibenzo-18-crown-6 as template.

Scheme 3.42. Synthesis of (3,6) *tris*-triple-decker system **135**.

Scheme 3.43. Synthesis of *bis*-triple-decker system **144**.

List of tables

Table 1.1. Example of electronic configuration of lanthanide ion (**Eu³⁺** and **Dy³⁺**).

Table 1.2. Lanthanides sizes (ionic radii from La³⁺ to Lu³⁺).

Table 3.1. Some attempted conditions for optimising the yield of required product **92**.

Table 3.2. Optimisation of bromoalkoxyporphyrin synthesis with different reaction conditions.

Table 3.3. Using different solvents to produce product **89**.

Table 3.4. Methodologies for synthesising test reaction for close triple-decker **117**

Chapter 1: Introduction

1. Introduction

1.1 Molecular Building Blocks

Porphyrin and phthalocyanine are related materials that are the focus of this thesis. In recent years, porphyrins (Por) and phthalocyanines (Pcs) proved interesting because of their unique chemical and physical characteristics and many possible applications.¹ These unique characteristics highlight their significance as technically advanced materials and make them valuable for applications in molecular electronics and nonlinear optics.²

(Pc) and (Por) have a structural relationship, resulting in the formation of highly stable planar macrocycles.³ The connection between these two molecules becomes evident when analysing the formula depicted in (Fig. 1.1). Porphyrins **1** are composed of tetrapyrrole linked by four methine bridges,^{4, 5} whereas phthalocyanine **2** is comprised of four isoindole units connected by nitrogen atoms.^{3, 6} (More details will be provided later in this chapter).

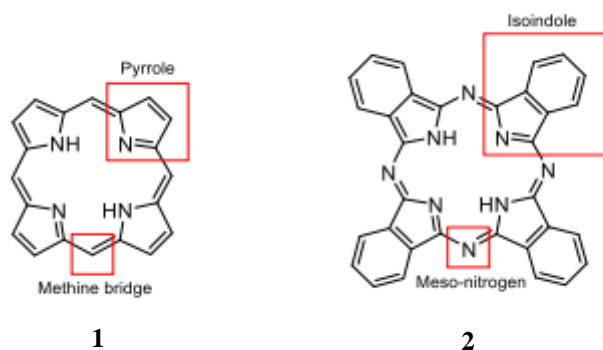


Figure 1.1. The basic structure of porphyrins **1** and phthalocyanines **2**.

1.2 Tetrapyrrolic aromatic system

The tetrapyrrolic aromatic system of porphyrins and phthalocyanines is a unique molecular structure consisting of four pyrrole rings connected in a cyclic arrangement (Fig. 1.2). This system forms a large, planar, and conjugated structure with alternating double bonds, resulting in a highly stable aromatic structure.

Lash and Steiner, along with their colleagues have also mentioned that the results of ^{13}C NMR-spectroscopy and X-ray studies as evidence that the 16-membered ring of the 18 π -electron system can be more favoured for the delocalisation pathway in the porphyrins.⁸
⁹ This is shown in (Fig 1.4).

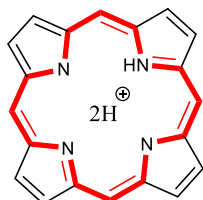


Figure 1.4. The preferred π -electron delocalization pathway.

Phthalocyanine derivatives, similar to porphyrins, are highly conjugated flat systems and display the same pathway.⁹ Phthalocyanines (Pcs) also have 18 delocalized π -electrons and are well-known for their remarkable stability against both thermal and chemical influences.^{10, 11} The most significant organic colourants are phthalocyanine derivatives, which are readily accessible and have exceptional photostability.¹¹

1.2.2 The nomenclature and structure of porphyrins and phthalocyanines

There exist two recognised nomenclature systems of porphyrins. Hans Fisher initially introduced the system of nomenclature for porphyrins.¹² In this system, the eight outer C-atoms of the pyrrolic sub-units are designated with numbers 1 to 8, and the four methine carbon-atoms are labelled as α , β , γ , and δ ,¹³ as illustrated in (Fig. 1.5). However, as also shown in Figure 1.5, the IUPAC introduced a nomenclature system in 1979 that assigns precise numbers to every atom in the macrocycle, excluding N-atoms.¹⁴ Due to the high level of symmetry, porphyrins allow for the replacement of only two specific types of carbon atoms within the ring during chemical reaction. The bridging methine carbons are referred to as *meso*-positions, whereas the pyrrolic carbons are designated as β -positions.^{14, 15}

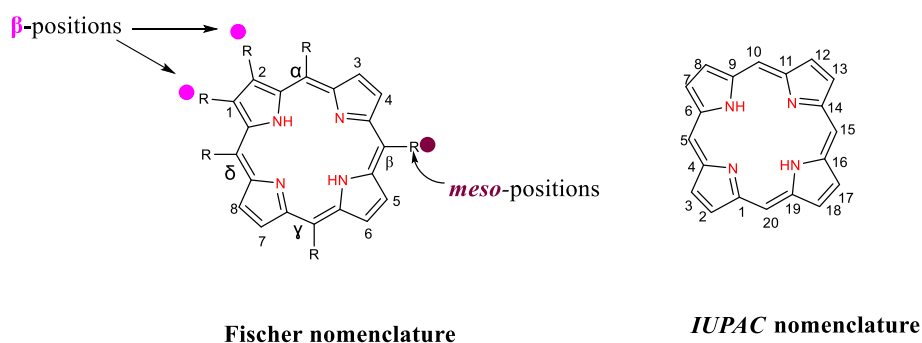


Figure 1.5. Porphyrins Nomenclature: Fischer and *IUPAC* nomenclature.

The phthalocyanine core provides the opportunity to introduce various substituents at positions designated as α (non-peripheral) and β (peripheral).^{10,16} Substituents found at positions 1, 4, 8, 11, 15, 18, 22, and 25 on the phthalocyanine ring in (Fig. 1.6, α -positions) are termed α -substituents, whilst those situated at positions 2, 3, 9, 10, 16, 17, 23, and 24 in (Fig. 1.6, β -positions) are referred to as β -substituents.¹³ This flexibility allows for tuning electronic and solubility properties to meet specific application requirements.^{17,}

18

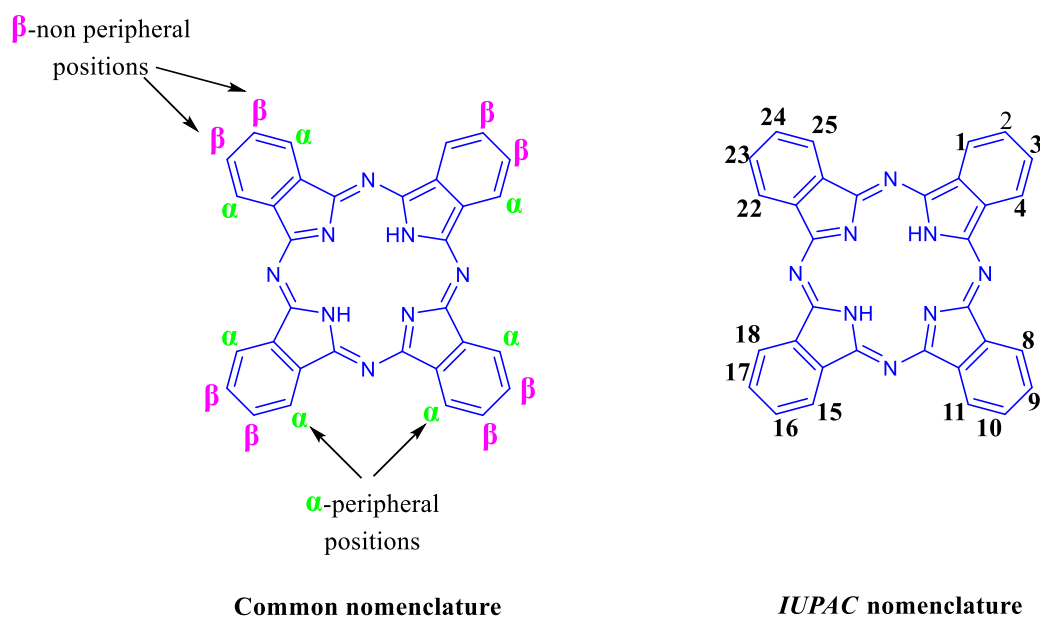


Figure 1.6. Phthalocyanine Nomenclature: Common and *IUPAC* nomenclature.¹⁰

1.3 Natural and synthetic porphyrins

1.3.1 Early development in naturally occurring porphyrins

The derivation of the name “porphyrin” is from the Greek word for purple *porphura*, because the pigments of porphyrin molecules are very dark.¹⁹ Porphyrins were first identified in the 19th century and, since that time they have been studied extensively because they are so important to the biological processes of everyday life.^{20, 21}

Metallo-porphyrin derivatives are common in nature and have a vital function in maintaining life on Earth. Figure 1.7 depicts four well recognised natural compounds which have similarities to porphyrins. These molecules play a vital role in essential biochemical processes. (A) Heme B **3**, which contains iron, is found in mammalian blood, and serves as a prosthetic group in haemoglobin and myoglobin proteins. The reversible binding of this substance with O₂ is crucial for the transportation²² and storage of oxygen in living organisms.²³ (B) Chlorophyll a **4** is a chromophore similar to a porphyrin that is metalated with Mg(II).²⁴ It has a crucial function in the light-driven process of photosynthesis.²⁵ Significantly, it captures sunlight and acts as an antenna that directs excited-state energy to the response centre via a sequence of energy-transfer processes.^{4, 26} (C) Methylcobalamin, often known as vitamin B12 **5**, is an essential nutrient for the proper functioning of the neurological system.²⁷ (D) Coenzyme F430 **6**, a nickel derivative containing a partially porphyrin core structure, functions as a prosthetic group in the enzyme methyl coenzyme found in methanogenic Archaea. It has a vital function in the final stage of methanogenesis by facilitating the release of methane.²⁸

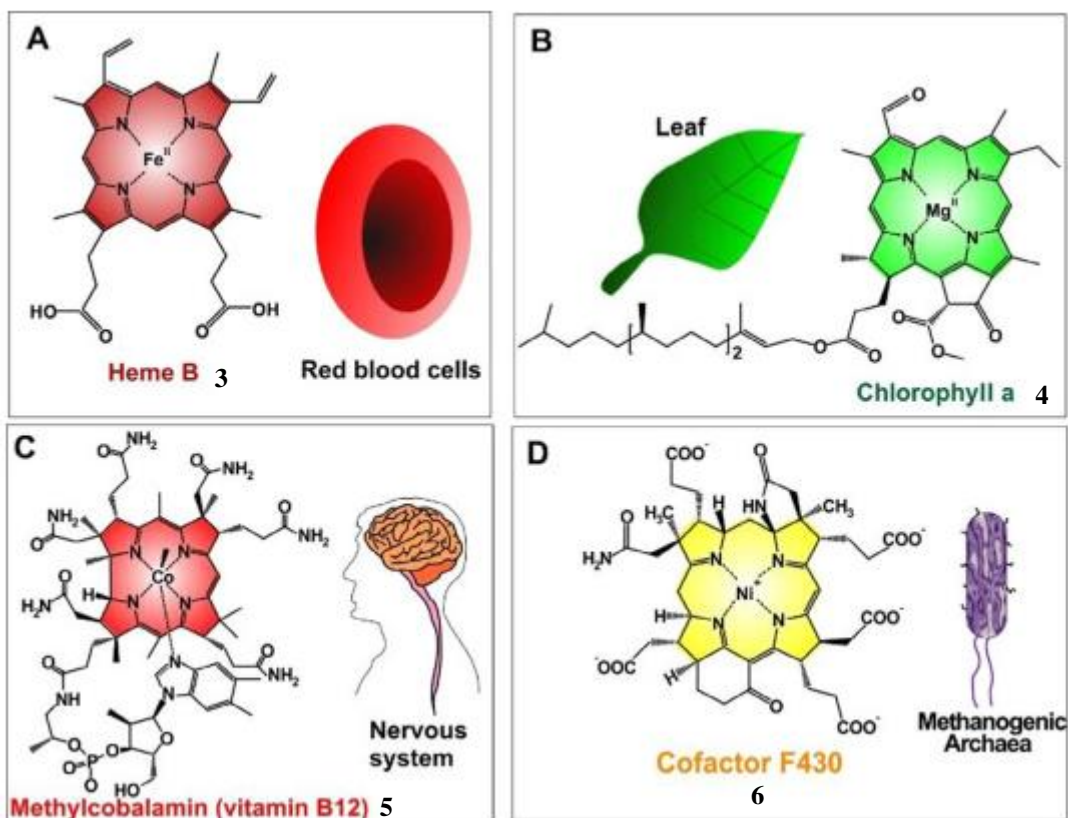
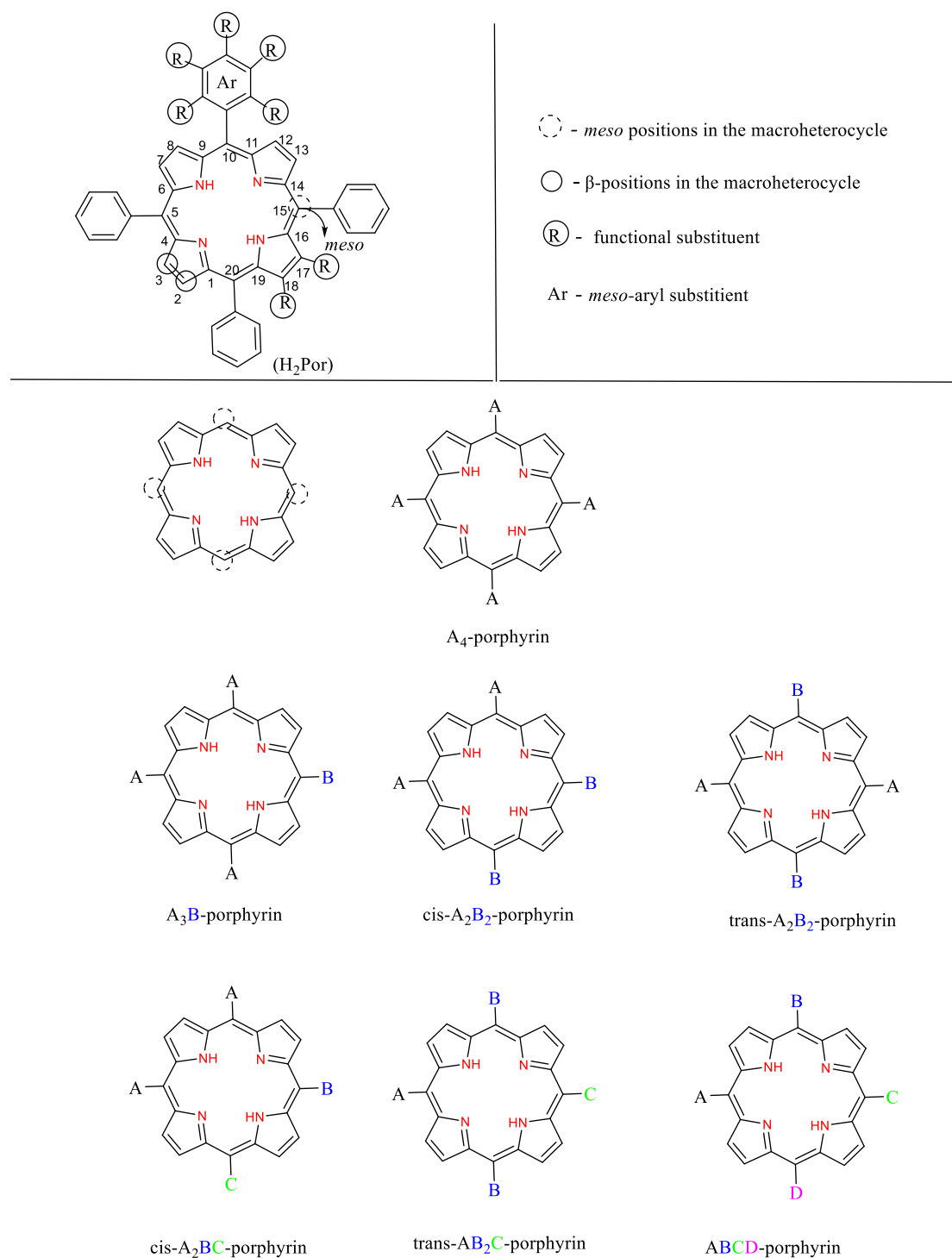


Figure 1.7. Several examples of natural compounds that resemble porphyrins.^{27, 29}
 Reproduced with permission from (27).

While porphyrins are found in natural biological substances, it is also possible to synthesise them; synthetic porphyrins have therefore been used as molecular components and in artificial systems of photosynthesis.³⁰

1.3.2 The synthesis of porphyrins

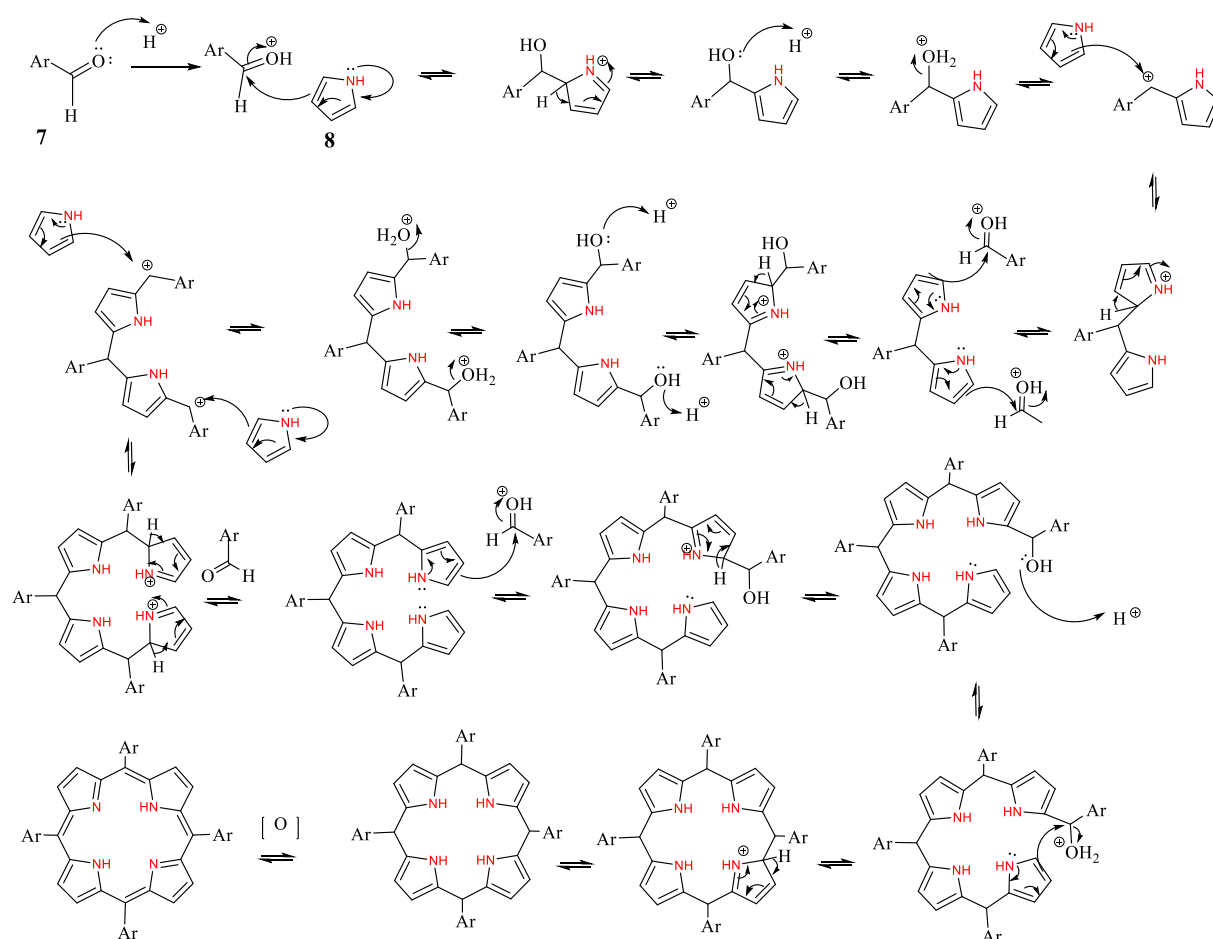
The synthesis of *meso*-substituted porphyrins is contingent upon the arrangement of various substituents. As the quantity of varied substituents expands the synthesis methods generally become increasingly complex. Scheme 1.1 illustrates seven common categories of *meso*-substituted porphyrins.³¹



Scheme 1.1. The fundamental structure of *meso*-arylporphyrin and various possibilities for modifying the macroheterocycle.³¹

1.3.2.1 Synthesising symmetrical porphyrins

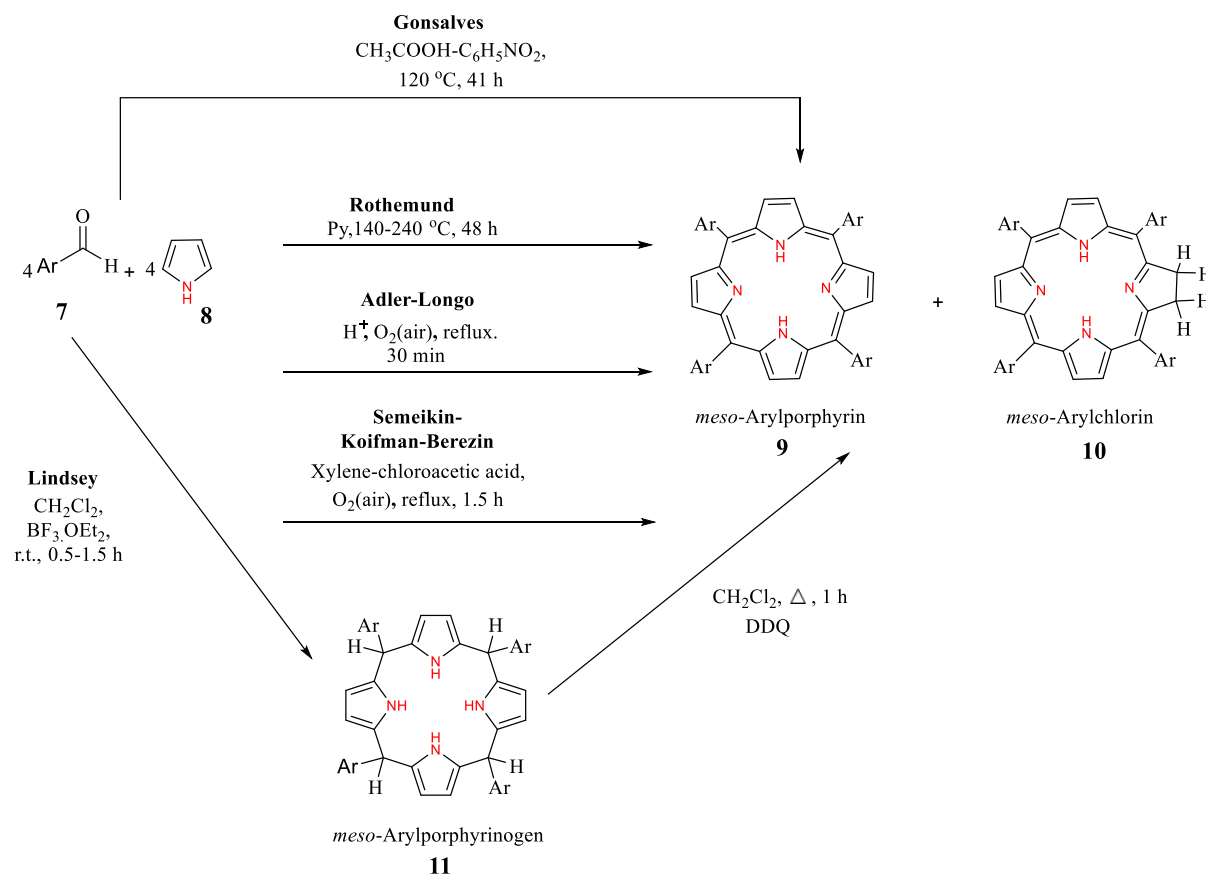
As previously mentioned, porphyrin substitution can be divided into two categories: *meso*- and β -substituted porphyrins. *Meso*-substituted porphyrins are among the most intriguing compounds in synthetic chemistry, while β -substituted porphyrins can be found naturally in a variety of forms.³² The main strategies of synthesis for *meso*-arylporphyrins is demonstrated in the scheme 1.2 below. In the condensation stage, pyrrole **8** reacts with aldehyde **7** in the presence of an acid catalyst. The nitrogen atom in pyrrole acts as a nucleophile, enabling the formation of an imine (C=N). Subsequently, multiple pyrrole molecules condense, resulting in the formation of a linear tetrapyrrole intermediate.³¹ This intermediate experiences cyclization in the presence of oxidative conditions, ultimately leading to the creation of a porphyrin macrocycle.^{31, 33}



Scheme 1.2. The mechanism of *meso*-arylporphyrins.³¹

The most significant challenges in tetrapyrrole macrocyclic chemistry revolve around developing a straightforward synthetic procedure for this material, improving the yield obtained from the reaction between pyrrole and aldehyde, and simplifying the isolation

and purification processes of the molecule. As a result, various synthesis approaches have been employed to create symmetrical *meso*-arylporphyrins, (Scheme 1.3).



Scheme 1.3. The main procedures for synthesis of *meso*-arylporphyrins with symmetric substitution.³¹

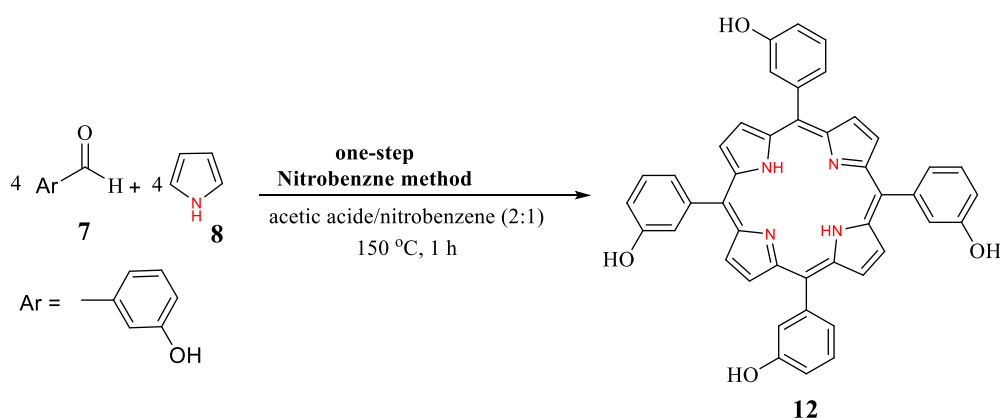
In 1935, **Rothemund** made an achievement by being the first to develop the process of creating *meso*-substituted porphyrins by synthesis.²¹ The synthesis involved applying of heat to acetaldehyde or benzaldehyde **7** and pyrrole **8** in a sealed flask containing MeOH at a temperature of 140°C . This resulted to the production of 5,10,15,20-tetraphenylporphyrins **9**, as shown in (Scheme 1.3). To improve the reaction conditions, MeOH was replaced with pyridine as a solvent and the temperature was increased to 240°C . As a consequence, compound **9** was obtained with a yield of 10%.^{32, 34}

Adler and Longo improved Rothemund's method for increasing the yield of *meso*-substituted porphyrins by using acidic conditions instead of harsh conditions.³⁵⁻³⁷ A solution of pyrrole **8** and benzaldehyde **7** in propionic acid was refluxed for 30 minutes

under open-air conditions. This reaction produced the required porphyrin **9** with a yield of 20% (Scheme 1.3).^{36, 38}

By employing the **Semeikin–Koifman–Berezin** approach, the synthesis of *meso*-tetraarylporphyrin in a mixture of xylene and chloroacetic acid demonstrated an average double increase in production compared to the yield achieved in propionic acid.^{39, 40} Usually, the reaction takes place under refluxing conditions, sometimes with ambient oxygen flowing through the mixture. The quantity of tetraarylporphyrins **9** collected is dependent upon the specific aldehyde utilised and the temperature at which the reaction takes place, with the highest yield produced at approximately 140°C, (Scheme 1.3).^{31, 40}

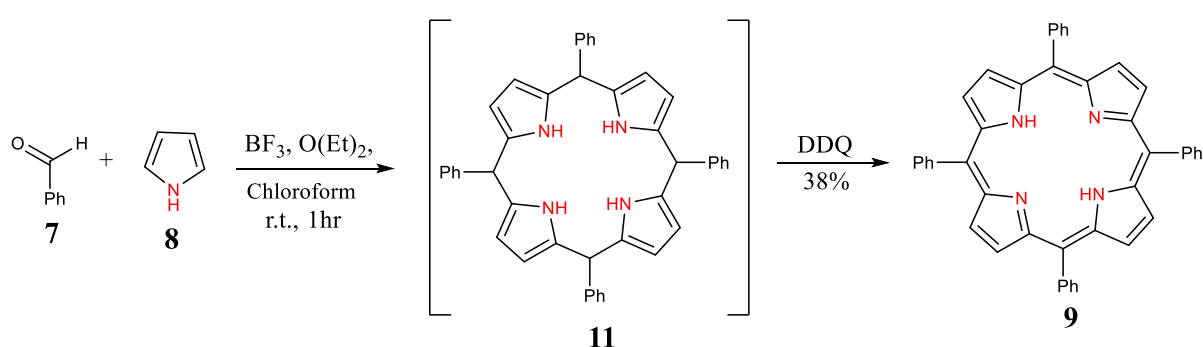
To improve the Adler-Longo process and remove chlorin, in 1985, **Rocha Gonsalves** and colleagues proposed a simplified, one-step nitrobenzene approach.⁴¹ This technique involves the synthesis of symmetrical *meso*-substituted porphyrins by reacting pyrrole **8** with aromatic or aliphatic aldehydes using acetic or propionic acid. Nitrobenzene (30%) is used as an oxidising agent for the intermediate tetraarylporphyrinogen **11** (Scheme 1.3).^{42, 43} The nitrobenzene method produced a 40% yield of 5,10,15,20-tetrakis(3-hydroxyphenyl)porphyrin **12**, which was not achievable with the Adler-Longo procedure (Scheme 1.4).⁴³



Scheme 1.4. Synthesis of 5,10,15,20-tetrakis(3-hydroxyphenyl)porphyrin **12** by Rocha Gonsalves and colleagues.⁴³

In 1979-86, **Lindsey** further improved the method for synthesising *meso*-substituted porphyrins. He was driven by the need to use gentler conditions for condensing aldehydes and pyrroles, in order to increase the range of aldehydes that could be utilized, and hence the number of porphyrins that could be produced.⁴⁴ This innovative procedure

has two steps, carried out at room temperature, and uses a sequence of steps of oxidation and condensation, and has come to be known as the Lindsey method, or the two step one flask method, (Scheme 1.5). The purpose of using gentle conditions was to try to reach equilibrium during the condensation step, but also to minimise side reactions throughout the process. Pyrrole is condensed with aldehydes, in the presence of an acid catalyst, such as TFA or BF_3 , in either chloroform or dichloromethane. This is carried out at room temperature, in an inert atmosphere. Oxidation of the initially formed porphyrinogen **11** can be achieved by the addition of a stoichiometric quantity of DDQ or *p*-chloranil, isolating porphyrin **9** in 38% yield.^{29, 45, 46}



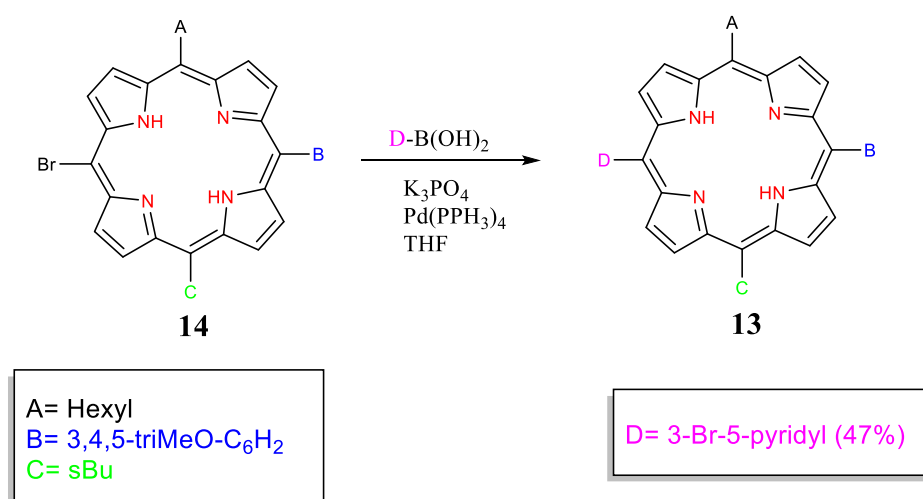
Scheme 1.5. The synthesis of porphyrins, using the two-step, one flask method.^{45, 47}

In summary, three primary techniques still exist for creating symmetrical porphyrins. The Rothmund process is inefficient and yields poor results. Adler's technique, although it produces a greater amount, encounters difficulties with unstable substituents under high temperatures and acidic conditions. The Lindsey method yields a higher quantity of porphyrin while reducing the formation of by-products. However, the purification process, which involves chromatography, limits the scale of the reaction. Therefore, Adler's approach provides a significant competitive advantage.

1.3.2.2 Synthesising unsymmetrically substituted porphyrins

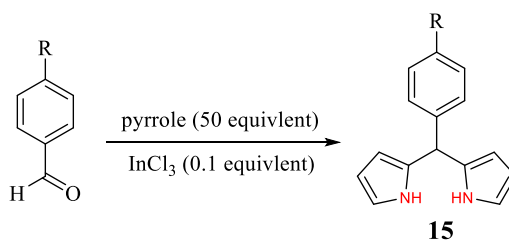
The methodologies developed by Adler-Longo and Lindsey are suitable for the synthesis of symmetrical porphyrins, nevertheless they are not very useful for creating complex unsymmetrical porphyrins.²⁹ Progress in porphyrin synthesis research has been rapid, with new methods of synthesis being developed. ABCD-type porphyrins are a good example of unsymmetrical substituted porphyrins. These have four different substituents occurring at the *meso*-position (Scheme 1.1).^{48, 49}

A new route for synthesising ABCD-type porphyrins **13** was developed by Senge and co-workers.⁴⁹ In this instance, the ABC porphyrins **14** are subjected to bromination, followed by coupling reaction using Pd as catalyst, as depicted in (Scheme 1.6).



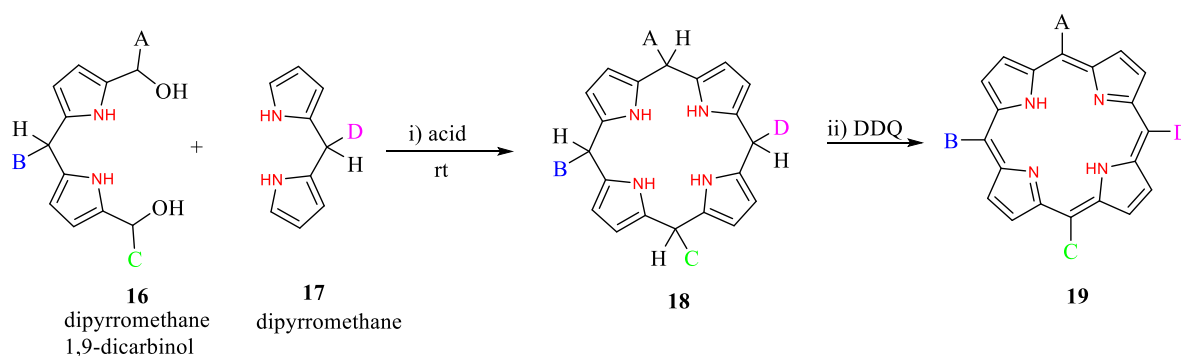
Scheme 1.6. Synthesis of ABCD-type porphyrin.⁴⁹

Dipyrromethanes (DPMs) **15** play a crucial role in the field of porphyrin chemistry.⁵⁰ Their preparation involves a reaction between an aldehyde and excess pyrrole in the absence of a solvent. This reaction takes place at room temperature and is facilitated by the presence of a moderate Lewis acid, such as InCl₃ (Scheme 1.7).^{50, 51}



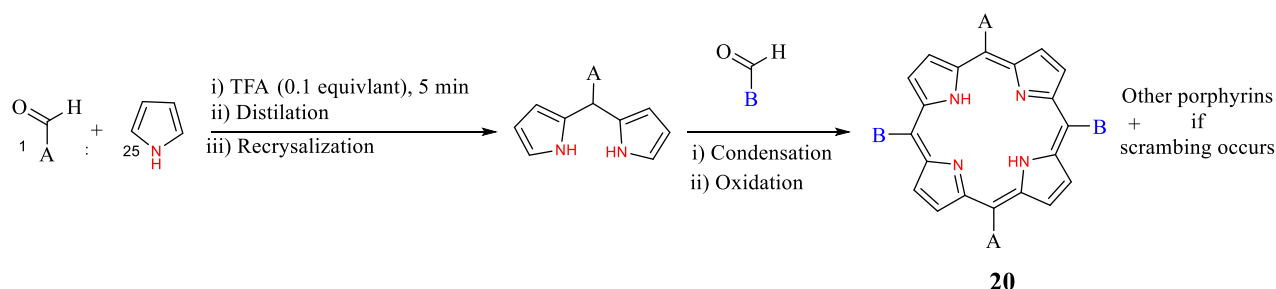
Scheme 1.7. Illustration example of the synthesis of dipyrromethanes **15**.⁵⁰

The synthetic procedure of an ABCD-porphyrin was accomplished using dipyrromethanes⁴⁶ and employing the MacDonald-type 2+2 condensation method.^{52, 53} In the "2+2" condensation reaction between a dipyrromethene dicarbinol **16** (with A, B, and C substituents) and a dipyrromethane **17** (with the D substituent), the D substituent is only subjected to mild acid catalysis conditions for the formation of dipyrromethane and porphyrin, as well as mild oxidation conditions for porphyrin creation **19**,⁵³ as shown in (Scheme 1.8).⁵⁴



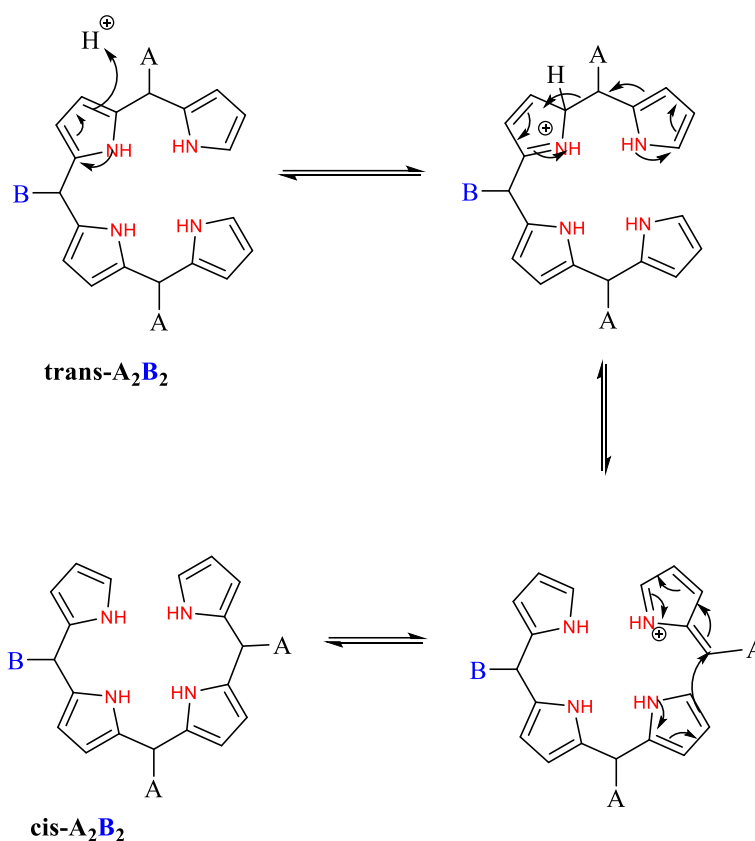
Scheme 1.8. Another route for making ABCD- porphyrins.⁵⁴

The reaction of a dipyrromethane and an aldehyde by a MacDonald-type⁵² 2+2 condensation, as shown in (Scheme 1.9), has also been employed to synthesise a diverse array of *meso*-substituted *trans*-porphyrins A_2B_2 **20**.⁵⁵



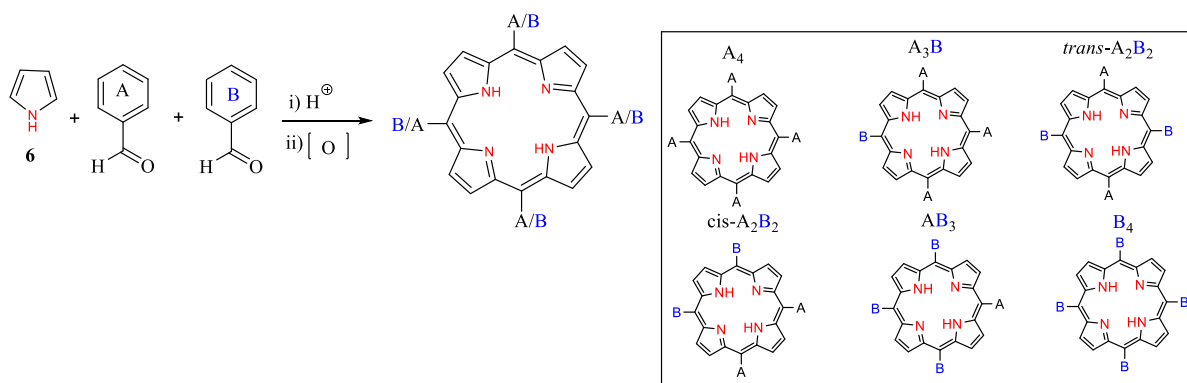
Scheme 1.9. Synthesis of *trans*-porphyrin **20**.

Ultimately this process often leads to the production of a scrambled mixture of porphyrins. The factors that promote the scrambling process in MacDonald-type 2+2 condensations are poorly understood, but suppression of scrambling is essential for preparing large quantities of pure *trans*-porphyrins.⁵⁶ Despite various synthetic methods outlined in the literature, creating porphyrins with specific functional groups is challenging.⁵⁵⁻⁵⁸ However, a major issue is the undesired rearrangement of substituents, known as "scrambling," leading to low yields of the target product.⁵⁷ While the use of dipyrromethane (DPMs) in the synthesis of porphyrins was expected to result in just the *trans*- A_2B_2 arrangement, it actually yields a variety of forms. This occurs by employing acid catalysts to condense pyrrole or DPMs with aldehydes, producing a mixture that includes *cis*- A_2B_2 , *trans*- A_2B_2 , and additional porphyrin types (A_4 , A_3B), (Scheme 1.10).⁵⁷



Scheme 1.10. Scrambling cyclization mechanism.⁵⁶

Unsymmetrically substituted porphyrin A₃B can be also synthesised using a variety of pathways. One such is the mixed aldehyde condensation. In this method, the precursors are a mixture of two aldehydes and pyrrole. This can generate a mix of products, from pyrrole building blocks in various combinations.⁴⁹ An acid-catalysed is required for such condensations but it has the potential to scramble the pyrrole units, which puts a limit on the reaction's yields (Scheme 1.11).^{31, 49, 59}



Scheme 1.11. Examples of the synthesis of unsymmetrical porphyrins, using mixed condensation.^{54, 56, 59}

The synthesis of porphyrins with various *meso*-substituents has posed several difficulties due to concerns related to scrambling.⁵⁴ To address these limitations, various approaches have been developed, including the use of linear tetrapyrroles **21**,⁶⁰ tripyrrans **22** (Fig. 1.8),⁵⁰ dipyrromethane derivatives, and other novel methodologies.^{46, 52, 61}

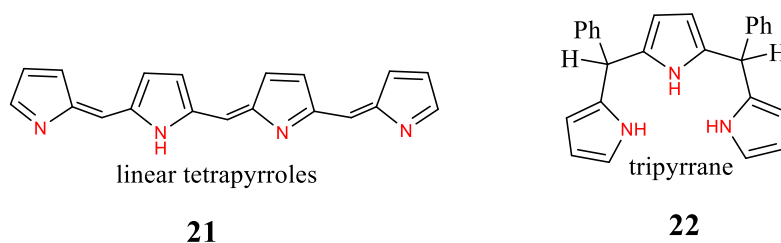


Figure 1.8. The structure of linear tetrapyrroles and tripyrrans.^{50, 60}

1.4 Phthalocyanine chemistry

1.4.1 Symmetrical and unsymmetrical phthalocyanines

In 1933, the word 'phthalocyanine' was introduced by P. Linstead,⁶² (Fig. 1.1). The term is derived from a combination of "phthalo" (relating to rock oil) and 'cyanine' (indicating a dark blue colour).^{62, 63} Phthalocyanines consist of four distinct subunits, each containing four potential substitution positions. In each subunit, the substituents can either be identical or different, leading to various substitution arrangements, as depicted in the (Fig. 1.9).^{64, 65} A_3B and A_4 phthalocyanines are commonly found, while A_2B_2 phthalocyanines are less prevalent. A few instances of $ABAC$ ⁶⁶ and $ABCD$ ⁶⁷ phthalocyanines are previously reported.⁶⁵

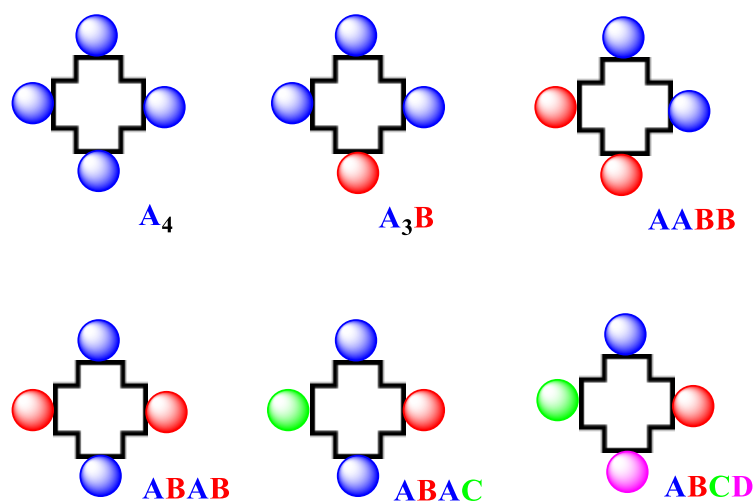


Figure 1.9. Various substitution structures for phthalocyanines.⁶⁵

Phthalocyanines are tetrabenzo-substituted⁶⁸, and (Fig 1.10) depicts some other structural examples.^{67, 69, 70}

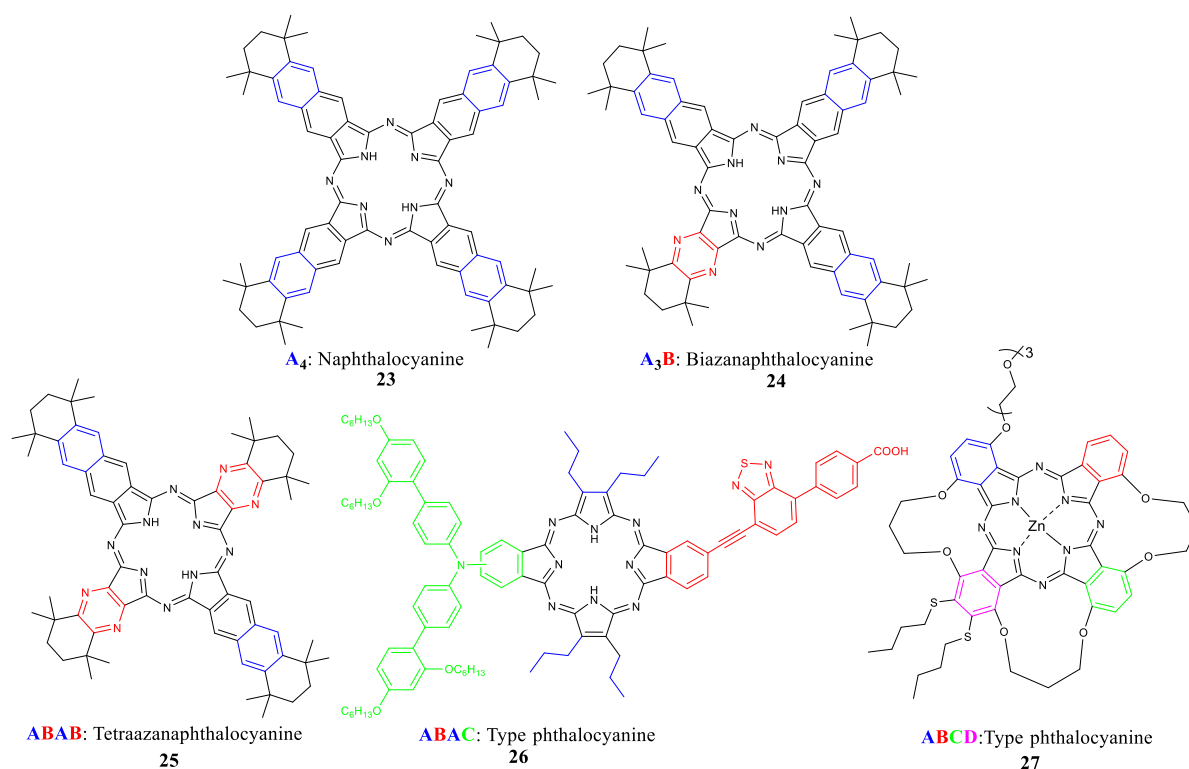


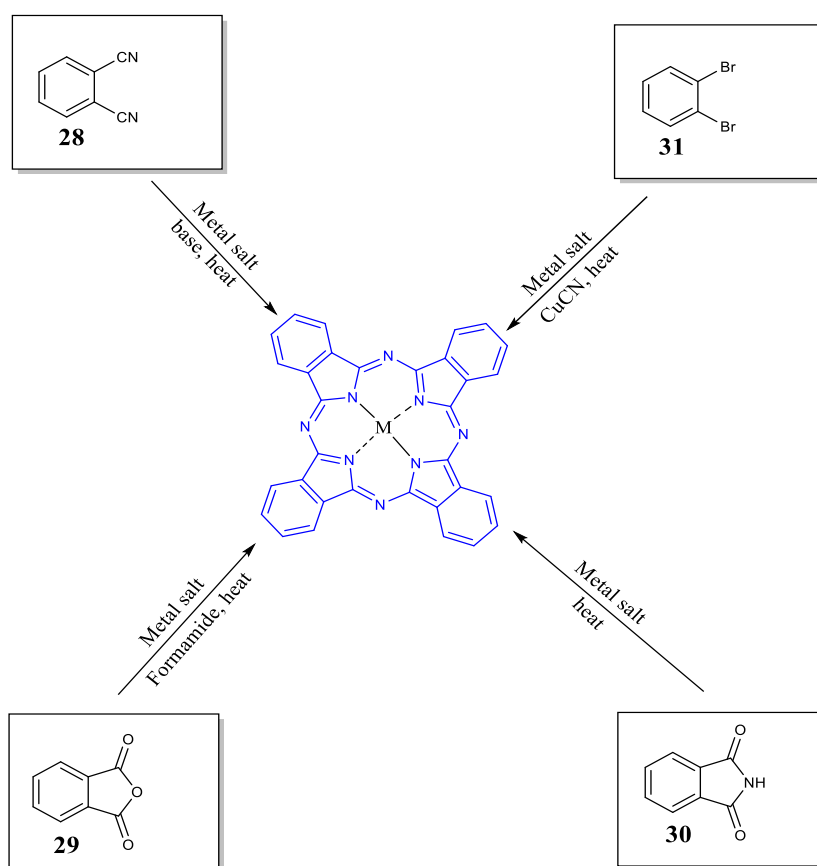
Figure 1.10. Illustration of some examples of substituted phthalocyanines-like molecules **23**,⁷¹ **24**,⁷² **25**,⁷² **26**⁶⁹ and **27**.⁶⁷

1.4.2 General synthetic procedure for the formation of phthalocyanines

Phthalocyanines can be produced synthetically using a variety of methods, and their synthesis can be affected by several factors. Among these factors are the phthalocyanine preparation technique, such as metal-free, metallated, symmetrical, or unsymmetrical. Furthermore, the method of introducing metal ions into the phthalocyanine core is important. Another important factor to consider is the type of functional group that can be attached to phthalocyanines, such as alkoxyalkyl or alkyl groups.⁷³ Moreover,

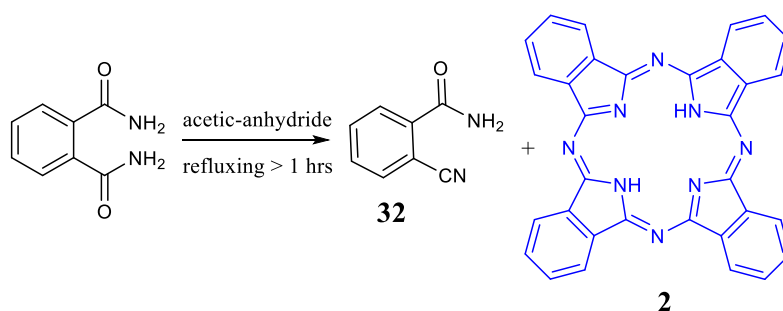
temperature, solvents, and bases, all affect how starting materials react to generate phthalocyanines influences the synthesis process.⁷⁴

Scheme 1.12 outlines various starting materials for producing phthalocyanines by cyclotetramerizing derivatives of aromatic *ortho*-dicarboxylic acids. Several starting substances, such as phthalonitrile **28**, phthalic anhydride **29**, phthalimide **30**, and *o*-dibromobenzene **31**, can be employed.^{75, 76} Metal salts are used to create metallo-phthalocyanines, whereas the absence of metal salts results in the production of metal-free phthalocyanines.⁷⁴



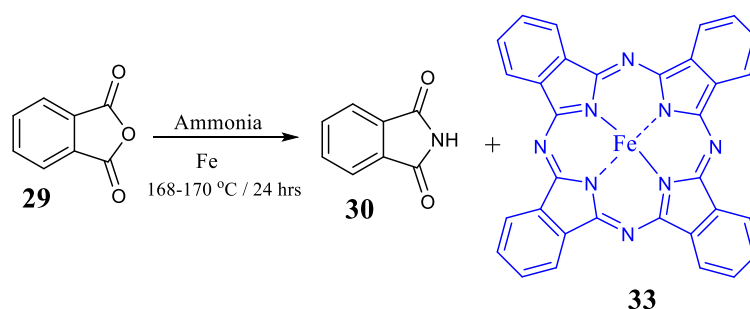
Scheme 1.12. General starting materials for forming phthalocyanines.⁷⁵

Braun and Tcherniac found the unexplained blue substance known as phthalocyanines in 1907, as a by-product of the *o*-cyanobenzamide **32** synthesis from phthalamide in acetic anhydride (Scheme 1.13).^{77, 78}



Scheme 1.13. The synthesis of the first metal-free phthalocyanine.

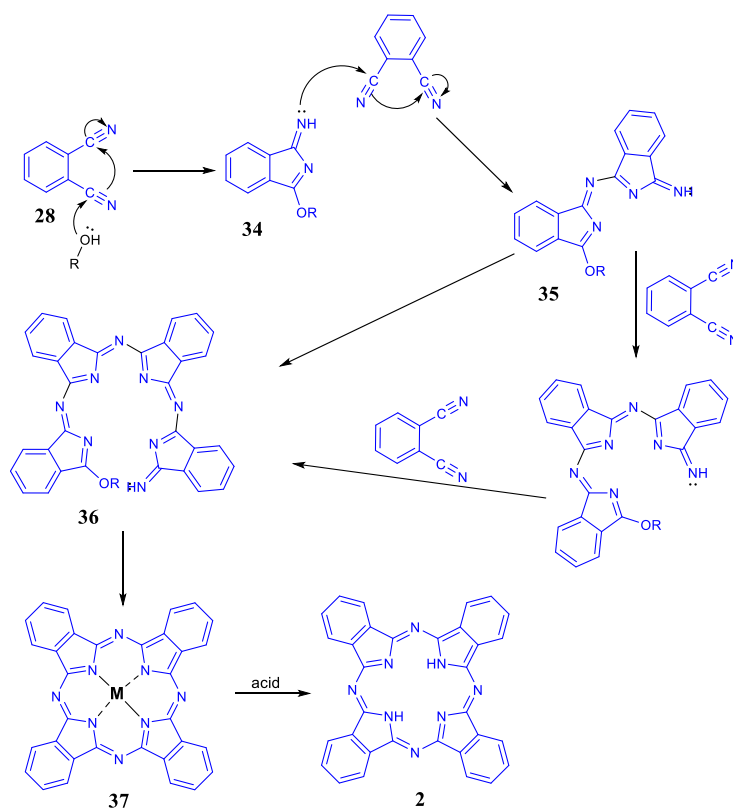
When trying to create phthalonitriles in 1927, Swiss researchers unintentionally discovered copper phthalocyanines, copper naphthalocyanines, and copper octamethyl phthalocyanines.⁷⁹ In the same year, Scottish Dyes of Grangemouth found iron phthalocyanine **33** while producing phthalimide **30** from phthalic anhydride **29** and ammonia (Scheme 1.14). Iron phthalocyanine was formed as a dark blue product.^{78, 80}



Scheme 1.14. Synthesis of iron phthalocyanine **33**.

The most common method to form substituted phthalocyanines is by using phthalonitrile **28** (1,2-dicyanobenzene). The production of metal-free phthalocyanines entails the combination of phthalonitrile **28** with an alkali metal and a primary alcohol to initiate the creation of a phthalocyanine structure surrounding the metal template (Scheme 1.15).^{81, 82, 83} Phthalocyanine synthesis begins with phthalonitrile and alcohol. Alcohol deprotonation by base promoters such as DBU forms nucleophilic alkoxide species, which attack phthalonitrile, creating intermediate **34**. This intermediate can bond with another phthalonitrile or dimerize to form **35**. In the proposed mechanism, **35** undergoes condensation to produce tetrameric intermediate **36**. Cyclization of **36**, followed by aldehyde elimination, resulting in the formation of the metal phthalocyanine **37**. Consequently, the alkali metal ions can be easily removed from the phthalocyanine due

to their weak binding when exposed to acidic conditions.⁸³ Generally, unsubstituted Pcs **2** can be synthesised in high amount of yield in a very short period.^{83, 84}



Scheme 1.15. Cyclization mechanism of phthalocyanine **2**.⁸³

1.5 Spectral properties of porphyrins and phthalocyanines

1.5.1 UV-vis Spectroscopy

The intense colour of porphyrins and phthalocyanines are a result of their highly conjugated system of π -electrons. This makes it possible to study them by making use of their distinctive UV-vis spectra.

These UV-visible spectra consist of two distinct regions. One is near ultra violet, while the other is in the visible region.⁸⁵ They exhibit strong Soret-band or B-band absorption from 380 to 420 nm, which is the transition from the ground state to the second excited state (S_0 - S_2), and weaker Q-band absorption in the longer wavelength visible light region (500–700 nm), which corresponds to the transition from the ground state to the first excited state (S_0 - S_1).⁸⁵ as shown in (Fig. 1.11).

However, Research on porphyrins has demonstrated that the UV-vis absorption spectrum of porphyrin can be altered by its conjugation pathway and its symmetry.⁸⁶ The

Q-bands pattern is simplified and two Q-bands emerge when the porphyrin macrocycle is coordinated with any metal, which creates a more symmetrical condition than in the free base porphyrin. In contrast to metallo-porphyrins, which have two smaller Q-bands between 500 and 700 nm (Fig. 1.11 (b)), metal-free porphyrins exhibit four smaller Q-bands between 500 and 700 nm due to the LUMO levels becoming non-degenerate (Fig. 1.12 (a)).⁸⁷

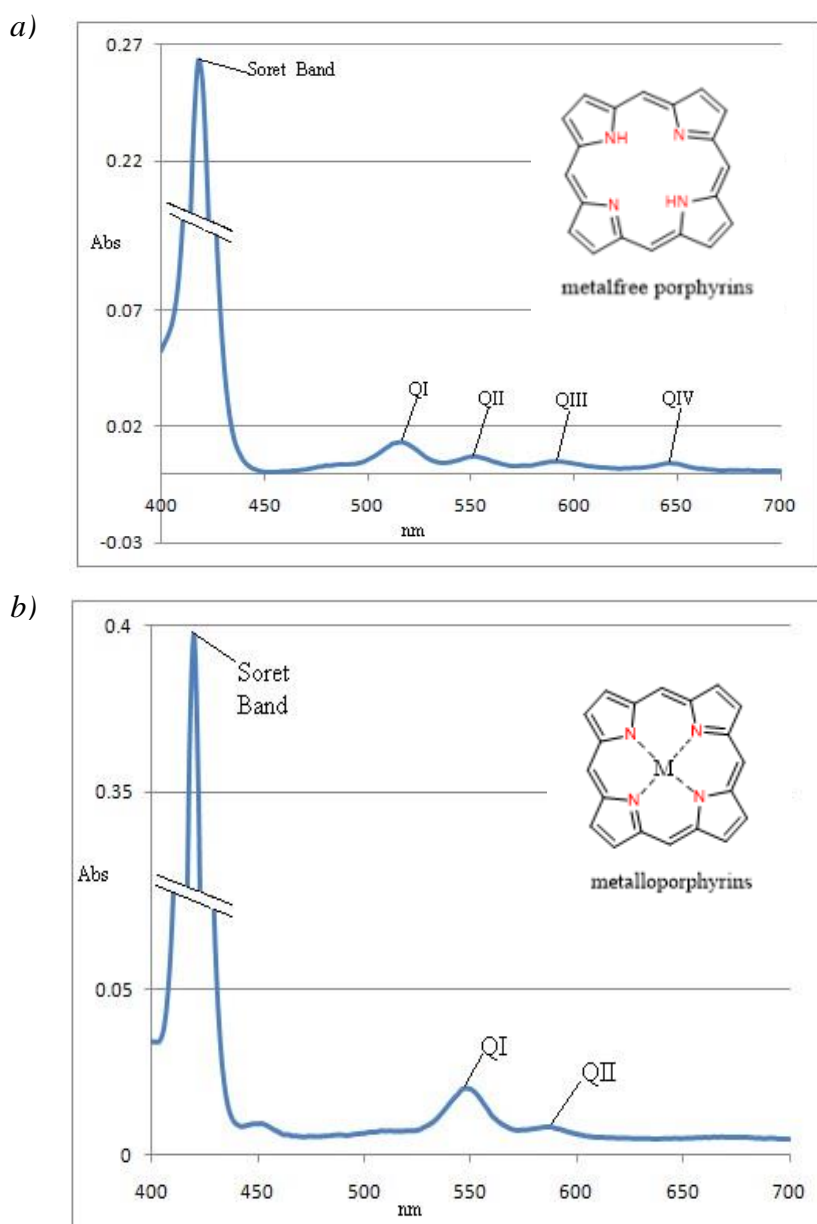


Figure 1.11. UV-Vis spectra for metal-free porphyrins (a), and for metalloporphyrins (b).⁸⁷

Phthalocyanines have lower energy absorption (Q-band) compared to porphyrins, due to the more extensive π -electron conjugation.⁸⁸ They exhibit one main Q-band when metallated compared to metal-free phthalocyanines, which have two main Q-bands. They substantially absorb light between 650 and 720 nm. This is what gives the phthalocyanine its vibrant colour.⁸⁵ The second band (the *Soret* or B- band) is seen as a broad band between 300 and 400 nm.^{85, 88} as shown in (Fig 1.12). However, as demonstrated below, when phthalocyanine is metalated, it has just one main Q-band (**b**) compared to two main Q-bands (**a**) in the case of metal-free phthalocyanine.).^{75, 89}

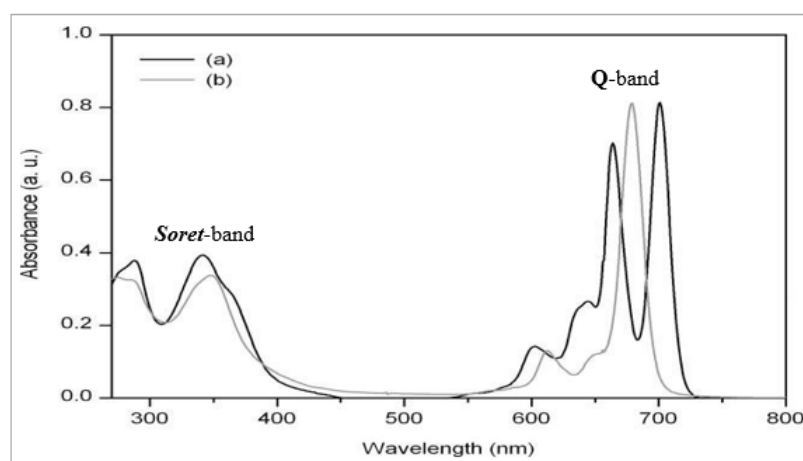


Figure 1.12. UV-vis spectra of phthalocyanine as (a) a metal-free and (b) a metallated-Pc.⁷⁵

1.5.2 NMR Spectroscopy

Although porphyrins and phthalocyanines both contain an expanded conjugated π -system, they exhibit distinct differences in terms of structural analysis. Porphyrins typically yield distinctive spectra in NMR spectroscopy, offering comprehensive insights into their molecular structure. However, it can be difficult to obtain distinct and interpretable spectra for unsubstituted-phthalocyanines, mainly because they have low solubility in typical NMR solvents. In porphyrins, it can be seen that signals are strongly shifted downfield for the β -pyrrole and *meso*-protons due to the paramagnetic ring current which causes de-shielding effect and the N-H protons of the rings are shifted up field to the negative region resulting from the shielding effect for the ring current as show below in (Fig. 1.13).⁹⁰

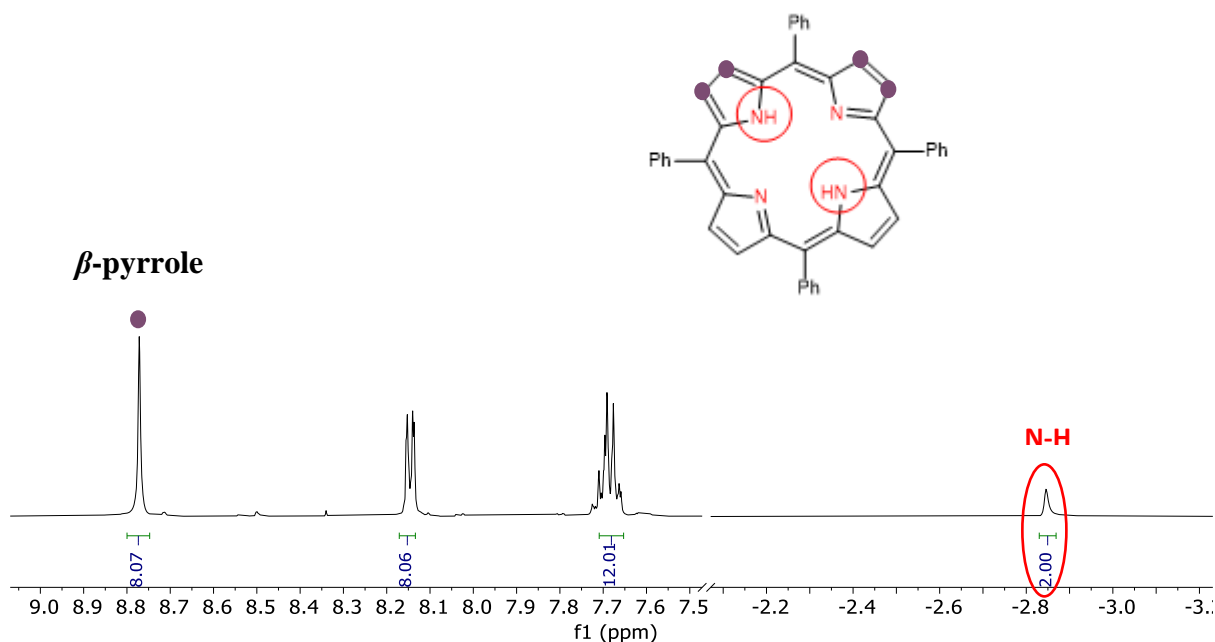
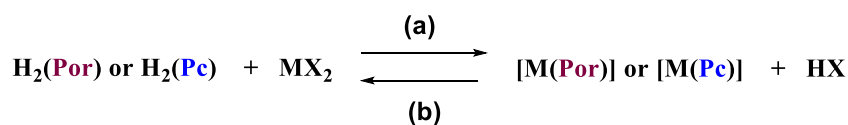


Figure 1.13. The NMR spectrum of porphyrin TPP 9.

1.6 General metalation of porphyrins and phthalocyanines

A metallo-porphyrin or metallo-phthalocyanine refers to a compound derived from porphyrin $H_2(\text{Por})$ or phthalocyanine $H_2(\text{Pc})$ in which at least one central nitrogen atom forms a bond with a metal atom. The basic form of this compound is the monometallic metallo-porphyrin $[M(\text{Por})]$ or metallo-phthalocyanine $[M(\text{Pc})]$, and its synthesis is outlined in Equation 1.⁹¹ Typically, the formation of such metallo-porphyrins or metallo-phthalocyanines involves a reaction between the free base forms, $H_2(\text{Por})$ or $H_2(\text{Pc})$, and a metal salt MX_2 , resulting in the production of $[M(\text{Por})]$ or $[M(\text{Pc})]$ and the corresponding acid molecule HX , as depicted in (Eq1 (a)).⁹¹ This process is termed "metalation," and its reverse counterpart, as shown in (Eq1. (b)), is referred to as "demetallation."⁹¹⁻⁹³

Equation 1.



The size of the cavity is well matched to various metal ions, and a wide range of metals (e.g., Zn^{2+} , Cu^{2+} , Ni^{2+} , Co^{2+} , etc.) can be inserted into the central core of

phthalocyanines, porphyrins, as well as other tetrapyrrole derivatives,⁸⁸ and many of these can fit into the central cavity without changing its structure,^{85, 92, 94} (Fig. 1.14).

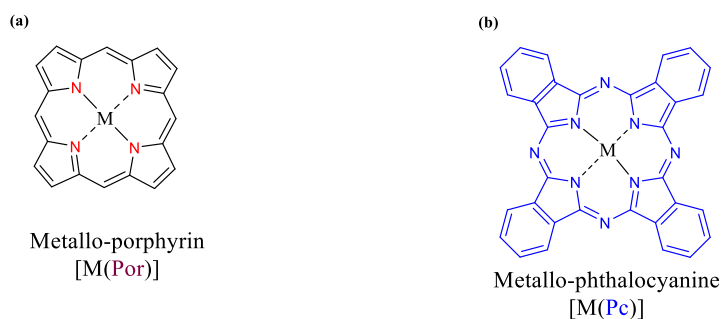


Figure 1.14. The structures of [M(Por)] and [M(Pc)] complexes where the metal fits inside the cavity.

1.7 Porphyrins and phthalocyanines arrays

Connecting two porphyrins or phthalocyanines by conjugated bonds can enhance the electronic interaction among the constituent porphyrin units due to a forced coplanar structure.

These arrays have attracted considerable attention because of their remarkable photophysical properties such as extensively red-shifted absorptions, very short excited-state lifetimes and large nonlinear optical properties.⁹⁵ These arrays also have potential use as conducting molecular wires by virtue of their conjugated electronic characteristics.

The structure of some conjugated porphyrinoids, which includes π -to- π directly linked polymers can be seen in (Fig 1.15).⁹⁵

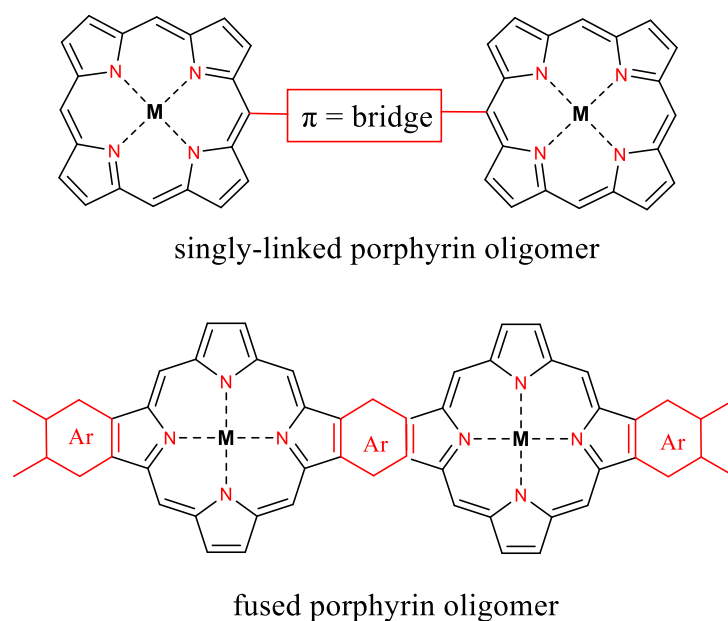


Figure 1.15. Porphyrin wires with various conjugated configurations.⁹⁵

1.7.1 linear arrays

Linear arrays are porphyrin or phthalocyanine molecules that are placed in a straight line to produce a chain-like structure. This configuration allows for efficient energy and electron transport along the chain.⁹⁵ Because of the short centre-to-centre distance and the high excitonic interaction, *meso-meso* directly connected porphyrins exhibit rapid energy and electron transfer rates, (Fig. 1.16).⁹⁶

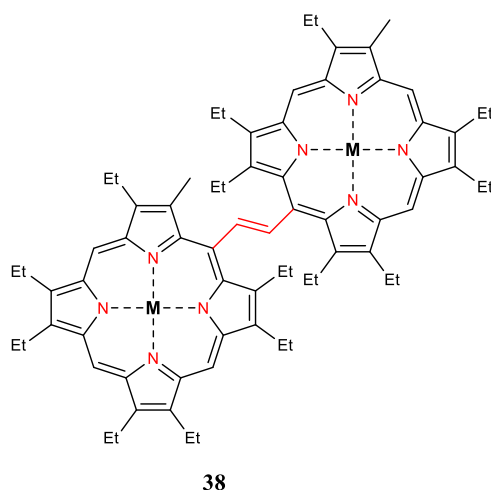


Figure 1.16. Ethene-bridged diporphyrins as single linkages.⁹⁵

Another type of porphyrin array is pyrazinoquinoxaline-fused trimeric porphyrin arrays **39**. The bridging unit **39** can be extended to the synthesis of L-shaped trimer array **40** and diporphyrin array **41** (Fig. 1.17).⁹⁵

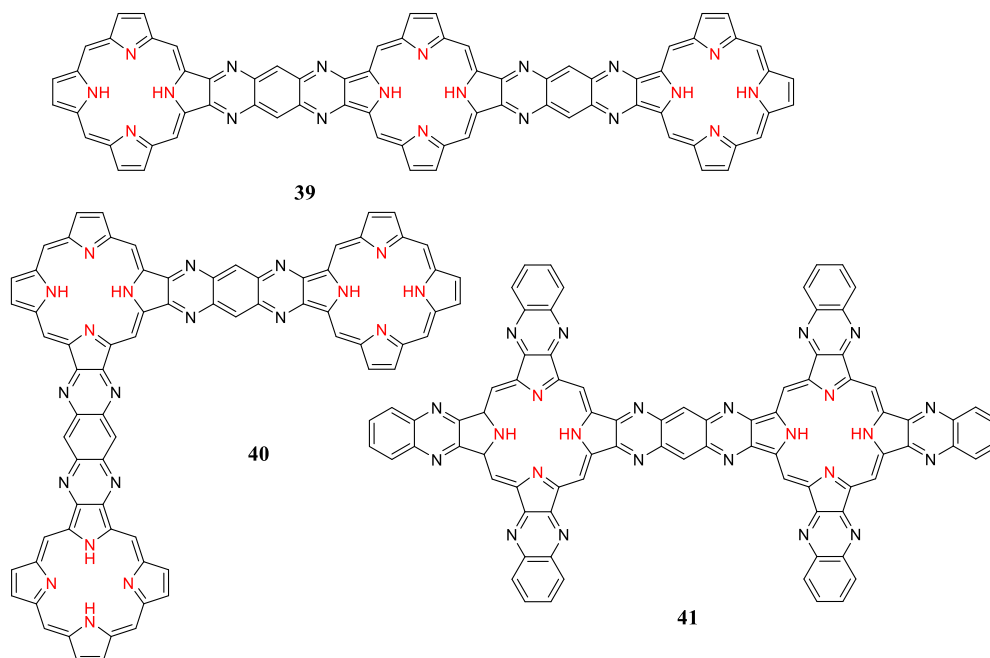


Figure 1.17. Some examples of fused-porphyrin structure.⁹⁵

In a further example, the structure of zinc porphyrin and free base porphyrin with diphenylethyne-linker **42** was applied also for the study of energy transfer, as shown in (Fig. 1.18)⁹⁷

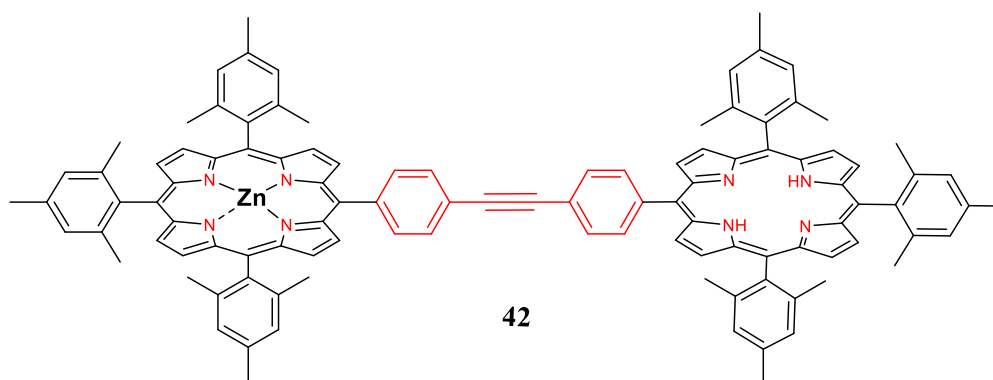


Figure 1.18. Diphenylethyne linker between diporphyrin units,⁹⁷ resulting in weak conjugation between the porphyrin units.

Isomeric linear metalated phthalocyanines **43** and **44** were connected via a series of benzene rings. These structures have been studied due their fluorescence spectroscopy and electronic chemistry absorption , (Fig. 1.19).⁹⁸

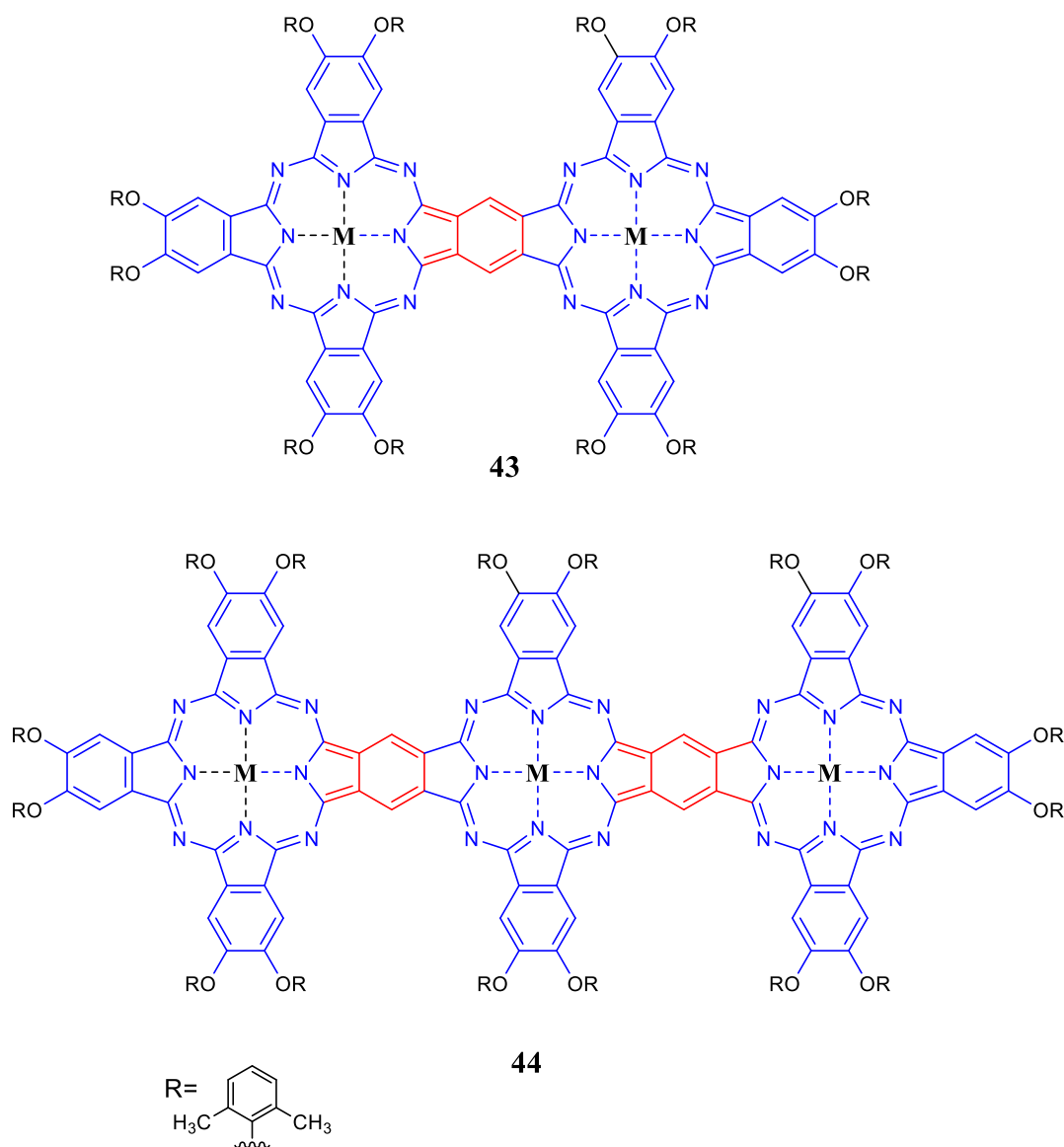


Figure 1.19. Linear arrays example using metalated phthalocyanine.⁹⁸

1.7.2 Cyclic array

Porphyrin cyclic arrays are a sort of organised porphyrin molecular arrangement in which the porphyrin units are connected to form a cyclic or ring-like structure. These cyclic arrays can be generated artificially for a variety of purposes.⁹⁵ For

example, cyclic porphyrin arrays **45** and **46** can be used in catalysis, sensing, light harvesting, and molecular electronics, (Fig. 1.20).^{95, 99}

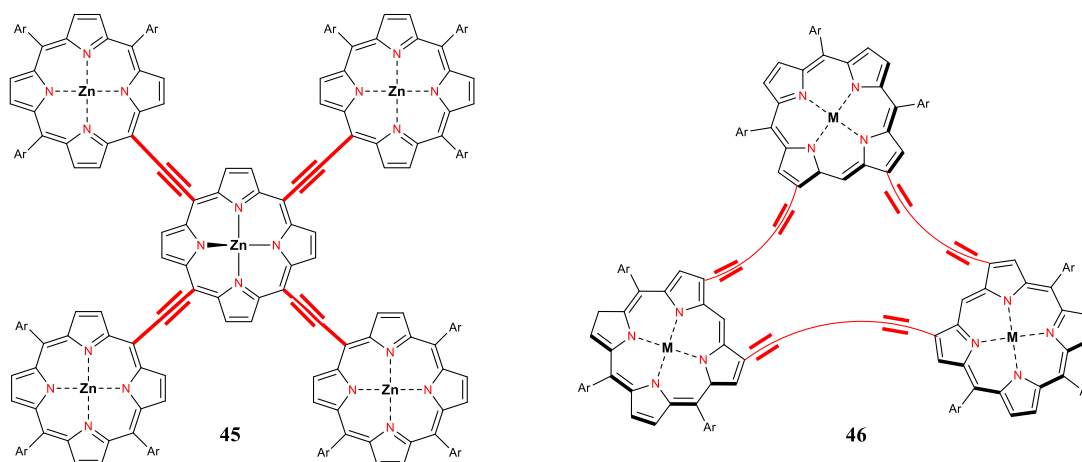


Figure 1.20. An example of multi-porphyrins by ethyne-bridged **45** (left), and cyclic porphyrin trimers by butadiyne-bridged **46** (right).⁹⁵

Kim and colleagues,¹⁰⁰ produced a range of covalent and non-covalently built cyclic porphyrin arrays as biomimetic models of light harvesting antennae. The key to creating these systems is the *meso-meso*-linked diporphyrin **47**, as shown below in (Fig 1.21).⁹⁶

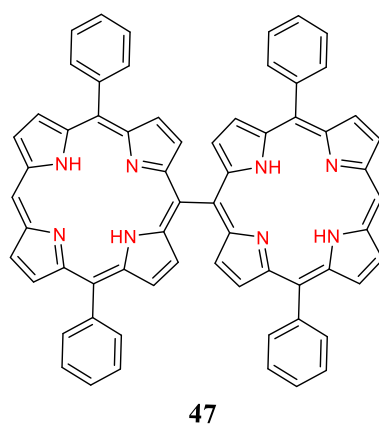


Figure 1.21. *Meso-meso*-linked diporphyrin.⁹⁶

Another example of structures of [M(Por)] and [M(Pc)] in cyclic arrays is **48**, used for increasing the photocatalytic effect of polymers,¹⁰¹ and **49** used for efficient electrocatalysts in organic electrochemistry, (Fig. 1.22).¹⁰²

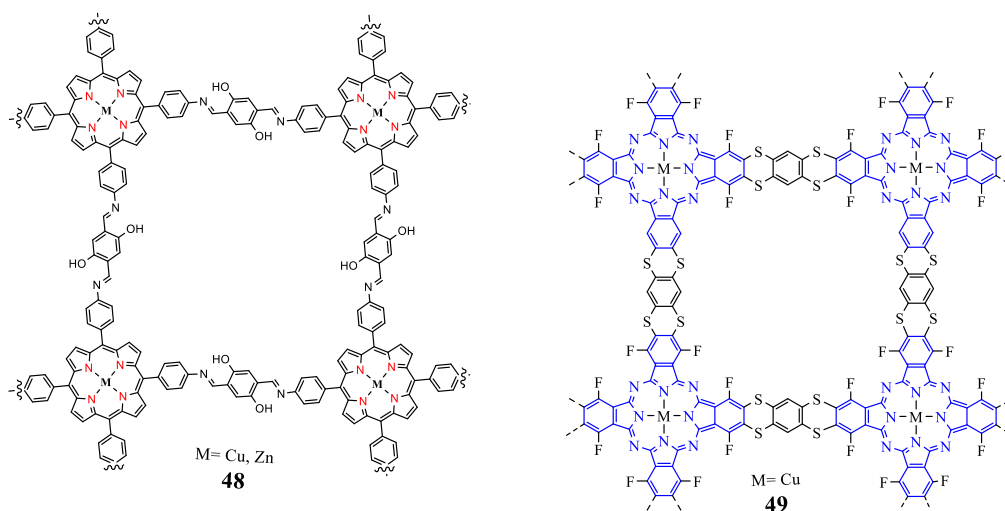


Figure 1.22. Example structures of cyclic metallo-porphyrin **48** and metallo-phthalocyanine **49**.^{101, 102}

Porphyrin arrays, in summary, serve an important role in biological processes, particularly in light-capturing systems such as chlorophyll. Furthermore, synthetic phthalocyanine or porphyrin linear and cyclic arrays show promise in the development of novel materials with distinct features for a wide range of technological applications.

1.7.3 Nanoparticles arrays

The extensive research on porphyrins and phthalocyanines across various advanced disciplines has yielded numerous favourable results due to their exceptional characteristics. Introduction of substituents and construction of complex variants often retains the remarkable characteristics of the original compounds such as catalysis, imaging, and energy transfer. Carefully designed derivatives possess the capacity to self-assemble creating nanomaterials,¹⁰³ and they can further encapsulate host materials in aqueous solutions. Some such functional nanoparticles demonstrate considerable promise in Photo-Dynamic Therapy (PDT), a cancer treatment method that involves the destruction of tumours by the production of oxygen species that are reactive upon the activation of a photosensitizer.¹⁰³⁻¹⁰⁵ Nanoparticles can have inherent surfactant capabilities, making them highly valuable in diverse applications, particularly in the

development of useful materials or nanoscale assemblies with specific characteristics, an illustrative instance of such designs is gold nanoparticles.^{105, 106}

Porphyrins or Phthalocyanines on gold nanoparticles

The Figure 1.23, illustrates an example of gold nanoparticles **50** that have been modified with a ligand derived from thiolated porphyrin (shown in red) and a ligand derived from thiolated polyethylene glycol (shown in black), attached to an antibody (shown in green).¹⁰³

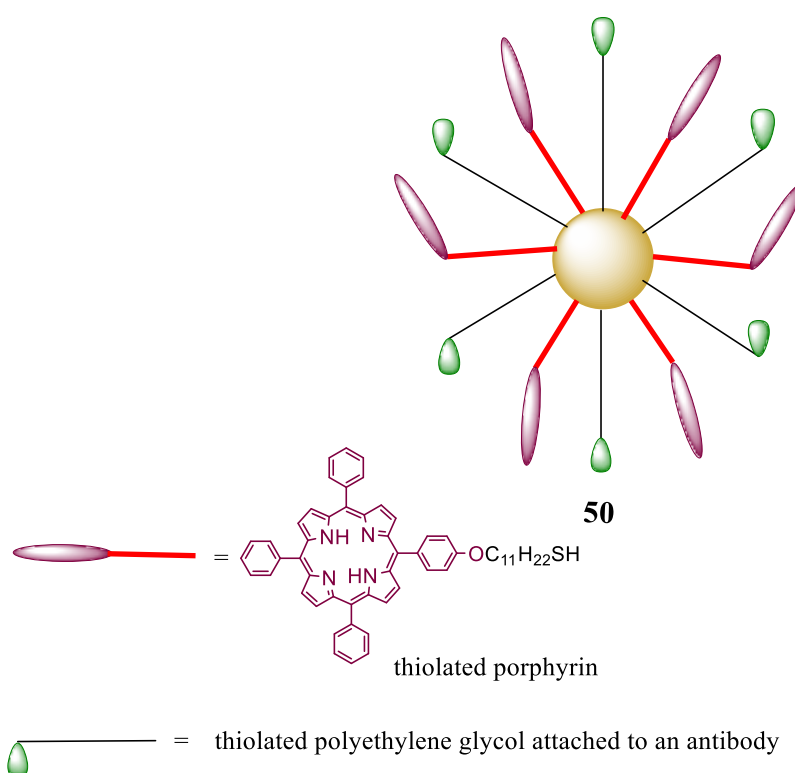


Figure 1.23. Example of gold nanoparticles, connected with porphyrin units.¹⁰³

Camerin and colleagues in 2015 synthesised and applied gold nanoparticles (NP) stabilised by the hydrophobic zinc-phthalocyanine co-self-assembly **51** (Fig. 1.24).¹⁰⁷

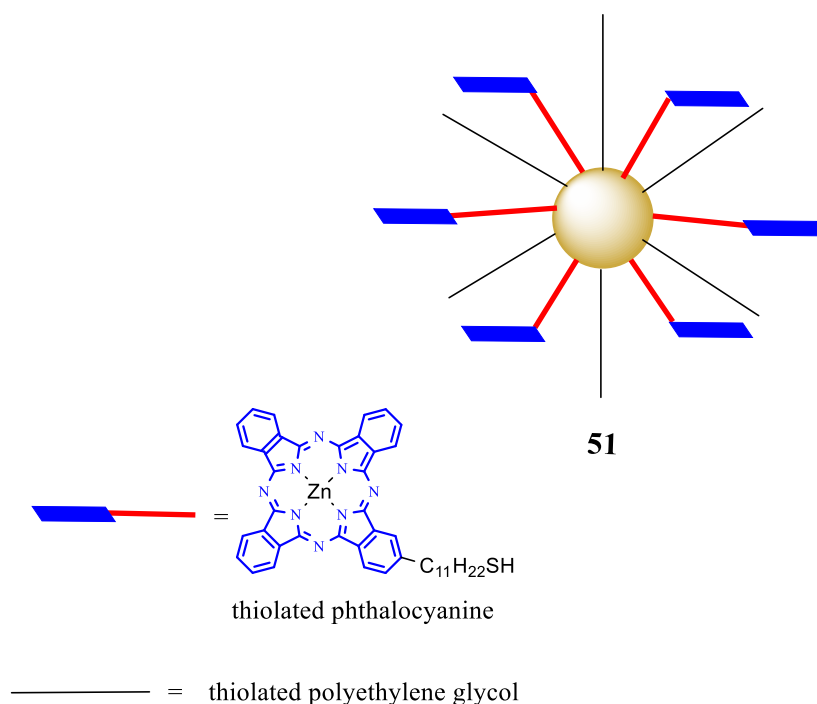


Figure 1.24. Example of gold nanoparticles coated with phthalocyanine cores .¹⁰⁷

Metallo-porphyrins have been thoroughly examined due to their capacity to generate species of reactive oxygen and their strong role as photosensitizers in photodynamic therapy (PDT).^{106, 108} The structure of another gold nanoparticle **52** is depicted in (Fig. 1.25). This multifunctional water-soluble nanomaterial, was synthesised by attaching a thiolated polyethylene glycol (PEG) and the thiolated porphyrin (PR-SH).¹⁰⁸

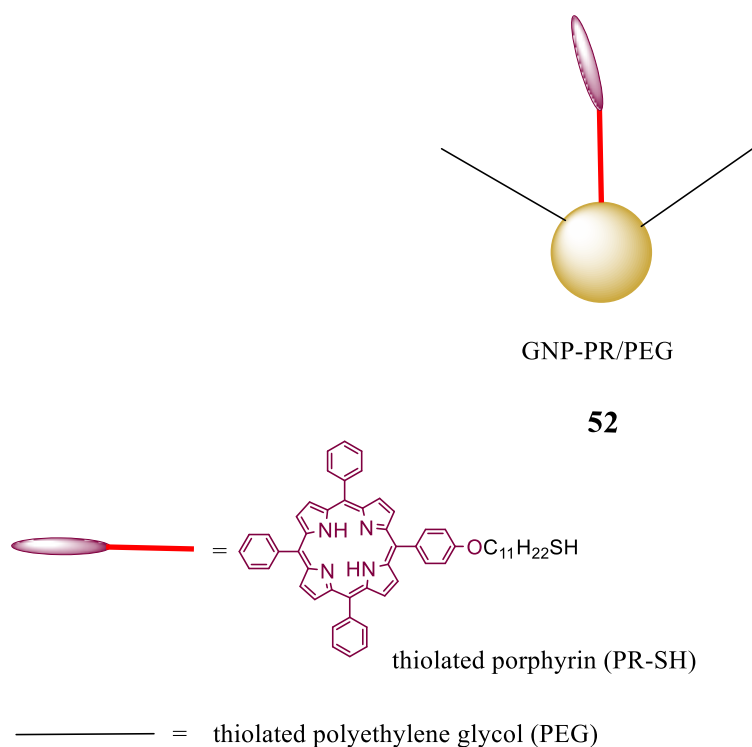


Figure 1.25. The structure of gold nanoparticle **52**, using PR-SH porphyrins and thiolated polyethylene glycol (PEG), which induces the production of singlet oxygen, resulting in increased effectiveness of the photosensitizer.¹⁰⁸

Examples of some porphyrins which are inherent amphiphiles and can self-assemble to form nanoparticles are shown in (Fig. 1.26).¹⁰⁴

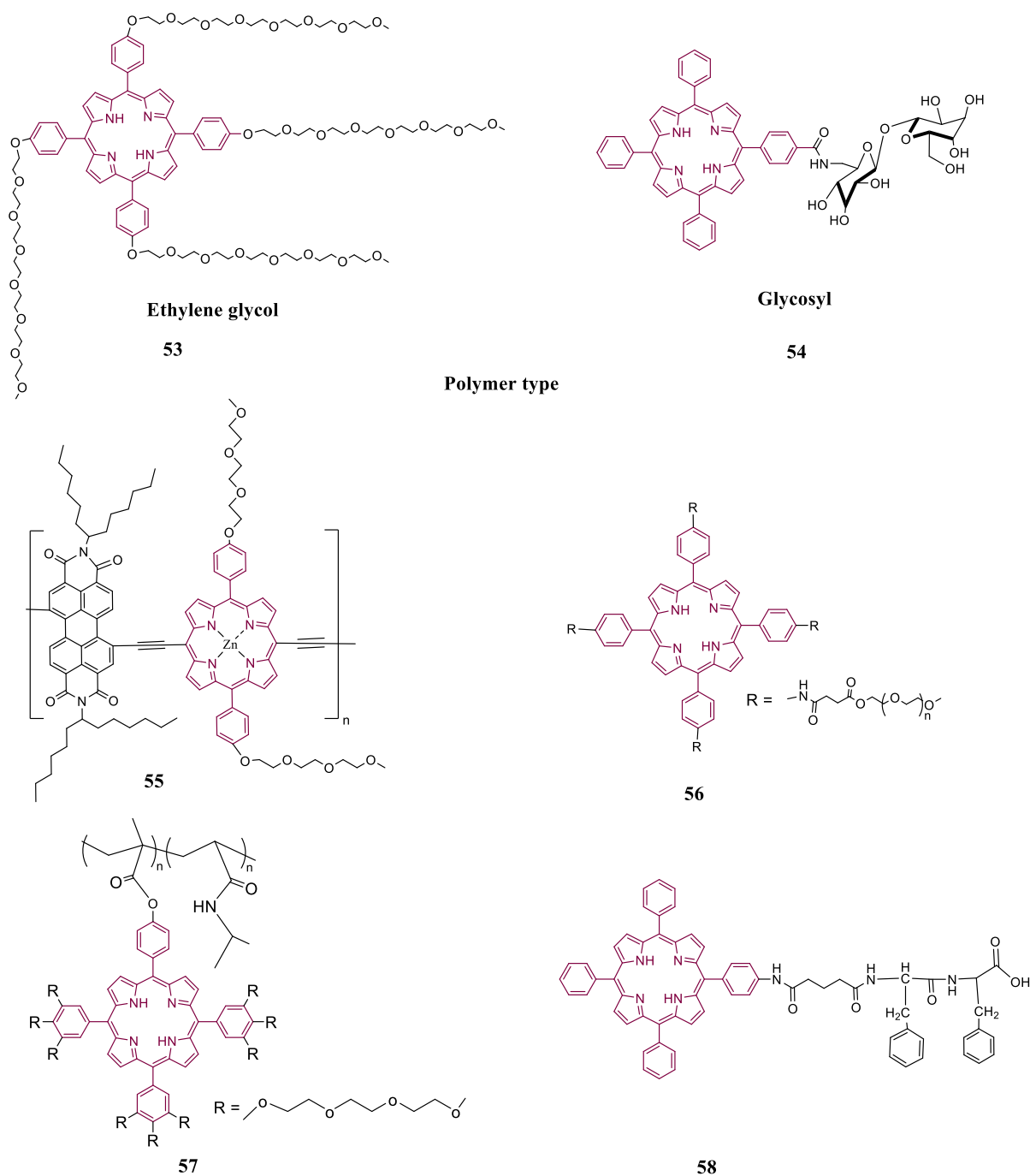


Figure 1.26. Molecular Structures for self-assembling nanoparticles using amphiphilic porphyrins or metallo-porphyrins **53-58**.¹⁰⁴

Porphyrins and phthalocyanines can therefore be assembled to build nanoparticles with unique electronic and optical properties. They have a semi-rigid arrangement and elements of controlled assembly at the nanoscale. They are the perfect building blocks for nanoparticle arrays in a variety of applications, such as electronics, catalysis, sensing,

imaging, and phototherapy, and represent an assembly arrangement that complements the fully defined multi-macrocyclic assemblies targeted in this work.

1.7.4 Rare-earth complexes (double- and triple-decker arrays)

Sandwich complexes created by rare-earth elements (REEs) and tetrapyrrole macrocycles, specifically porphyrins (Por) and phthalocyanines (Pc), are distinct structures that provide numerous possibilities for both fundamental study and practical uses.¹⁰⁹ They have already made significant contributions to diverse areas of contemporary materials science, involving organic electronics,¹¹⁰ nonlinear optics,¹¹¹ , sensing technologies,¹¹² and particularly in the development of Single-Molecule Magnets (Ln-SMMs).^{113, 114} Utilising porphyrins and phthalocyanines as ligands to connect lanthanide metals in single complexes results in the formation of double- and triple-decker arrays.^{115, 116}

1.7.4.1 The reaction of porphyrins and phthalocyanines with lanthanide metals

The lanthanide or 'lanthanoid' series consists of at least 14 metallic elements. Within the periodic table, these elements have occupied 4f orbitals and have the electron configuration $[Xe]4f^{(n-1)}$ where n = number of 4f electrons (which filled from 4f¹ to 4f¹⁴, varying on specific lanthanide metal).¹⁰⁹ Each lanthanide element consistently exhibits an oxidation state of +3.¹¹⁵ The relationship that exists between SMMs and lanthanide metals comes from the unique magnetic properties that certain lanthanide ions display, such as their large magnetic moments and magnetic anisotropy.¹⁰⁹ Because of the unpaired electrons that exist in their f-orbitals, lanthanide ions often have large magnetic moments, which makes them excellent candidates for SMMs.¹¹⁵

The lanthanide ions, specifically **Eu³⁺** and **Dy³⁺** both display the greatest magnetic properties due to 4f orbitals accommodating 6e⁻ and 9e⁻ unpaired electrons, respectively (Table. 1.1).¹⁰⁹

Element	Atomic electron configuration (all begin with [Xe])	Ln ³⁺ electron configuration
Eu	4f ⁷ 6s ²	4f ⁶
Dy	4f ¹⁰ 6s ²	4f ⁹

Table 1.1. Electronic configuration of lanthanide ion (**Eu³⁺** and **Dy³⁺**).^{109, 117}

When it comes to lanthanide metals, experimental evidence demonstrates that the ionic size of the lanthanide metals progressively decreases from lanthanum to lutetium as the atomic number increases¹¹⁸ and it can be observed that after transitioning from La³⁺ to Lu³⁺, the ionic radius decreases from (La³⁺) 103 picometers to (Lu³⁺) 86 picometers, as depicted in the (Table. 1.2).^{115, 118, 119} The effect occurs because of the poor shielding of the 4f electrons against the increasing nuclear charge, resulting in a continuous decrease in ionic radius across the series.¹⁰⁹







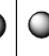




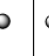



Chemical element	La	Ce	Pr	Nd	Pm	Sm	Eu	Gd	Tb	Dy	Ho	Er	Tm	Yb	Lu
Atomic number	57	58	59	60	61	62	63	64	65	66	67	68	69	70	71
Ln ³⁺ size															
Ln ³⁺ radius (Picometers pm)	103	102	99	98.3	97	95.8	94.7	93.8	92.3	91.2	90.1	89	88	86.8	86.1

Table 1.2. Lanthanide sizes (ionic radii from La³⁺ to Lu³⁺).¹¹⁹

Furthermore, the combination of porphyrins (**Por**) and phthalocyanine (**Pc**) with strong bonds to lanthanide metals leads to an impactful and distinctive magnetic behaviour, generating a strongly linked spin system. The spin system refers to the presence of unpaired electrons in a double- or triple-decker complexes, either using one or more of these metals.^{115, 120} Figure 1.23 displays the structure of these complexes formed by lanthanide metals with tetrapyrrolic macrocycles (**Por** and **Pc**, with mixed systems offering potential additional complexity that can be exploited in information storage protocols) used as SMMs system. This alignment creates the spin magnetic behaviour in

molecules, as electrons prefer to stay unpaired.¹²¹ This behaviour influences the complex's magnetic and electronic properties such as (Ln-SMMs).^{115, 122, 123}

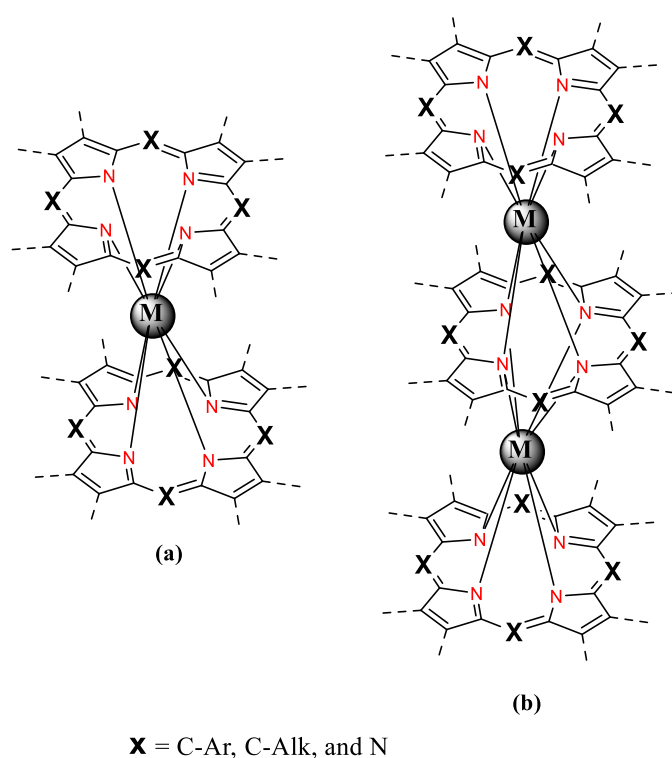


Figure 1.23. An illustration of a double (a) and triple (b) decker-system of molecules employed as SMMs.¹⁰⁹

In complexes with tetrapyrroles, lanthanide metals are located above the macrocycle's plane and create a bridge connecting the porphyrin and phthalocyanine units as shown in (Fig. 1.24).^{124, 125} Complexes containing two Lanthanide ions (Ln^{3+} - Ln^{3+}) display dual magnetic system, by building Ln-N bond, (Ln^{+6} , N^{-6}) with 3 Por/Pc systems.¹⁰⁹ Conversely, double-decker complexes that consist of a single ion lead to the formation of a free-radical electron system,¹⁰⁹ as shown in (Fig. 1.24).

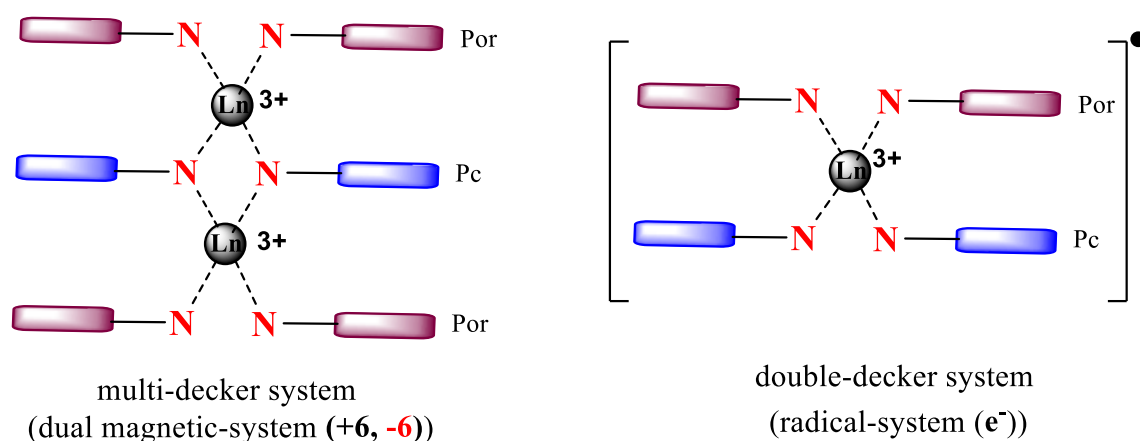


Figure 1.24. The sites of lanthanide metals of the double-and triple-decker complexes and their magnetic structure system.¹²⁵

The potential of double- and multi-decker complexes has greatly inspired researchers to concentrate on creating high-performance Single-Molecule Magnets (Ln-SMMs) using lanthanide ions. For further information on SMMs, see references (109).

1.7.4.2 Synthesis of porphyrin and phthalocyanine double-and triple-decker arrays

The development of materials with unique magnetic properties, designated Ln-SMMs complexes, has made extensive use of lanthanide metals by scientists. Phthalocyaninato and/or porphyrinato ligand combinations can be used to form these complexes, which can appear as double- or triple-decker arrays.¹²⁶ These mixed complexes have the capability to produce a wide range of both homoleptic and heteroleptic structures.¹²⁷ Homoleptic sandwich complexes, which consist of identical phthalocyaninato or porphyrinato ligands, can be easily differentiated from heteroleptic sandwich complexes, as illustrated in (Fig. 1.25).^{128, 129}

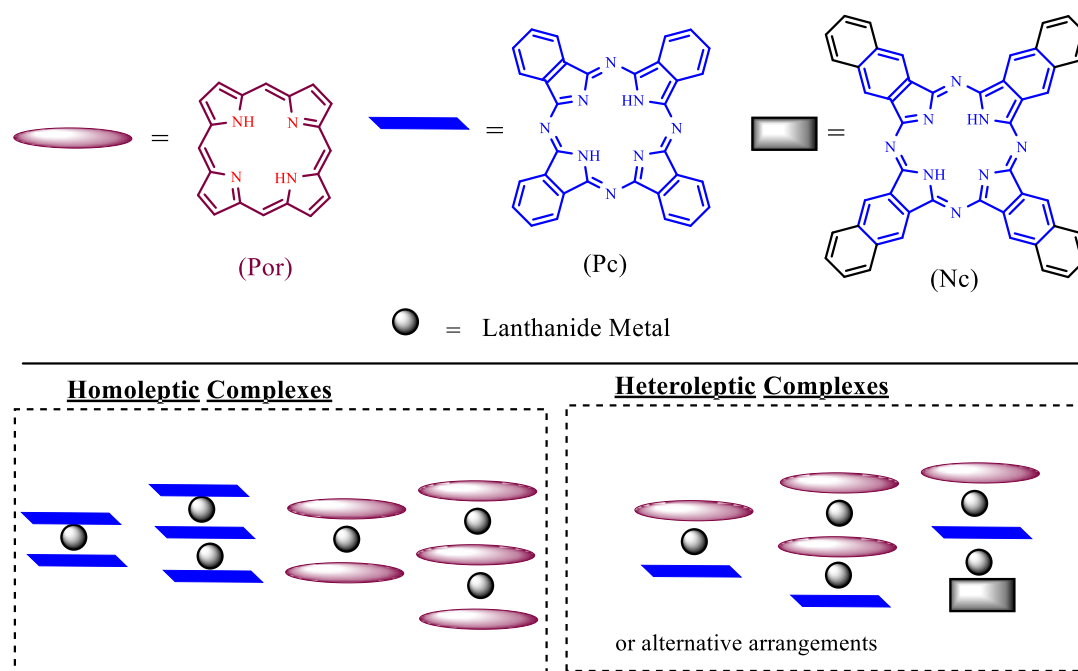
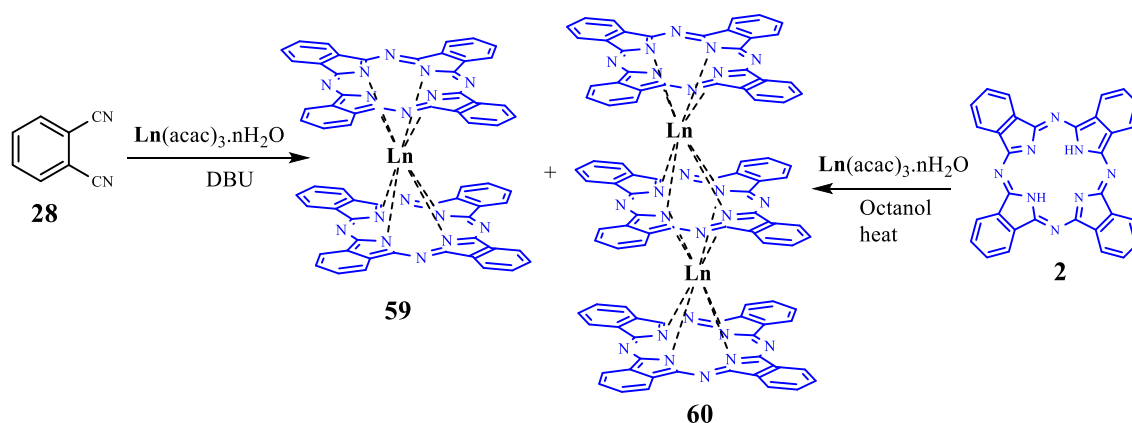


Figure 1.25. Schematic structures for both homoleptic and heteroleptic complexes.¹²⁹

Both homoleptic and heteroleptic sandwich-type complexes are supramolecular compounds. There are two main procedures by which these rare-earth complexes can be produced. In the first method, they are often synthesised using what has been termed a “**one-pot**” reaction, whereby starting materials are all combined and reacted.¹³⁰ The second method is called a “**stepwise raise-by-one-storey**” reaction that could be optimised into a “one-pot” process.¹³¹ This synthetic procedure involves reacting the porphyrin or phthalocyanine molecule with lanthanide metal salts $[\text{Ln}(\text{acac})_3 \cdot n\text{H}_2\text{O}]$ to produce a mono-decker of $[\text{Ln}(\text{acac})(\text{Por})]$ or a mono-decker of $[\text{Ln}(\text{acac})(\text{Pc})]$, which is a “**half sandwich**” complex.^{125, 131, 132}

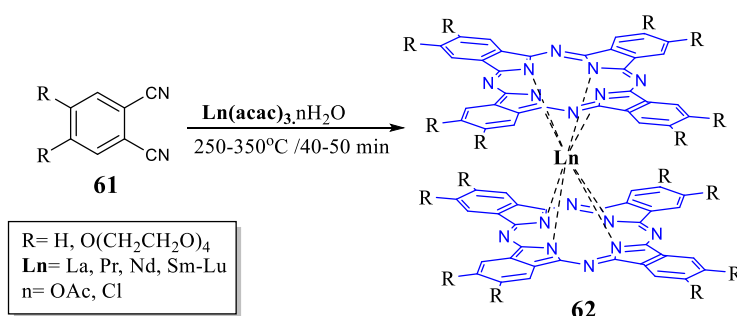
1.7.4.2.1 Homoleptic complex arrays

Homoleptic complexes can be achieved by using the “one-pot” reaction of phthalonitriles **29** which undergo cyclo-tetramerization in the presence of lanthanide metal salts $[\text{Ln}(\text{acac})_3 \cdot n\text{H}_2\text{O}]$.¹³³ This is achieved using such organic bases as 1,8-diazabicyclo undec-7-ene (DBU). An alternative is to react $\text{H}_2(\text{Pc})$ **2**, with metal salts, in a solvent with a high boiling point, such as octanol. This, however, produces only a low yield of the double- **59** and triple-decker **60** (Scheme 1.16).¹³⁰



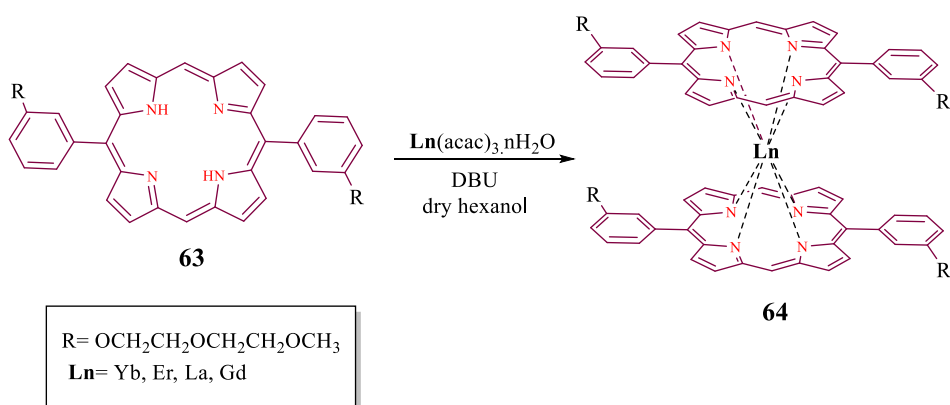
Scheme 1.16. Preparation method for homoleptic complexes.

Kirin and Moska synthesised and analysed the initial phthalocyanine lanthanide double-decker in 1965,^{134, 135} by heating the mixture of phthalonitriles **61** with $[\text{Ln}(\text{acac})_3 \cdot n\text{H}_2\text{O}]$ for 40-90 min at high boiling point 250-350°C resulting in *bis*-phthalocyanine complexes $[\text{Ln}^{3+}(\text{Pc})_2]$ **62** in 10-15% yields (Scheme 1.17).



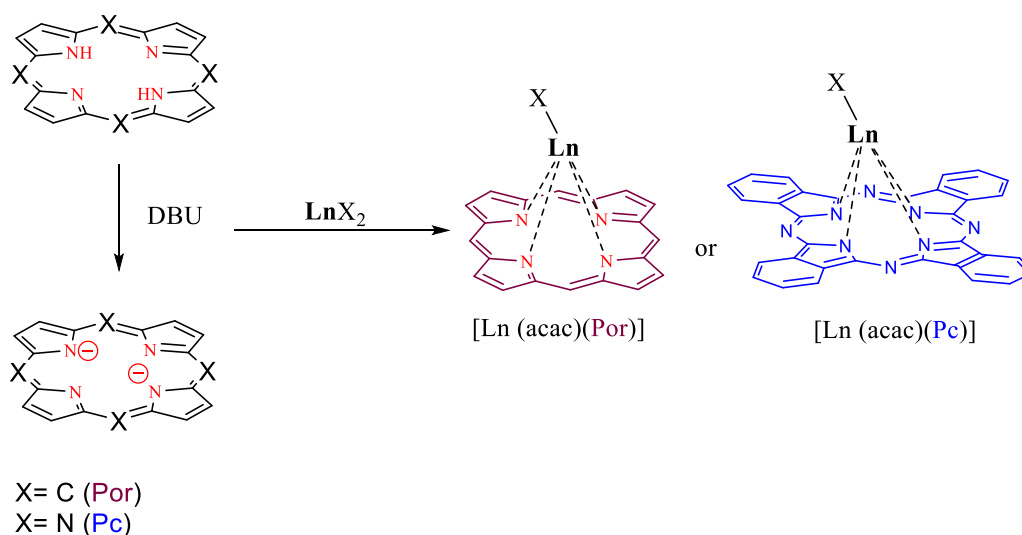
Scheme 1.17. The synthesis of homoleptic double-decker complexes **62**.^{133, 134}

A recent study successfully synthesised a homoleptic double-decker lanthanide *bis*-porphyrinate, with the aim to enhance the design and production of water-soluble molecular theranostics.¹³⁶ The synthesis consisted of a reaction in which 5,15-*bis*(3-(2(methoxyethoxy)ethoxy)phenyl)porphyrin **63**, $[\text{Ln}(\text{acac})_3 \cdot n\text{H}_2\text{O}]$, and DBU were heated in dry hexanol. This led to the creation of the double-decker complex **64** as the final product (Scheme 1.18).



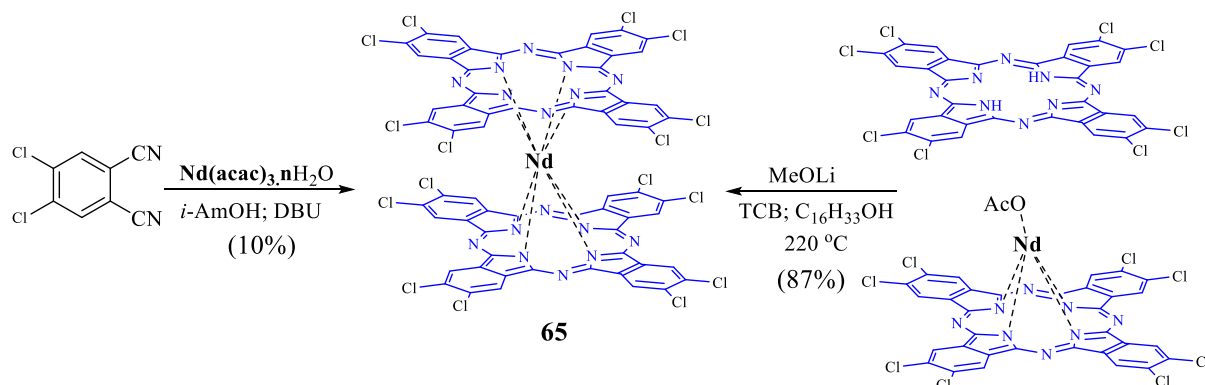
Scheme 1.18. Synthesis of homoleptic porphyrin double-decker complex.¹³⁶

Further developed methods for the synthesis of homoleptic complexes create mono-complex "half sandwiches" through the "stepwise raise-by-one-storey" reaction, which depends on the interactions between lanthanide salts [Ln(acac)₃.nH₂O] and a free macrocyclic ligand. Thus, ligands were changed into dianion forms in order to prepare different mono-decker complexes of Pc or Por.^{133, 137} The simplest strategy involves deprotonating the starting material using a concentrated solution of DBU at temperatures ranging from 180 to 200 °C. Subsequently, an organic solvent extraction was performed to isolate the mono-decker complex, as outlined in Scheme 1.19.¹³⁷



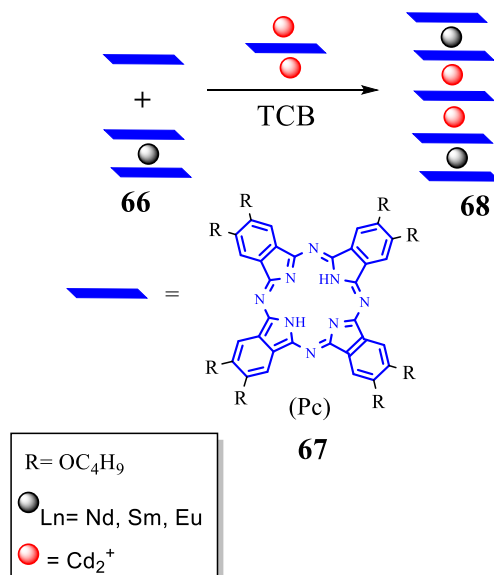
Scheme 1.19. A general method for producing mono-decker complexes of porphyrins or phthalocyanines.¹³⁷

In a comparable instance, a chloro-substituted Nd³⁺ *bis*-phthalocyanine of the sandwich homoleptic complex type was synthesised applying the two above methods. As result, using “stepwise raise-by-one-storey” method can produce a high yield 78% of the desired double-decker **65**,¹³⁸ as shown in (Scheme 1.20).



Scheme 1.20. The synthesis of phthalocyanine double-decker complex **65**.¹³⁸

In addition, a straightforward synthesis method began with a combination of Cd(OAc)₂·2H₂O, the neutral double-decker molecule [(Pc (OC₄H₉)₈)Ln(Pc (OC₄H₉)₈)] **66**, and metal-free Pc(OC₄H₉)₈ **67** in 1,2,4-trichlorobenzene (TCB). The mixture was subjected to reflux in the presence of nitrogen for 3 hrs. This led to the creation of a blue band that consisted of the quintuple-decker complex [(Pc)Ln(Pc)Cd(Pc)Cd(Pc)Ln(Pc)] **68**, with yields between 14.1% to 21.5% (Scheme 1.21).^{139, 140}

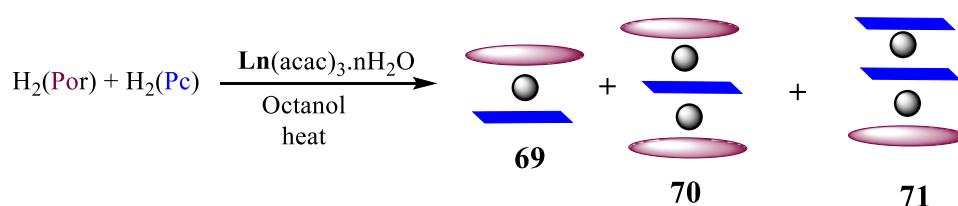


Scheme 1.21. Another example of homoleptic complex, pentakis(phthalocyaninato)-Ln³⁺-Cd^{II} **68**.¹³⁹

1.7.4.2.2 Heteroleptic complex arrays

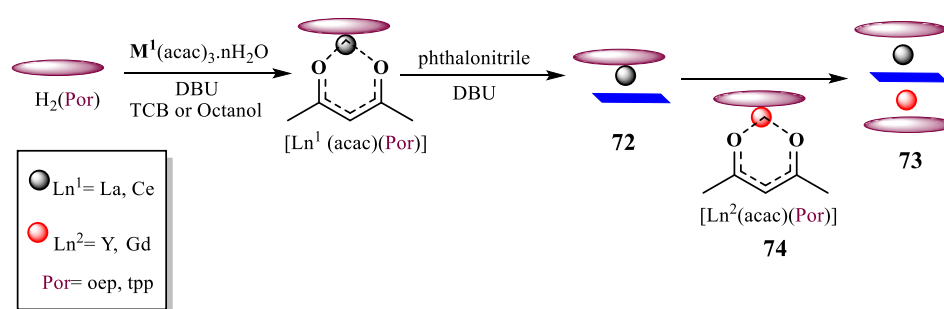
Recently, there has been a growing interest in heteroleptic analogues that incorporate a combination of several macrocyclic ligands. The distinct chromophores within these complexes may exhibit very varied optical and redox characteristics, enabling an exploration of the π - π interactions between the ligands and the metal ion's f-f interaction.¹⁴¹ Right now, there are few published articles that describe these heteroleptic complexes, and they are still uncommon and limited to a specific group of lanthanide metals.¹⁴¹⁻¹⁴³

The "one-pot" reaction is a simple but inefficient way to make heteroleptic double- or triple-decker complexes. This involves heating the $H_2(\text{Por})$, $H_2(\text{Pc})$ and $[\text{Ln}(\text{acac})_3 \cdot n\text{H}_2\text{O}]$ in solvent with a high boiling point of alcohol at reflux.^{143, 144} The reaction mixture also contains double-decker **69** and other triple-decker structures **70** and **71**, as depicted in (Scheme 1.22).



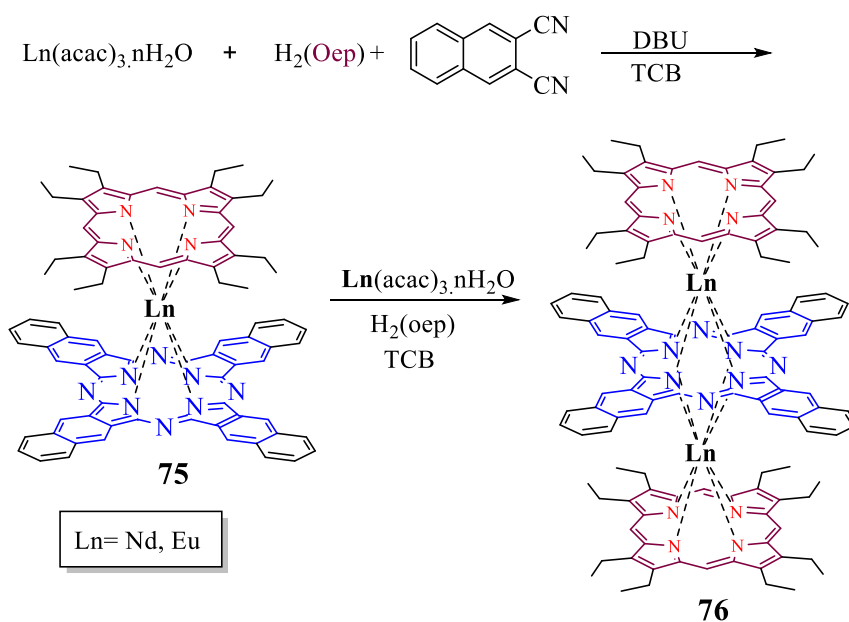
Scheme 1.22. Synthesising heteroleptic double and triple-decker complexes, using a "one-pot" reaction.^{143, 144}

Weiss and colleagues discovered that employing the "stepwise raise-by-one-storey" approach is an effective strategy for synthesising heteroleptic double- and triple-decker complexes of porphyrins and phthalocyanines.^{125, 131, 145} Scheme 1.23 demonstrates the synthesis of heteroleptic double-decker complexes $[\text{Ln}^1(\text{Por})(\text{Pc})]$ **72**, which are formed by cyclo-tetramerization of phthalonitrile with $[\text{Ln}^1(\text{acac})(\text{Por})]$. Additionally, the mixed-metal triple-decker complexes $[(\text{Por})\text{Ln}^1(\text{Pc})\text{Ln}^2(\text{Por})]$ **73** are obtained by reacting $[\text{Ln}^1(\text{Por})(\text{Pc})]$ **72** with $[\text{Ln}^2(\text{acac})(\text{Por})]$ **74**.



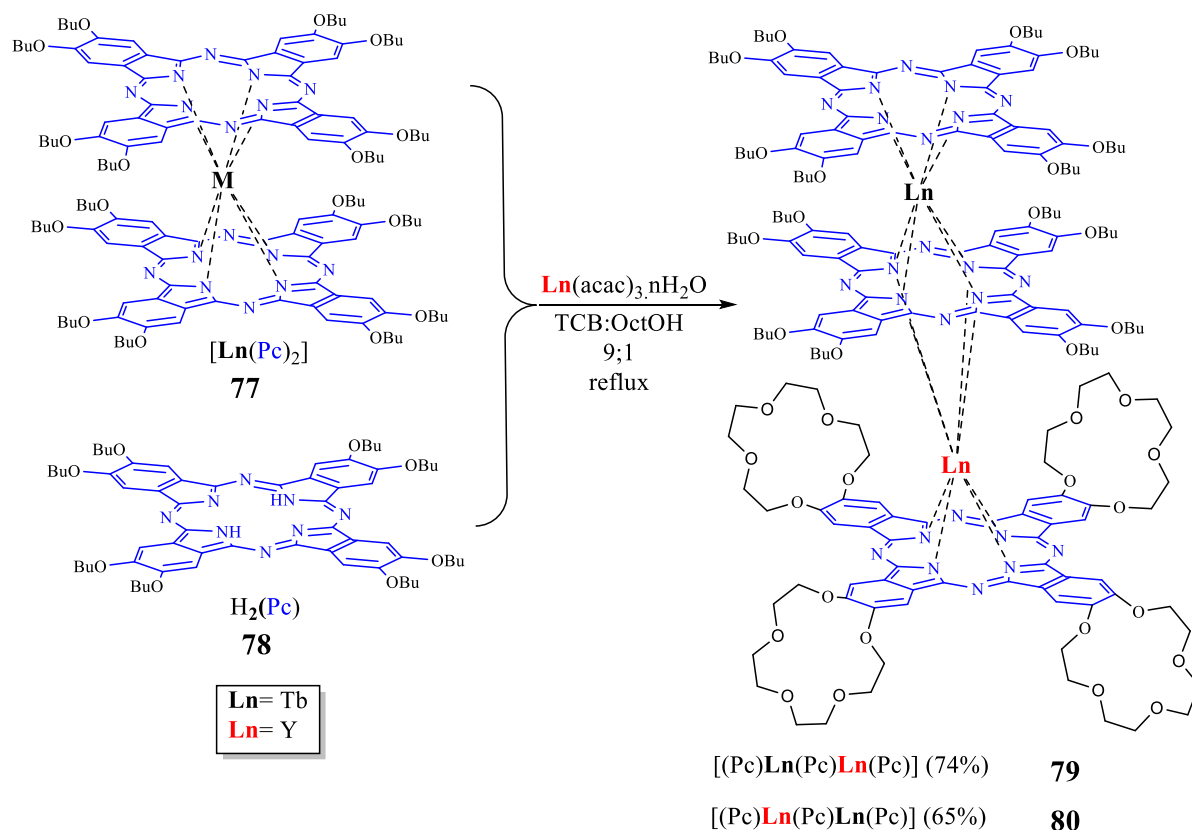
Scheme 1.23. Synthesis of heteroleptic complexes.¹²⁵

However, according to Jiang and co-workers,¹³¹ the synthesis of mono-decker porphyrin $[\text{Ln}^{3+}(\text{acac})(\text{Por})]$ "half sandwich" complex was deemed superfluous for the production of heteroleptic porphyrin and phthalocyanine double and triple-decker complexes. This was prepared by repeating the "stepwise raise-by-one-storey" reaction, reacting porphyrin molecule $\text{H}_2(\text{Oep})$ with the $[\text{Ln}(\text{acac})_3 \cdot n\text{H}_2\text{O}]$ in the presence of substituted-phthalonitrile with DBU to produce a double-decker complex $[\text{Ln}^{3+}(\text{Por})(\text{Pc})]$ **75** as starting material.¹³¹ Treatment of these double-deckers with $\text{H}_2(\text{Oep})$ and $[\text{Ln}(\text{acac})_3 \cdot n\text{H}_2\text{O}]$ in refluxing (TCB) as solvent gave the desired of heteroleptic triple-deckers complex $[\text{Ln}^{\text{III}}_2(\text{Pc})(\text{Por})_2]$ **76** (Scheme 1.24)



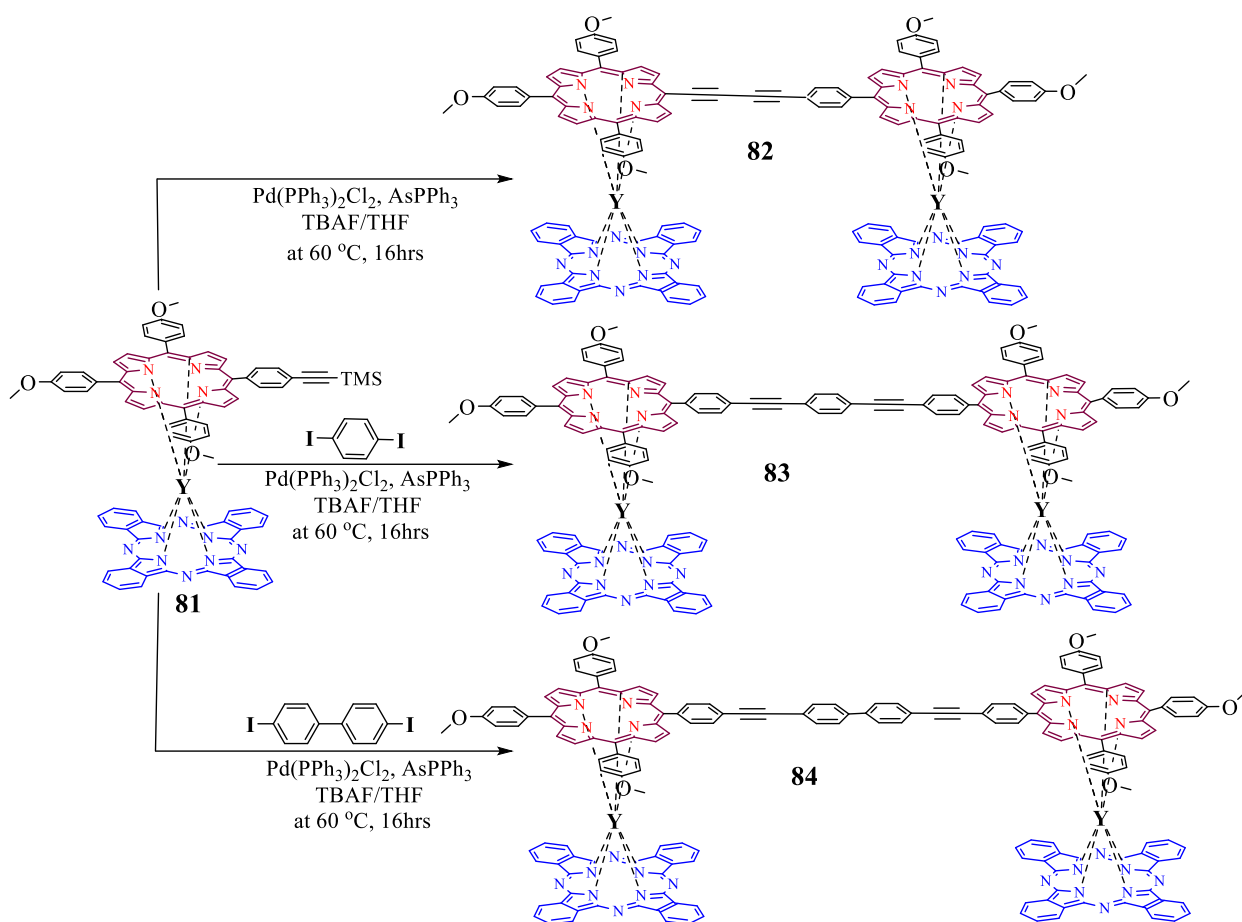
Scheme 1.24. Synthesis of double- and triple- decker complexes.¹³¹

The modification of using mixed solvents condition, has been demonstrated to enhance the stability of various sandwich phthalocyaninates, as indicated by the formation of triple-decker complexes including heteroleptic Y^{3+} and Tb^{3+} .^{114, 146} Briefly, butoxy-substituted double-deckers $[\text{Ln}(\text{Pc})_2]$ **77** (homoleptic complex) was reacted with $\text{H}_2(\text{Pc})$ tetra-15-crown-5-phthalocyanine **78** and $[\text{Ln}(\text{acac})_3 \cdot n\text{H}_2\text{O}]$, (where $\text{Ln} = \text{Y, Tb}$), in a mixture of TCB and 1-octanol (9:1 v:v). The resulting final complexes **79** and **80** were easily isolated with high yields of 74% and 65% respectively (Scheme 1.25).¹⁴⁶



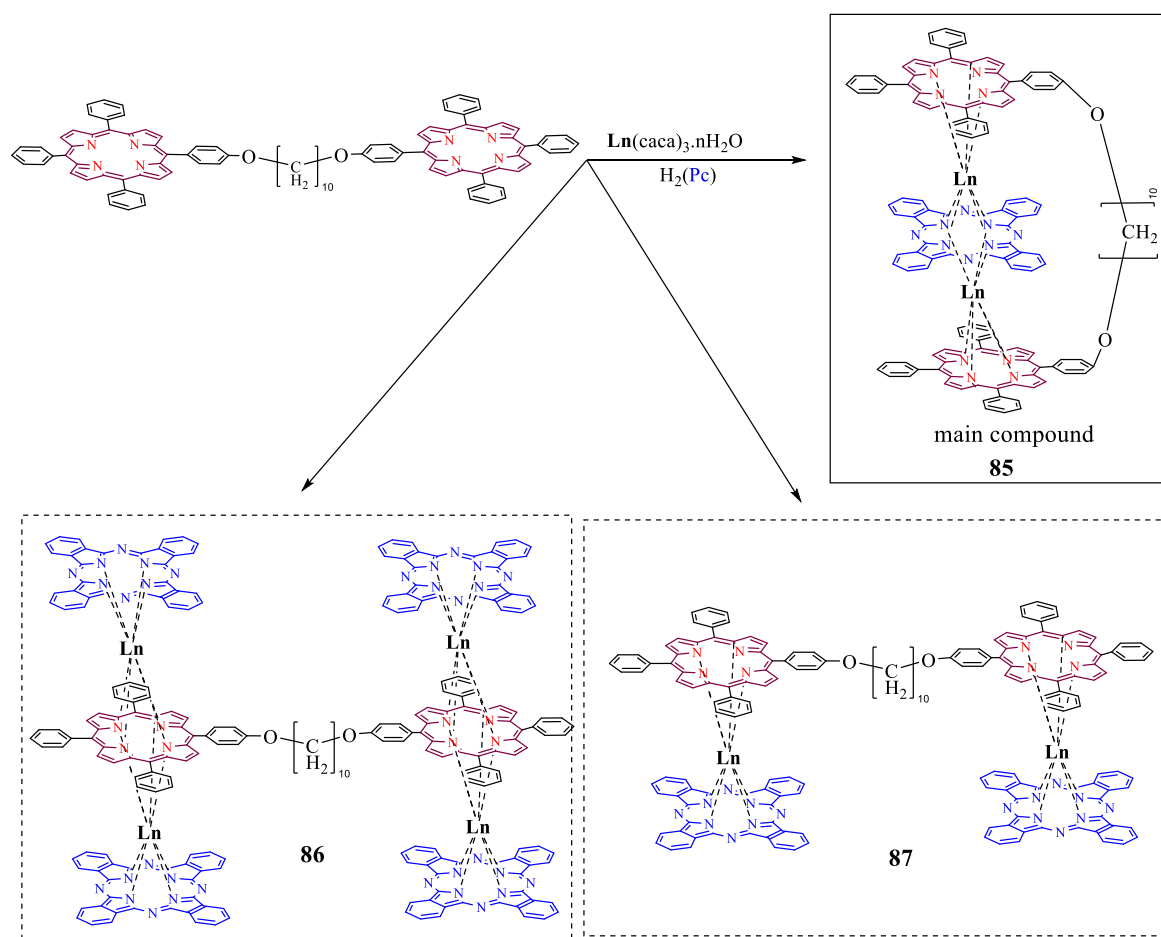
Scheme 1.25. Synthesis of heteroleptic triple-decker complexes **79** and **80**.¹⁴⁶

Recently, the specially made 5,10,15-tris(4-methoxyphenyl)-20-(4-((trimethylsilyl)ethynyl)phenyl)porphyrin was used to synthesise mixed-ligand porphyrins and phthalocyanines Y^{3+} double-decker complexes. First, $[\text{Y}^{3+}(\text{Por})(\text{Pc})]$ double-decker **81** was formed by applying the “stepwise raise-by-one-storey” reaction in TCB.¹⁴⁷ Then, using the ethyne functionality, two of these complexes were coupled forming biradicals (two double-decker complexes with one metal each, generating biradical system) through rigid tethers; a short-tethered biradical **82** was created using Glaser coupling, while longer-tethered ones **83** and **84** were created using Sonogashira coupling.¹⁴⁷ Although this method maintains a fixed distance around the metal centres, it in principle enables scientists to imagine shared ligands of different lengths, adjusting the bridging complexes' distance (Scheme 1.26).



Scheme 1.26. A recent synthesis of double-decker complexes **82-84**.¹⁴⁷

To date, our group has built on the work of Birin and co-workers^{128, 148} to attempt synthesising the heteroleptic structure of double and triple-deckers by using linked porphyrin and phthalocyanine derivatives as illustrated in (Scheme 1.27). They found that the triple-decker of porphyrin-phthalocyanine was the main compound produced **85**.¹⁴⁹ When an excess of Pc was used, the *bis*-TD was the sole product.



Scheme 1.27. Triple-decker complex **85** by Cammidge group, using “one-pot” reaction.¹⁴⁹

Thus far, several synthetic methods have been used to study the double- and triple-decker homo and heteroleptic sandwich-type tetrapyrrole family.^{150, 151}

1.8 Rare-earth elements (double- and triple-decker arrays) applications

Rare-earth double- and triple-decker complexes, synthesised with porphyrin or phthalocyanine macrocycles, have significant potential applications in material science.^{152, 153}

In general, these novel complexes exhibit distinct properties which do not occur in corresponding non-sandwich complexes. These features are a result of the intrinsic natures of their metal centres and their unique intramolecular π - π interactions that gives the complexes the potential to be used in a variety of areas.^{151, 152} The following are a few of the specific goals and benefits of synthesising a system of this type:

1. Improved Spin Information: By inserting lanthanide metals into a multi-decker structure with porphyrins and phthalocyanine, the effective length of spintronic interactions and electron delocalization can be increased. This may lead to wider absorption spectra and better light-harvesting capacities, both of which are desirable for photovoltaic and photodetection applications.¹⁵⁴

Recent example, both Scanning Tunnelling Microscopy (STM) and Scanning Tunnelling Spectroscopy (STS) can be used to detect and analyse individual magnetic atoms on a surface, as well as directly monitor the density of states (DOS).¹⁰⁹ Consequently, there has been a growing interest in utilising rare-earth sandwich tetrapyrrole complexes as a method for detecting individual spins.¹⁰⁹ These complexes are attractive for the development of various (STM) and (STS) techniques, (Fig. 1.30).

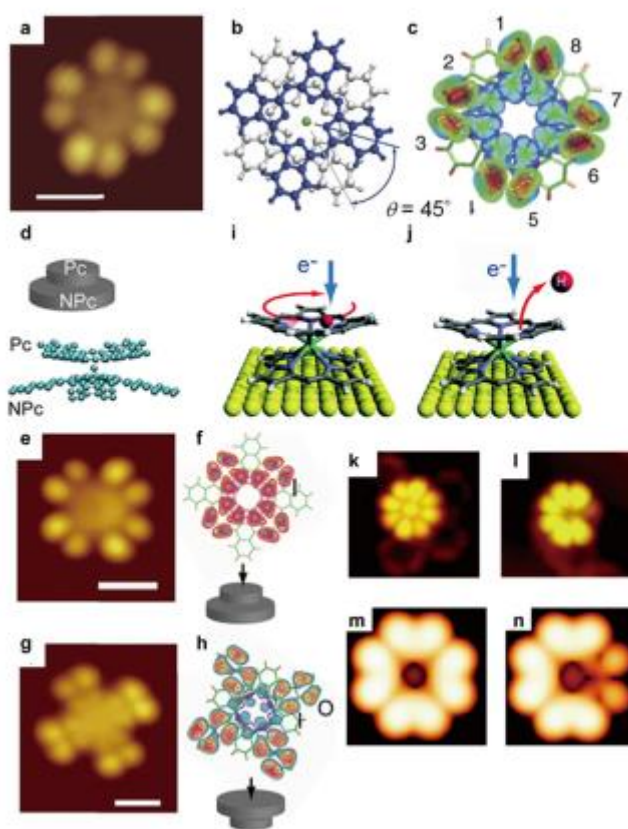


Figure 1.30. An example of (STM) image using rare-earth metal complexes.¹⁰⁹ Reproduced with permission from (109).

Another example, Magnetic Resonance Imaging (MRI) is a diagnostic technique used in medicine to generate detailed images of the anatomical and physiological aspects of the body, (Fig. 1.31). MRI scanners utilise powerful magnets, magnetic gradients, and radio waves to provide highly detailed images of internal organs.¹⁵⁵ It utilises nuclear magnetic resonance (NMR), which is also employed in NMR spectroscopy.¹⁵⁵ The development of Single-Molecule Magnets (Ln-SMMs) complexes has the potential to enhance MRI procedures.

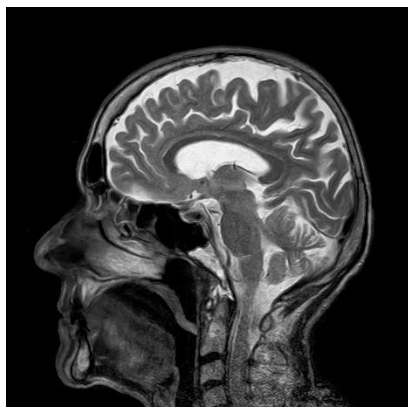


Figure 1.31. Providing an example of the application of MRI imaging technique through the utilisation of Ln-SMMs design of multi-decker complexes.¹⁵⁵

Reproduced from ([Free Stock Illustration Image - Pixabay](#)), no permission is required.

2. Supramolecular Organisation: The multi-decker system functions as a basis for coordinated assembly and accurate self-arrangement. This system improves the capabilities and operations, which are crucial for applications in molecular electronics and optoelectronic devices.^{128, 156}

In the 1990s, Simon and his colleagues initially observed the dual semiconducting capabilities of rare earth complexes. Then, density functional theory (DFT) calculations were used to look into how these complexes handle ambipolar charge transfer.¹⁰⁹ These calculations showed that there is a dispersed radical. By integrating suitable electron transport, triple-decker compounds were effectively modified to operate as air-stable ambipolar semiconductors at standard conditions, (Fig. 1.32).¹⁰⁹

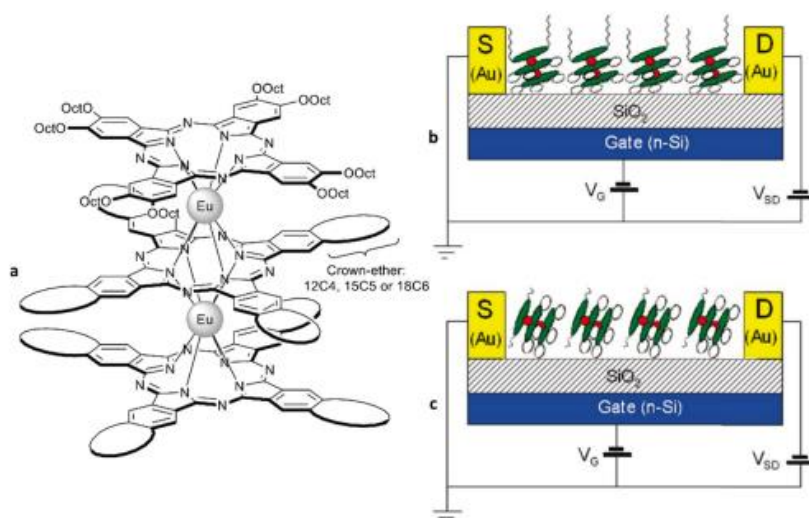


Figure 1.32. An ambipolar OFET device was assembled using a triple-decker complex.¹⁰⁹ Reproduced with permission from (109).

3. Novel Optical and Electronic capabilities: When porphyrins and phthalocyanines are combined in a multi-decker structure via lanthanide metals, new optical and electronic capabilities may arise that are not present in the individual chromophores. New absorption bands, changing energy levels, and changed excited-state dynamics can all result from the interactions between the two chromophores. Numerous applications, including as sensors, light-emitting components, nonlinear optics and quantum computers can be investigated using these features.^{156, 157}

Quantum technology is utilising rare-earth sandwich tetrapyrrole, specifically Ln-SMMs, which are recognised for their exceptional stability in terms of both chemical and physical properties, particularly in relation to magnetic fields. This characteristic allows for their utilisation in quantum devices.¹⁰⁹ The successful development of spintronic devices is highly dependent on the precise manipulation of the interaction between spin and vibrations, (Fig. 1.33).¹⁰⁹

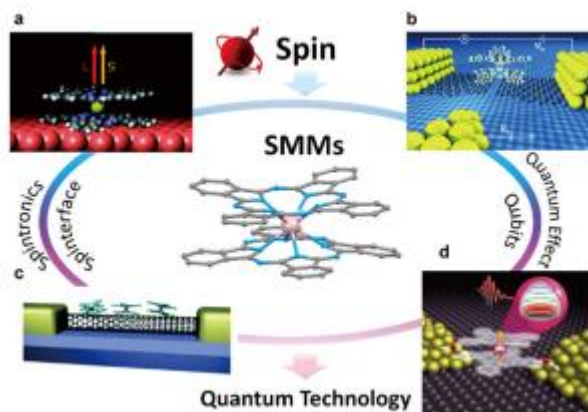


Figure 1.33. Applying tetrapyrrole complex for developing quantum technology.¹⁰⁹
 Reproduced with permission from (109).

4. Perovskite-based Solar Cells(PSCs): Perovskite solar cells have attracted considerable interest in recent years because of their high-power conversion efficiency, ease of manufacturing, and potential for low cost.¹⁵⁸ The often-employed Perovskite substance is a hybrid compound consisting of both organic and inorganic components, specifically lead halide. Multi-decker structures refer to the arrangement of layers made from various materials in order to maximise the movement of electric charge and improve the overall efficiency of solar cells. A potential approach for PSCs is to create a multi-layered structure consisting of perovskite, porphyrin, and phthalocyanine, their power capacity for conversion has grown significantly from 3.9% to over 20%.¹⁵⁸ This design aims to take advantage of the unique features of each material, as they were mainly employed as the charge selecting layers in these types of cells,^{17, 158, 159} (Fig. 1.34).

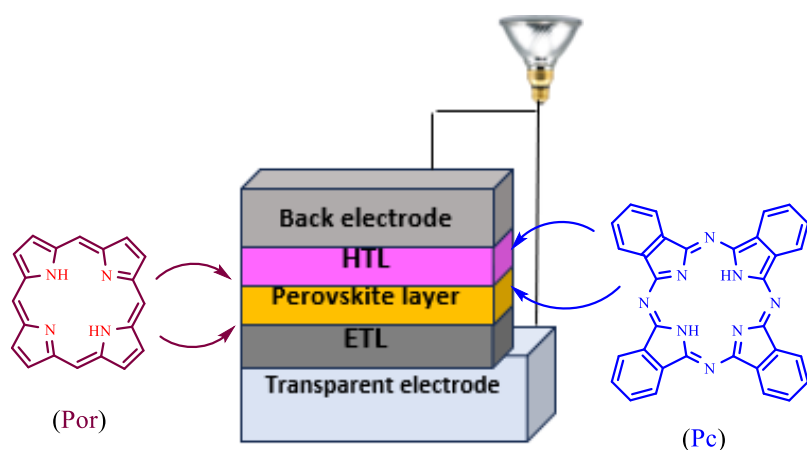


Figure 1.34. An example of using porphyrin and phthalocyanine in layering Solar Cells.¹⁵⁸

In conclusion, multidecker systems based on lanthanide-bridged porphyrins and phthalocyanines offer a versatile platform with enhanced electrical and optical capabilities, suitable for a wide range of applications.^{149, 150, 160}

Chapter 2: Project aim

2. Aim of this project

Formation of sandwich complexes (particularly for SMMs) are a recent focus of interest. They have been widely synthesised as double- and triple-decker but still few works have reported making multiple multi-deckers combed in one molecular system. In this project, the aim is the synthesis and assembly of 3×triple-deckers of porphyrins and phthalocyanines to create *tris* triple-decker system, as shown in (Fig. 2.1). Such a structure holds potential to generate enhanced memory storage capacity.

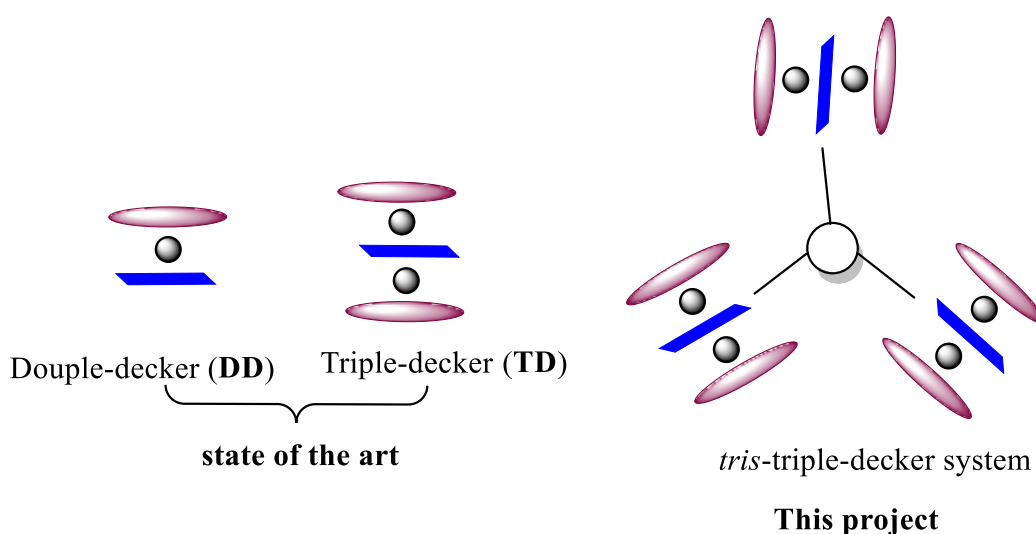


Figure 2.1. Connecting 3×triple-decker for making *tris*-triple-decker system.

The core needs to be easy to synthesise and should present six porphyrin units with different spacing. The chosen core in this project is the triphenylene nucleus **89**, where our lab has much experience in producing triphenylenes due to its use as a liquid crystal core. There are twelve possible substitution sites on triphenylene molecules but the most accessible position for substitution of this compound is 2,3,6,7,10 and 11 positions which allow to create a *hexa*-system. Spacing between attached groups (porphyrins) is controlled by the linking bridge relationship. 2,3-Linking via oxygen gives 4 atoms, while 3,6 gives 8. Previous work has shown stable TD complexes form from C₁₀ O-alkyl bridges, so C₃ chains between core and porphyrin mimic this for the 2,3-arrangement, (Fig. 2.2).

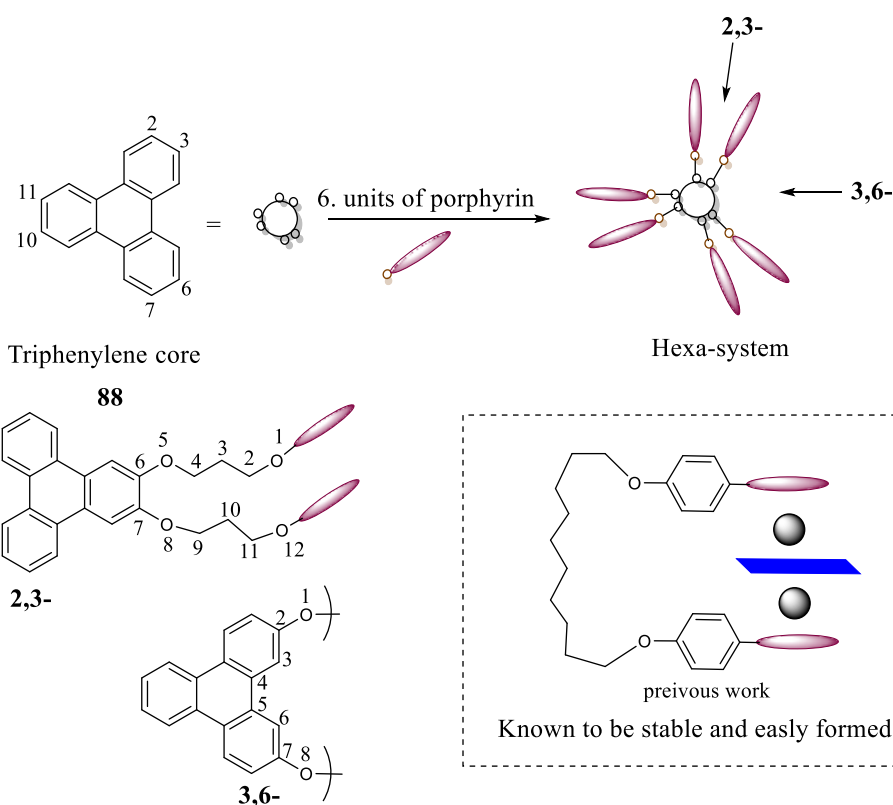
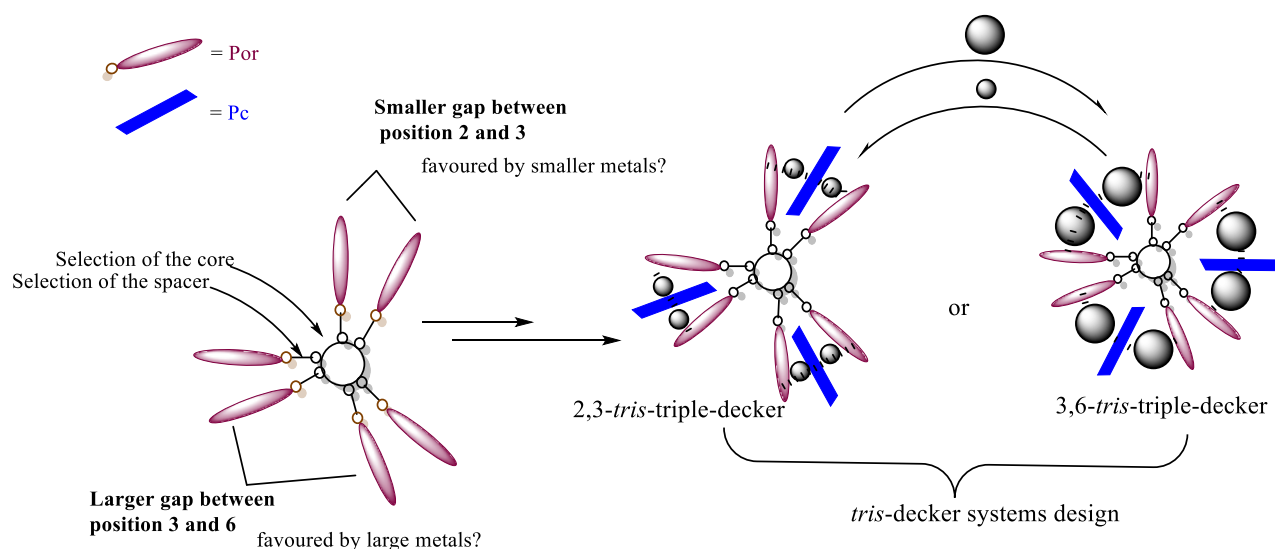


Figure 2.2. The structure of *hexa*-system and the linking in triphenylene.

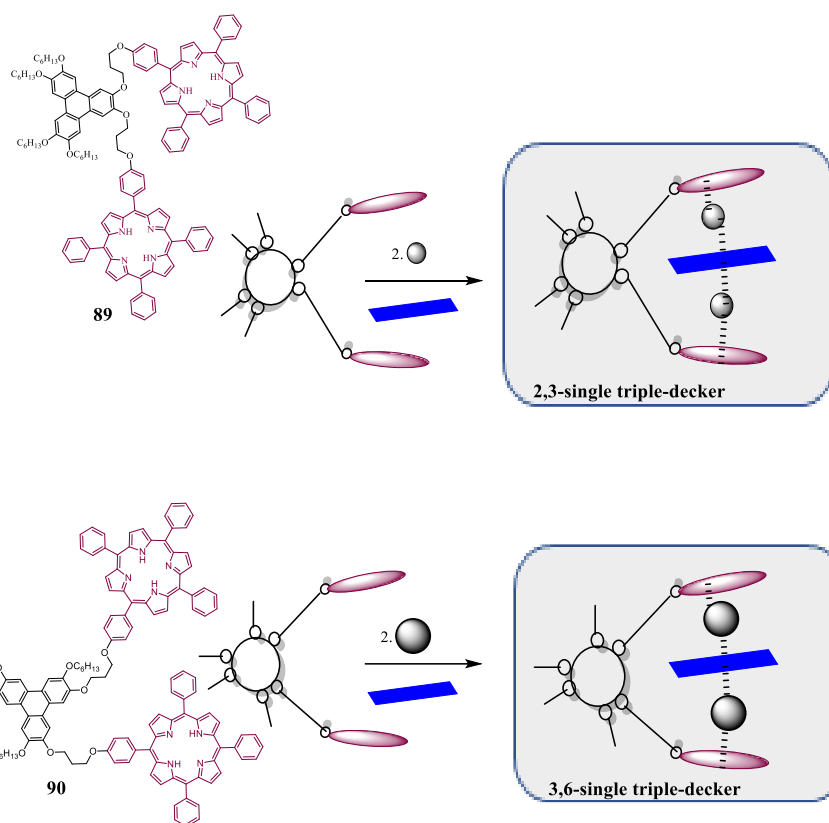
When it comes to the structure of *hexa*-system using triphenylene core, an arrangement of two-porphyrin units in pairs around a rigid core is targeted. As the separation gap between position 3 and 6 is much bigger than the separation between position 2 and 3, the *hexa*-substituted triphenylene is ideally suited to this. Switching between assembly modes may then be possible depending on the size of the metal components and the rigidity of spacer units. Therefore, the aim was to investigate possible equilibration when metal size is varied, as shown in (Scheme 2.1). Full chemical characterisation would be achieved for the highly complex materials, and it was anticipated that preliminary measurement of spectroscopic properties (particularly UV-Vis) would give an indication of their suitability in potential applications.



Scheme 2.1. The design of *tris*-triple-decker system and how assembly can be controlled.

In order to investigate the assembly modes, it is necessary to initially design and investigate model systems.

1. Synthesising triphenylenes with two porphyrins attached at both 2,3 and 3,6 positions (yielding two isomers **89** and **90**) is required. Subsequently, the formation of their TD complexes with various metals needs investigation. The isolated TDs would also give useful spectroscopic characterisation for understanding later *tris*-systems, (Scheme 2.2).



Scheme 2.2. The design of *single* 2,3 and 3,6 triple-decker complexes.

2. The need arises to investigate the selectivity of these *single* triple-decker formations (2,3 versus 3,6 isomeric TDs). Thus, determining the preference between these two isomeric TDs based on metal size is essential. This enables the accurate assessment of any selectivity for these TDs. For an optimal result, the final design of the *tris* triple-decker system can be anticipated, taking into account the metal preference. This involves either favouring the 2,3 *tris* triple-decker system by smaller metals, or the 3,6 *tris* triple-decker system by larger metals.

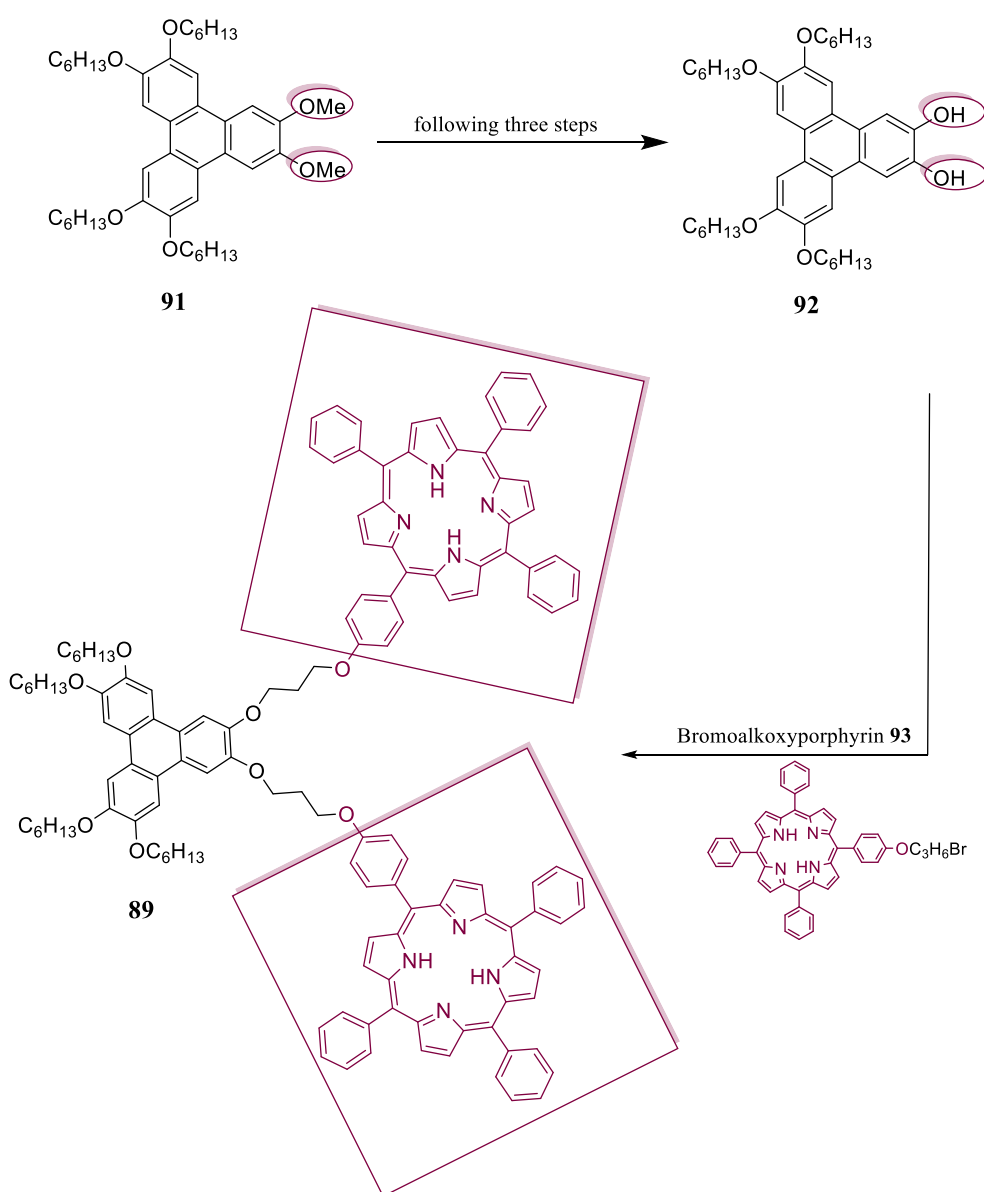
Theoretically, the selectivity based on the length of the chain and the metal ions sizes can control the final formation of *tris* triple-decker system as a single design.

Chapter 3: Results and discussion

3. Results and discussion

3.1 Synthesis of 2,3-triphenylene-linked *bis*(porphyrin) model **89**

It is necessary to synthesise the triphenylene core before making the first model compound. This allows to control where the porphyrins can be attached. In this molecule, the two chromophores of porphyrins were relatively linked in positions 2 and 3 to the triphenylene core by three carbon-diether linkers. The synthetic route can place the linker initially on either the triphenylene core or the porphyrin compound, but the preferred route was found to be the latter (scheme 3.1).



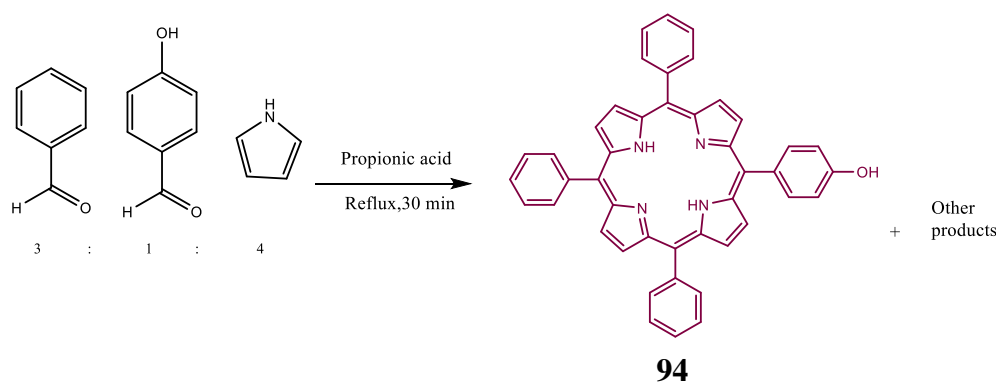
Scheme 3.1. Proposed synthesis of 2,3-linked *bis*(porphyrin)triphenylene **89**.

3.1.1 Preparation of unsymmetrical tetraphenyl-porphyrin ((10,15,20-triphenylporphyrin-5-yl)phenol) TPP-OH 94

The first stage of our work was to synthesise an unsymmetrical porphyrin (unsymmetrical tetraphenyl-porphyrin) TPP-OH, which bears a single link point.

As previously described, *meso*-substituted porphyrins with an A₃B substitution pattern have been synthesised altogether in one step using a variety of reported reaction conditions,¹⁶¹ such as the Alder^{35, 36, 162} and Lindsey procedures^{44, 54, 163}.

In this part, a modification of Adler and Longo's methodology³⁶ was used to generate TPP-OH 94, by reacting pyrrole, benzaldehyde with 4-hydroxybenzaldehyde in 4:3:1 ratio⁴⁴ as shown below in (scheme 3.2).



Scheme 3.2. The synthesis of TPP-OH 94.

Conditions for the reproducible production and isolation of TPPOH 94 were refined and the preferred procedure was as follows. 4-Hydroxybenzaldehyde and benzaldehyde were mixed in refluxing propionic acid. Then, freshly distilled pyrrole was added dropwise to the mixture and reflux continued for an additional 30 minutes open to the atmosphere. After cooling, methanol was added and, the crude was left in a fridge overnight to complete precipitation of the product. The solid was purified by column chromatography using DCM:PET (v:v 1:1). Efficient separation initially proved challenging, with the first fractions showing a mixture of TPP and TPP-OH 94. Good conditions for chromatographic separation (at scale) were eventually identified, allowing TPPOH to be isolated in >5% yield.

¹H NMR spectroscopy verified the TPP-OH compound (Fig. 3.1 B). The spectrum for TPPOH is more complicated than symmetrical TPP (Fig. 3.1 A). The OH group at the *para*

position gives a broad signal (~5.2 ppm) but the most characteristic signal for TPPOH is the doublet at ~7.2 ppm that corresponds to the protons *ortho* to OH. Protons that are found in the macrocycle's plane but at the periphery of the porphyrin are deshielded. [94] The ring current effect causes the shielded imino protons of the macrocycle to resonate at approximately -2.77 ppm.

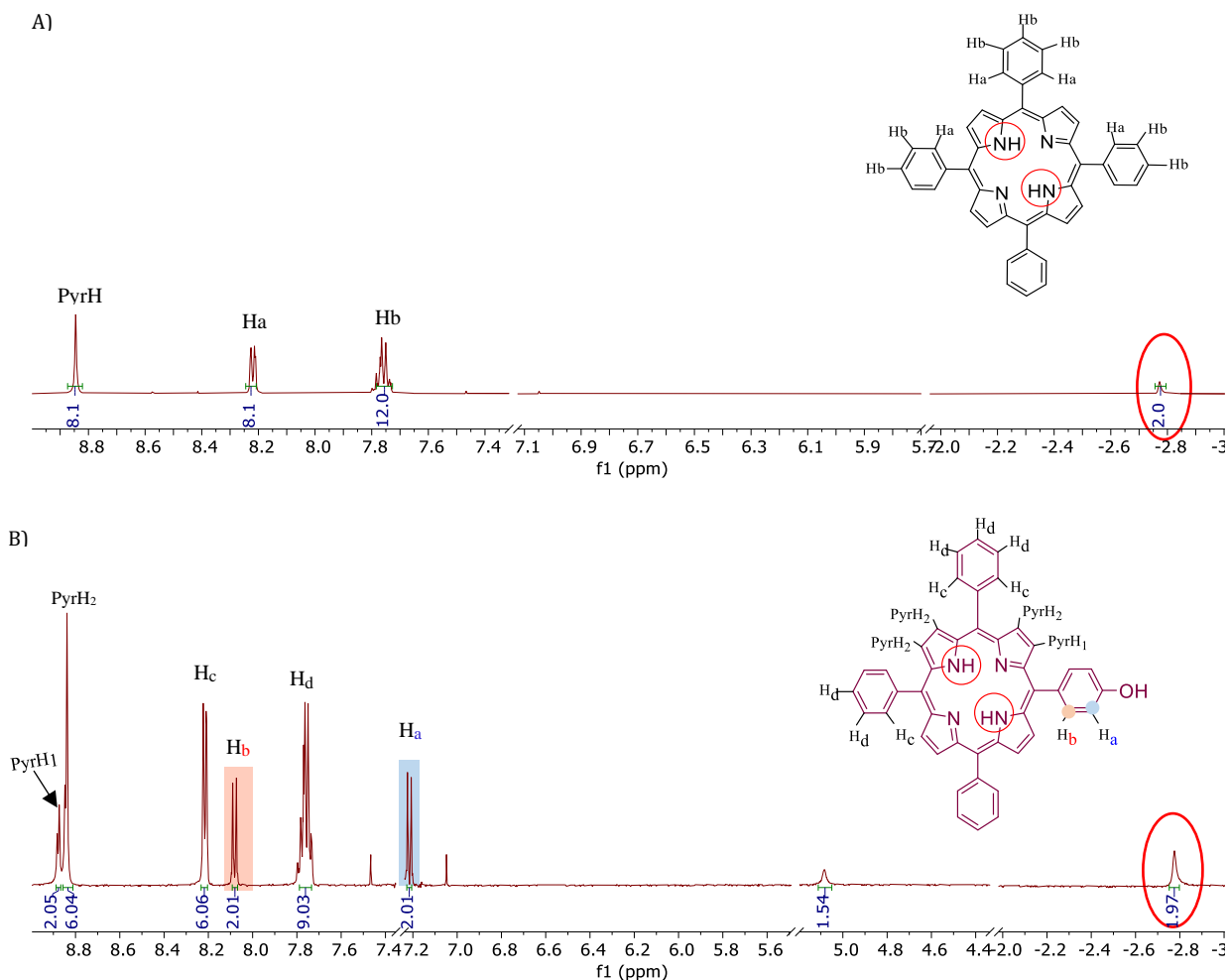


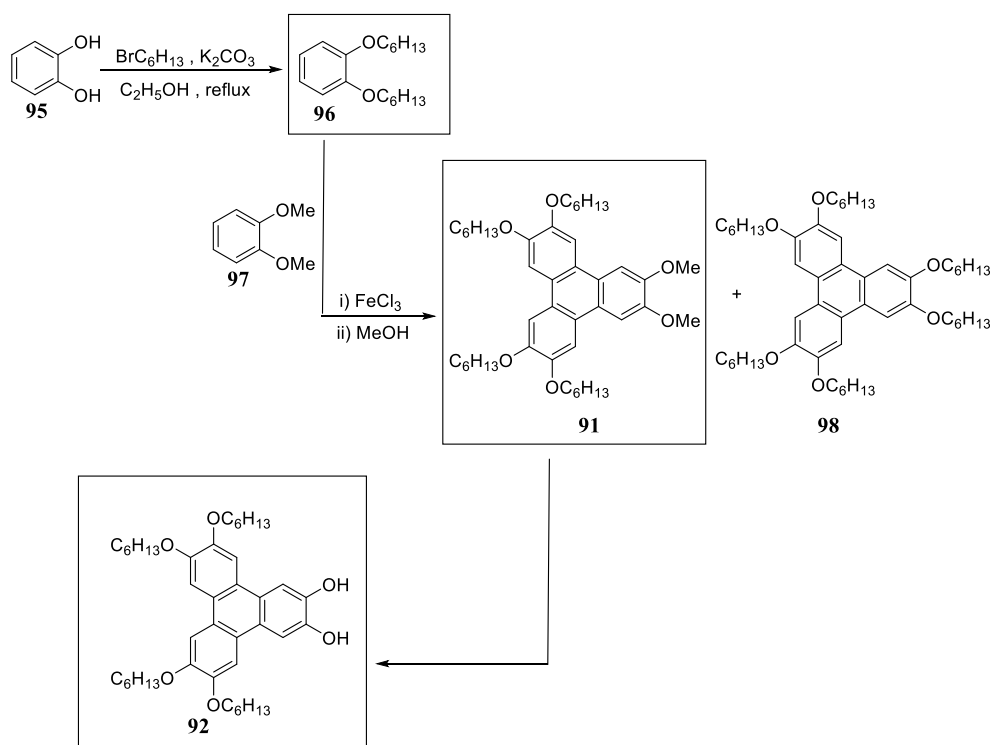
Figure 3.1. The ^1H NMR spectra of symmetrical porphyrin TPP (A) and unsymmetrical tetraphenyl-porphyrin TPP-OH 94 (B), (500 MHz, CDCl_3).

3.1.2 The triphenylene core

Triphenylene has been extensively researched in the literature for more than a century.^{164, 165} Many triphenylene derivatives form liquid crystalline mesophases, and they have been widely investigated.¹⁶⁶ They can exhibit energy migration and one-dimensional charge.¹⁶⁷ The compounds of triphenylene are thermally and chemically stable. There are a range of synthetic methods that have been developed to yield the triphenylene with numerous substituents.^{165, 168}

3.1.2.1 Preparation of the triphenylene core (2,3-bis(hydroxy)triphenylene **92**)

Several steps were completed in the synthesis processes to get triphenylenes, which served as the project's primary core. Scheme 3.3 below illustrates the procedure used to create 2,3-bis(hydroxy)triphenylene **92**, (scheme 3.3).



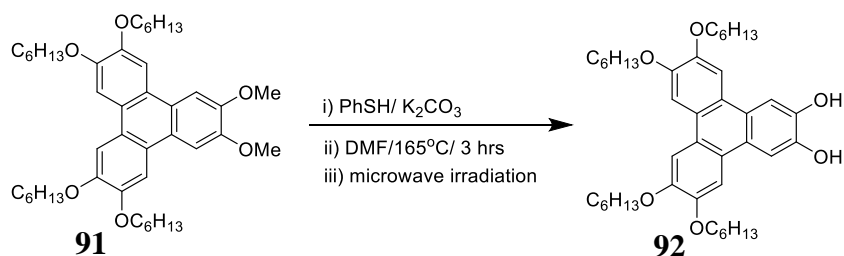
Scheme 3.3. Stepwise synthesis of triphenylene core **92**.

Alkylation of catechol **95** was achieved by using excess of 1-bromohexane in refluxing ethanol, adding potassium carbonate as a base. The crude product was purified by careful distillation¹⁶⁹ giving 1,2-dihexyloxybenzene **96** in 66% yield.

The synthesis of the required unsymmetrical triphenylene intermediate **91** was achieved by using a mixture of DHB **96** and dimethoxybenzene **97**. Following a reported

method¹⁷⁰⁻¹⁷² a mixture of 1,2-dihexyloxybenzene **96** and **97** was added to a stirred suspension of iron(III) chloride in DCM. After 2-4 hrs of stirring, the reaction was complete. TLC showed a top spot ($R_f = 0.60$ cm) for the symmetrical product as side product of the cyclization (HAT₆ **98**) and a new low spot ($R_f = 0.15$ cm) for the desired triphenylene **91**, using (DCM:PET v:v 2:1). The reaction, it was quenched with MeOH to precipitate the triphenylene directly. The solid purified by column chromatography using DCM:PET (v:v 2:1). , then recrystallized from DCM:MeOH to give the product **91** with a 21% yield.

Finally, selective demethylation of 2,3-dimethoxytriphenylene **91** was achieved employing thiophenol.¹⁷³ This is illustrated in Scheme 3.4 below.



Scheme 3.4. The reaction conditions for forming 2,3-*bis*(hydroxy)triphenylene **92**.

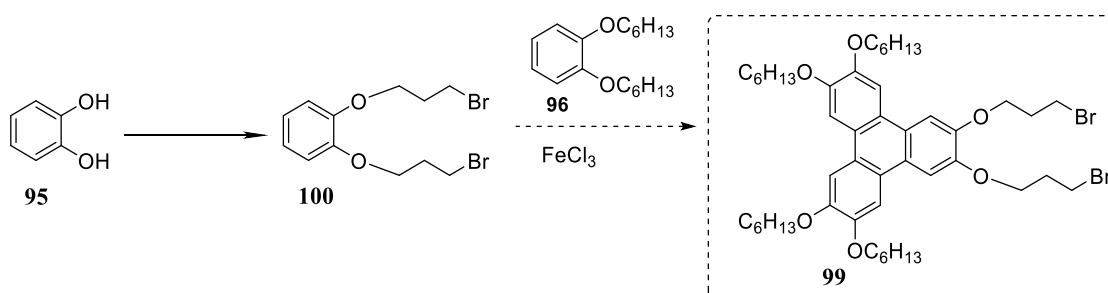
2,3-dimethoxytriphenylene **91** was reacted with PhSH in the presence of K₂CO₃ as the base in dry DMF at reflux. After workup the crude product was recrystallized slowly from DCM: MeOH to generate 2,3-dihydroxytriphenylene **92**. However, this product was quickly decomposed in air and needs to be handled carefully in a controlled atmosphere when possible. In the reaction optimisation good conditions (microwave) were identified to achieve demethylation in 74% yield (Table 3.1).

Entry (No of attempt)	SM (58) Quantity g	Agent Thiophenol eq	Base K ₂ CO ₃ eq	Solvent Dry DMF	Temp (°C)	Time	Reaction Condition	Results
1	1 g	3 eq	4.5 eq	DMF	80°C	2 hrs	Normal refluxing	no product (decomposed)
2	1 g	3 eq	4.5 eq	DMF	150°C	5 hrs	Sealed tube Under Argon	SM + product (Decomposed during the reaction)
3	1 g	3 eq	4.5 eq	DMF	165°C	6 hrs	Microwave tube In oil Bath	Product (35%)
4	1 g	Excess (5 eq)	Excess (6.5 eq)	DMF	165°C	3 hrs	Microwave tube In the microwave irradiation	Pure product (74%)

Table 3.1. Some attempted conditions for optimising the yield of required product **92**.

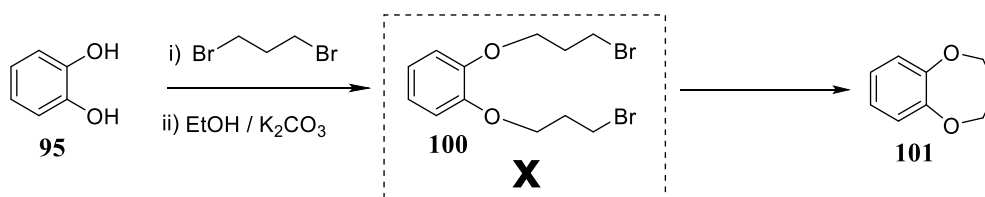
3.1.2.2 Synthesis of 2,3-bis(3-bromopropoxy) triphenylene **99** (linker-1st attempt)

The linker was first placed on the catechol molecule **95** to generate compound **100** using the basic S_N2 substitution reaction.¹⁷⁴ Then compound **100** could react with 1,2-dihexyloxybenzene **96** to yield 2,3-bis(3-bromopropoxy)triphenylene **99** using FeCl₃ as previously described (Scheme 3.5).



Scheme 3.5. General synthesis plan for 2,3-bis(3-bromopropoxy)triphenylene **99**.

Initially, the linker (C₃) chain was connected with compound **95** for forming 1,2-bis(3-bromopropoxy) benzene **100** as shown in scheme 3.6.



Scheme 3.6. Forming side product **101** by reacting with dibromopropane.

Catechol **95** was reacted with an excess of 1,3-dibromopropane and K_2CO_3 in refluxing ethanol. After workup the crude product was purified by distillation. Unfortunately, compound **100** was not isolated, but instead the main product of this reaction was from cyclization (compound **101**).

The 1H NMR-spectrum of **101** presented two aliphatic signals as a consequence of the chain cyclization. Fig. 3.2 below, shows one triplet of H_a around 4.29 ppm assigned to the 4H of $-OCH_2$ group and the multiplet of H_b at 2.32-2.24 ppm refers to the 2H of the $-CH_2$ group. Indeed, NMR analysis of **101** compound has previously been reported in other literature publications.¹⁷⁵

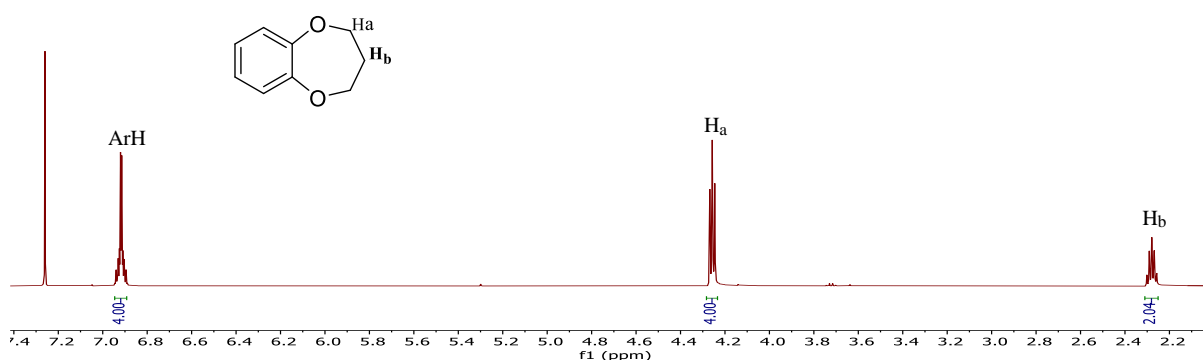
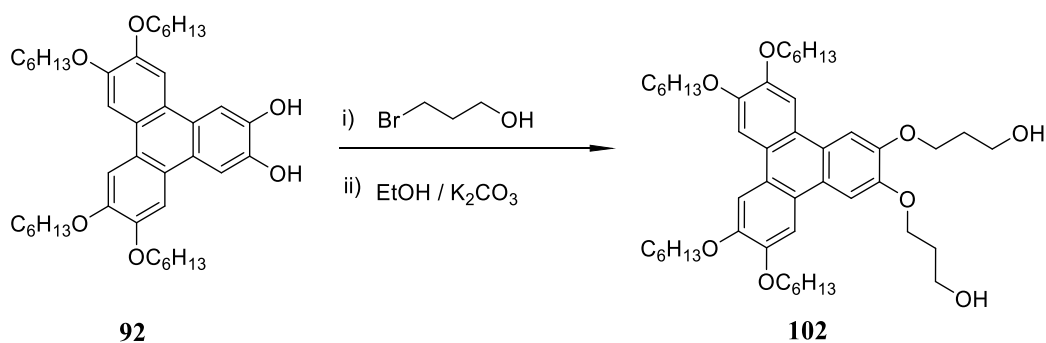


Figure 3.2. The 1H NMR-spectrum for unwanted cyclized product **101**.

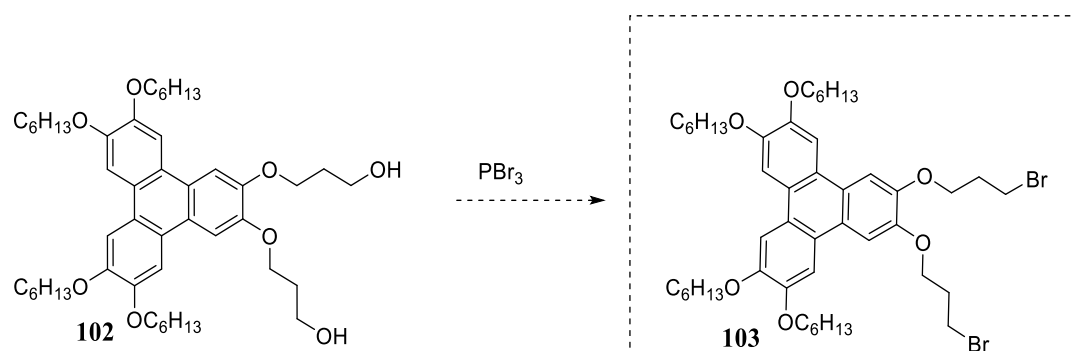
Competing cyclisation¹⁷⁶ could not be avoided for catechol, and reasoned the same problem would be encountered if 2,3-dihydroxytriphenylene **92** was used, so an alternative strategy was developed to attach the three-carbon linker to the triphenylene core **92**. 1-Bromo-3-propanol was employed instead of 1,3-dibromopropane in the reaction with 2,3-dihydroxytriphenylene **92**, as shown in Scheme 3.7 below



Scheme 3.7. Converting compound **92** into compound **102**.

Compound **102** can be obtained by reacting dihydroxytriphenylene **92** with 1-bromo-3-propanol and K_2CO_3 in refluxing in ethanol. The crude product was purified by column chromatography to produce 2,3-bis(hydroxypropanyloxy)triphenylene **102** but in relatively low yield. The conditions were optimized for this reaction by adding an excess of linker. However, it did not show any improvement. This could be due to the fact that many studies have demonstrated that 1-bromo-3-propanol chains have the ability to generate polymeric structures.¹⁷⁷

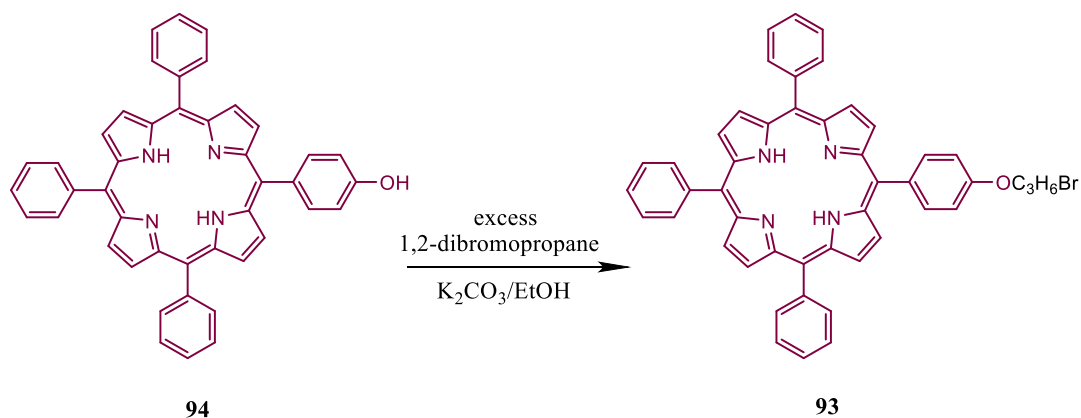
This intermediate could be converted to the required bromide required **103**¹⁷⁸ as shown in scheme 3.8, but this was not attempted because an alternative strategy proved more convenient.



Scheme 3.8. Converting **102** to the required compound **103**.^{178, 179}

3.1.2.3 Synthesis of bromoalkoxyporphyrin **93** (linker-2nd attempt)

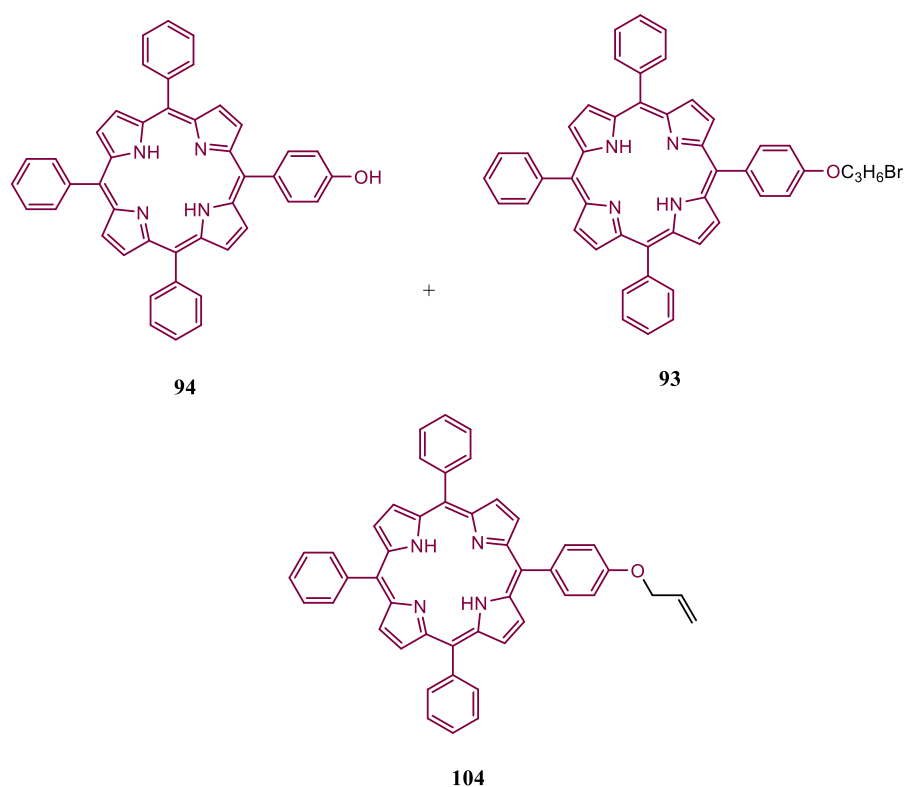
the linker was placed on porphyrin **94** to generate compound **93** using 1,2-dibromopropane, (Scheme 3.9). This strategy avoids any cyclisation problems.



Scheme 3.9. The formation of bromoalkoxyporphyrin **93**.

Consequently, 1,2-dibromopropane was reacted with TPPOH **94** in EtOH employing K_2CO_3 . The crude product was crystallized using DCM and MeOH, yielding a very good 98% yield.

Although the process of forming compound **93** seems straightforward, managing the mixture of by-products turned out to be somewhat challenging. As shown in scheme 3.10 below.



Scheme 3.10. The possible side products that can be presented in a mixture in synthesising the desired compound **93**.

As a result, this reaction can be influenced by the amount of the base, the nature of the solvent, the temperature, and the reaction conditions as well (Table 3.2).

Entry	SM (61) Eq/g	SM (linker) Eq/g	Solvent	Base K ₂ CO ₃ Eq/g	Reaction Condition	Reaction Time	Target product yield
1	1 eq/0.5 g	5 eq/0.8 g	acetone 10-15 ml	3 eq/0.33 g	Sealed tube 70°C	1-2 days	Mixed-
2	1 eq/0.5 g	10 eq/1.5 g	DMF	5 eq/0.54 g	Sealed tube 120°C	2-3 days	--
3	1 eq/0.5 g	adding excess 2.4 - 3.1 g	EtOH	Adding excess 0.6 - 0.8 g	Sealed tube 80°C	2-3 days	75%
4	1 eq/0.5 g	25 eq/4 g	EtOH 20 ml	10 eq/1.09 g	Normal refluxing 80°C	24 hrs	98%

Table 3.2. Optimisation of bromoalkoxy porphyrin synthesis with different reaction conditions.

The ¹H NMR-spectrum of **94** shows a doublet peak of H_a (Fig. 3.3 A) for the two protons around 7.15 ppm, while in **93** we see a shift from 7.15 to 7.30 ppm (Fig. 3.3 B).

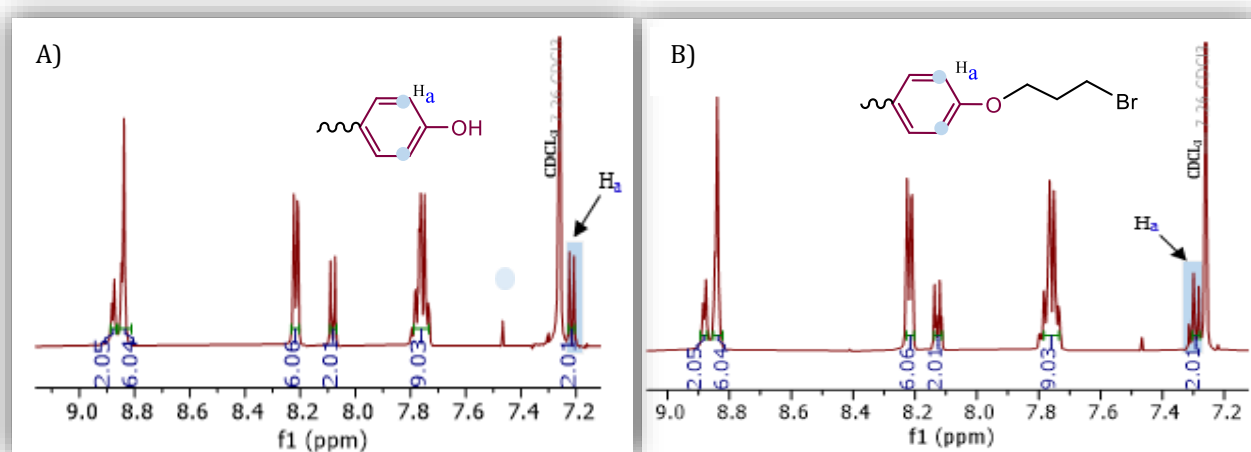


Figure 3.3. Comparison of ¹H NMR spectra for TPP-OH **94** A) and compound **93** B), (500 MHz, CDCl₃), inset: expansion of the 9.0-7.0 ppm area.

In addition, the ¹H NMR-spectra analysis of **93** exhibited well-defined of all aliphatic signals; one quintet of H_d (2.53 ppm) for the protons of -CH₂ in the middle, two triplet of H_b (4.41 ppm) and H_c (3.79 ppm) for the -OCH₂ group and -CH₂Br, respectively (Fig. 3.4).

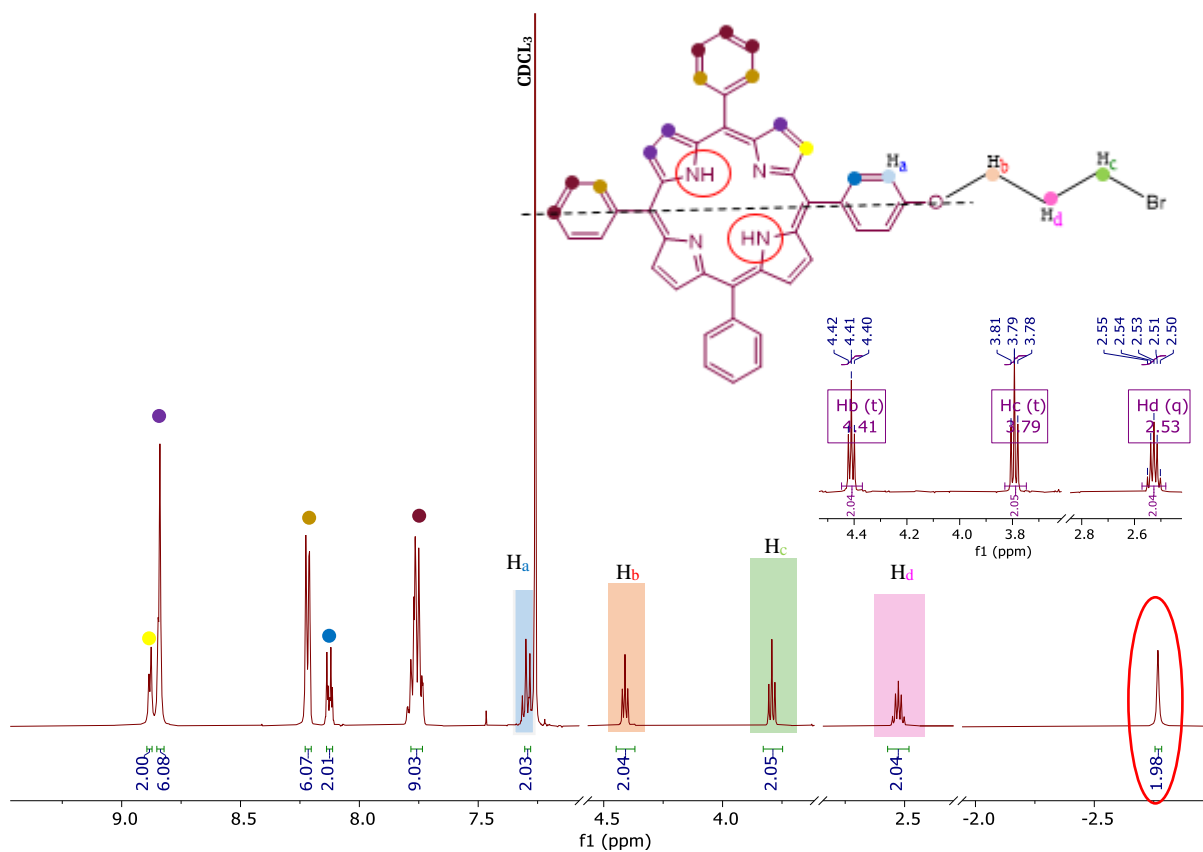


Figure 3.4. ¹H NMR spectrum of forming bromoalkoxy porphyrin **93** compound, (500 MHz, CDCl₃).

The MALDI-TOF-MS also confirmed the peak relating to the molecular ion of m/z 752.00, calc. : 752.19 (Fig. 3.5).

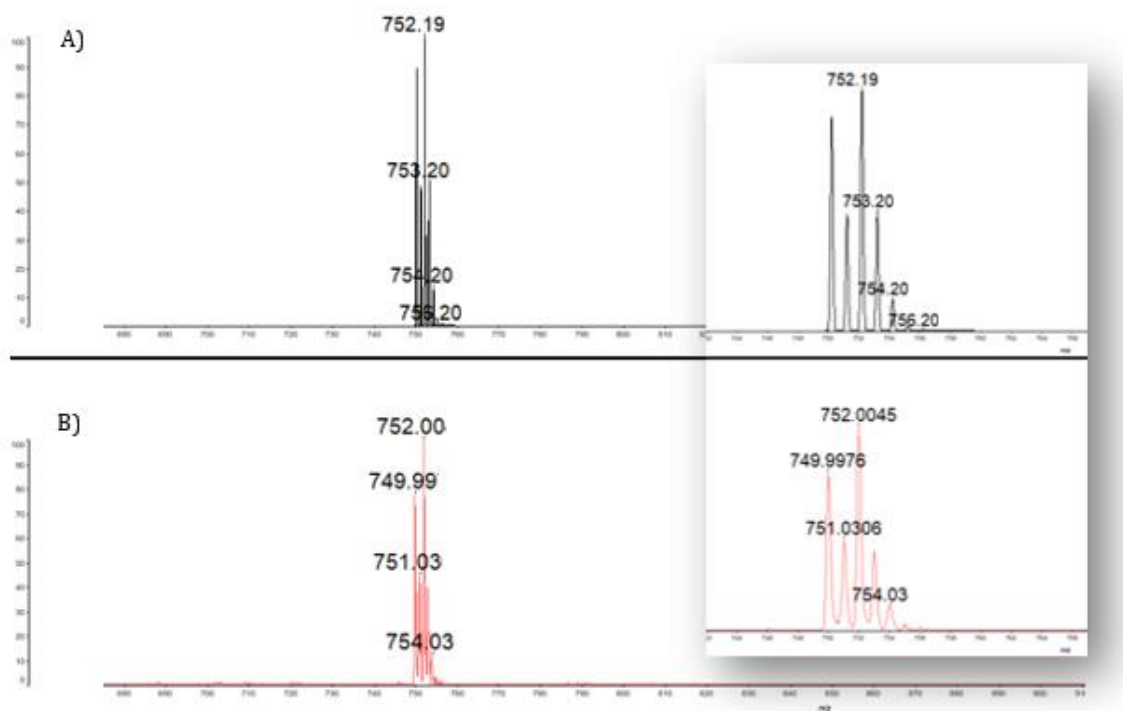


Figure 3.5. The MALDI-TOF-MS for bromoalkyloxyporphyrin **93**. The inset shows (B) obtained and (A) theoretical isotopic patterns.

This compound is also detectable in UV spectroscopy, and the characteristic peaks for porphyrin have been obtained, the first peak corresponds to a Soret band at 419 nm, indicating a transition to a higher energy level (from $\pi \rightarrow \pi^*$ transitions within the porphyrin ring). Additionally, four peaks have been observed in the Q-band at 518, 553, 593, and 653 nm (Fig. 3.6), indicating a lower energy level (from $n \rightarrow \pi^*$ transitions). Compound **93**, identified as metal-free porphyrin, exhibits four Q-bands due to the reduced symmetry caused by interior hydrogens.

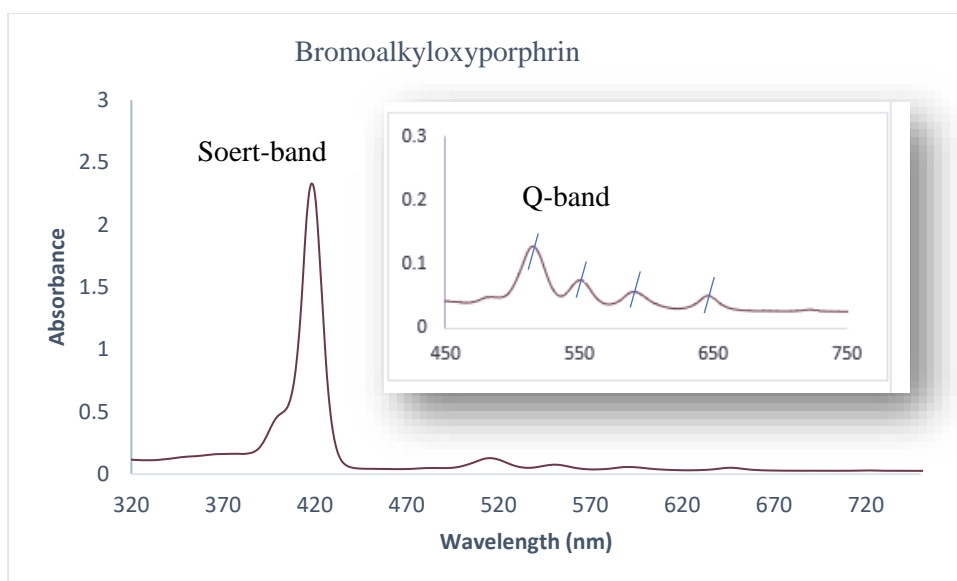
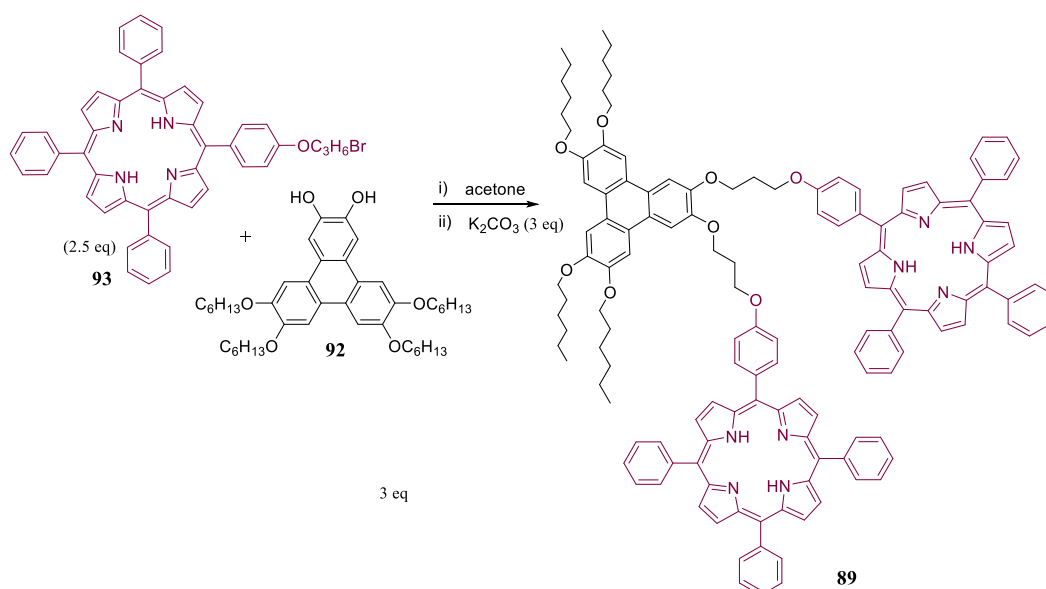


Figure 3.6. The UV-vis spectrum of bromoalkoxy porphyrin **93** compound, inset: expansion of the 450-750 nm area.

3.1.3 Preparation of 2,3-bis(porphyrin)triphenylene model **89**

The last step was to combine 2,3-bis(hydroxy)triphenylene **92** with our chromophore bromoalkoxy porphyrin **93** as illustrated in scheme 3.11.

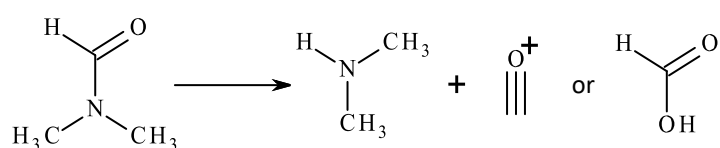


Scheme 3.11. Synthesis of the first model porphyrin triphenylene **89**.

Bromoalkoxy porphyrin **93** (2.5 eq) was reacted with 2,3-bis(hydroxy)triphenylene **92** employing K_2CO_3 in refluxing acetone in a sealed tube at $70^\circ C$ for 7 days. The crude

product was purified by a column chromatography to yield a dark purple fraction that was recrystallized with DCM:MeOH, giving the desired product, 2,3-bis(porphyrin)triphenylene compound **89**, in an acceptable yield of 22%.

After determining that the reactants were not sufficiently soluble in acetone, the reaction was repeated using dry DMF as the solvent instead of acetone. Therefore, 2,3-dihydroxytriphenylene **92** was reacted with bromoalkoxyporphyrin **93** in refluxing DMF using K₂CO₃ and KI at 120 °C. However, when TLC was used to check the reaction, it showed that the process created a large number of by-products, possibly due to DMF decomposing at high temperatures, (Scheme 3.12).¹⁸⁰



Scheme 3.12. Dimethylformamide degradation.

the reaction's temperature was reduced to 80 °C to try to avoid any side product formation. As a result, 2,3-dihydroxytriphenylene **92** was reacted with an excess of bromoalkoxyporphyrin **93** in DMF using K₂CO₃ and KI at 80 °C for 2–3 days. Following the workup, the crude product was purified using column chromatography to isolate the required compound in double this yield (Table 3.3).

<i>NO of attempt:</i>	Condition:	Time of reacting:	Yield%:
1	Sealed tube-acetone	6-7 days	22%
2	Sealed tube-dry DMF-High T(120°C)	-	-
2	Normal heating - dry DMF-Lower T (80 °C)	2-3 days	43%

Table 3.3. Using different solvents to produce product **89**.

The formation of 2,3-bis(porphyrin)triphenylene model **89** was fully analysed by ¹H- and ¹³C{¹H}-NMR, IR, UV-vis, and the MALDI-TOF-MS spectroscopy, as reported in the experimental chapter. In the ¹H NMR-spectrum of **89** (Fig. 3.7), the protons of the triphenylene ring exhibited three singlets between 7.98 and 7.81 ppm. Two triplets for H_a (4.31 ppm) and H_b (4.26 ppm), and two triplets of H_d (4.64 and 4.55 ppm) correspond to the O-CH₂ groups.

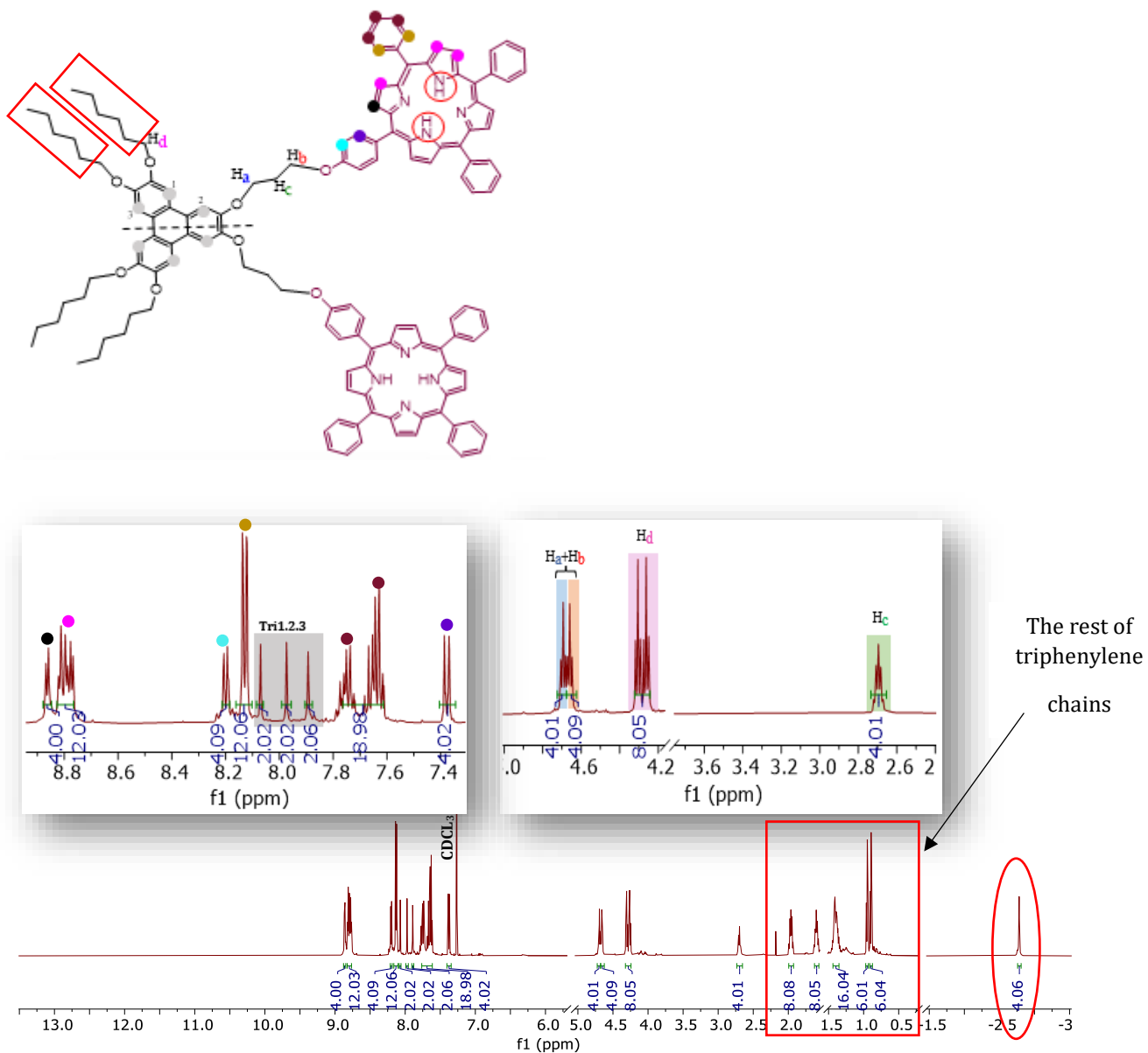


Figure 3.7. The full ¹H NMR spectrum of 2,3-*bis*(porphyrin)triphenylene **89**, (500 MHz, CD₂Cl₂), expansion of the 8.9-7.3 ppm aromatic area and of the 4.8-2.5 ppm aliphatic area.

The MALDI-TOF-MS spectrum of **89** model displays a peak which corresponds to the molecular ion at m/z 2001.88 [M]⁺ (C₁₃₆H₁₂₈N₈O₈⁺), calc.: 2001.98, as shown in (Fig. 3.8).

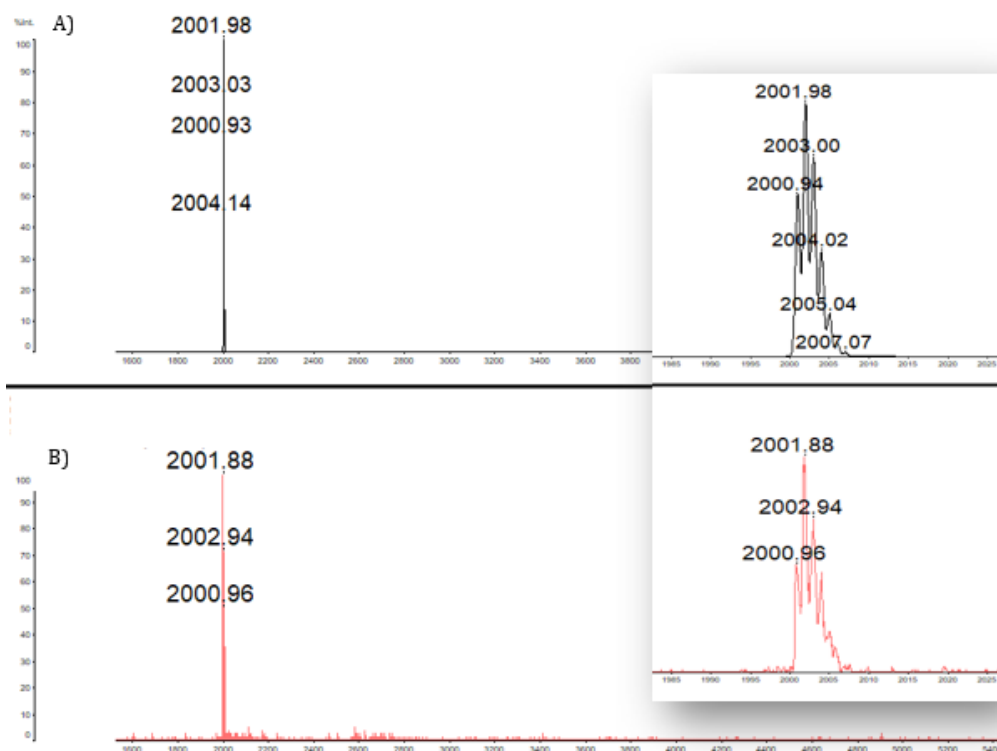


Figure 3.8. MALDI-MS spectrum of 2,3-bis(porphyrin)triphenylene **89**. The inset shows (B) obtained and (A) theoretical isotopic patterns.

UV-vis spectroscopy can be used to analyse the building blocks of this model, which shows the Soret and Q-band of porphyrin. Importantly, the existence of triphenylene may be determined by the single peak (282 nm) found in this region, indicating that the triphenylene core was successfully connected to porphyrin chromophores. (Fig. 3.9).

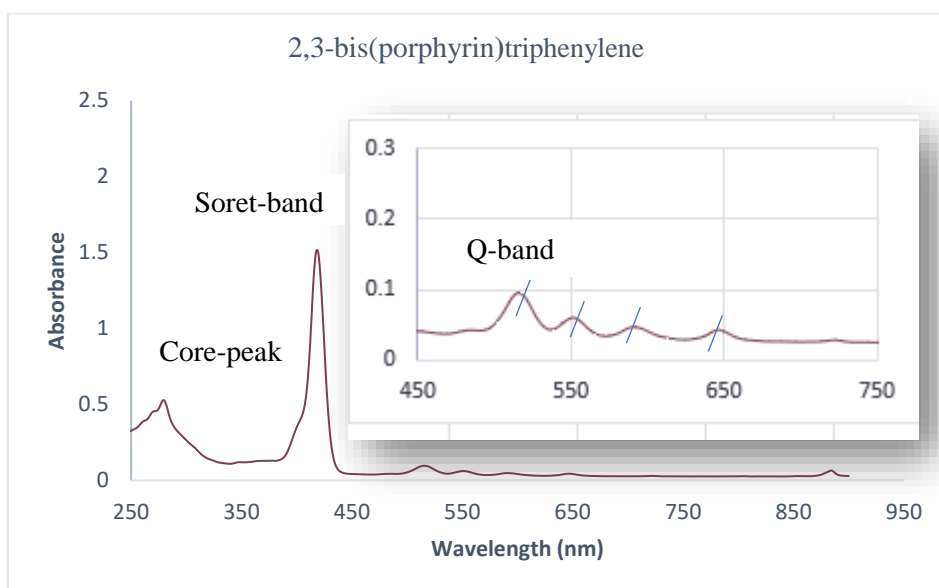
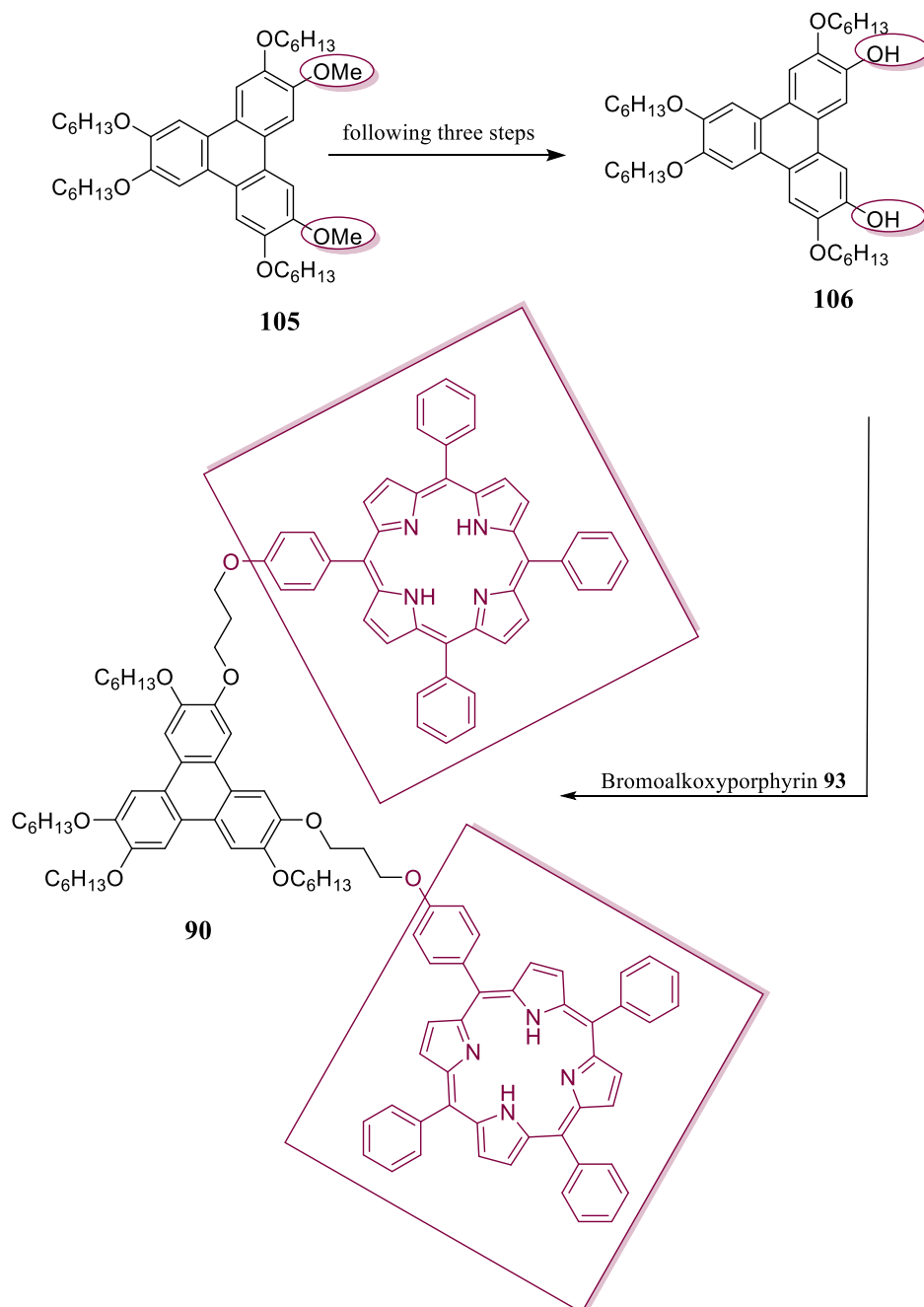


Figure 3.9. The UV-vis spectrum of 2,3-bis(porphyrin)triphenylene **89**, inset: expansion of the 450-750 nm area.

3.2 Synthesis of 3,6-triphenylene linked *bis*(porphyrin) model **90**

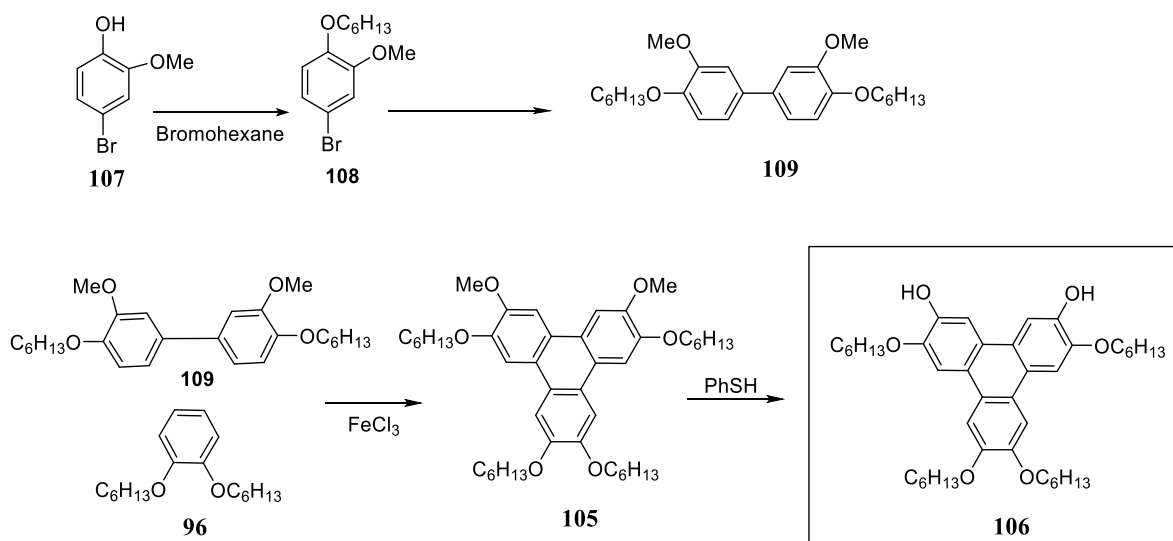
Since the initial target model on positions two and three **89** was successfully built, it has now possible to synthesise the other isomer (3,6) within the triphenylene core, as indicated by scheme 3.13. This isomer places the porphyrins different apart.



Scheme 3.13. Proposed synthesis of 3,6-linked *bis*(porphyrin)triphenylene **90**.

3.2.1 Preparation of triphenylene core (3,6-bis(hydroxy)triphenylene **106**)

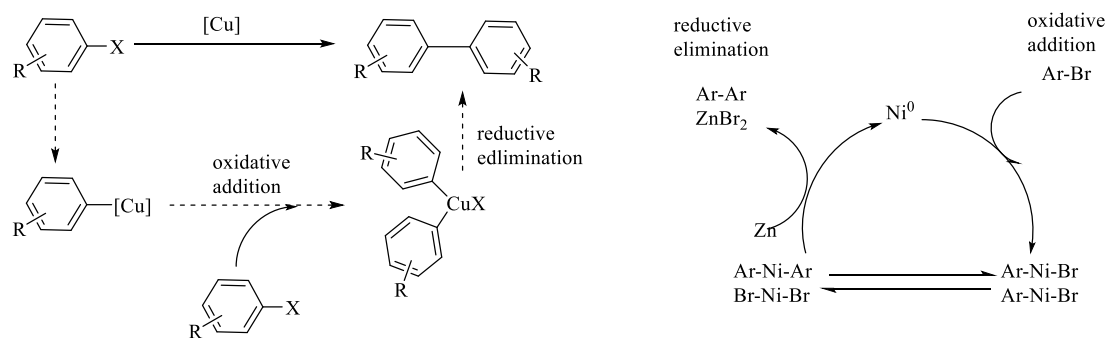
Scheme 3.14 reveals first a method for using a biphenyl **109** to produce triphenylene **105**, as previously reported.¹⁸¹ Then, the deprotection of 3,6-dimehoxytriphenylene **105** was applied. So, this method consists of four stages.



Scheme 3.14. The steps for formation 3,6-bis(hydroxy)triphenylene **106**.

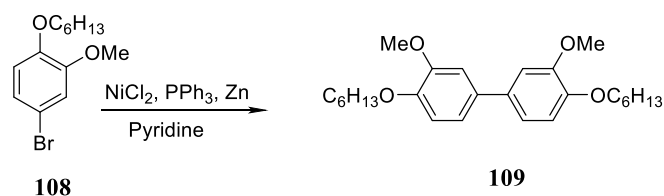
The synthesis started began with the straightforward alkylation of the hydroxy group on the 4-bromo-2-methoxyphenol **107**.¹⁷² This was achieved using excess 1-bromohexane in ethanol with **107** and potassium carbonate. This mixture was refluxed for more than 48 hrs at 80°C. The crude product was then distilled to give 4-bromo-1-hexyloxy-2-methoxybenzene **108** as a clear oil in 95 % yield.

In the second step the classic Ullman coupling for the synthesis of biaryls via copper coupling¹⁸² (Scheme 3.15) was replaced with an adaption by Lin and co-workers utilizing nickel as a catalyst.^{181, 183, 184}



Scheme 3.15. Ullman coupling catalytic cycle with copper and with nickel. ^{181, 183}

Thus, the di(hexyloxy)di(methoxy)biphenyl **109** can be successfully obtained by reacting two molecules of bromide **108** catalysed by nickel as illustrated in scheme 3.16.



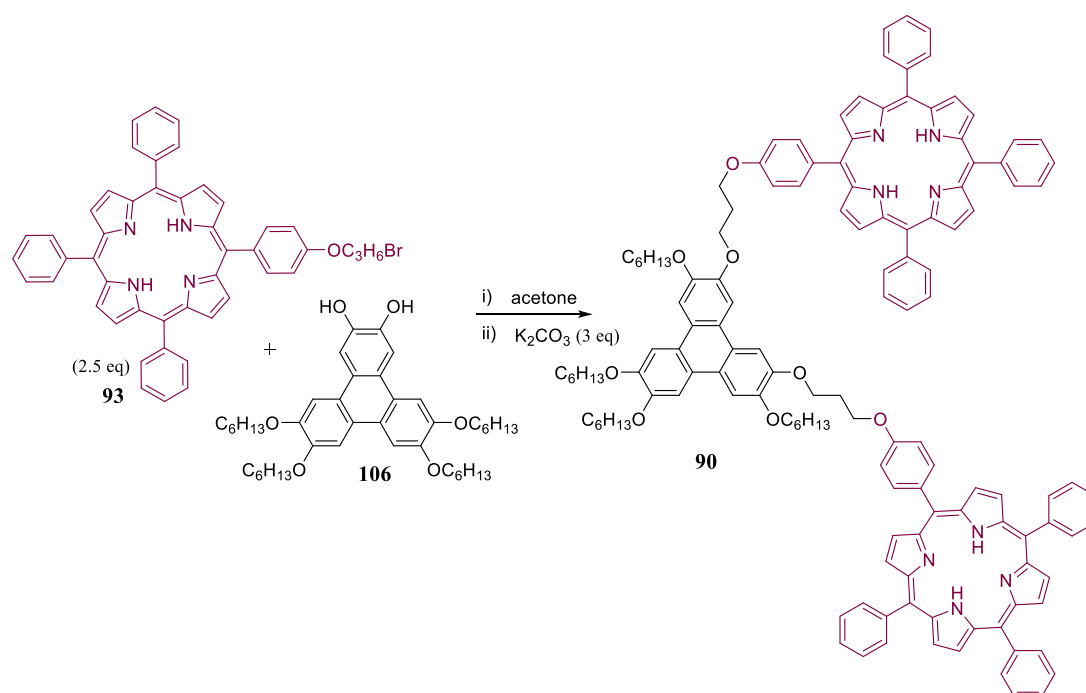
Scheme 3.16. The formation of di(hexyloxy)di(methoxy)biphenyl **109**.

4-Bromo-2-methoxyhexyloxybenzene **108** was reacted in refluxing pyridine in the presence of NiCl_2 , PPh_3 and Zn powder, giving biphenyl **109** in a yield of 44%.

As previously described,^{170, 181, 185} biphenyl **109** was then cyclised with 1,2-bis(hexyloxy)benzene **96** to produce the 3,6-di(methoxy)triphenylene core **105**, again employing iron(III) chloride to cyclise in DCM. Then, the resulting product was purified by column chromatography to isolate the target compound in 49% yield.

Finally, deprotection of 3,6-dimethoxytriphenylene **105** followed the procedure earlier developed, using PhSH in microwave-irradiation with DMF at 120°C for 3 hrs. Then, the crude product was purified by column chromatography to produce the 3,6-di(hydroxy)triphenylene core **106** with yield of 72%.

3.2.2 Synthesis of 3,6-bis(porphyrin)triphenylene model **90**



Scheme 3.17. Synthesizing the second model **90**.

Following the procedure employed for isomer **90**, 3,6-dihydroxytriphenylene **106** and excess of bromoalkoxyporphyrin **93** were combined in DMF and was heating at $80^\circ C$ in the presence of K_2CO_3 and KI. After work up and purification by column chromatography, the target product, 3,6-bis(porphyrin)triphenylene **90**, was generated with a yield of 50% (scheme 3.17).

The 1H NMR signals of 3,6-bis(porphyrin)triphenylene **90** are mostly identical to the signals of the first model **89**, with a few minor variations because of different positions. The 1H NMR-spectra of 3,6-bis(porphyrin)triphenylene **90** demonstrated the significant distinction in the protons that correlated to the triphenylene rings; three singlets of $ArH_{1,2,3}$, shifted to 8.03(H_1), 7.83(H_2) and 7.81 ppm(H_3), (Fig. 3.10).

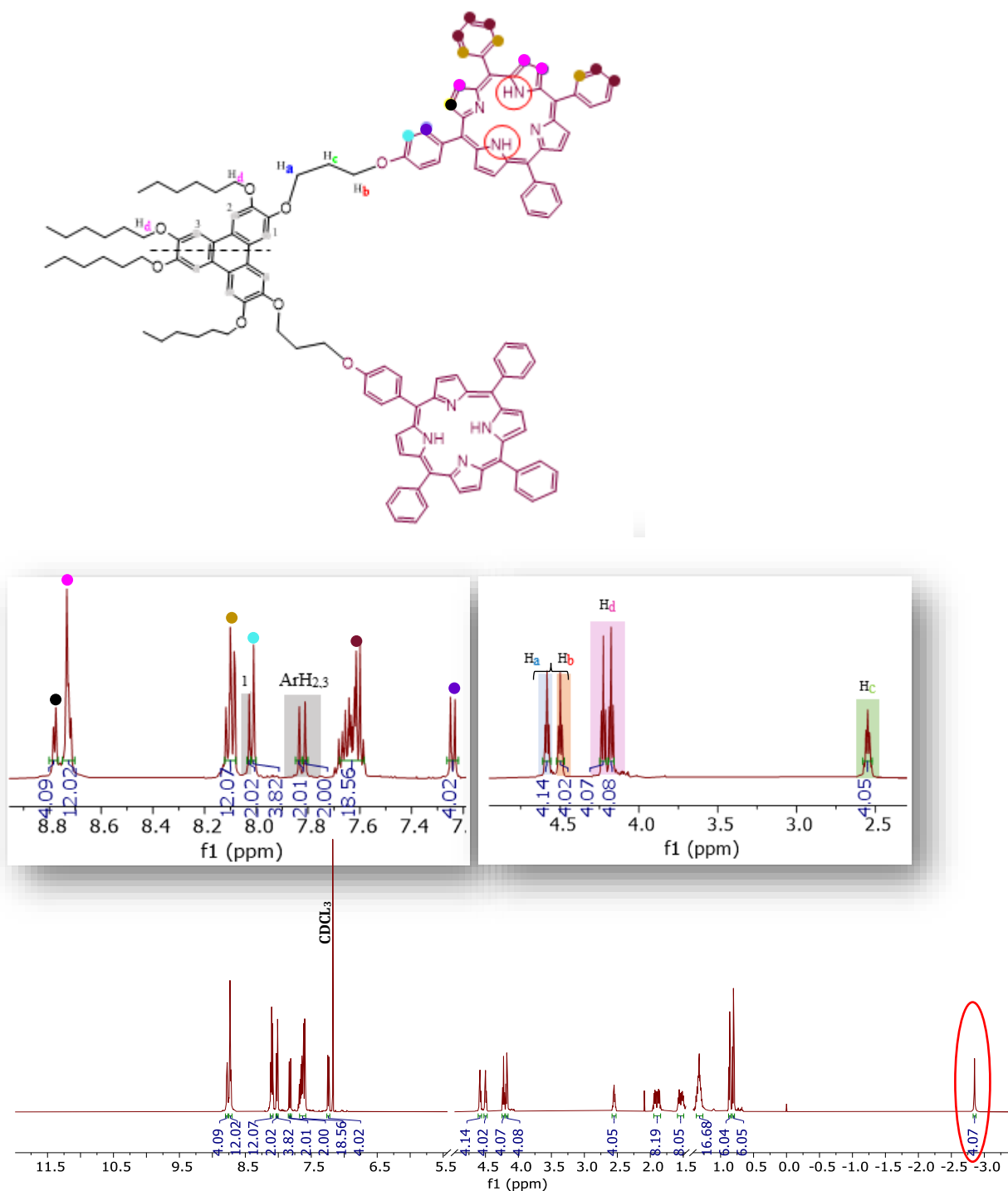


Figure 3.10. The 1H NMR spectrum of synthesizing 3,6-bis(porphyrin)triphenylene **90** compound, (500 MHz, $CDCl_3$), expansion of the 9.0-7.2 ppm aromatic area and of the 4.7-2.49 ppm aliphatic area.

2D Homonuclear Correlation spectroscopy (COSY) was additionally carried out to give more evidence supporting the assigning of the observed signals to the proper aromatic and aliphatic protons (Fig. 3.11). The COSY spectrum of **90** presents that the two doublets of protons (*m*) and (*o*) to porphyrin at 8.01, 7.24 ppm correlates with each other (Figure 3.25, dashed lines). Therefore, both triplet of H_a at 4.58 ppm and H_b at 4.50 ppm correlates with the quintet of H_c at 2.55 ppm, all belonging to the alkyl chain, also the two triplet of H_d at 4.23, 4.18 ppm correlates with the two multiples of H_e at 1.93, 1.87 ppm on the triphenylene core.

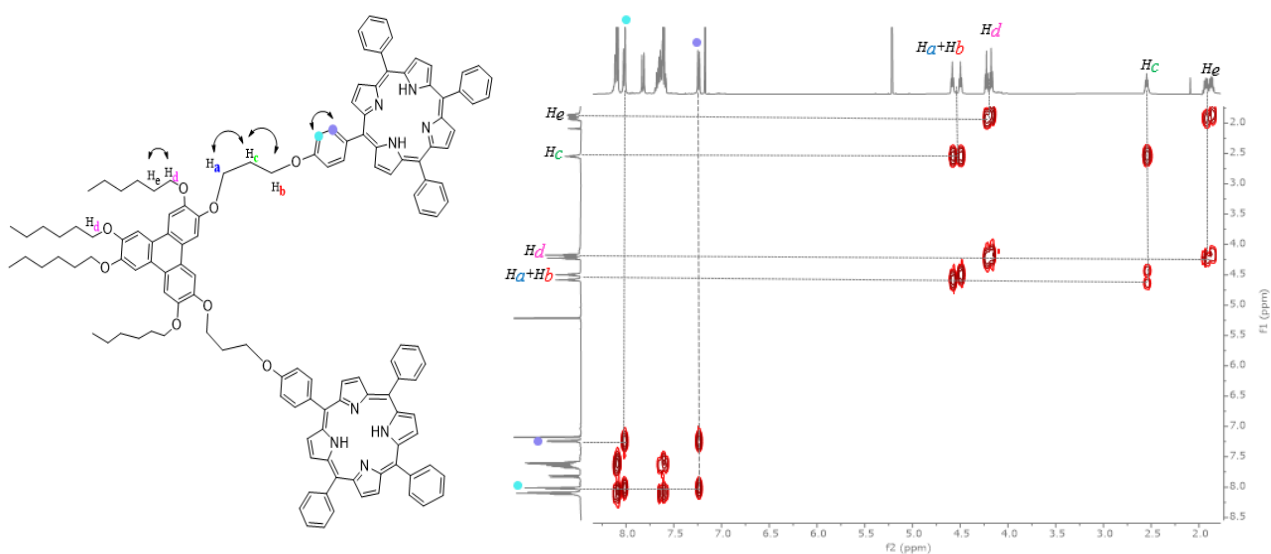


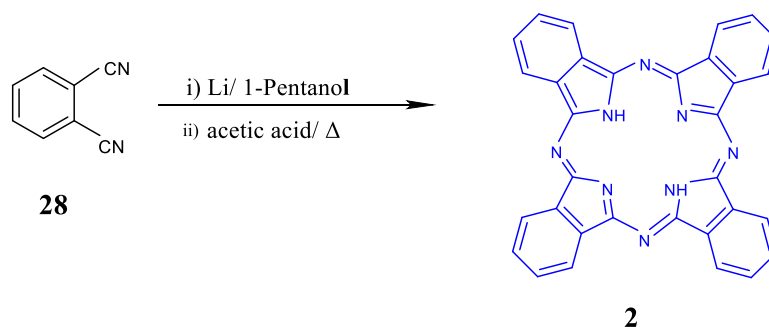
Figure 3.11. 2D COSY-NMR spectrum of second model **90**, zoom of the 8.25-1.89 ppm area.

3.3 Synthesis of 2,3- and 3,6-novel of triple-decker (LnTD)

After successful synthesis of two isometric di-porphyrin triphenylenes (2,3- **89** and 3,6- **90** models), these isomers were used to synthesise *single* triple-decker complexes using phthalocyanine as the central unit with different series of lanthanide metals. This is because the formation of these complexes is ideal to study and investigate their selectivity depending on the metal size.

3.3.1 Synthesis of metal-free phthalocyanine **2** (central unit-Pc)

The metal free phthalocyanine is an essential central core to synthesise the lanthanide multi-decker systems. A previously reported procedure¹⁴⁹ to synthesise phthalocyanine is shown in scheme 3.18.



Scheme 3.18. Formation of metal-free phthalocyanine **2**.

A solution of phthalonitrile **28** was refluxed in 1-pentanol. Lithium metal was added to the reaction mixture and was left to reflux for an hour. Following this, acetic acid was added, then refluxed to another hour. Finally, the mixture of this reaction was cooled down at room temperature and was precipitated using methanol to obtain the product. A dark blue solid was filtered and phthalocyanine product was synthesized with a 50% yield. UV-vis (Fig. 3.12) indicated that the presence of the metal-free phthalocyanine H₂(Pc) **2**. However, there was no further characterisation of this product due to the high insolubility of Pc **2** in any organic solvents.¹⁴⁹

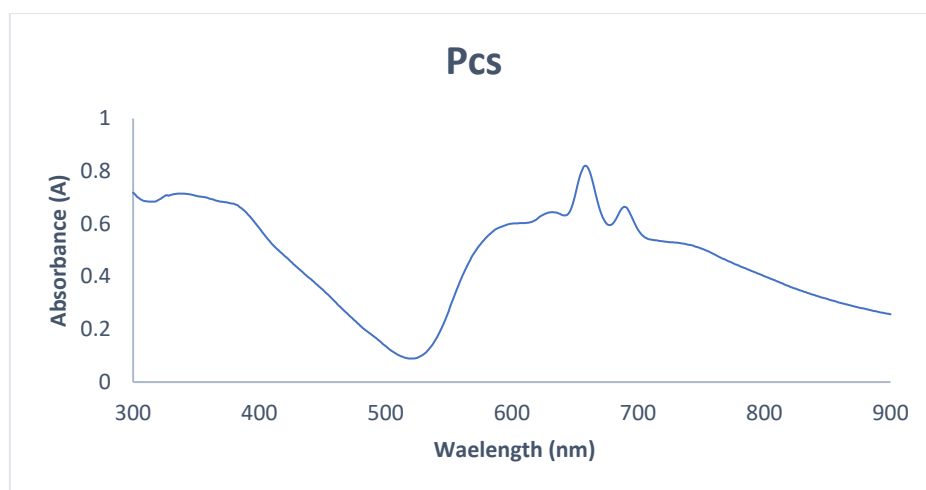
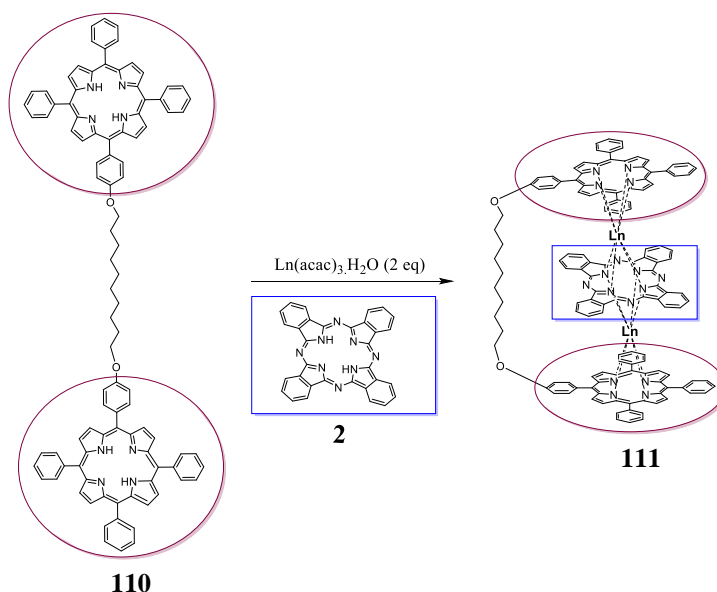


Figure 3.12. UV-vis spectra for metal-free phthalocyanine **2**.

3.3.2 Synthesising a closed triple-decker complex of porphyrin and phthalocyanine **111**

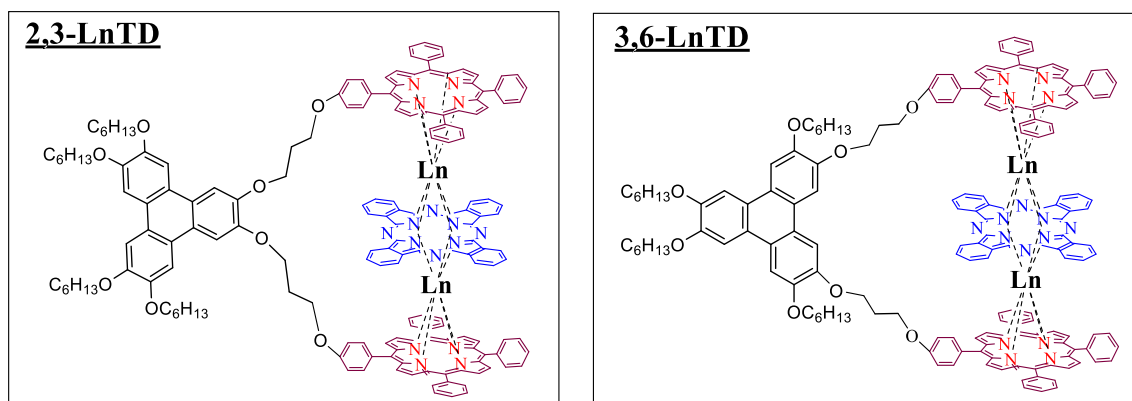
According to Cammidge's group,¹⁴⁹ the sandwich type triple-decker **111** was synthesised using a “one-pot” reaction. This reaction was between one equivalent of porphyrin dyad **110** and two equivalents of $M(\text{AcAc})_3 \cdot \text{H}_2\text{O}$, treated with one equivalent of phthalocyanine **2** (Scheme 3.19).



Where Ln = La, Nd, Eu, Tb, Dy, Yb

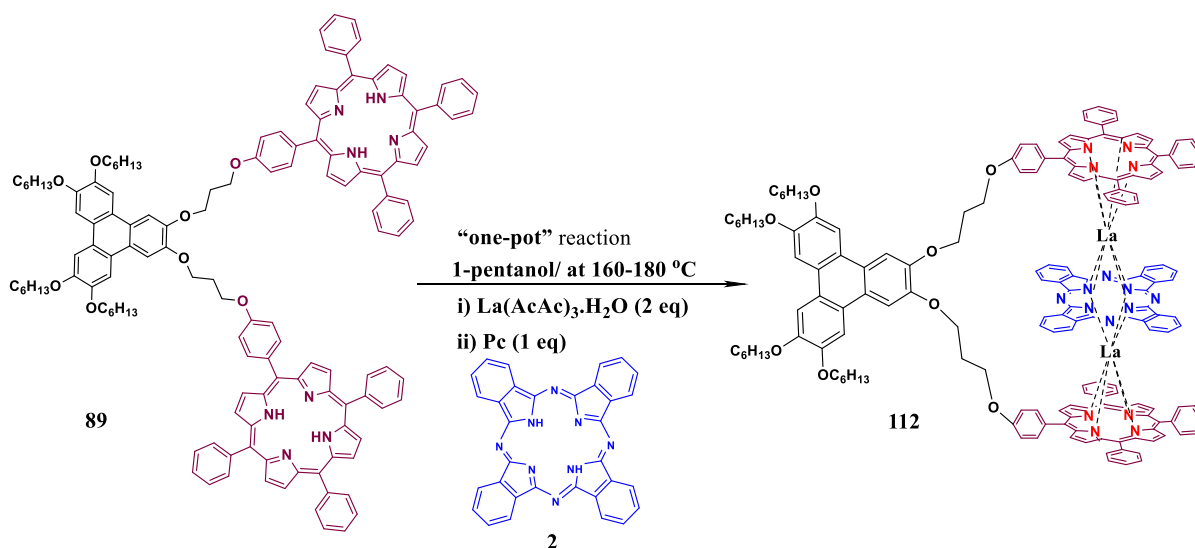
Scheme 3.19. Reaction process for closed triple-decker **111**.¹⁴⁹

In this case, the *single* triple-decker can be produced with different isomers of triphenylene-bridged di-porphyrins, as shown in scheme 3.20.



Scheme 3.20. Proposed structure of 2,3 and 3,6 *single* triple-decker complex.

An attempt was made to synthesise the heteroleptic triple-decker complex **112** from the 2,3-isomer **89**, (Scheme 3.21).



Scheme 3.21. Synthesis of 2,3-*bis*(porphyrin)triphenylene triple-decker **112**.

According to the previously mentioned protocol (Scheme 3.19), the reaction was performed using a **“one-pot”** reaction. A mixture of the di-porphyrin **89**, freshly prepared pure Pc **2** and two equivalents of $\text{La}(\text{AcAc})_3 \cdot \text{H}_2\text{O}$ was refluxed in 1-pentanol at 165°C for 4 hrs. A TLC was performed each hour during the reaction, which confirmed that no new products were detected. Multiple attempts were made by:

- 1- Using several alternative solvents to 1-pentanol, including distilled octanol, quinoline and DCB. These solvents allowed higher temperatures (200-250 ° C) to be reached due to their higher boiling points.
- 2- Increasing reaction time from 4-6 hrs to 24-48 hrs.
- 3- Adding some amounts of base DBU.

They all failed to produce the triple-decker complex; unreacted starting materials were only observed.

Efforts were made to modify the amounts of Pc **2** and metal of this reaction. Unexpectedly, a new product emerged, with MALDI-TOF-MS analysis revealing a lower mass range of $m/z = 2654.83$ representing the molecule **113**, (calc. :2654.83), instead of our triple-decker mass. This indicates that Pc and one metal were bonded to one side of the porphyrin unit as shown in (Fig. 3.13) below.

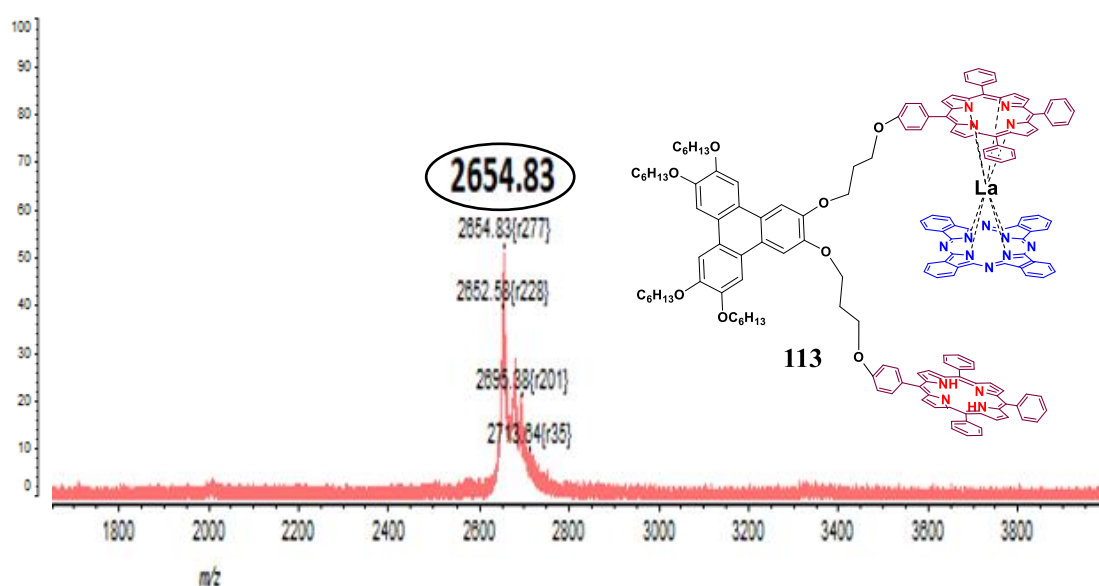
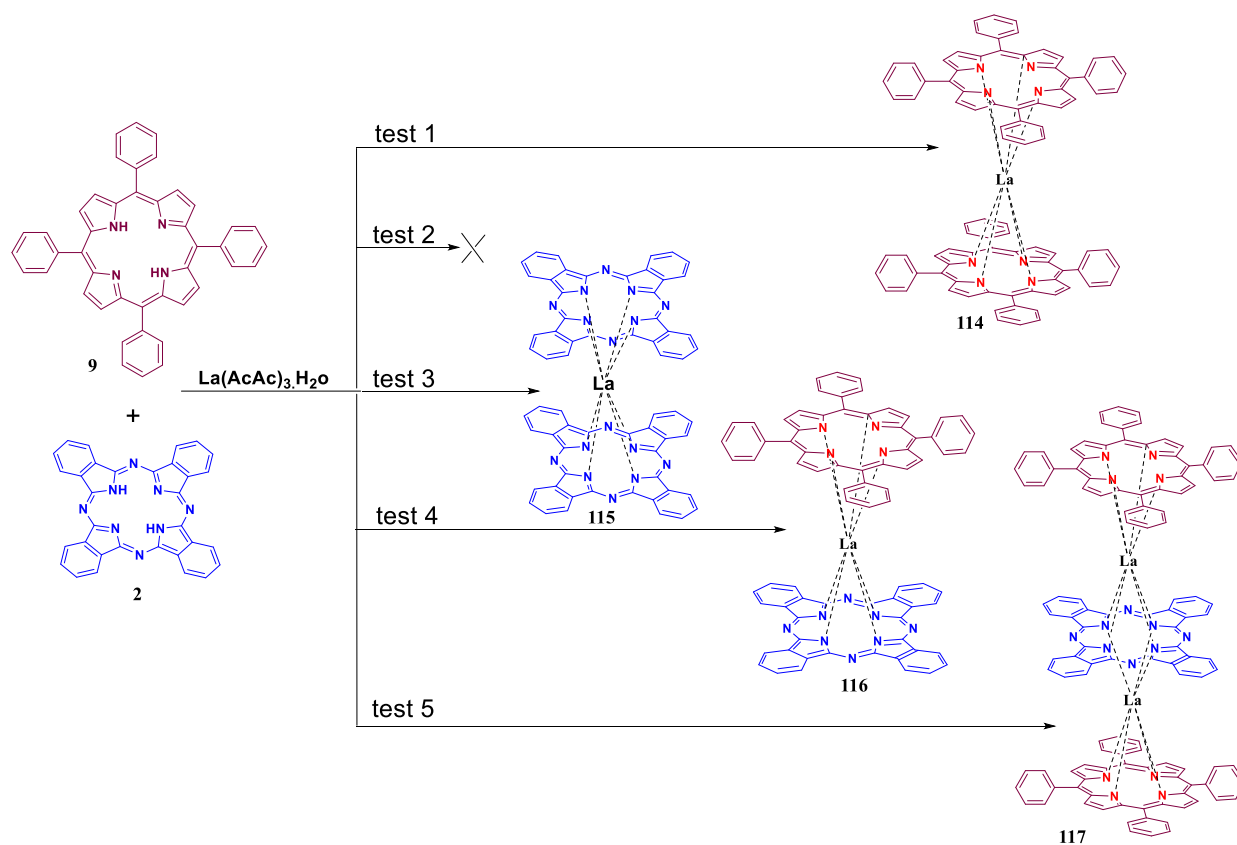


Figure 3.13. MALDI-TOF-MS result for one porphyrin linked to Pc central unit, product **113**.

3.3.2.1 Triple-decker formation from TPP **9** and Pc **2**

As previously discussed, no triple-decker had successfully formed. To check that the reaction process and equipment were satisfactory, a test reaction was investigated from **89**^{139, 186}. This was carried out using metal-free phthalocyanine **2**, porphyrin (TPP **9**) and La(AcAc)₃.H₂O (Scheme 3.22).



Scheme 3.22. General synthesis of test reaction by using TPP 9.

Several test reactions were performed to obtain triple-decker **117**, using a “one-pot” reaction each time. most methodologies afforded the TPP double-decker except the reaction number 5 as indicated in (Table 3.4).

<i>No of reaction:</i>	<i>No of equivalent</i>	<i>Condition:</i>	<i>Results:</i>	<i>MALDI-TOF-MS:</i>
1	TPP (2 eq) Pc (1 eq) La(acac) ₃ .H ₂ O (2 eq)	1-pentanol 165°C/ 4-6 hrs	double decker 114	(m/z=1306)
2	TPP (2 eq) Pc (1 eq) La(acac) ₃ .H ₂ O (2 eq)	quinoline 250 °C/ 6-24 hrs	No result	-
3	TPP (2 eq) Pc (2 eq) La(acac) ₃ .H ₂ O (2 eq)	1-pentanol 165 °C/ 3-4 hrs	double decker 115	(m/z=1268)
4	TPP (2 eq) Pc (1 eq) La(acac) ₃ .H ₂ O (8 eq)	1-pentanol 165 °C/ 3-4 hrs	double decker 116	(m/z=1173)
5	TPP (2 eq) Pc (2 eq) La(acac) ₃ .H ₂ O (4 eq)	1-pentanol 165 °C/ 3-4 hrs	triple decker 117	(m/z=2015)

Table 3.4. Methodologies for synthesising test reaction for close triple-decker **117**.

Initially, test 1 was performed by mixing two equivalents of the porphyrin **9** and one equivalent of Pc **2**. Two equivalents of La(AcAc)₃.H₂O were added. The mixture was refluxed for 4-6 hrs. Although TLC analysis revealed the presence of a new product, a double-decker porphyrin **114** was obtained, rather than the desired triple-decker **117**, as confirmed by MALDI-TOF-MS.

Consequently, in test 2, the same approach was repeated using an alternative solvent, quinoline and heated to 250°C, but no outcome was detected. Therefore, the reaction was repeated during test 3, by utilising the identical solvent as in first attempt, but with the addition of an excess quantity of Pc (two equivalents). Test 3 was analysed using MALDI-TOF-MS revealed the presence of a Pcs double-decker **115**.

In test 4, an increasing excess of the metal was added, (8 equivalents). The resulting product was analysed using MALDI-TOF-MS to confirm the formation of a heteroleptic double-decker of phthalocyanine and porphyrin **116**. Finally, in test 5, a double excess of Pc (two equivalents) and the metal (four equivalents) was employed based on prior results. The new product was analysed using MALDI-TOF-MS, and the expected mass of the triple-decker **117** was successfully achieved (Fig. 3.14).

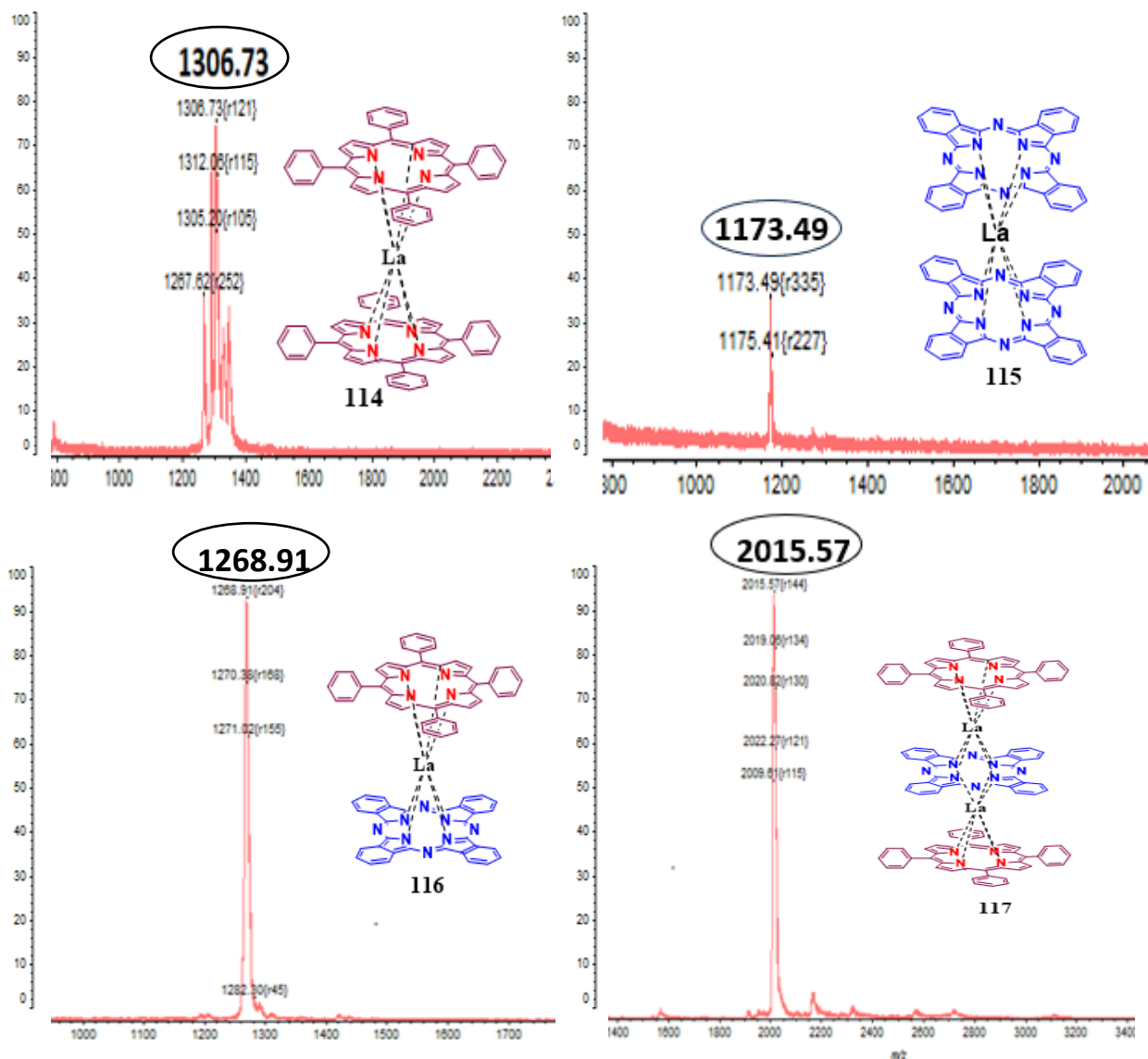
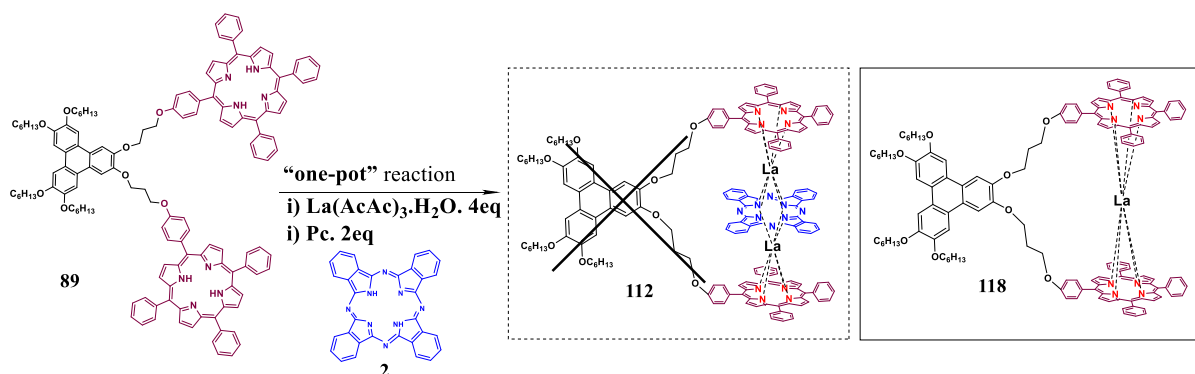


Figure 3.14. MALDI-TOF-MS results for test reactions 1-5.

3.3.2.2 New attempts of synthesis 2,3-LaTD **112** from 2,3-isomer **89**

The earlier conditions outlined in test number 5 gave heteroleptic triple-decker of TPP **9** and Pc **2**. By applying this condition with 2,3-isomer **89**, double-decker **118** was observed instead of the required triple-decker complex **112**. Therefore, using a “**one-pot**” reaction, two equivalents of Pc **2** and four equivalents of $\text{La}(\text{AcAc})_3 \cdot \text{H}_2\text{O}$ with one equivalent of 2,3-*bis*(porphyrin)triphenylene **89**, were directly mixed and refluxed at 165 °C. TLC analysis

confirmed that after 1 hr of the reaction, the new product double-decker **118** was formed, as shown in (Scheme 3.23).



Scheme 3.23. Double-decker formation **118**.

MALDI-TOF-MS of double-decker **118** shows a molecular mass of 2,3-isomer combined with the weight of one lanthanum metal, giving an m/z value of 2134.39 $[M]^+$, as illustrated in (Fig. 3.15).

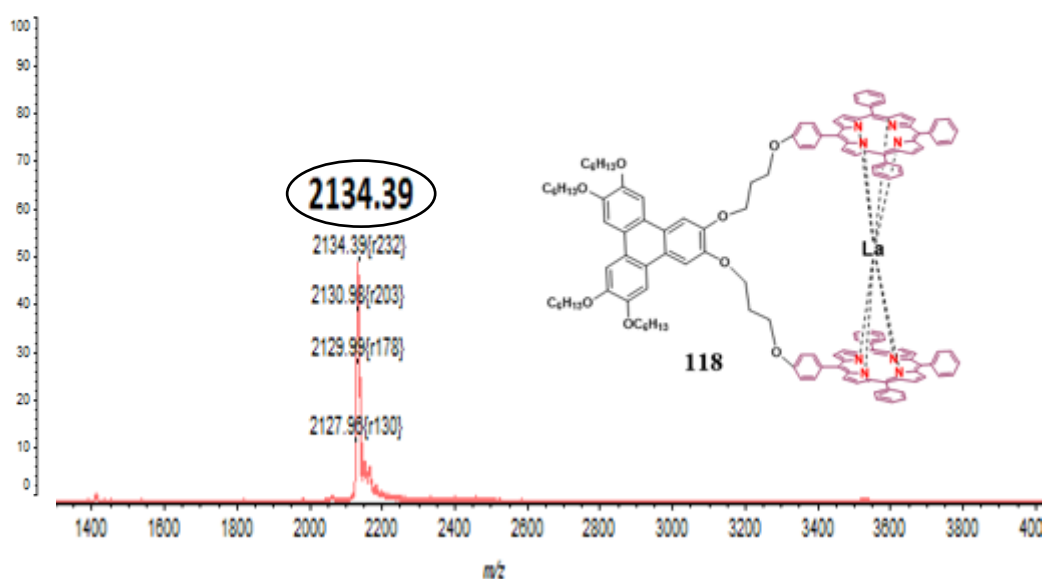


Figure 3.15. MALDI-TOF-MS result for double-decker **118** by testing first model with “one-pot” reaction.

The UV-vis spectrum of the metal-free porphyrin **89** displays four Q-band peaks (Fig. 3.16, **A**), whereas the peaks decrease on metalation of **118** (Fig. 3.16, **B**). The UV-spectrum of **118** confirms that lanthanide metal has caused these effects, and it was bonded between these two chromophores. Graph (**B**) signals for **118** were extremely close to those previously reported for the double-decker complex ¹⁸⁷ (Fig. 3.16, **C**).

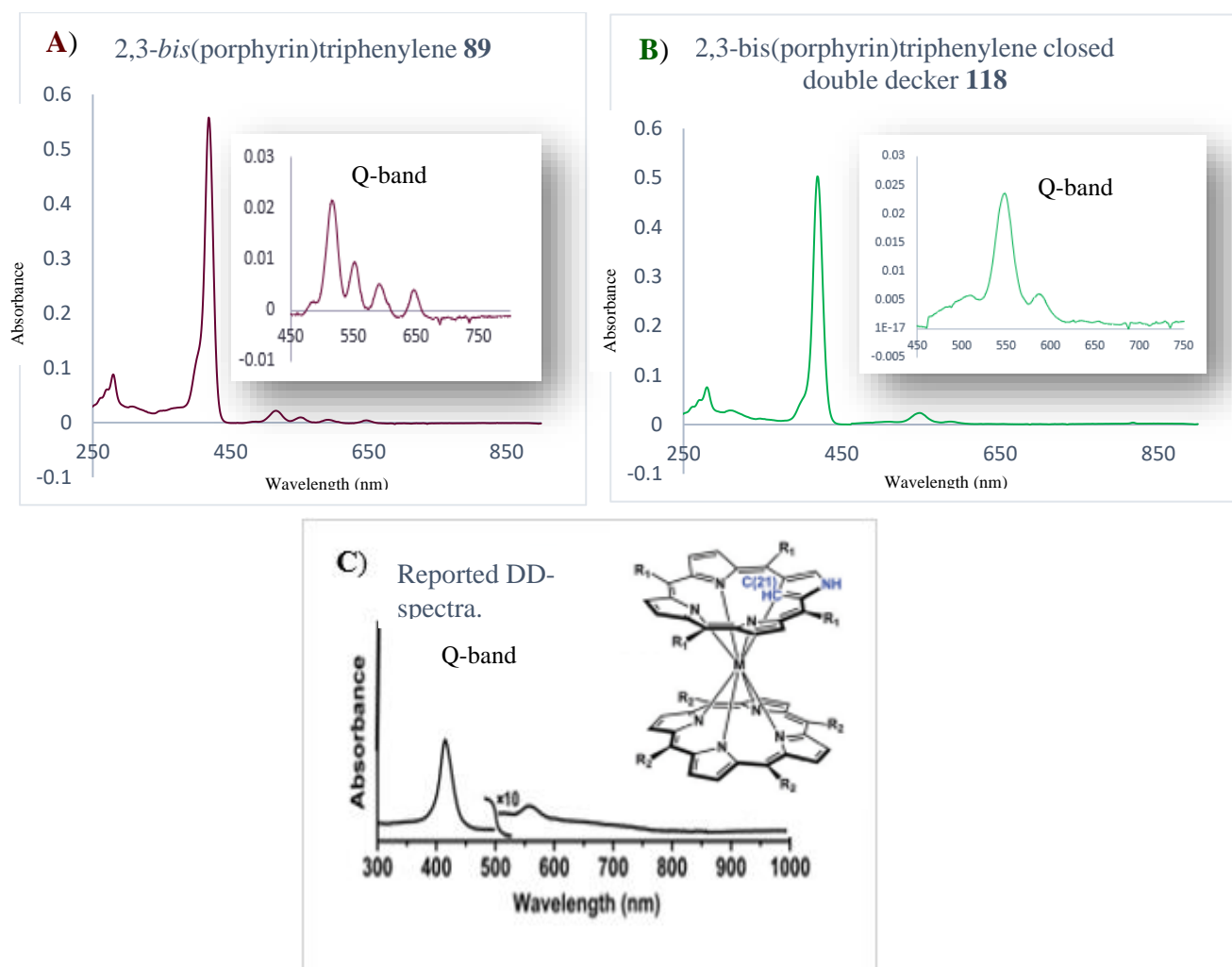


Figure 3.16. Comparison between UV-vis spectra of starting material **89** (**A**), double-decker complex **118** (**B**) and double-decker from literature¹⁸⁷ (**C**).

The chemical structure of the double-decker was also investigated by ¹H NMR-spectroscopy. The ¹H NMR-spectra of the metal-free porphyrin model **89** showed a singlet peak of 4H for N-H around -2.81ppm. Whereas, due to metalation in **118**, the N-H peak is absent, and all the signals were slightly shielded, particularly in the aromatic area for porphyrins rings; all the protons of pyrrole rings were around 8.85-8.74 ppm in **89** (metal-free porphyrins), while in **118** showing a shift to around 8.93-8.82 ppm (metalated-porphyrins), (Fig. 3.17). The porphyrin peaks shifted significantly and triphenylene signals remained unchanged as expected.

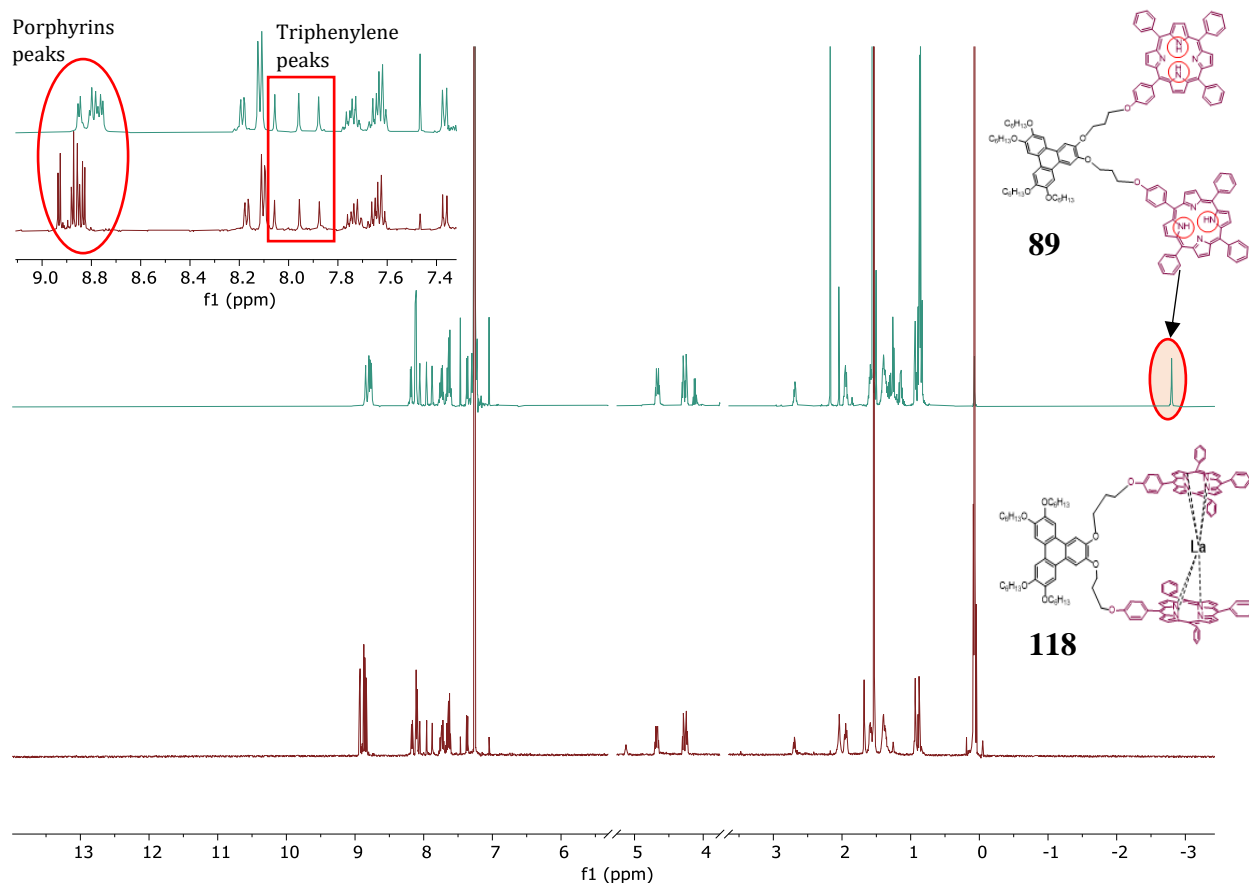


Figure 3.17. Comparison of ^1H NMR-spectrum between (starting materials **89** and double-decker complex **118**).

However, ^1H NMR-spectra of complex **118** showed only small shifts of porphyrin peaks, notably different from open DD examples¹⁸⁸, (Fig. 3.18).

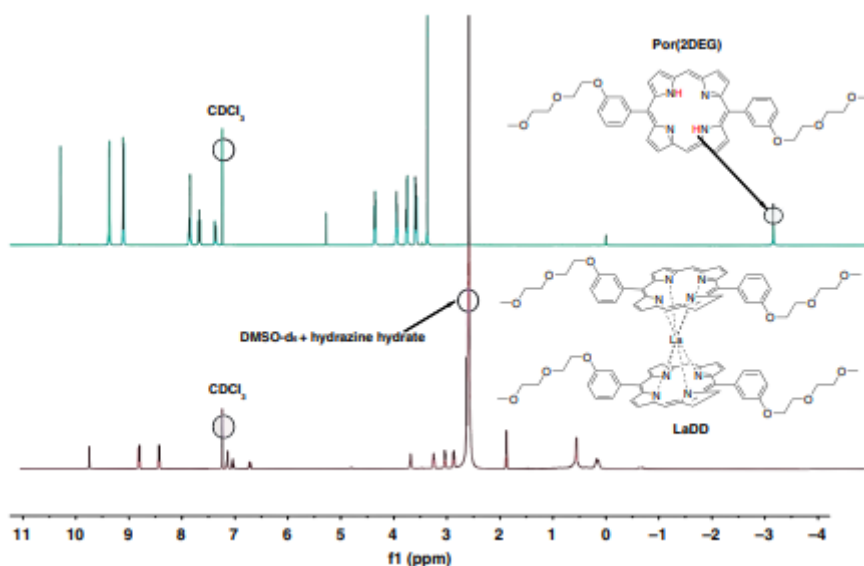
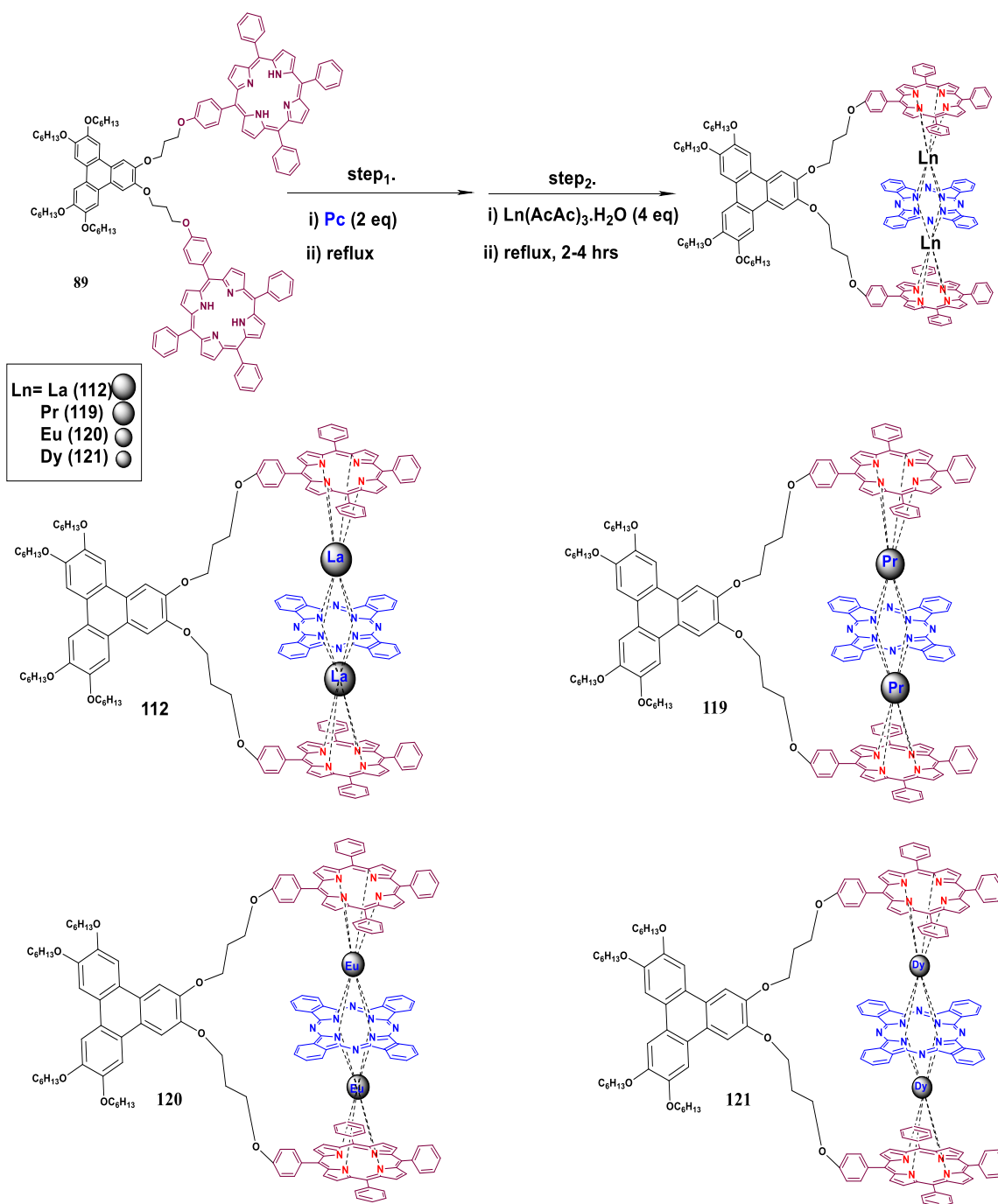


Figure 3.18. ^1H NMR-spectrum of a porphyrin starting material and double-decker from literature¹⁸⁸.

3.3.3 Successful synthesis of 2,3-bis(porphyrin)triphenylene triple-decker (2,3-LnTD)

From the test reaction for the formation of triple-decker **117** with TPP and Pc, using a “one-pot” reaction with different ratio of the equivalents, (2eq of Pc and 4eq of metal salt), is essential. Unfortunately, using this condition, model **89** with Pc **2** (two equivalents) in the presence of La(AcAc)₃.H₂O (four equivalents) generates a double-decker complex **118** instead. The outcome of “one-pot” reaction indicates that the starting material **89** was mostly consumed and reacted with the metal itself without inserting the Pc core, failing to produce required triple-decker complex **112**. From this observation it was concluded that this problem was low solubility of Pc in the reaction so that **89** was reacting with Lanthanum ion to give stable dyad rather than the required TD **112**. In order to prevent this, modified reaction protocols were investigated.

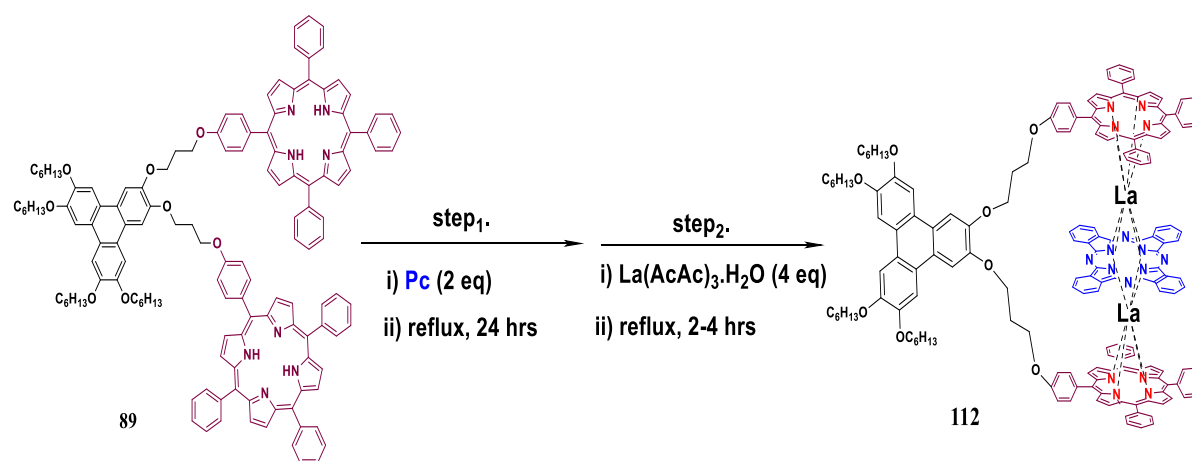
Therefore, considering modification, synthesis of 2,3-bis(porphyrin)triphenylene triple-deckers were performed in alternative reaction pathways by refluxing and mixing starting materials of **89** and Pc **2** overnight in 1-pentanol as solvent, before adding the metal (to avoid any low solubility problems of Pcs product). Thus, the triple-deckers, with a series of different metals sizes, were successfully obtained, (Scheme 3.24).



Scheme 3.24. The reaction process for synthesizing a *single* triple-decker complex **2,3-LnTD**.

3.3.3.1 Lanthanum triple-decker (2,3-LaTD) **112**

Here, the first successful attempt to synthesis lanthanum triple-decker **112**, (Scheme 3.25), as lanthanum is the main example in the lanthanide series, having the biggest size among all the lanthanide elements.¹¹⁹



Scheme 3.25. 2,3-La triple-decker **112**.

One equivalent of model **89** with 2 equivalents of Pc **2** were refluxed in 1-pentanol at 165°C for 24 hrs. Next, four equivalents of La(acac)₃.H₂O was added to the mixture and left to reflux for 2-4 hrs. TLC was performed on aliquots from the reaction to check formation of the triple-decker complex, which showed a new green spot after 1 hour of adding the metal. This product was analysed using MALDI-TOF-MS which confirmed the formation of 2,3-LaTD **112**, displaying the molecular ion m/z 2787.23 [M]⁺ (C₁₆₈H₁₄₀La₂N₁₆O₈), calc.: 2787.90, as illustrated in (Fig. 3.19).

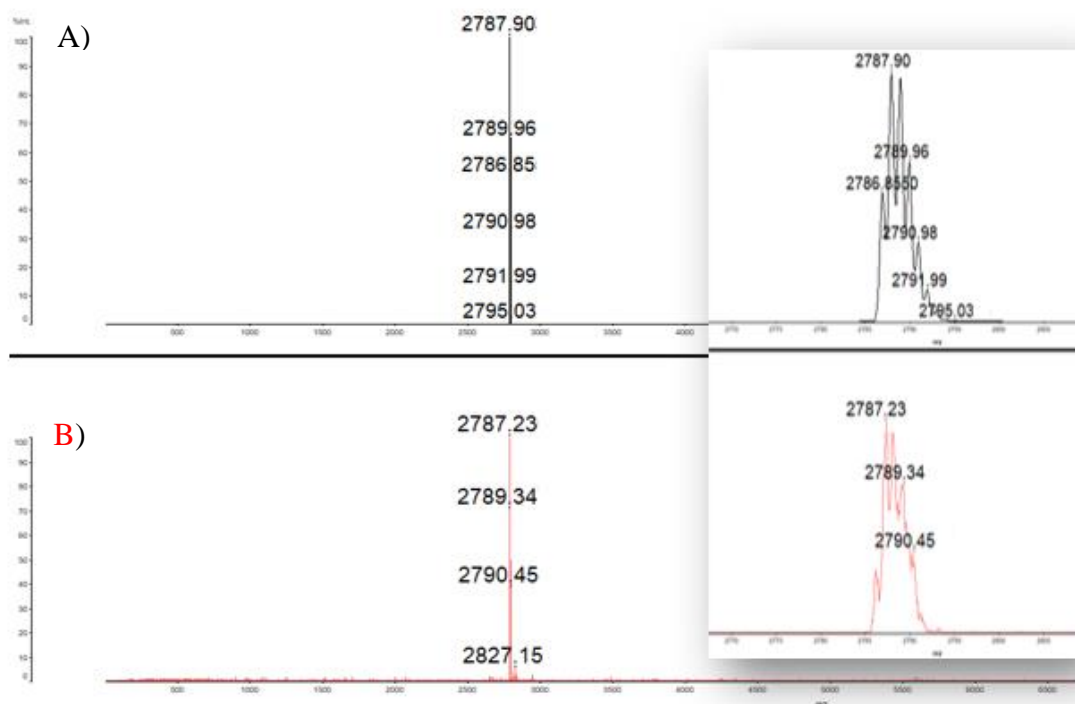


Figure 3.19. The MALDI-TOF-MS for a green solid for lanthanum triple-decker of 2,3-*bis*(porphyrin)triphenylene **112**. The inset shows (B) obtained and (A) theoretical isotopic patterns.

Attempts to purify the green solid consistently produced a mixed fraction containing unreacted starting materials. However, with the addition of TEA to the column chromatography eluents PET:DCM:TEA (v:v:v 10:3:1), a green solid of the TD product was obtained. This was recrystallized using DCM: MeOH to obtain the triple-decker **112**, with a yield of 47%.

Analysis of UV-vis spectrum

The UV-vis spectrum of 2,3La-TD is different from that of the starting material's, **89**, as shown in (Fig. 3.20). Interestingly, the UV-vis spectra of **112** presented three absorption peaks of Q-band instead of four (-red trace) and *Soret*- broad band (*) peak at 363 nm due to existing of the Pc core.

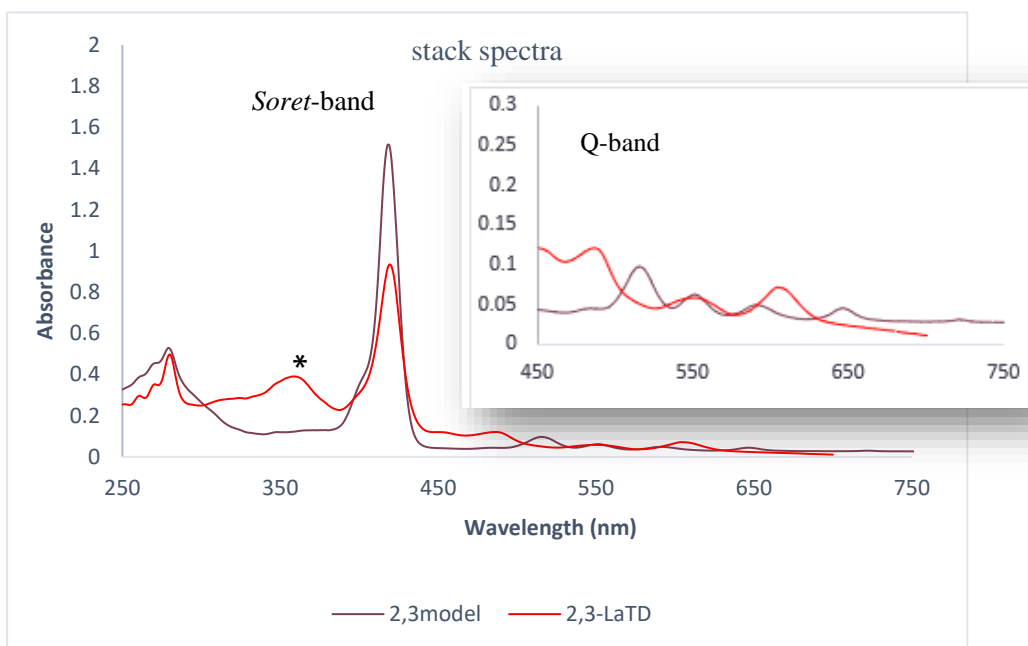


Figure 3.20. UV-vis spectrum obtained for the lanthanum triple-decker **89** compared to 2,3-model **112**, inset: expansion of the 450-750 nm area.

Analysis of NMR spectrum

The chemical structure of the lanthanum triple-decker **112** was also proved by ^1H and COSY NMR-spectroscopy. ^1H NMR-spectra of **112** display signals which correspond to Pc core, including two doublets of doublets of H_{pci} and **2** for 8H each around 9.35 and 8.29 ppm. All peaks related to the porphyrin molecule are observed in the high chemical shift region, giving clear split signals which can be explained by the structure of the TD complex. ^1H NMR-spectra of **112** shows a symmetrical triple-decker formation and clearly indicates free rotation. Ar-H signals in *meso*-phenyl of the substituted porphyrin (benzene ring **(A)** and **(B)**) displayed the inner and the outer phenyl protons for each of (*meta*) and (*ortho*) position because of restricted rotation of rings. For example, four distinct signals for the Ar-H in benzene ring **(A)** shows $\text{H}_{\text{mo}'}$ and $\text{H}_{\text{oo}'}$ for the outer phenyl protons of *meta* and *ortho* position at 7.04-7.02 ppm; $\text{H}_{\text{mi}'}$ and $\text{H}_{\text{oi}'}$ for the inner phenyl protons at 8.25 and 10.33 ppm. Furthermore, Ar-H in the benzene ring **(B)** shows a similar pattern. (Fig. 3.21).

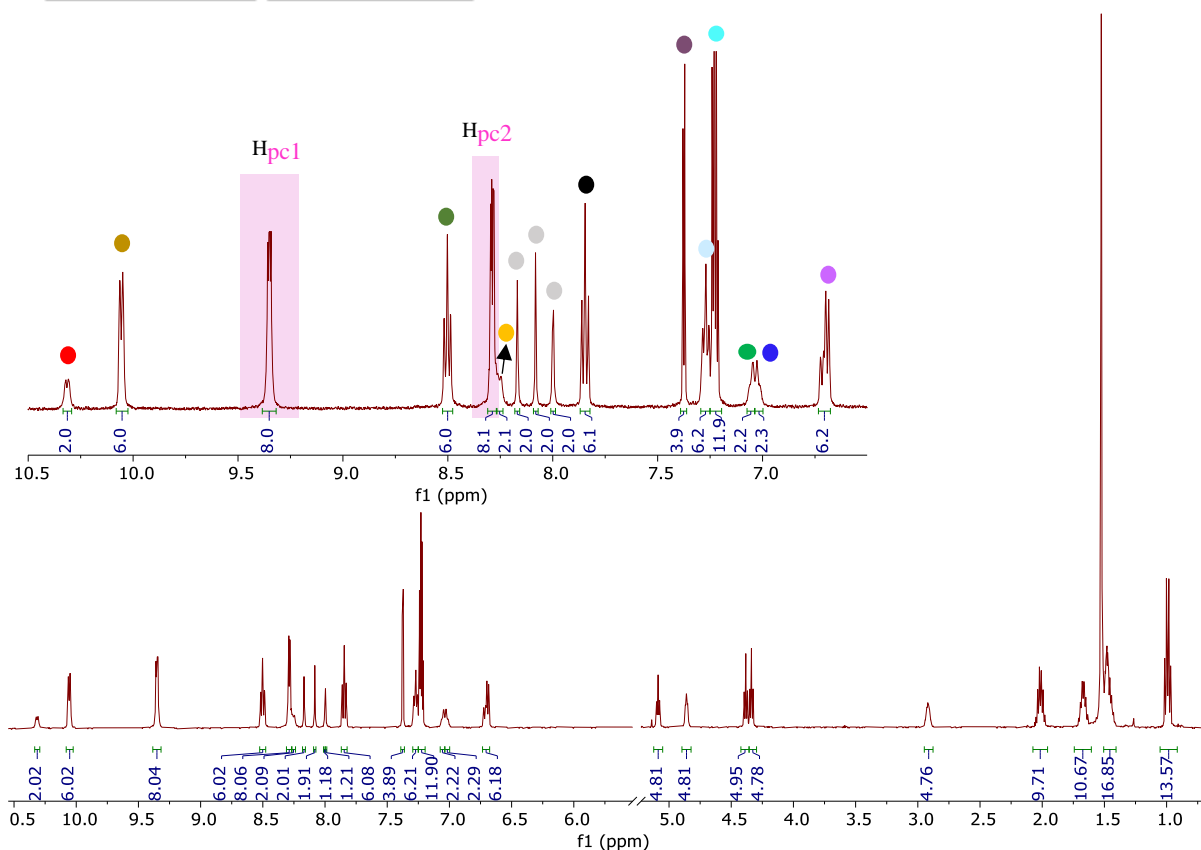
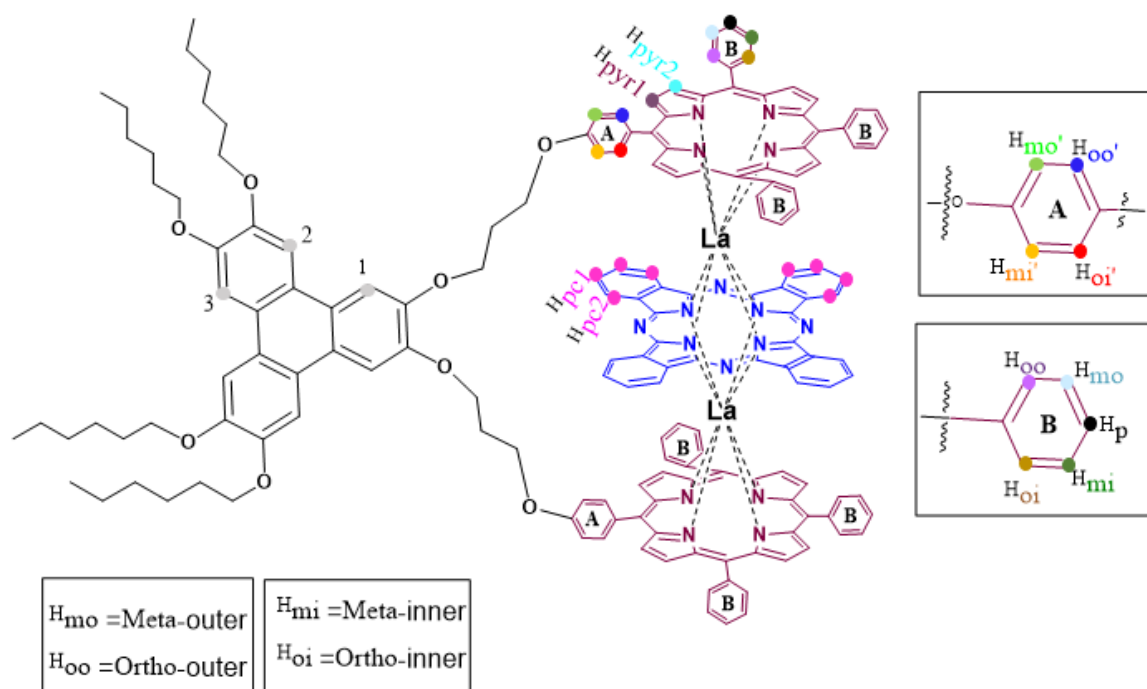


Figure 3.21. The ^1H NMR-spectrum of the lanthanum triple-decker **112** (500 MHz, CD_2Cl_2), expansion of 10.5-6.5ppm aromatic area.

The COSY-spectrum of 2,3-LaTD **112** presents that the doublet of doublets for H_{pc1} at 9.35ppm correlates with the doublet of doublets for H_{pc2} at 8.29 ppm, both belonging to the Pc core. Therefore, the spin-spin coupling between porphyrin hydrogens were revealed. As result, the rotation of benzene rings for di-porphyrins were observed, as they show ‘inner’ and ‘outer’ hydrogens location. Starting with benzene rings (A); both doublets of $H_{oi'}$ (*ortho*- inner’) at 10.31ppm correlate with the doublet of $H_{mi'}$ (meta-inner’) at 8.25ppm (overlapped with H_{pc2}). Also, protons $H_{mo'}$ (meta-outer’) and $H_{oo'}$ (*ortho*-outer’) were coupled to each other. Therefore, benzene rings (B) display a clear correlation pattern; the protons of H_{oi} at 9.08 ppm correlate to those of H_{mi} . H_{mi} correlates with both H_p and H_{oi} . The pattern also continues; H_p coupling again with both hydrogen in meta position (inner and outer) H_{mi} and H_{mo} ; the hydrogen in meta position (outer) H_{mo} correlate to both H_p and H_{oo} . Finally, H_{oo} in *ortho* position (outer) correlate with meta position (outer) H_{mo} , as shown in (Fig. 3.22).

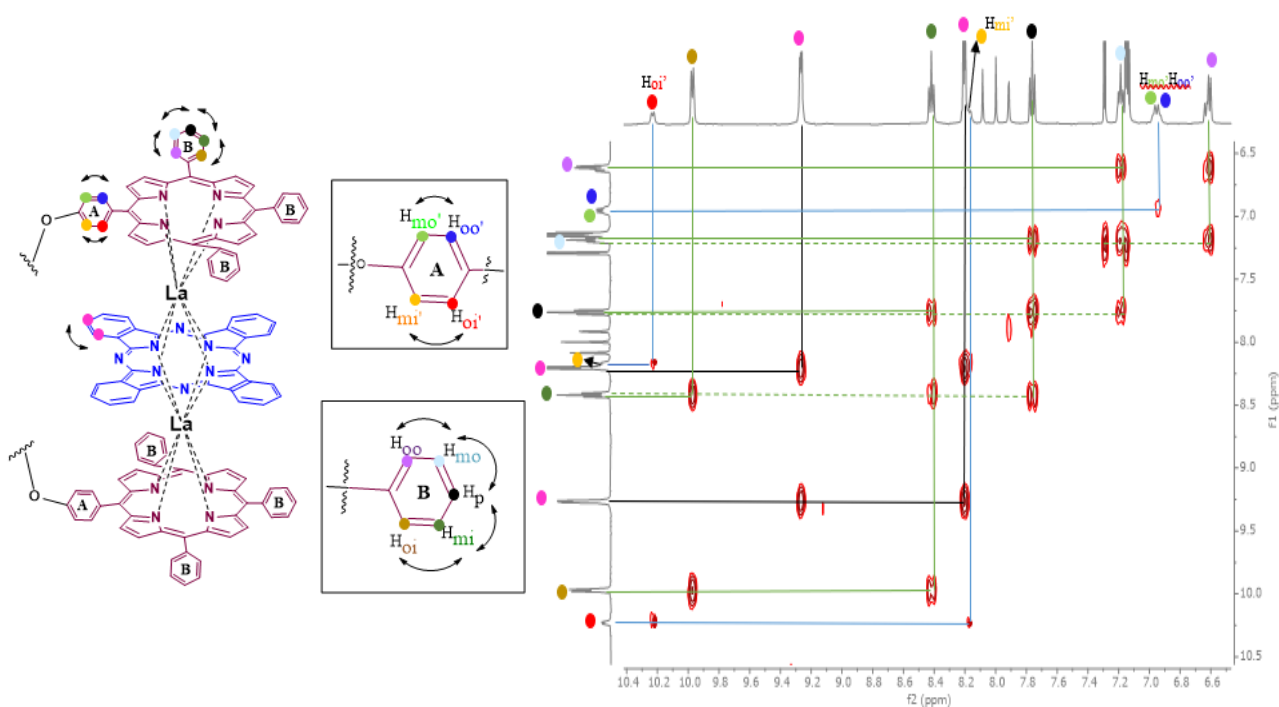
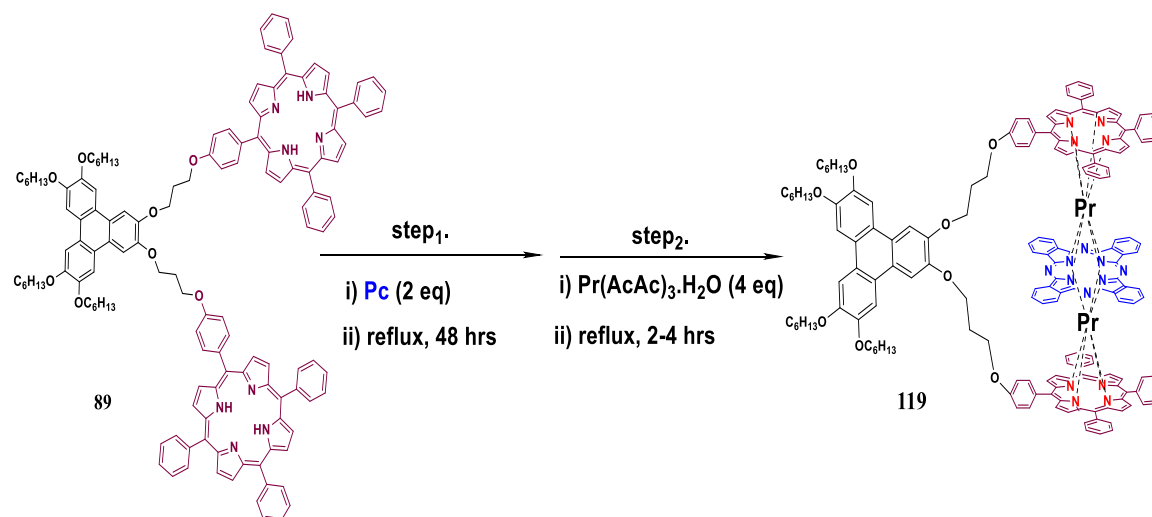


Figure 3.22. 2D Cosy NMR-spectra of 2,3-bis(porphyrin)triphenylene triple-decker **112**.

3.3.3.2 Praseodymium triple-decker (2,3-PrTD) 119

After the successful synthesis of the 2,3-LaTD, another triple-decker was also synthesised using praseodymium metal, as praseodymium is the third element in the lanthanide series and belongs to the rare-earth metals. The estimated atomic radius of Pr^{3+} is notably smaller, measuring 99 pm, compared to La^{3+} with a radius of 103 pm,¹¹⁹ (Scheme 3.26).



Scheme 3.26. Triple-decker with praseodymium ions **119**.

The optimized previous conditions were applied, changing the first step by; increasing both the time of refluxing and mixing initial starting materials from 24 hrs to 48 hrs and ensuring vigorous reflux. $\text{Pr}(\text{AcAc})_3 \cdot \text{H}_2\text{O}$ (4 equivalents) was then added. Full consumption of the starting material was observed after 4 hrs. The product was precipitated using MeOH then filtered off, and subjected to flash column chromatography, washed with (100% DCM) to separate any excess of Pc. After two attempts of recrystallisation, it was possible to get the product with 52% yield.

The compound 2,3-PrTD **119** was identified using MALDI-TOF-MS analysis, which displayed the molecular ion at m/z 2791.24 $[\text{M}]^+$, $[\text{C}_{168}\text{H}_{140}\text{Pr}_2\text{N}_{16}\text{O}_8]^+$, calc.: 2791.90 (Fig. 3.23).

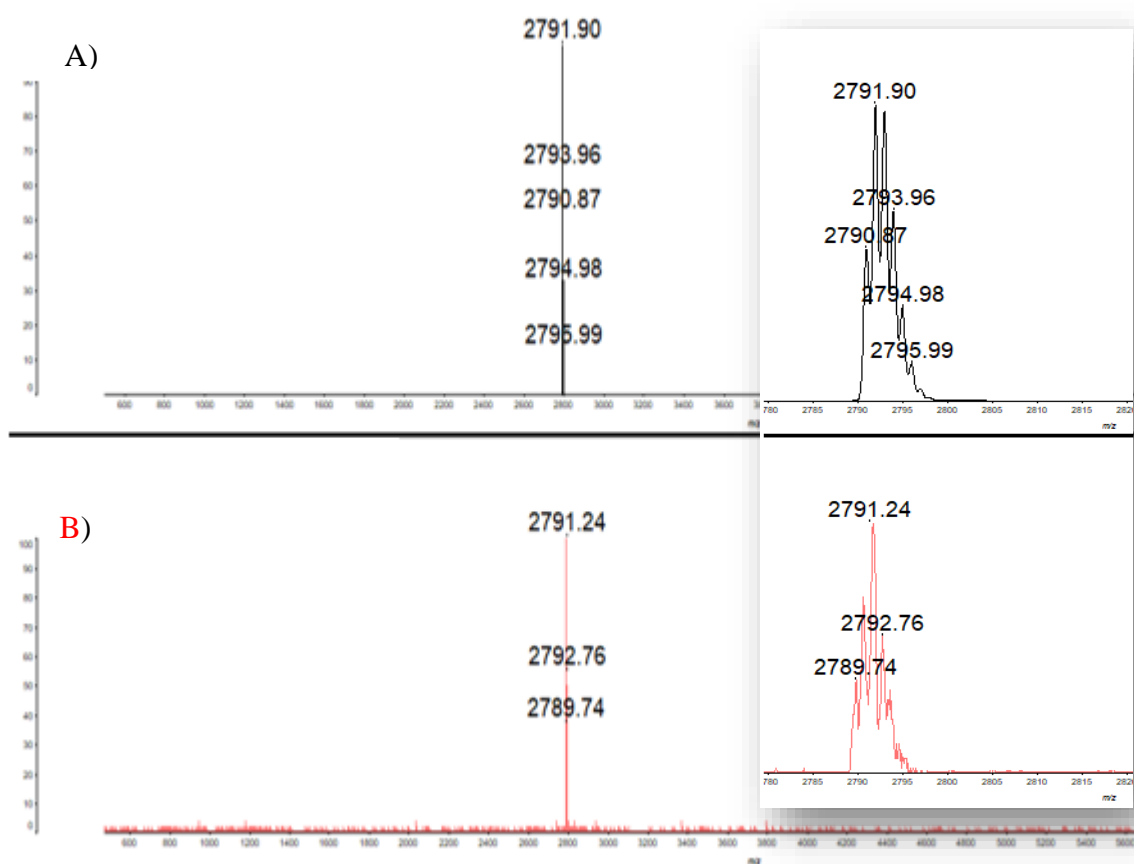


Figure 3.23. MALDI-TOF-MS obtained for a green solid for praseodymium triple-decker **119**. The inset shows (B) obtained and (A) theoretical isotopic patterns.

After characterising the 2,3-PrTD **119** using ^1H NMR-spectroscopy, the spectra were found to differ from those of 2,3-LaTD **112**, in terms of signal arrangement and placement. The ^1H NMR-spectra of 2,3-LaTD **112** displayed signals in the high deshielded region to around 10.33 ppm and gave a different splitting peaks from Praseodymium triple-decker **119**, (Fig. 3.24 (a) and (b)). As expected, the spectra of Praseodymium triple-decker derivatives markedly differ from those of Lanthanum triple-decker due to the paramagnetic nature of the Pr^{3+} ion. The spectra for the corresponding 2,3-LaTD **112** and simple C_{10} bridged PrTD were depicted as stacks with the new complex system 2,3-PrTD **119** in (Fig. 3.24 (a), (b) and (c)). Notably, the spectra between of the two PrTD ((b) and (c)) derivatives exhibit significant similarities, with several highlighted peaks. Specifically, porphyrins and Pc peaks are essentially identical in both derivatives; ($\text{H}_{\text{Pc1,2}}$) signals appearing at 5.80 and 3.90 ppm and $-\text{OCH}_2$ peaks at 3.08 ppm are also similar. However, in the 2,3-LaTD complex (a), the corresponding protons of $-\text{OCH}_2$ appear at 5.09 ppm and the influence of the praseodymium ion extends even to the triphenylene

singlets Ar-H*, which shift from 8.16 ppm in 2,3-LaTD complex (*a*), to approximately 7.50 ppm in 2,3-PrTD complex (*b*).

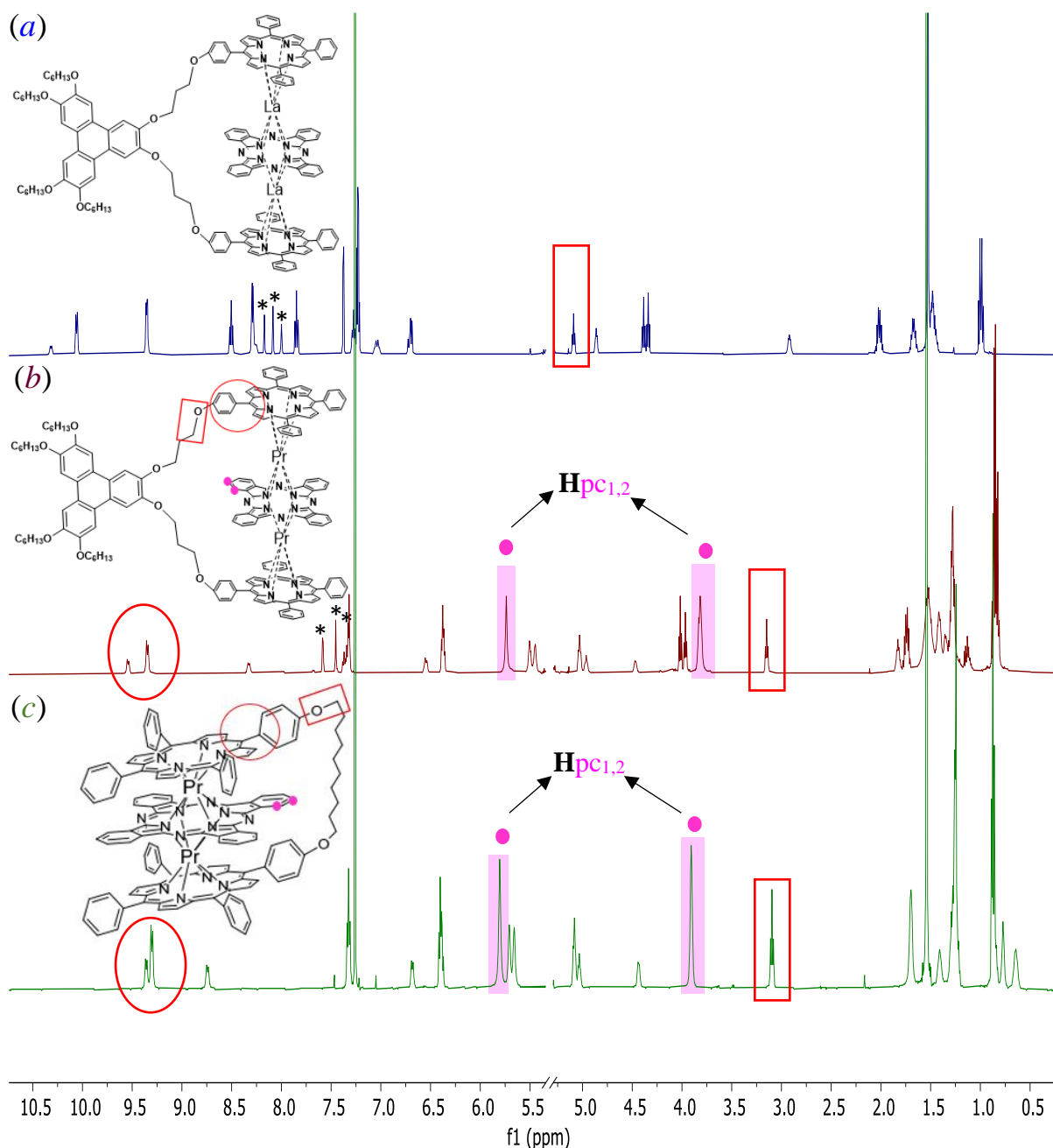
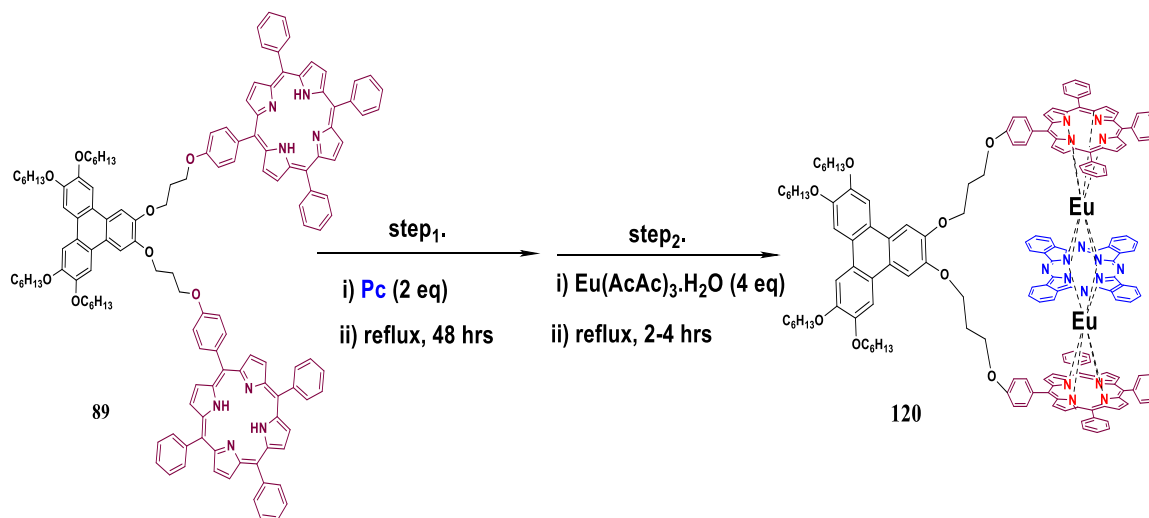


Figure 3.24. The ¹H NMR-spectrum obtained for 2,3-PrTD **119** (*b*) with comparing ¹H NMR-spectra to 2,3-LaTD **112** (*a*) and PrTD for Cammidge's group (*c*).

3.3.3.3 Europium triple-decker (2,3-EuTD) **120**

The europium metal was also used, as europium is one of the rarest rare-earth elements and has the lowest density compared to the other lanthanides, measuring ionic radii 95

pm.¹¹⁹ The triple-decker **120** was obtained following the same methodology, which was optimised above, (Scheme 3.27).



Scheme 3.27. Triple-decker via europium ion **120**.

This complex was proven by MALDI-TOF-MS analysis which displayed the molecular ion m/z 2814.98 [M]⁺, [C₁₆₈H₁₄₀Eu₂N₁₆O₈]⁺, calc.: 2814.96, (Figure 3.25). Additionally, it was verified using ¹H, ¹³C{¹H} and COSY NMR analysis. Due to complex NMR spectra, the data are reported in detail in the experimental chapter.

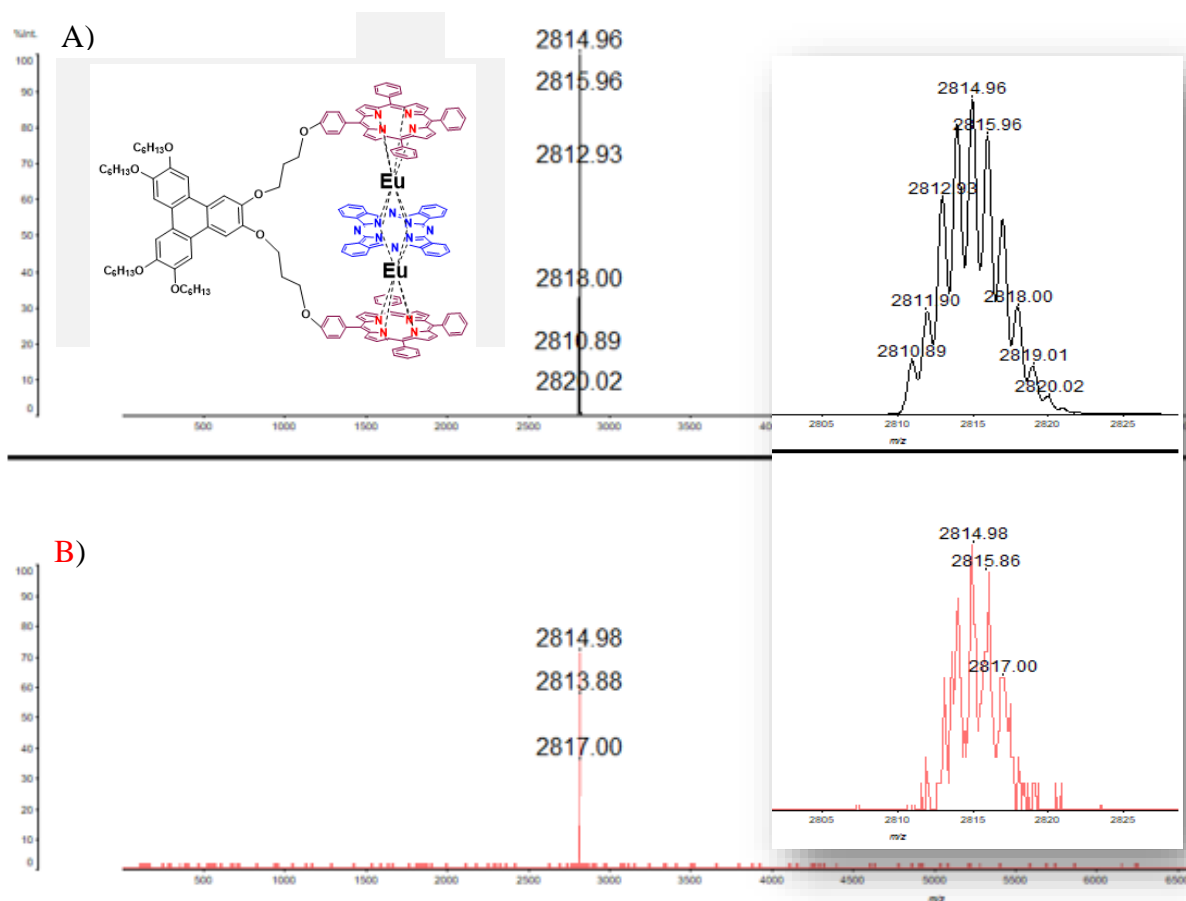


Figure 3.25. MALDI-TOF-MS obtained for a green solid for Europium triple-decker complex **120**. The inset shows (B) obtained and (A) theoretical isotopic patterns.

3.3.3.4 Dy triple-decker (2,3-DyTD) **121**

Dysprosium metal was employed, but it failed to generate a triple-decker complex **121**, likely due to its small size of ionic radii 90 pm, making it challenging to create effective links between di-porphyrin units and the phthalocyanine core.

3.3.3.5 Comparison of 2,3- triple-decker 112, 119 and 120

By comparing the UV-vis spectra of the produced La, Pr and Eu triple-decker complexes, they all display highly similar UV-vis absorption patterns, as illustrated in (Fig. 3.26).

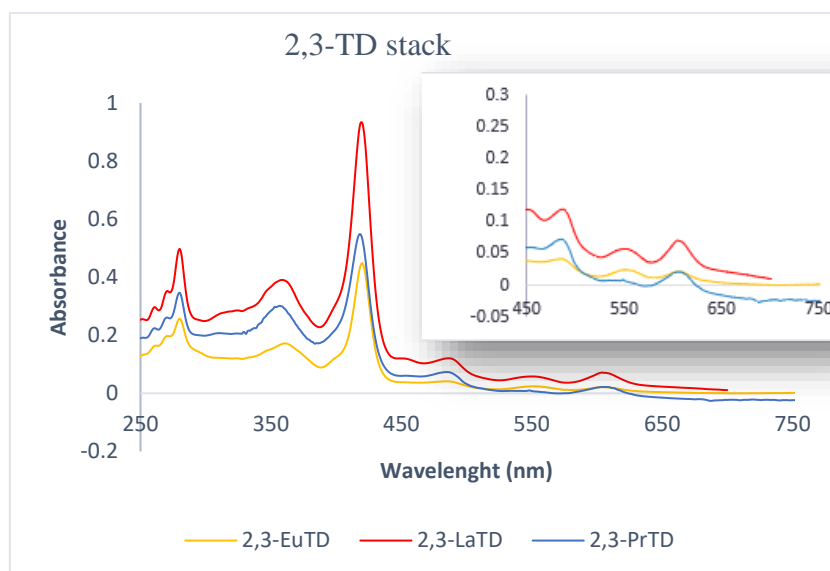


Figure 3.26. UV-vis spectra for 2,3-LnTD complexes for all three metals (La, Pr and Eu), inset: expansion of the 450-750 nm area.

3.3.4 Synthesis of 3,6-bis(porphyrin)triphenylene triple-decker (3,6-LnTD)

The next step involved using a second isomer, 3,6-bis(porphyrin)triphenylene model **90**, to produce another isometric *single* triple-decker with a series of different metal sizes, ranging from bigger to smaller. A more favourable selection was expected for larger metal sizes, given that the 3,6-isomer has a structure spanning a larger distance due to increased space between the di-porphyrin units, as shown in (Fig. 3.27).

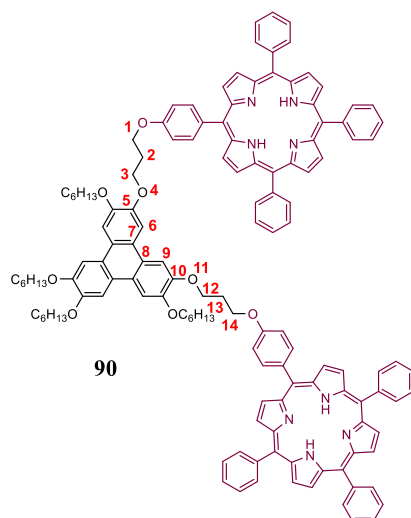
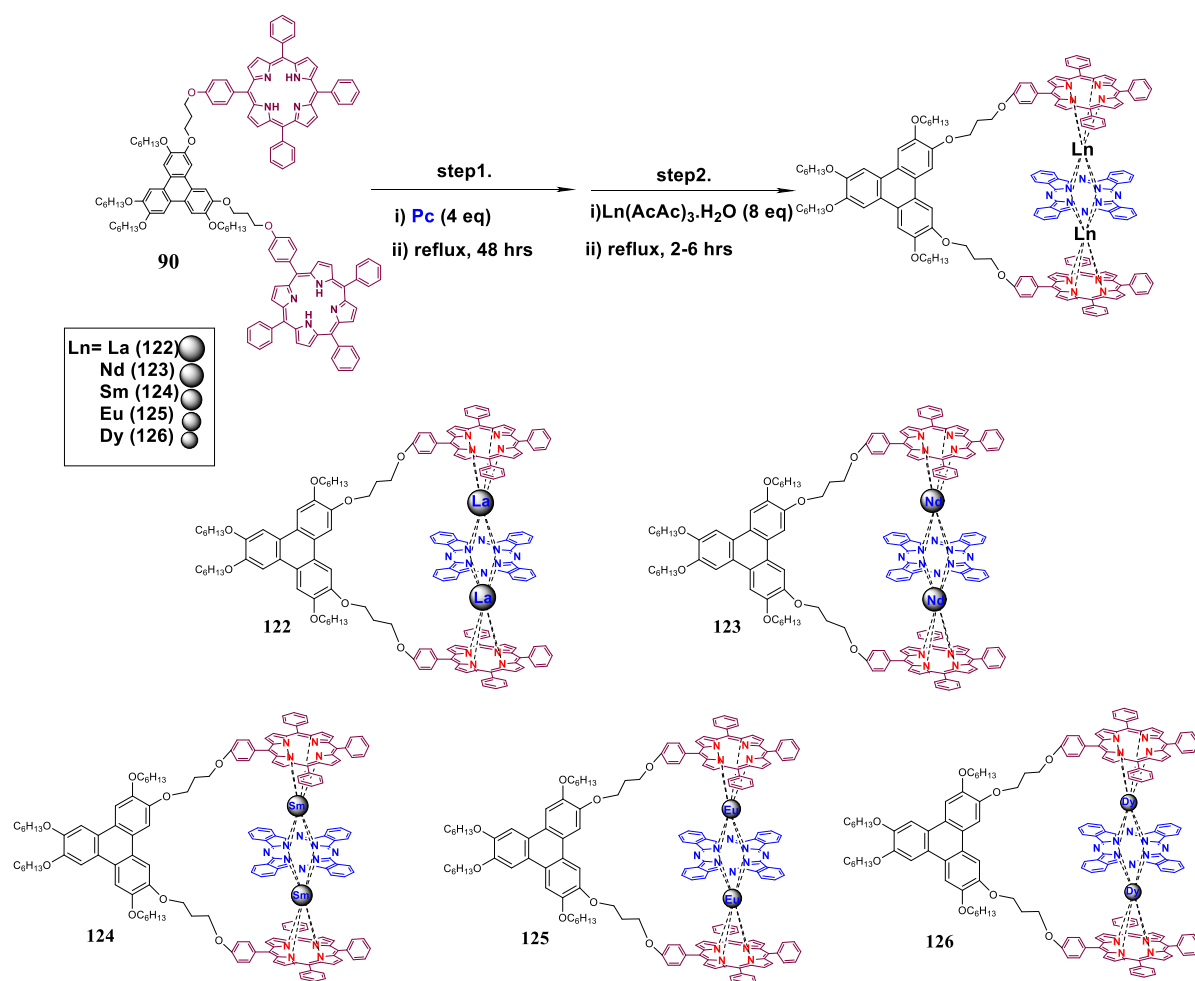


Figure 3.27. The spacing for 3,6-isomer **90**.

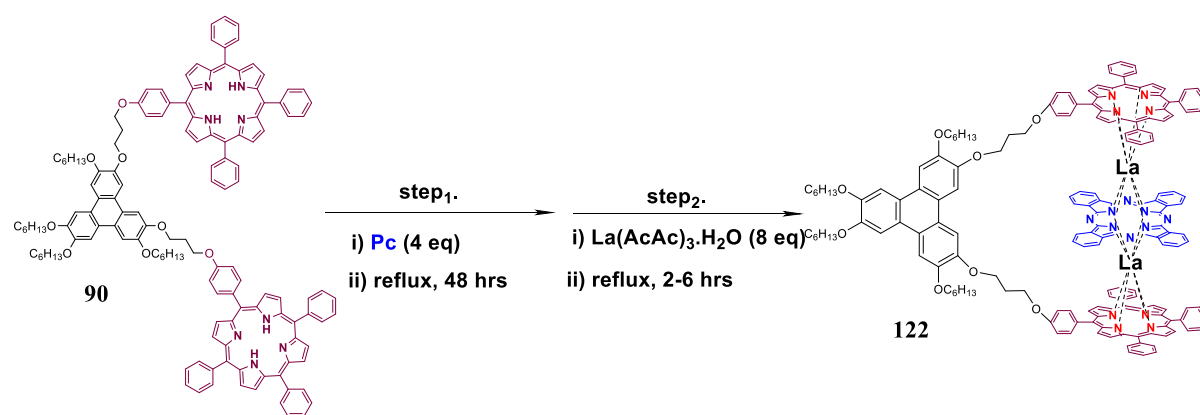
The same principles could then be applied to form the desired La, Nd, Sm, Eu and Dy *single* triple-decker complexes as illustrated in scheme 3.28 below.



Scheme 3.28. The reaction process for synthesizing a single triple-deckers **3,6-LnTD**.

3.3.4.1 Lanthanum triple-decker (3,6-LaTD) **122**

Applying the previously explained conditions for (2,3LnTD), a mixture of 3,6-*bis*(porphyrin)triphenylene model **90** (1 equivalent) with phthalocyanine (2 equivalents) were refluxed in 1-pentanol for 2 days. Following this, 4 equivalents of the La(acac)₃.H₂O were added to the reaction mixture and regularly checked by TLC. No TD was observed. Therefore, in the next attempt the amount of both the Pc **2** and the metal were doubled and pleasingly this led to successful formation of 3,6-*single* triple-decker after 2-6 hrs. Isolation was early achieved (as before) and 3,6-LaTD **122** was recrystallized using DCM:MeOH to obtain 51% yield, as shown in (Scheme 3.29)



Scheme. 3.29. 3,6-La triple-decker **122**.

Analysis of NMR spectra

By using ¹H and COSY NMR-spectroscopy, the chemical structure of the lanthanum triple-decker **122** was confirmed. ¹H NMR-spectra of lanthanum triple-decker **112** (for 2,3-isomer) and lanthanum triple-decker **122** (for 3,6-isomer) were similar. However, ¹H NMR of **122** complex demonstrated a clear pattern including two clear doublets of doublets of H_{mo'} (*meta*-outer) and H_{oo'} (*ortho*-outer) at 6.86 and 6.78 ppm which corresponded to the protons of the benzene rings (**A**), (Fig. 3.28).

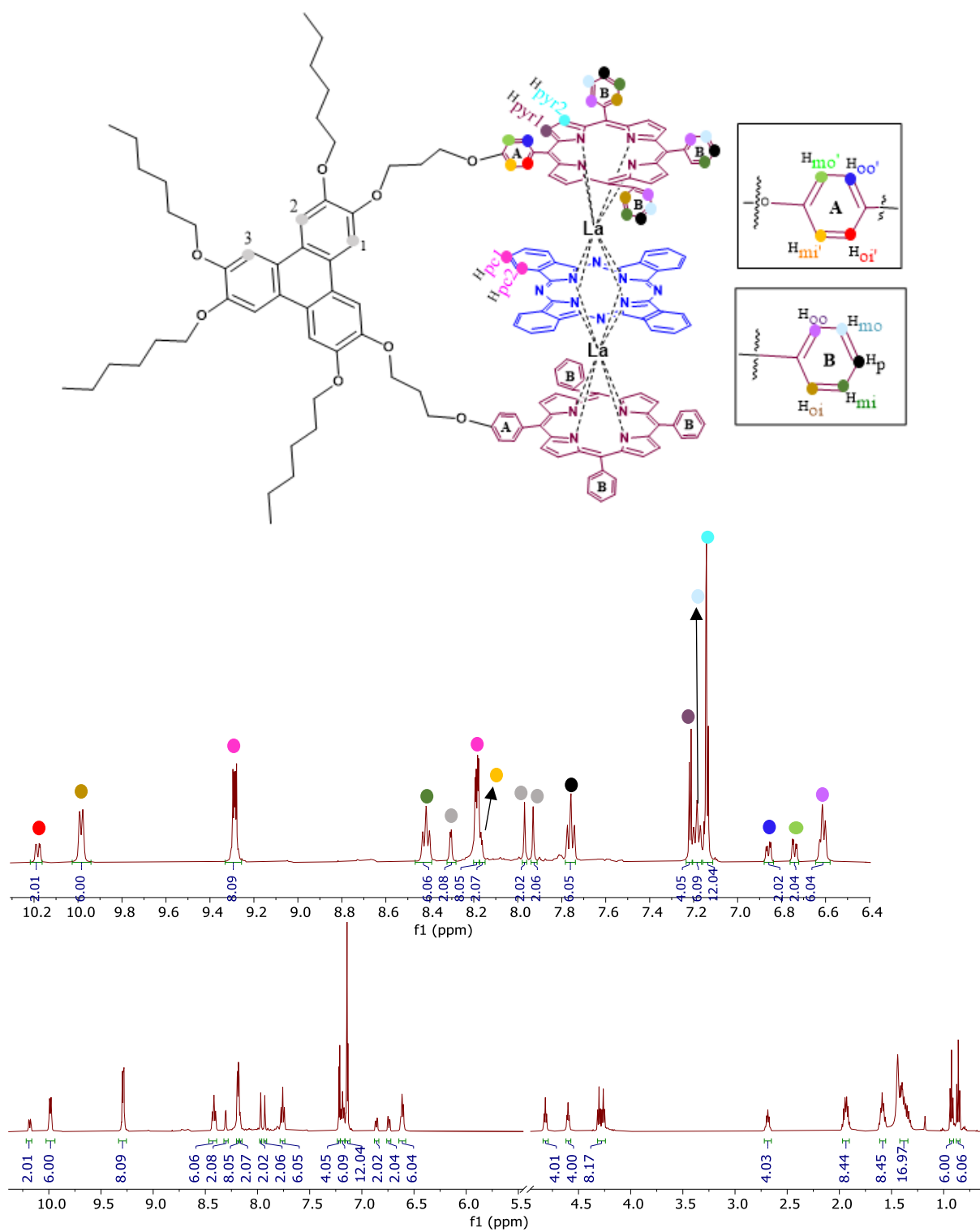


Figure 3.28. The ^1H NMR-spectrum of synthesizing complex **122** (500 MHz, CD_2Cl_2), expansion of 10.74-6.51 ppm aromatic area.

In order to provide additional proof that the detected signals correspond to the appropriate aromatic protons, 2D COSY NMR was performed. The COSY spectrum of **122** shows that the protons of H_{oi} at 9.08 ppm correlate to those of H_{mi} and vice versa. H_{mi} correlates with both H_p and H_{oi}. The pattern continues in this manner as shown in (Fig. 3.29).

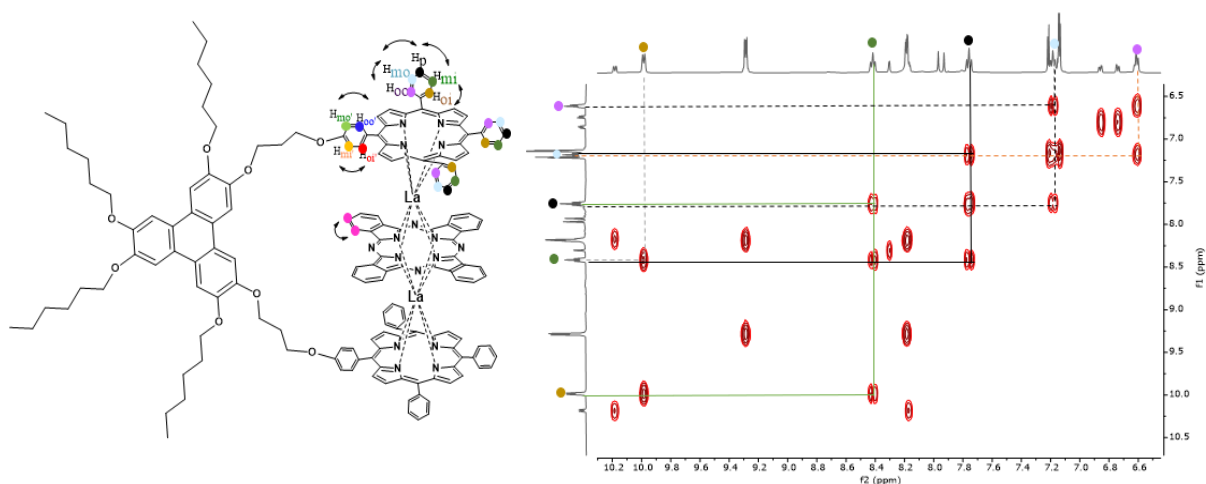


Figure 3.29. 2D COSY NMR 3,6-*bis*(porphyrin)triphenylene closed triple-decker **122**.

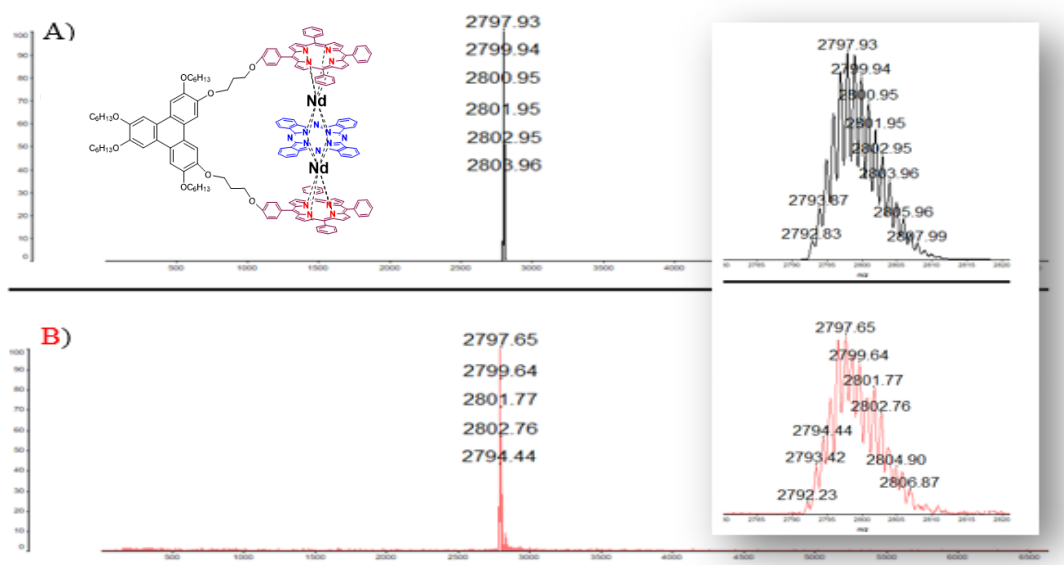
3.3.4.2 Neodymium, Samarium and Europium closed triple-decker ((3,6-NdTD)**123**, (3,6-SmTD) **124** and (3,6-EuTD) **125**, respectively)

The triple-decker of Nd, Sm and Eu were all successfully synthesised by using a modified conditions described above. Comprehensive spectroscopic techniques including MALDI-TOF-MS, NMR (¹H and COSY), UV and IR were employed to confirm these compounds, as reported in next part. Figure 3.28 below shows MALDI-TOF-MS data for this confirmation.

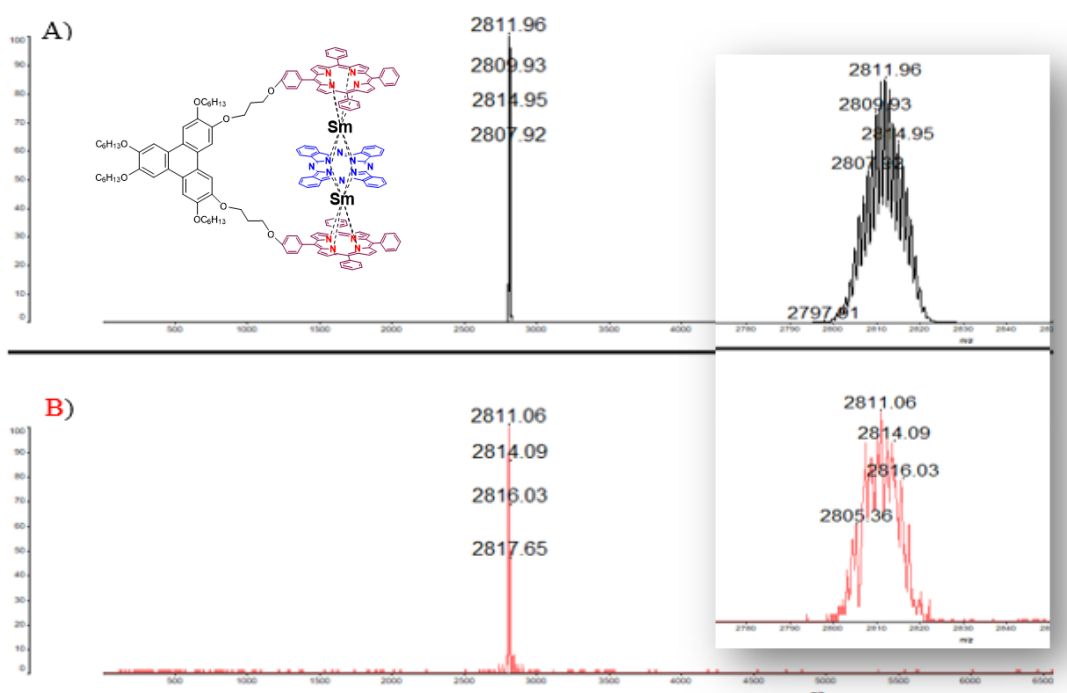
Based on their data, complexes with various metals exhibited distinct appearances especially in NMR and MALDI-TOF-MS spectroscopy. This is because they bonded to metals of different sizes, each having distinct paramagnetic level (ionic radii Nd³⁺ =98 pm (3e-), Sm³⁺ =96 pm (5e-), Eu³⁺ =95 pm(6e-)) that can impact differently on the molecular dimensions and influencing the overall behaviour of the system.

Here, MALDI-TOF-MS spectra shows an example of different isotopes pattern for each complex, (Fig. 3.30).

Nd- **triple-decker 123**; MALDI-TOF-MS analysis which displayed the molecular ion m/z 2797.65 $[M]^+$, $[C_{168}H_{140}Nd_2N_{16}O_8]^+$, calc.: 2797.93.



Sm- **triple-decker 124**; MALDI-TOF-MS analysis which displayed the molecular ion m/z 2811.06 $[M]^+$, $[C_{168}H_{140}Sm_2N_{16}O_8]^+$, calc.: 2811.96.



Eu- **triple-decker 125**; MALDI-TOF-MS analysis which displayed the molecular ion m/z 2814.82 $[M]^+$, $[C_{168}H_{140}Eu_2N_{16}O_8]^+$, calc.: 2814.96.

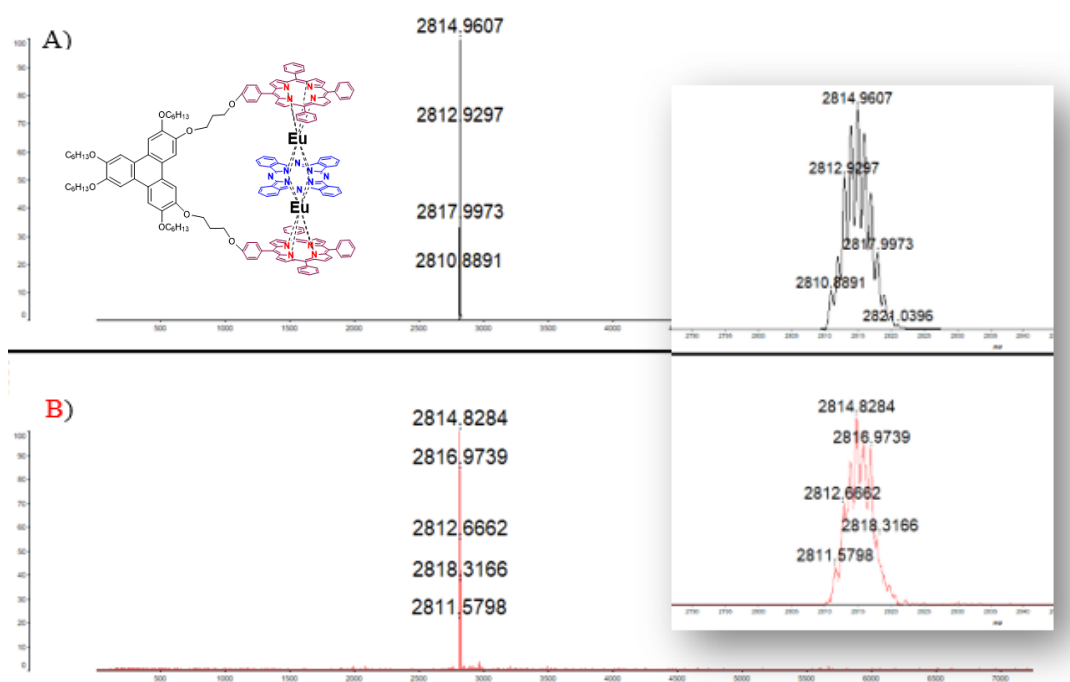


Figure 3.30. MALDI-TOF-MS obtained for 3,6-Nd, Sm and Eu- triple-decker **123**, **124** and **125**. The inset shows (B) obtained and (A) theoretical isotopic patterns.

3.3.4.3 Dy triple-decker (3,6-DyTD) **126**

Unfortunately, dysprosium metal failed once again to produce a triple-decker complex **126** due to its small-sized.

3.3.5 The spectroscopic characterization comparison

TDs formation was straightforward for La, Pr, Nd, Sm and EuTDs with full spectroscopic characterisation. However, the spectroscopic analysis of the two TD isomers, using same metals did not reveal any practically distinct signals that could be used to distinguish between the 2,3 or 3,6 formation modes.

3.3.5.1 Comparing between (2,3-LaTD) **112** with (3,6-LaTD) **122**

In this example, the ^1H NMR-spectra of both isomeric TD, utilizing the Lanthanum ion (2,3-LaTD) **112** and (3,6-LaTD) **122**, exhibited highly comparable splitting peak patterns. However, slight differences were observed in the appearance and positioning of these signals, for triphenylene signals (1,2,3); for the outer phenyl protons of the porphyrins ($\text{H}_{\text{m}o'}$ and $\text{H}_{\text{o}o'}$), as illustrated (Fig. 3.31).

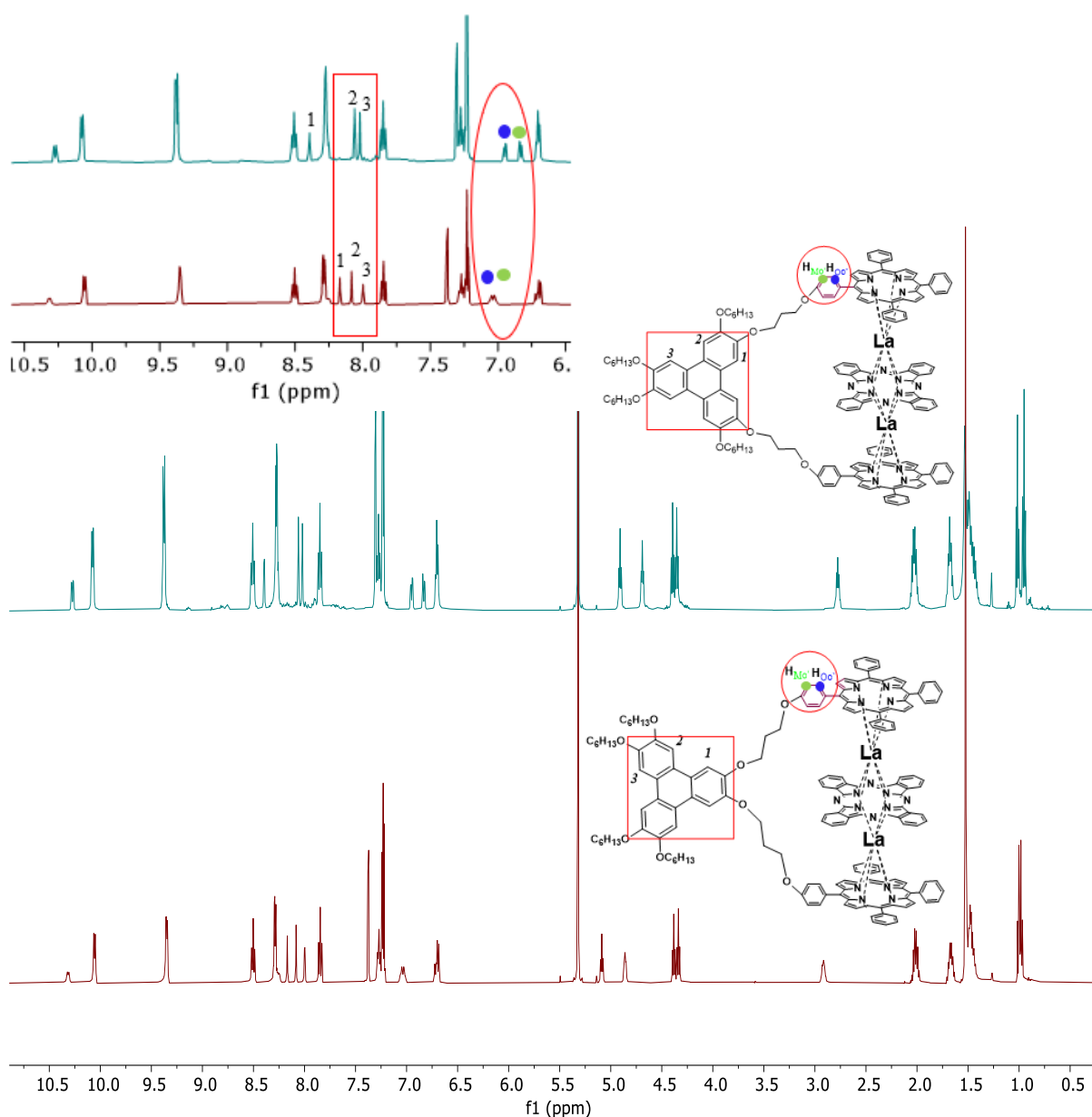


Figure 3.31. ^1H NMR-spectroscopy comparison between (2,3-LaTD) **112** with (3,6-LaTD) **122**.

3.3.5.2 Comparing between (2,3-EuTD) **120** with (3,6-EuTD) **125**

Another example, the ^1H NMR-spectra of both **120** and **125**, exhibited also highly comparable splitting peak patterns, Pc core signals ($\text{H}_{\text{Pc}1,2}$) for both TDs were observed at 12.94 and 10.07 ppm, as shows (Fig. 3.32). However, Europium metal showed minor variations, though not enough to give considerable confidence in identifying the isomer that might be produced from final target reaction.

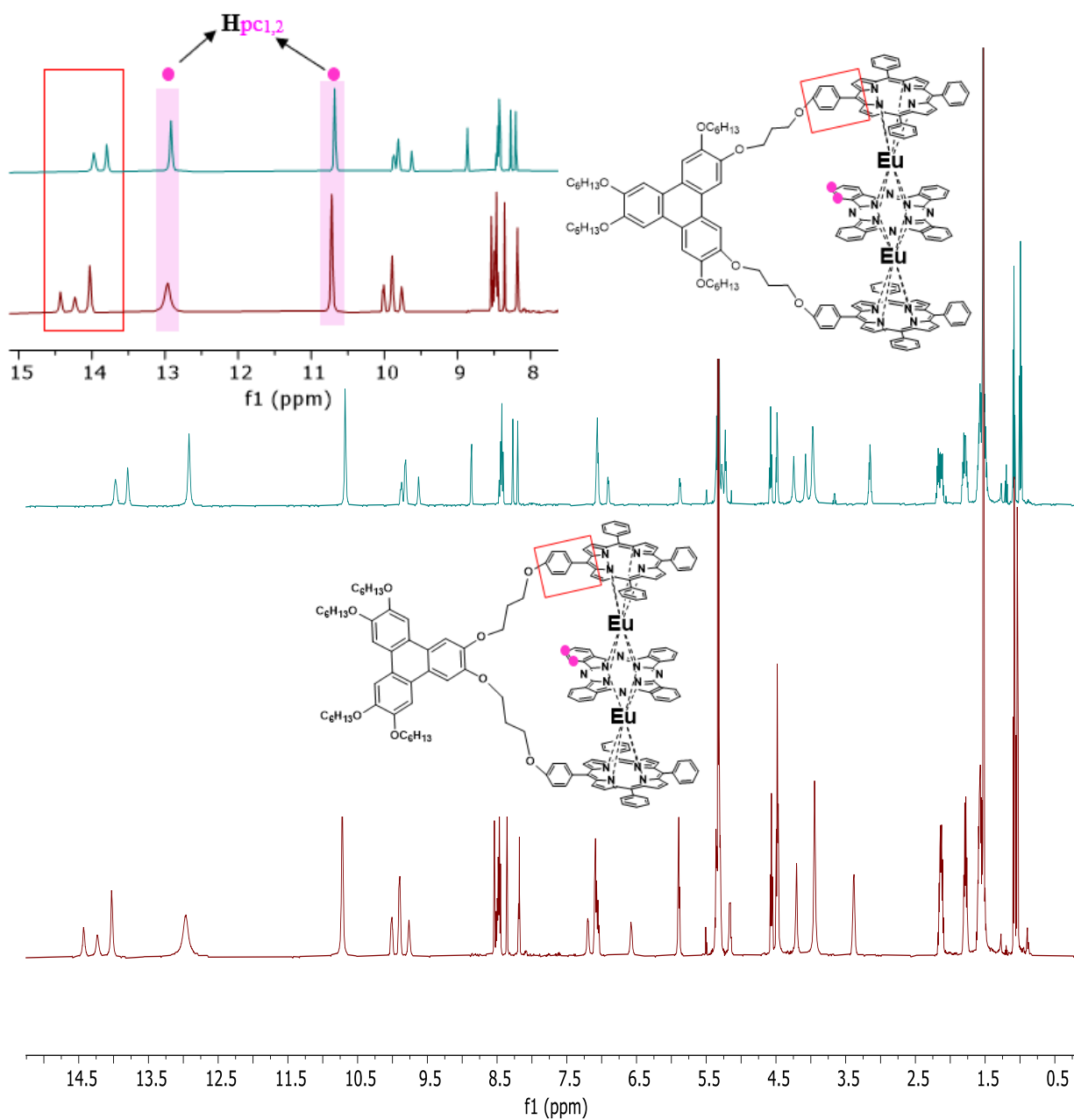


Figure 3.32. ¹H NMR-spectroscopy comparison between (2,3-EuTD) 120 with (3,6-EuTD) 125.

Conclusion

According to the synthesis results, it can conclude that both 2,3- and 3,6-isomeric *single* triple-deckers (using big or small metal size) were successfully synthesized and fully characterized with similar yields, and no significant differences were observed in stability between these triple-deckers in terms of metal size. It was expecting that by moving to smaller metals, there would be differences in stability, potentially resulting in reduced stability or the non-formation of one isomer. However, the failed attempt to use dysprosium metal was not a surprising result, given its small size. Furthermore, dysprosium metal did not work with the normal triple-decker reported by Cammidge's group. Unfortunately, the spectroscopic characterization for the two sets of TD isomers did not highlight any specific signals that could be used to identify linking mode in the target *hexa*-system.

3.4 TD formation study

As mentioned earlier, the direct synthesis did not reveal significant differences in metal size affecting the outcomes on their reactivities or stabilities. To understand the reactivity of porphyrins with lanthanide ions and determine levels of synthetic control, the two previously discussed isomers of novel triple-decker assemblies, containing various metals, will be used for three types of experiments aimed at investigating the selectivity and stability of these complexes.

3.4.1 Transmetallation using a different lanthanide ions

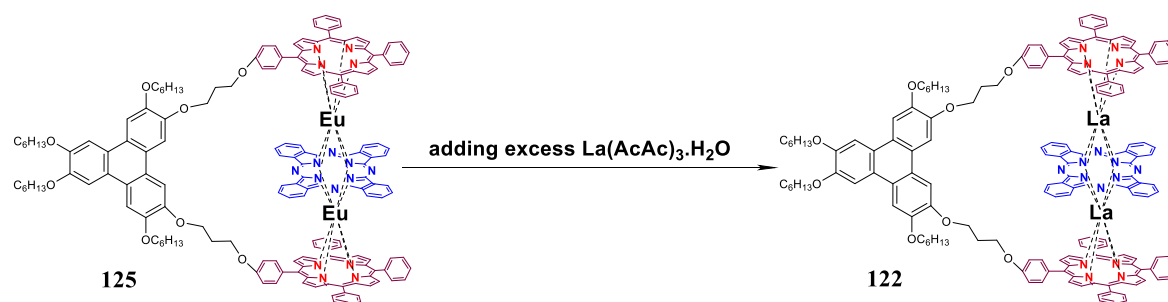
3.4.2 Transmetallation using a mixture of lanthanide ions

3.4.2.1 Distribution study (using 2,3 and 3,6-TD systems)

3.4.3 Mixed isomers experiment.

3.4.1 Transmetallation using a different lanthanide ions

In order to evaluate the stability of the 3,6-La-TD and 3,6-Eu-TD complexes previously synthesised, a metal exchange reaction was attempted. 3,6- Eu-TD was treated with an excess of $\text{La}(\text{acac})_3 \cdot \text{H}_2\text{O}$ under the standard reaction conditions of refluxing up to 24 hrs in 1-pentanol (Scheme 3.30).



Scheme 3.30. Exchange reaction of europium (**125**) to lanthanum (**122**) in 3,6-EuTD.

During this process, the europium metal ion was expected to be exchanged by lanthanum metal. The ^1H NMR-spectra of the La and Eu derivatives are conveniently distinct. Figure 3.33, displays the full ^1H NMR-spectra for both 3,6-LaTD (Fig. 3.33 (a)) and 3,6-EuTD (Fig. 3.33 (b)), highlighting the distinct signals in the aromatic region before applying transmetallation experiments. For instance, the ^1H NMR-spectrum of the 3,6-LaTD complex exhibited signals, around 10.18 ppm, whereas in the case of 3,6-EuTD, an even higher region that shifted up to around 14.52 ppm was observed.

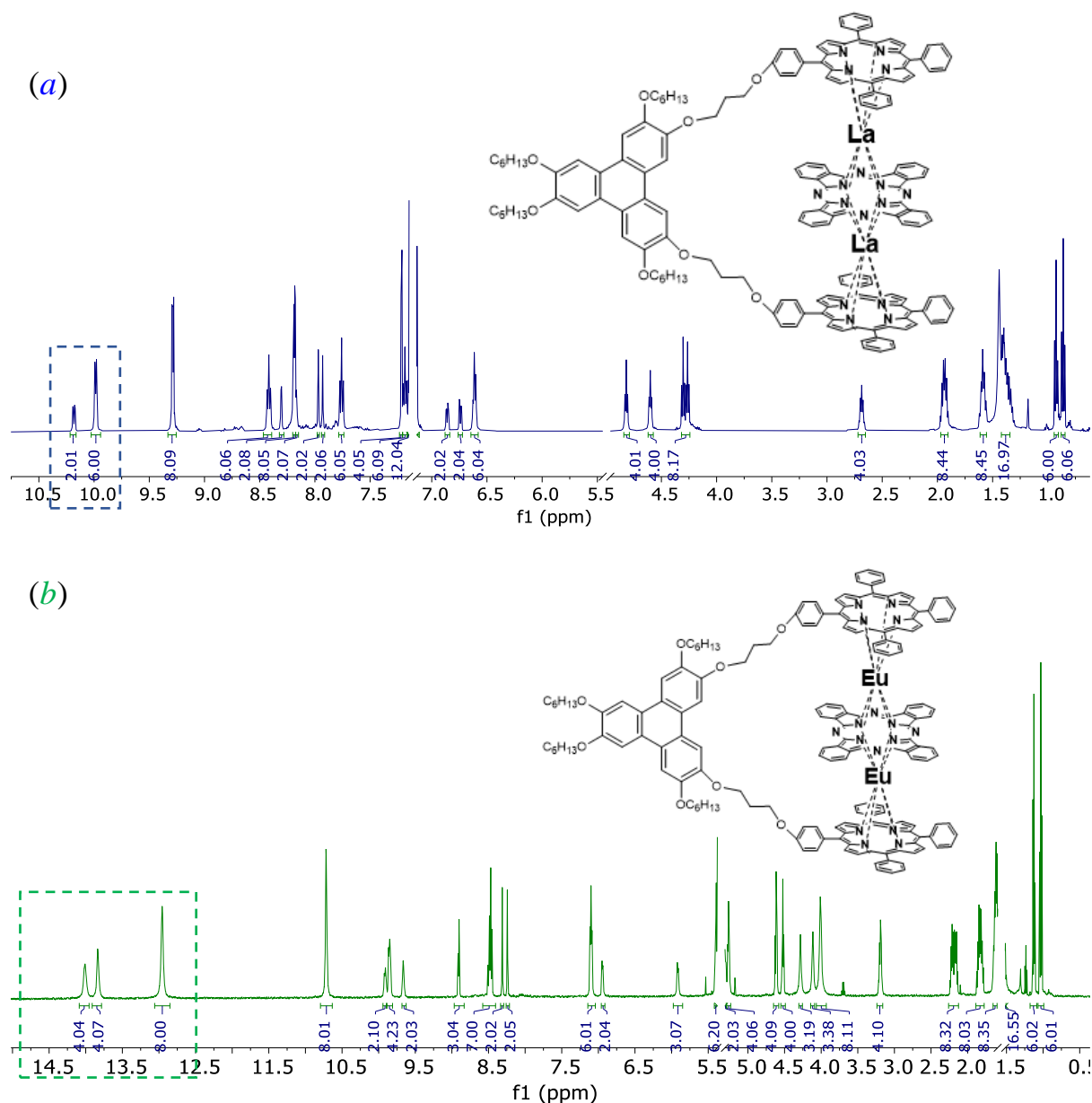


Figure 3.33. ^1H NMR-spectra for 3,6-LaTD (a) and 3,6-EuTD (b).

The metal exchange reaction was attempted, and reactions were therefore monitored by ^1H NMR-spectroscopy. All peaks corresponding to 3,6-EuTD **125** in the aromatic region (14.52-12.97ppm) would disappear and the peaks corresponding to 3,6-LaTD **120** should be observed (Fig. 3.34).

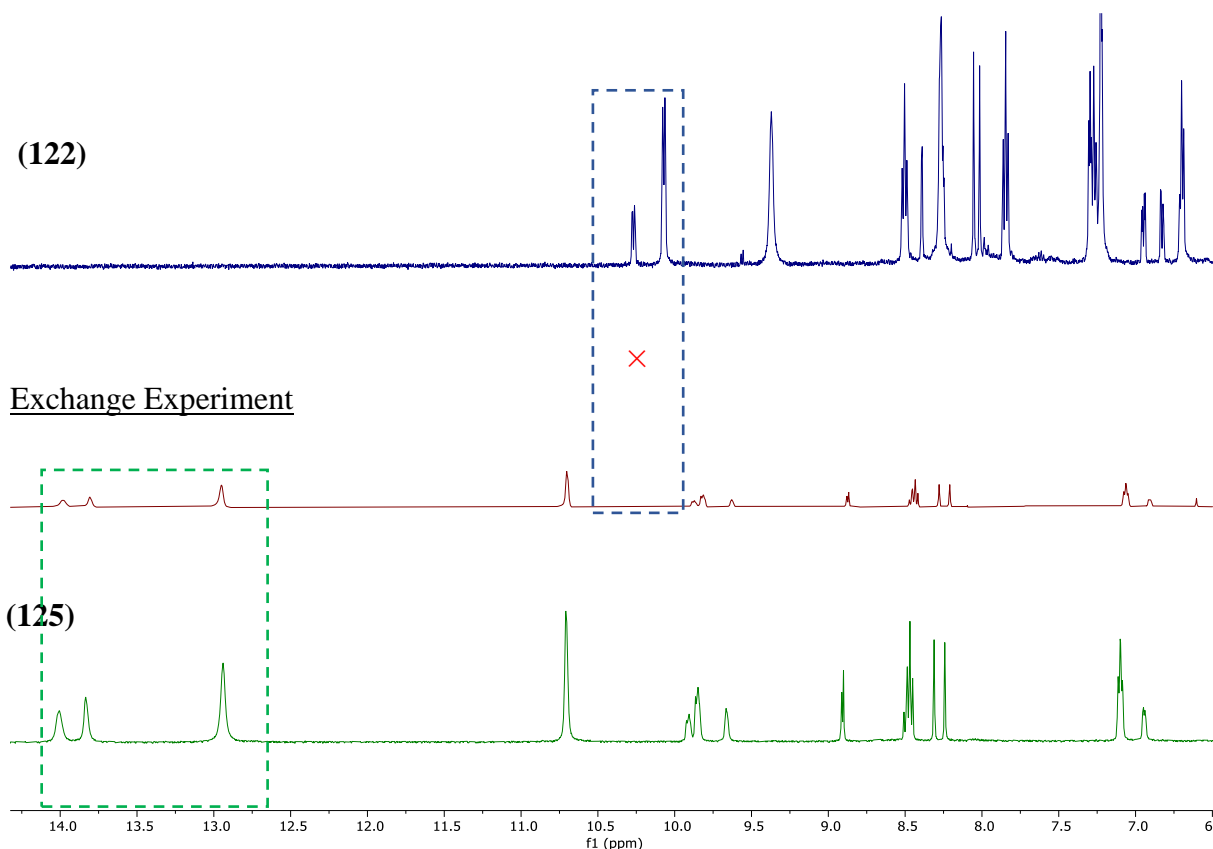


Figure 3.34. Comparing ^1H NMR-spectra for 3,6-EuTD (**125**) down, and 3,6-LaTD (**122**) up with an aliquot from the exchange experiment middle after reflux for 24 hrs (500 MHz, CD_2Cl_2), expansion of 14.5 - 6.00 ppm aromatic area.

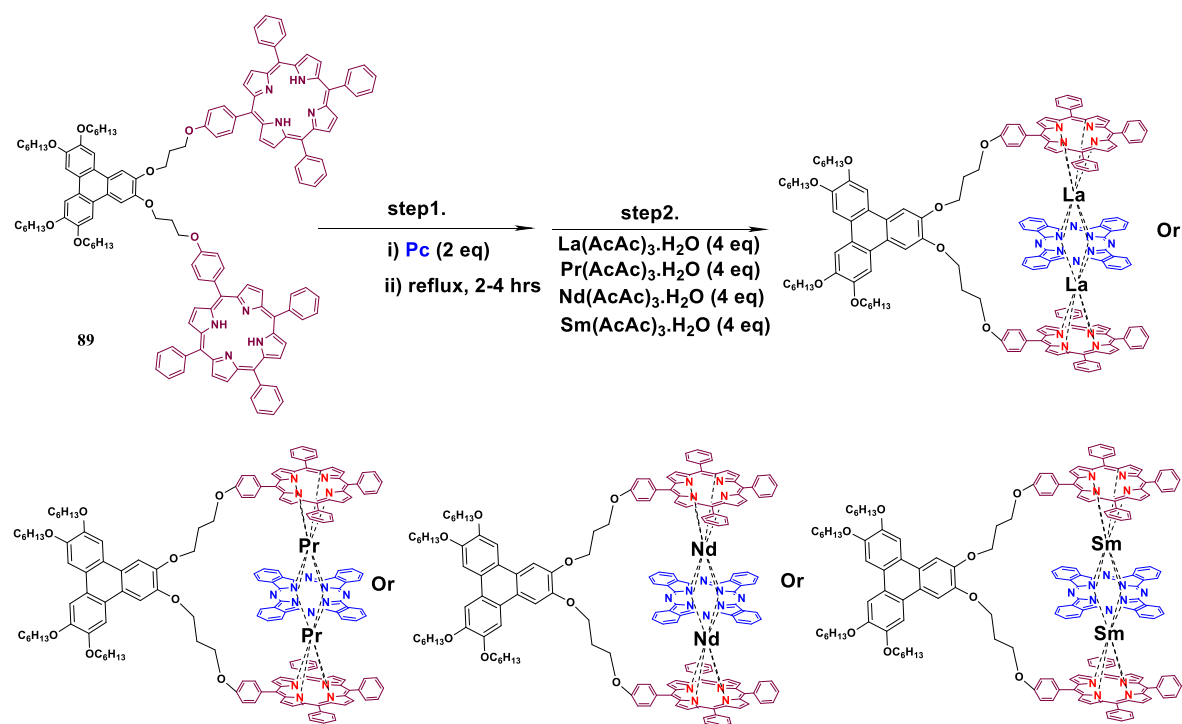
Unexpectedly, based on the ^1H NMR-spectra results, no exchange of Eu metal for La was observed. In the next attempt, 3,6-EuTD (whilst maintained in the original NMR tube) was heated and refluxed in 1,1,2,2-tetrachloroethane TCE- d_2 D at 250°C in the presence of excess of La metal. Unfortunately, no changes were recorded. The same process was also attempted using 2,3-EuTD. However, no changes were observed here either. These results indicated that the europium metal ion cannot be displaced by lanthanum metal ion in these systems under the standard reaction conditions.

It was therefore concluded that both 2,3 and 3,6- europium triple-decker complexes were robust and stable. Therefore, selective synthesis could not be achieved for this set of triple-deckers based on thermodynamic equilibration. The same reaction was not attempted the other way around (e.g., La displacing Eu), because the stability of La-TD is higher than Eu-TD, as previously recorded ¹⁴⁹.

3.4.2 Metallation using a mixture of lanthanide ions

3.4.2.1 Distribution study (using 2,3 and 3,6-TD complexes)

As the metal of La did not displace Eu metal, TD complex was investigated to show a preference for any lanthanide in the series. Therefore, a combination metals experiment was performed to observe if one of the metals forms TD complex faster than the others, as illustrated in (Scheme 3.31).

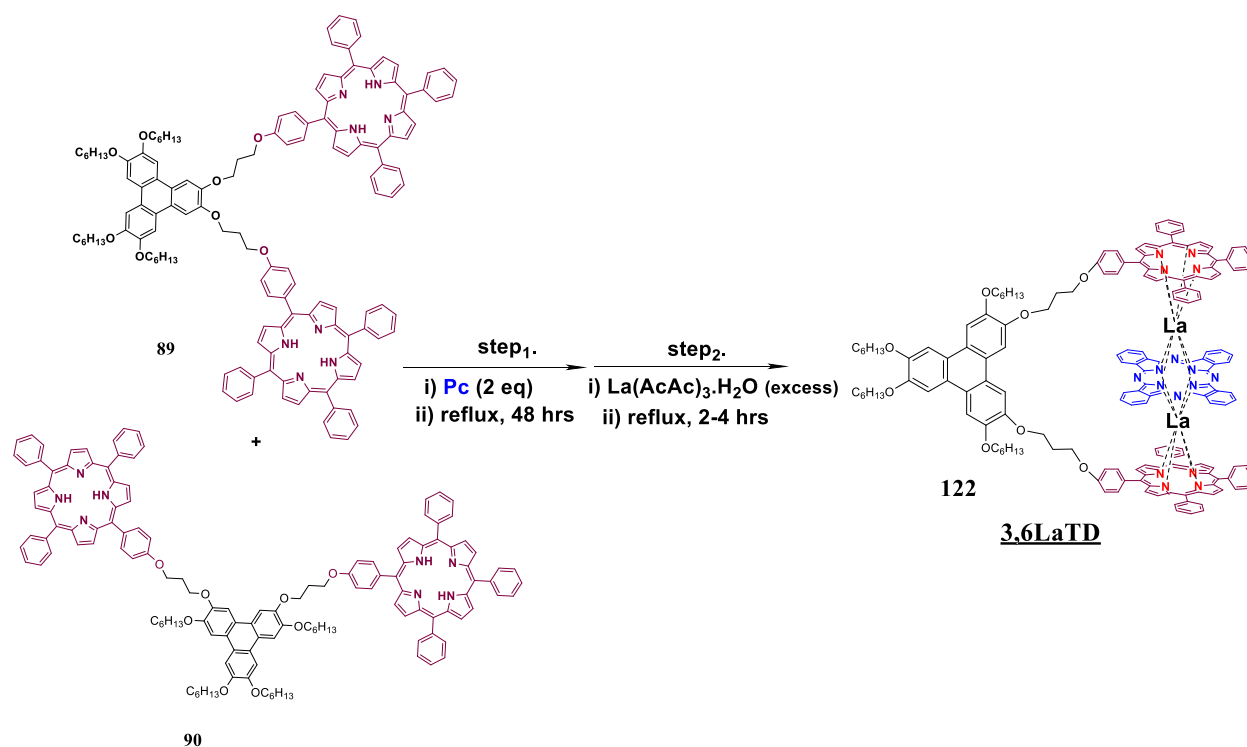


Scheme 3.31 General procedure for the combination metals experiment, to assess selective synthesis of one metal triple-decker.

The reaction was performed under the same conditions as previously described, however, four metal salts were combined. The mixture of 2,3-bis(porphyrin)triphenylene **89** and Pc **2** in 1-pentanol was refluxed overnight, then the excess of metal salts (La, Pr, Nd, and Eu(acac)₃.H₂O) were added. The crude mixture sample was analysed by MALDI-TOF-MS. Here, no distinct triple-decker relative mass could be identified, due to a mixture of metal TD complexes being present. Therefore, it was concluded that 2,3 or 3,6- TDs complexes were not lanthanide metal-selective. In other words, neither 2,3- or 3,6- porphyrins demonstrated a preference for forming a single complex.

3.4.3 Mixed isomers experiment

As the previous approach did not selectively synthesise TDs, one metal and a mix of 2,3- and 3,6- isomers were used to assess whether the selectivity, instead of using a mix of metals as shown in (Scheme 3.32). In this experiment, the aim was to observe if one of the isomers produces a *single* triple-decker more efficiently than the others, providing the desired selectivity crucial for achieving our project objectives.



Scheme 3.32. Selective reaction of mixed isomers.

The mixture of 2,3- and 3,6- isomers (1:1 equivalent) with Pc (2 equivalents) in 1-pentanol were refluxed overnight, then an excess of La(acac)₃.H₂O was added and refluxed for 2-4 hrs. TLC showed a new green spot formed. It was isolated (as described before with normal TD formation) and analysed by ¹H NMR-spectroscopy. It was found that only the 3,6-TD-complex had been successfully and exclusively formed. There was no sign for the formation of 2,3-TD-complex as illustrated below in (Fig. 3.35).

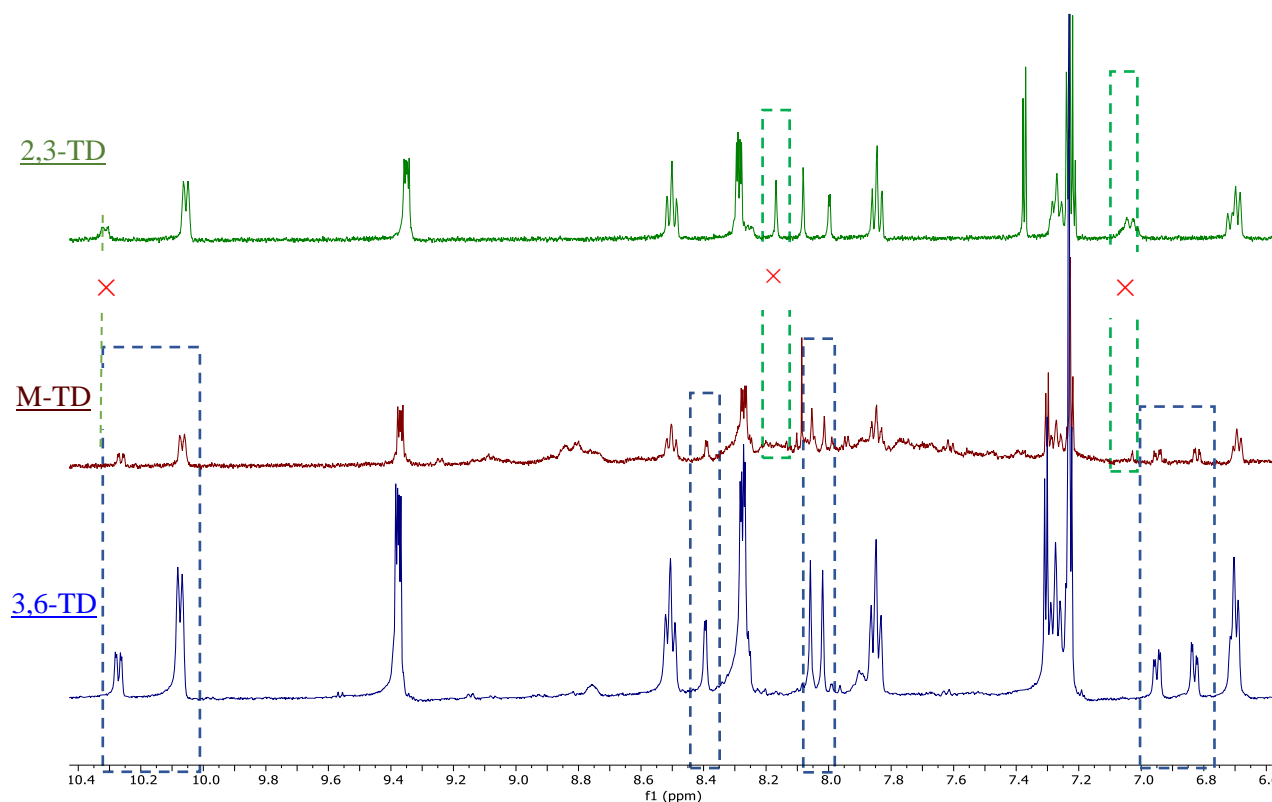


Figure 3.35. Comparing ^1H NMR spectra for 2,3 triple-decker complex **above**, and 3,6 triple-decker complex **down** with the mixed isomers experiment result **middle** (500 MHz, CD_2Cl_2), expansion of 10.45-6.55 ppm aromatic area.

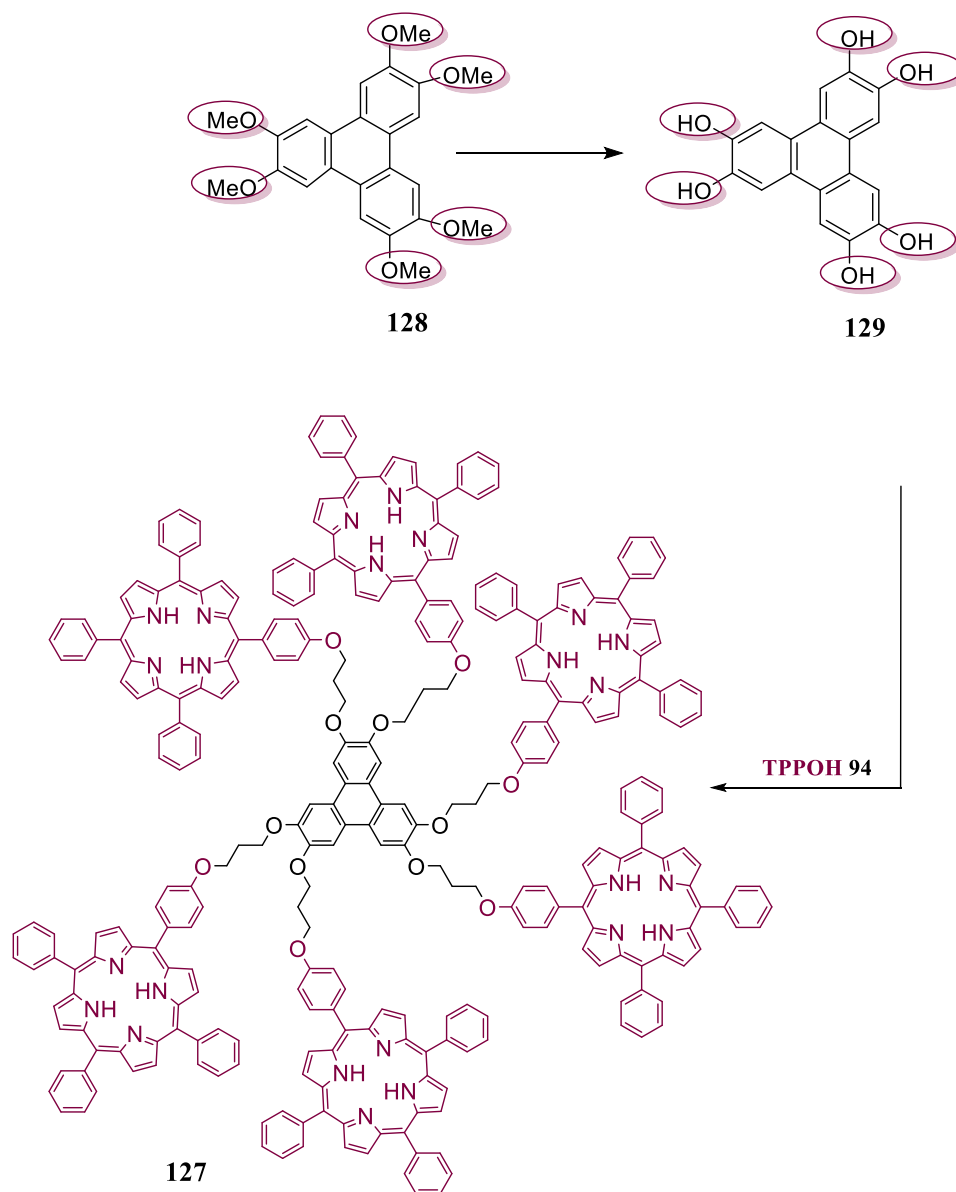
Figure 3.30 above displays three spectra; **2,3-LaTD** spectra shows three main peaks at 10.25, 8.16 and 7.04 ppm, however these are absent in **M-TD** spectra of mixed isomers experiment. Whereas the four peaks unique to **3,6-LaTD** spectra were recorded in the **M-TD** spectra. The newly shared signals at 10.27, 6.95 and 6.38 ppm can be assigned to the porphyrin units. The signals at 8.39, 8.06, 8.02 ppm which are assigned to the triphenylene core can also now be found in both spectra.

3.4.4 Conclusion

It appears that the mixed reaction of 2,3- and 3,6-isomers with Pc and Lanthanum salt leads exclusively to 3,6-LaTD complex. This is useful result for the successful progression of this project.

3.5 Synthesis of *hexa*-(porphyrin) triphenylene system **127**

After successfully synthesising *single* isomeric triple-deckers and assessing their synthetic control, the synthesis of the *hexa*-system itself was begun. The synthesis of the required triphenylene *hexa*-porphyrin is shown in (Scheme 3.33).

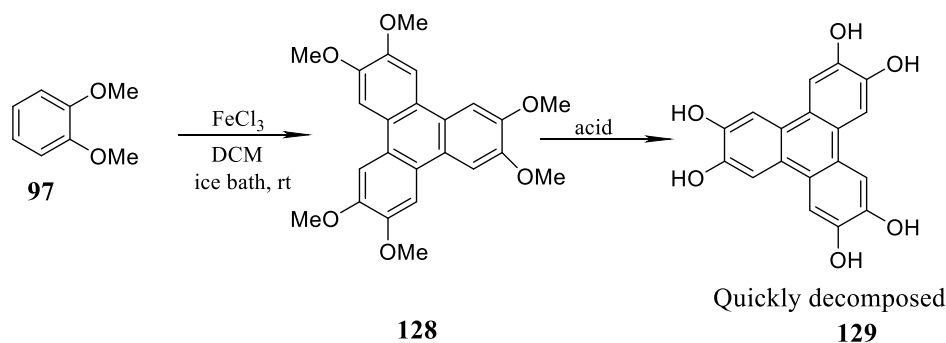


Scheme 3.33. Proposed synthesis of *hexa*-(porphyrin) triphenylene system **127**.

3.5.1 Preparation of triphenylene core

3.5.1.1 Synthesis of *hexa*-(hydroxy) triphenylene **129**

The symmetrical triphenylene core can simply be synthesised by cyclising veratrole to create *hexa*-(methoxy) triphenylene **128** and then deprotecting the methoxy groups to form *hexa*-(hydroxy) triphenylene **129** as shown in scheme 3.34.



Scheme 3.34. General synthesis of *hexa*-(hydroxy) triphenylene **129**.¹⁸⁹

Veratrole **97** was easily cyclised into *hexa*-(methoxy) triphenylene **128** using iron(III) chloride in DCM. Then, the resulting product was precipitated and recrystallized to give the product in 30% yield. Next, *hexa*-(hydroxy) triphenylene **129** was synthesised by deprotection of triphenylene **128** applying acid. The deprotection was first carried out by refluxing in a mixture of HBr and acetic acid (1:1). The demethylation was successful, but the product unfortunately quickly decomposed during the work up. The product **129** was decomposed directly to a black solid, even when a clean ^1H NMR spectra was observed. This is because compounds with multiple hydroxy groups are prone to oxidative decomposition.¹⁹⁰

^1H NMR-spectra of *hexa*-(methoxy) triphenylene **128** demonstrated a sharp singlet peak of Ha at 4.12 ppm for 18H of methoxy group and this peak disappeared due to the formation of *hexa*-(hydroxy) triphenylene **129** (Fig. 3.36).

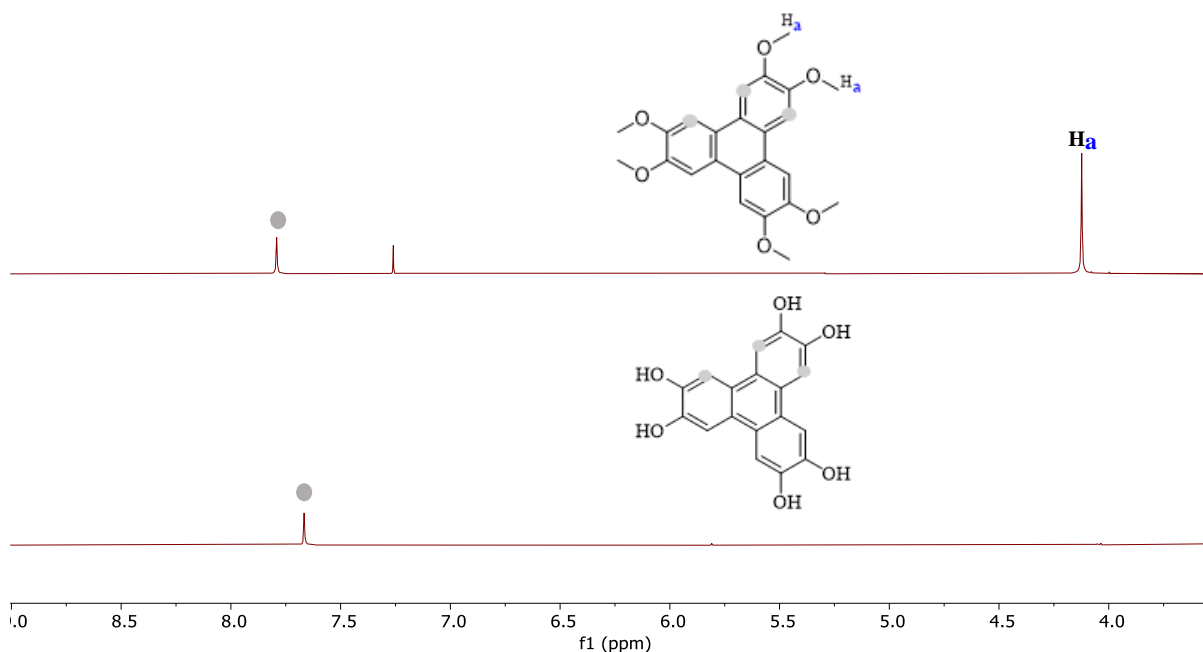
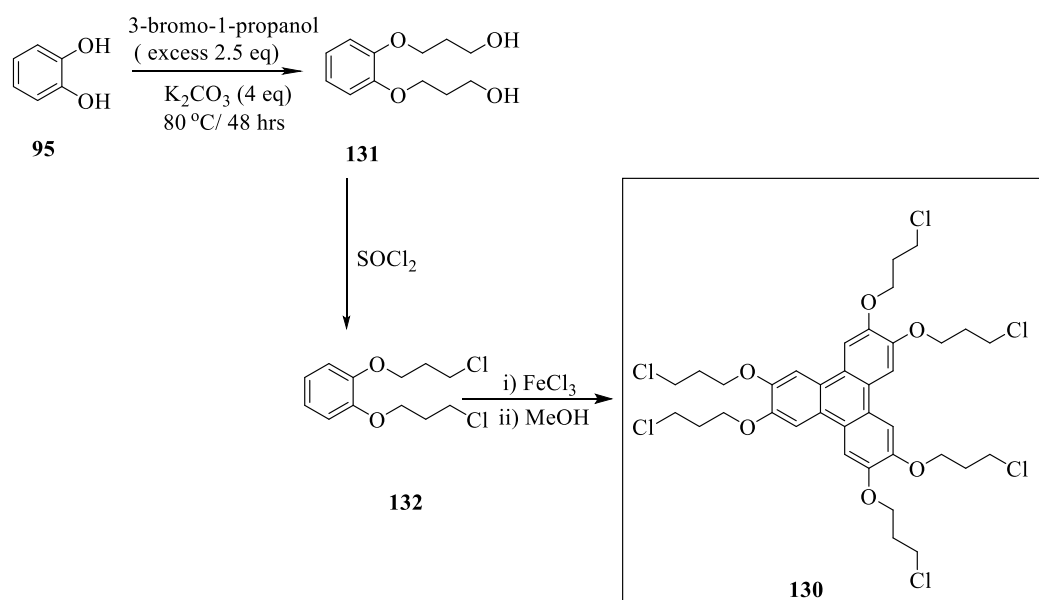


Figure 3.36. ^1H NMR-spectra for both triphenylenes **128** and **129**.

3.5.1.2 Synthesis of 2,3,6,7,10,11-Hexa-(3-chloropropoxy)triphenylene **130**

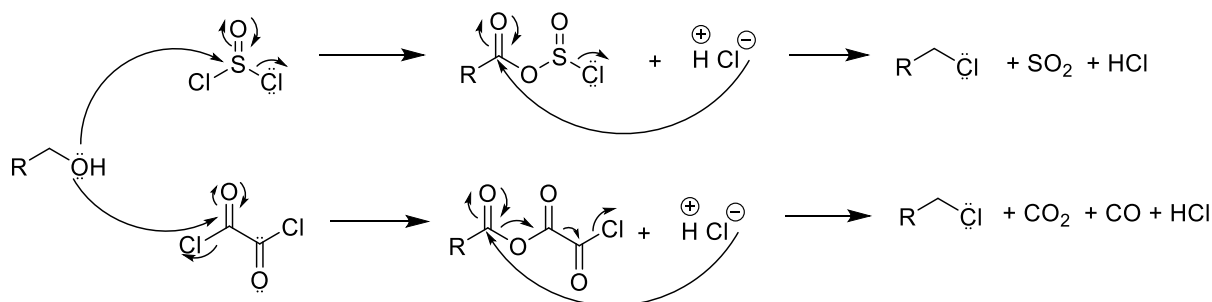
The core can be formed following a stepwise synthesis, as shown in scheme 3.35.



Scheme 3.35. Synthesis of the final triphenylene core **130** via stepwise process.

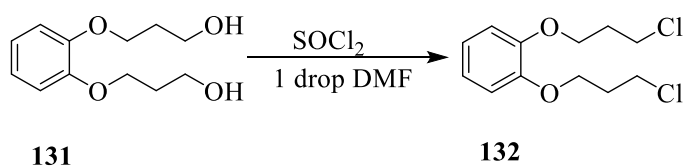
The first step was performed by reacting catechol **95** and excess 3-bromo-1-propanol in refluxing EtOH, with K_2CO_3 . The reaction mixture was then distilled and recrystallized to give **131** in 80% yield.

The second step involved the conversion of the hydroxy groups into halides. Scheme 3.36, provides a summary of the typical mechanism for activating acids using thionyl or oxalyl chloride.¹⁹¹



Scheme 3.36. Using oxalyl or thionyl chlorides to produce acyl chlorides.¹⁹¹

Accordingly, product **131** was converted to chloride product **132** by applying activation agents such as thionyl chloride (Scheme 3.37).



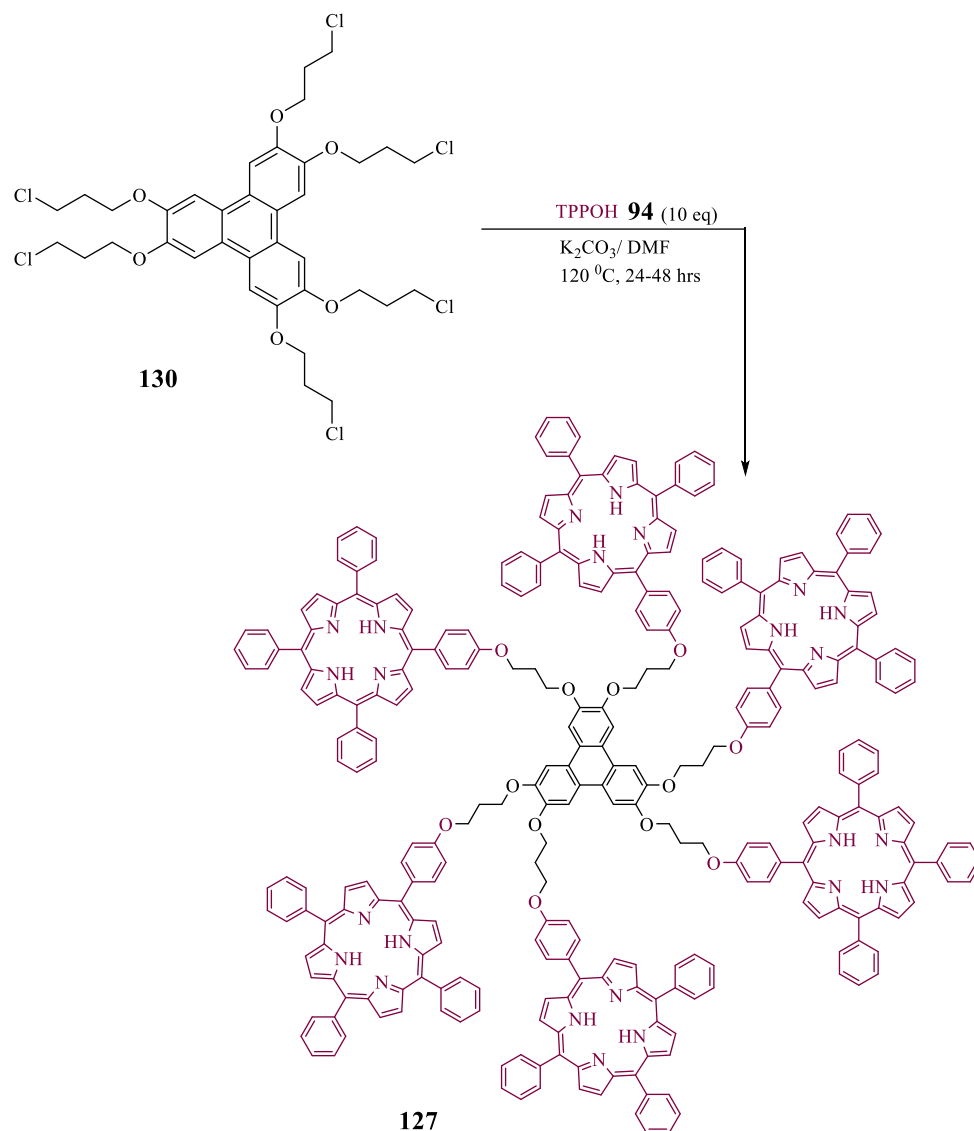
Scheme 3.37. Converting compound **131** to compound **132**.

o-Bis((3-hydroxypropyl)oxy)benzene **131** and thionyl chloride were refluxed in dry DCM under N_2 . One to two drops of DMF were added and left to reflux overnight. The product was filtered through a pad of silica to yield a colourless oil of **132**, 77%.

Finally, product **132** was then cyclised easily using $FeCl_3$ in DCM as described before, to produce 70% of the desired 2,3,6,7,10,11-*hexa*-(3-chloropropoxy)triphenylene **130** as white solid.

3.5.2 Synthesis of *hexa*-(porphyrin) triphenylene **127**

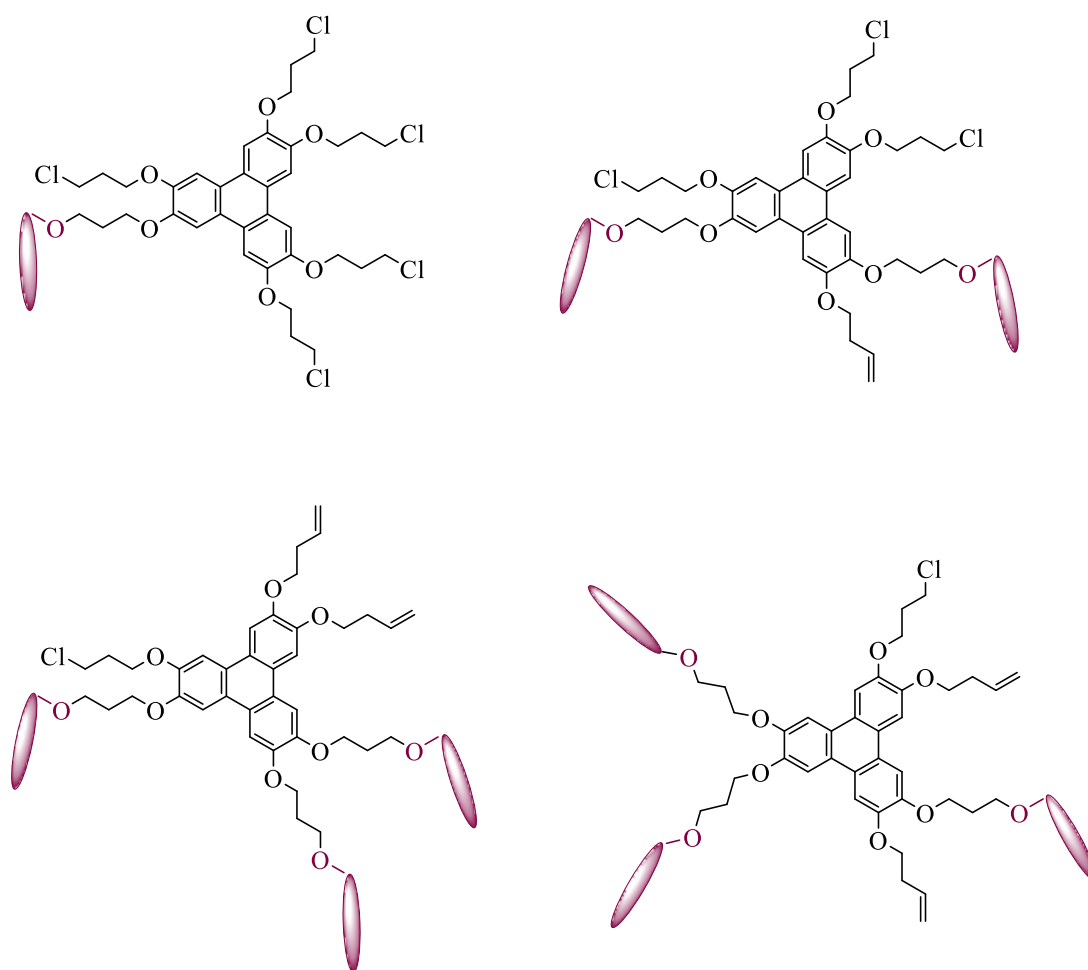
The six chromophores of porphyrins **94** can be now attached to final triphenylene core **130** by simple alkylation reaction S_N2 , as shown in (Scheme 3.38).



Scheme 3.38. New route for synthesis *hexa*-(porphyrin) triphenylene system **127**.

Multiple attempts were made to synthesise *hexa*-(porphyrin) triphenylene **127** by reacting the triphenylene core **130** with an excess of TPPOH **94**, utilising K_2CO_3 as a base, with DMF as the solvent.

It is more challenging to combine six chromophores with a central core to create a single molecule. The crude of the reaction was checked by TLC, which displayed many spots, suggesting many mixed by-products (Scheme 3.39).



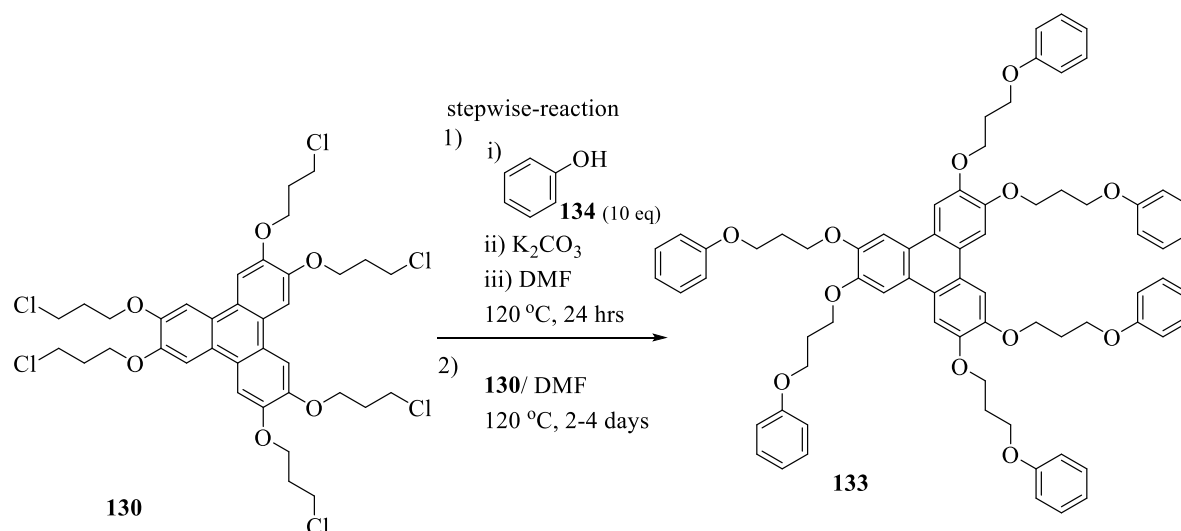
Scheme 3.39. Examples of side products which can be formed.

3.5.2.1 Optimisation procedure for the formation of target compound 127

For the chromophores to be attached to the triphenylene core **130**, at least 6.5 equivalents must be present. Therefore, a commercial product was tested instead of the **TPPOH 94**, to assess whether the triphenylene core could work under the conditions for making target compound.

3.5.2.1.1 Attempted synthesis of compound 133(test reaction)

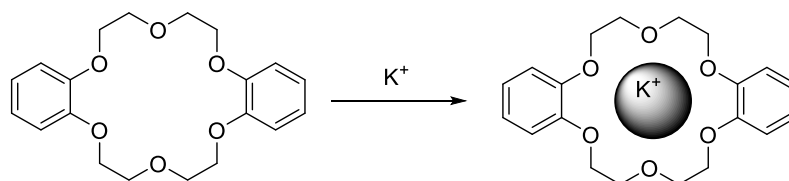
These same reaction conditions as before were used, but in this instance, the phenol molecule **134** was used in place of **TPPOH** (Scheme 3.40).



Scheme 3.40. Synthesis of compound **133** as tester.

A similar reaction was performed by refluxing triphenylene core **130** with a large excess of phenol **134** with K_2CO_3 in DMF. After 24 hrs of reflux, the crude mixture was analysed by MALDI-TOF-MS, which showed several peaks but only one tiny signal that belonged to the target substance. the decision was made to give the reaction a few more days to finish, but this had no further impact on the amount of product that formed. Along with the unreacted starting material (phenol), the products from elimination were increasing.

To prevent this elimination, a second attempt was performed by first modifying the reactions from a “one-pot” reaction to a “two-stepwise” reaction. An excess of phenol with K_2CO_3 was refluxed in DMF. This was followed by the addition of dibenzo-18-crown-6 as template^{192, 193} which interacts with K^+ in the solution as shown in (Scheme 3.41).



Scheme 3.41. Using dibenzo-18-crown-6 as template.¹⁹³

After refluxing of the mixture for 24 hrs, a solution of triphenylene core in DMF was added to the reaction mixture and left to react for 3 days. The MALDI-TOF-MS spectrum displayed a sharp peak that corresponded to the target product **133**, demonstrating the connection of triphenylene with six phenol units. Because there was no longer the elimination side effect, the reaction was stopped and purified by column chromatography

to remove any excess starting material using DCM: PET (v:v 3:2), to collect the **133** in 65% yield.

The ^1H NMR-spectra analysis of **133** exhibited well-defined aromatic signals: signal of H_o at (7.26 ppm for the 12 protons of *ortho*), and multiplets of both H_m and H_p at 6.95-6.89 ppm for 18H, (Fig. 3.37).

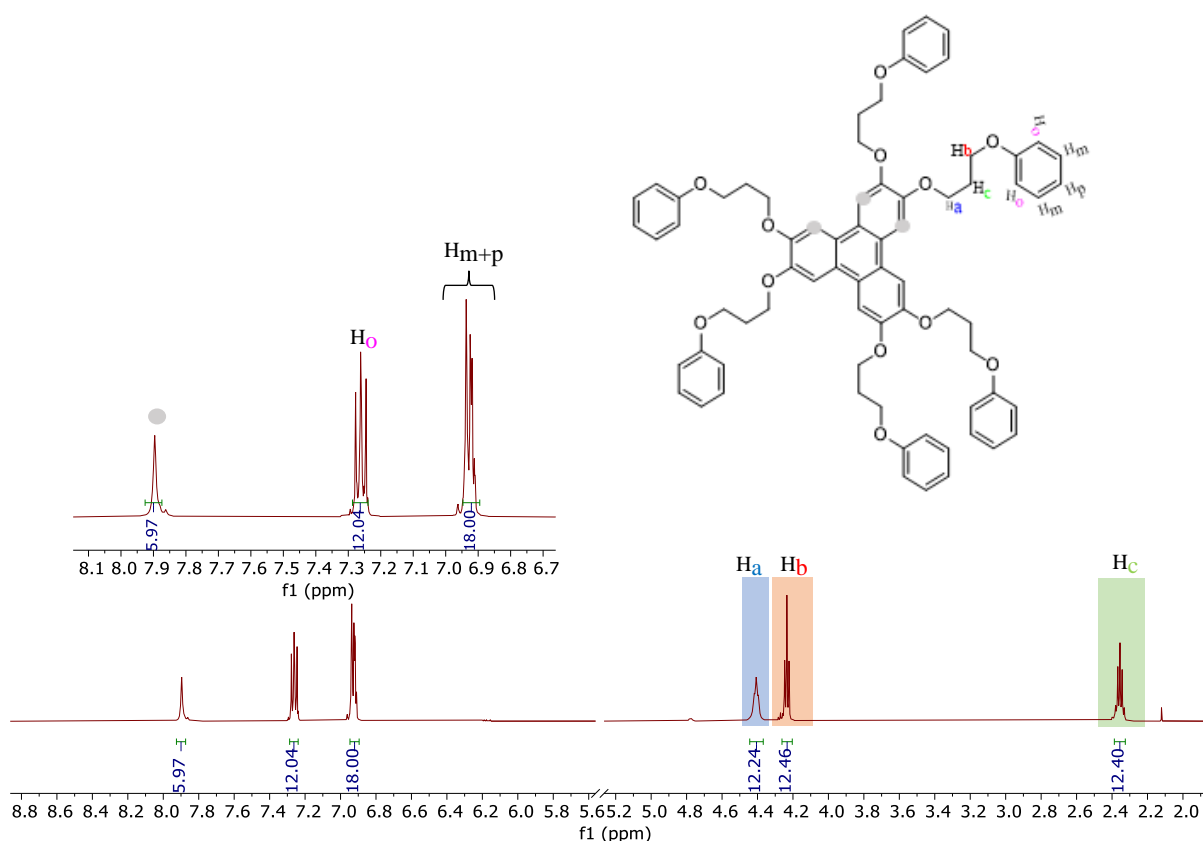


Figure 3.37. ^1H NMR spectra for test compound **133**.

As a result, *hexa*-(porphyrin) triphenylene system **127** was successfully synthesised following the same conditions of the test reaction above. The structure of **127** was confirmed using several spectroscopic techniques including NMR (^1H , Cosy, $^{13}\text{C}\{^1\text{H}\}$ and HSQC), IR, UV-vis, and MALDI-TOF-MS. These analysed data can be found in the experimental chapter. The MALDI-TOF-MS confirmed the molecular ion of m/z 4348.69, $[\text{M}]^+$ ($\text{C}_{300}\text{H}_{216}\text{N}_{24}\text{O}_{12}$), calc.: 4348.71 (Fig. 3.38).

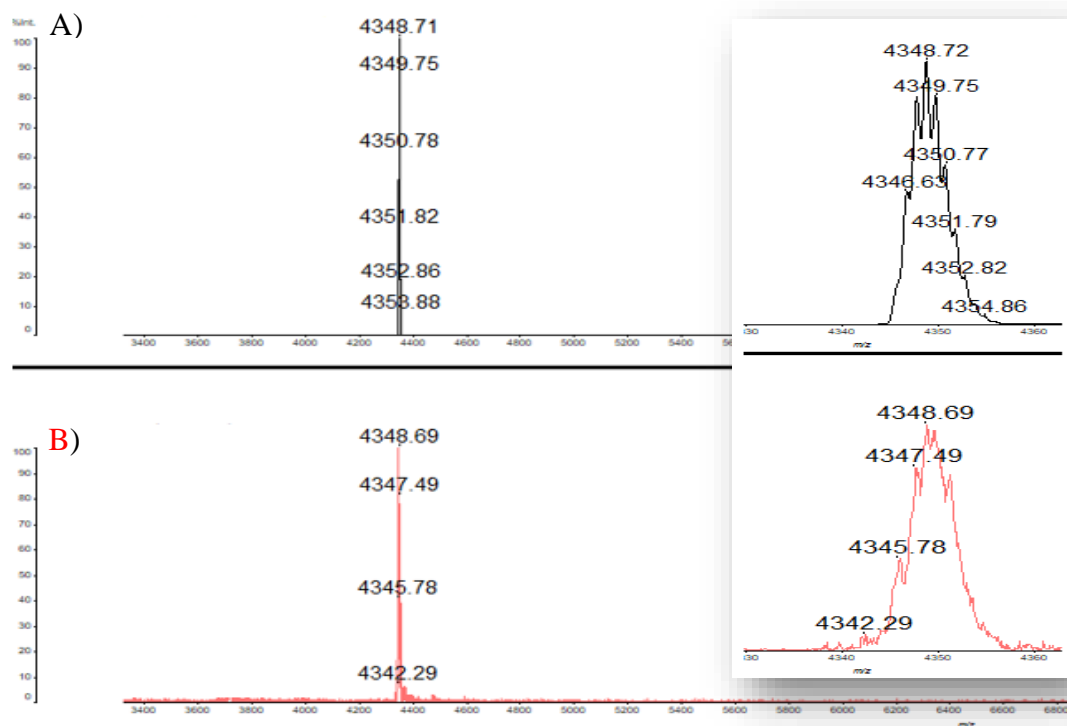


Figure 3.38. MALDI-TOF-MS of *hexa*-(porphyrin) triphenylene **127**. The inset shows (B) obtained and (A) theoretical isotopic patterns.

Analysis of NMR spectrum

^1H NMR-spectra of the *hexa*-system **127** showed a small singlet of Ar-H* at 8.11 ppm, corresponding to the 6 protons of the triphenylene ring, one singlet of 12H for N-H group at -2.92 ppm and two triplets for H_a (4.60 ppm) and H_b (4.45 ppm), and one quintet of H_c (2.51 ppm) related to the 12H each of the alkyl chain. Most importantly, ^1H NMR-spectra of **127** system reveals the symmetrical system was formed, showing free rotation of the 6-porphyrin units passing through the 6-linkers to the triphenylene core. This clearly indicates hydrogens of the *meso*-phenyl of porphyrins shows benzene ring **A**; doublet of *meta*-position $\text{H}_{m'}$ for 12H at 7.94 ppm and doublet of *ortho*-position $\text{H}_{o'}$ for 12H at 7.13 ppm. Benzene ring **B** and **B'**; doublet signals of H_1 and $\text{H}_{1'}$ for 12 and 24 hydrogens at 7.99 and 7.85 ppm; overlapped triplet signals of H_2 and $\text{H}_{2'}$ for 36H at 7.38 and 7.32 ppm; overlapped multiplet signals of H_3 and $\text{H}_{3'}$ for 18H at 7.60 and 7.32 ppm. Other important signals appear clearly, as labelled in (Fig. 3.39).

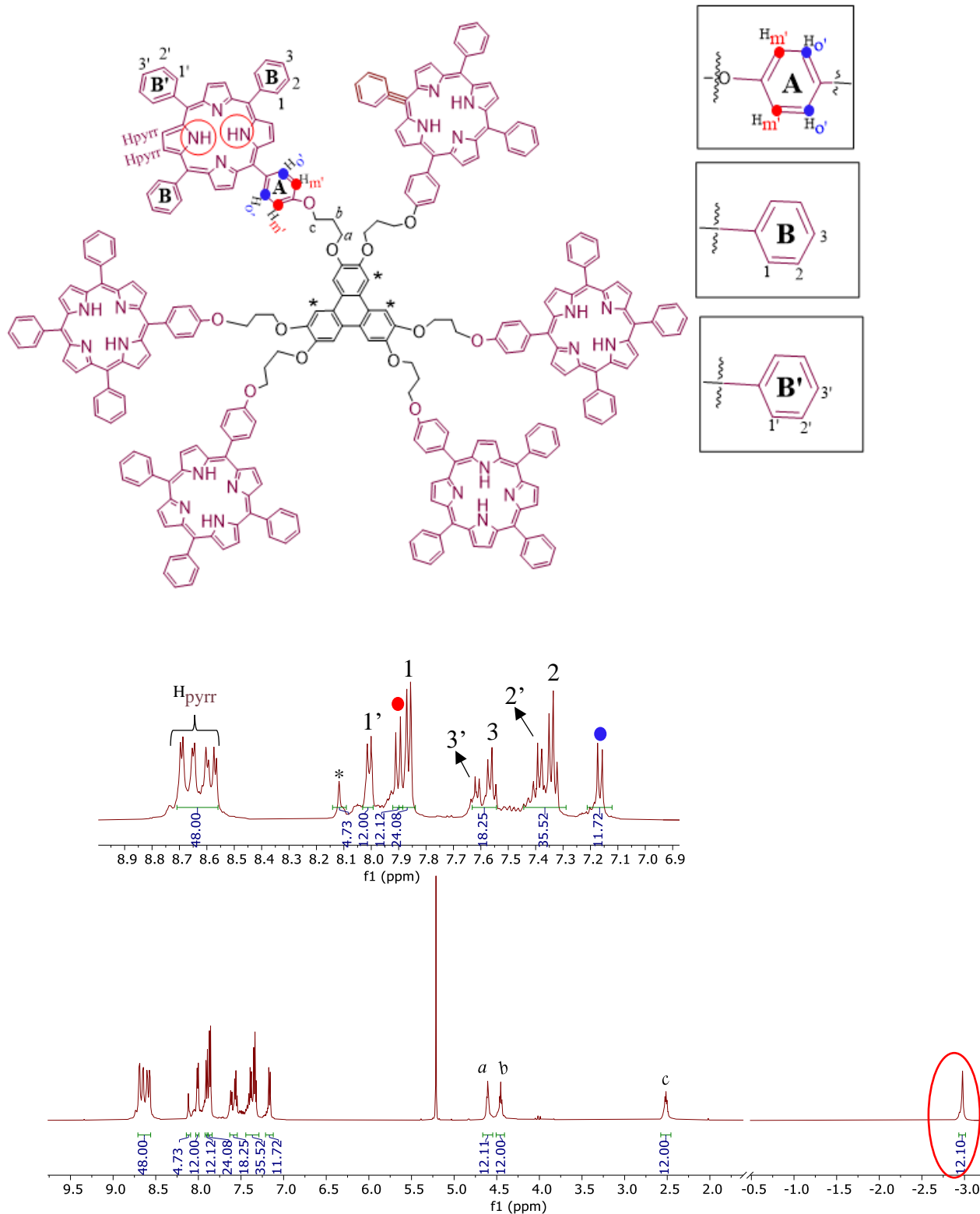


Figure 3.39. ^1H NMR-spectroscopy for hexa-(porphyrin) triphenylene system **127**, (500 MHz, CD_2Cl_2), expansion of 8.9-7.0 ppm aromatic area.

In addition, the HSQC-spectra displays a signal of Ar-H* for 6H correlates with a very small weaker peak C* because of no electronegative atoms bonded to the triphenylene benzene rings (Fig. 3.40).

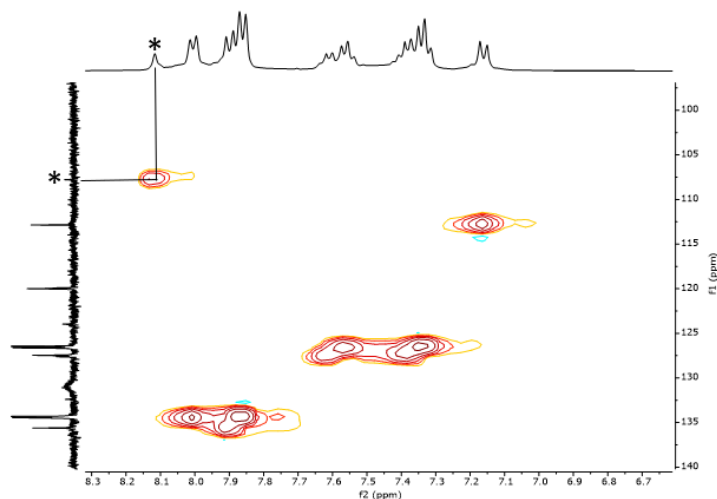
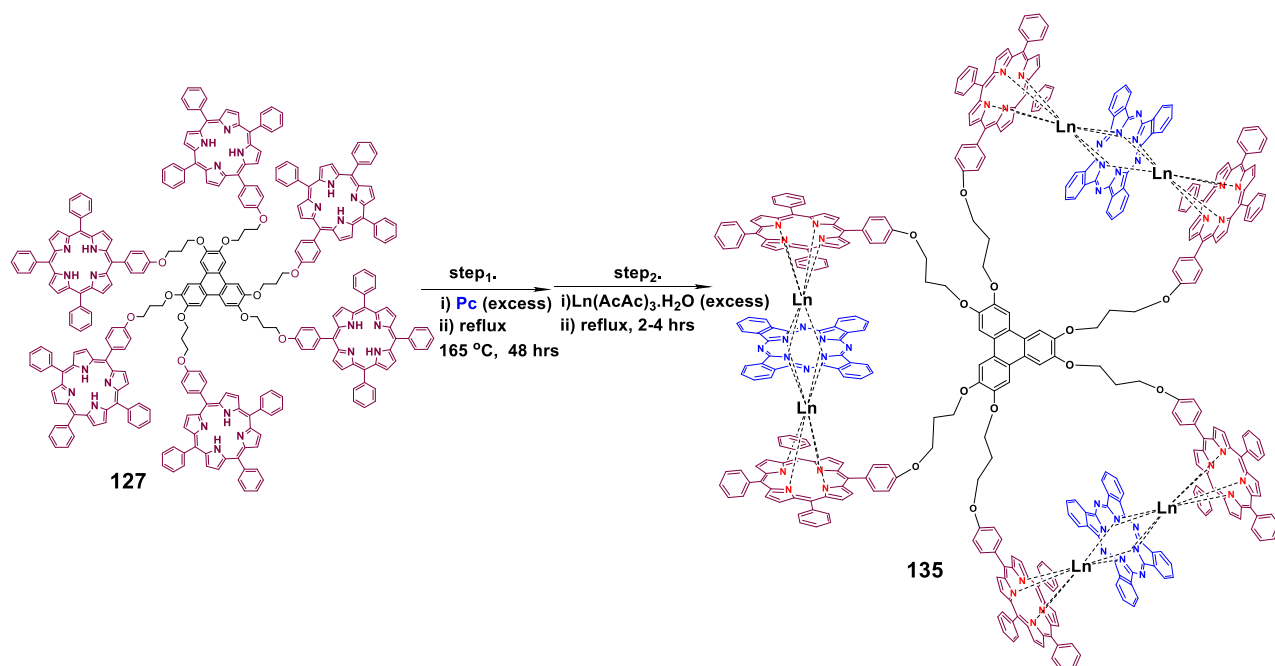


Figure 3.40. HSQC NMR-spectroscopy for *hexa*-(porphyrin) triphenylene system **127**.

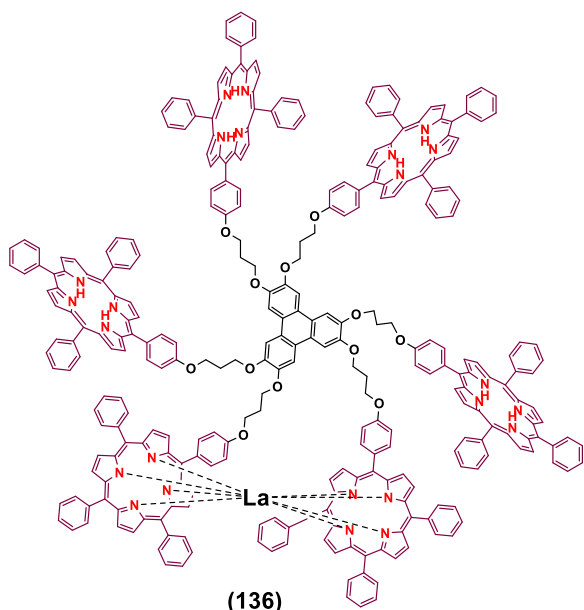
3.6 Synthesis of *tris*-triple-decker system **135**

The *hexa* porphyrin system was successfully synthesized and fully characterized, guiding towards the final step. To prepare *tris*-triple-decker system **135**, the same modified methodology used for the *single* triple-decker was followed, using an excess of both Pc **2** and the metal, as shown in Scheme 3.42 below.

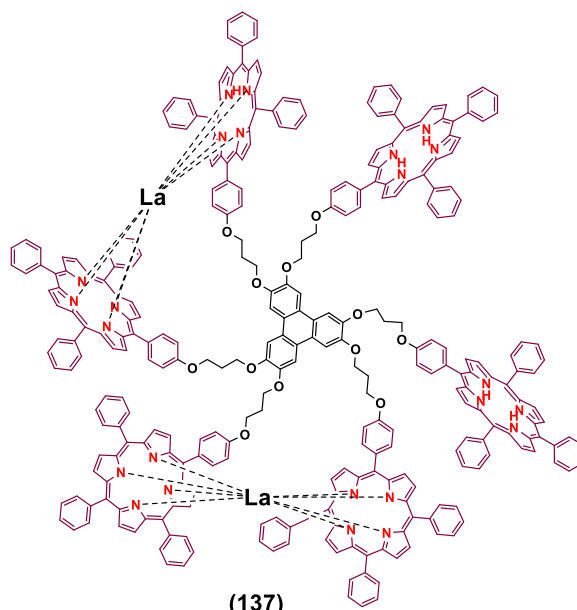


Scheme 3.42. Synthesis of (3,6) *tris*-triple-decker system **135**.

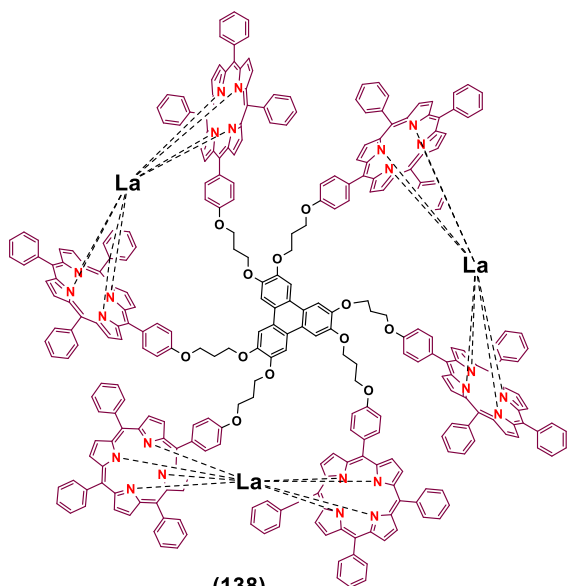
3,6-linkages were expected in the formed *tris* triple-decker system **135** due to earlier results that showed its preferential formation over 2,3-. In practice forming three triple-decker complexes around the central core, to form a single larger molecular mass system (6713 m/z) was more difficult. Multiple rounds of analysis were conducted to examine the reaction's crude using TLC and MALDI-TOF-MS. The results revealed numerous spots, indicating the presence of multiple side products. Analysis of the results indicated the same logical assumptions about the structural features of some products and they are illustrated in (Fig. 3.41).



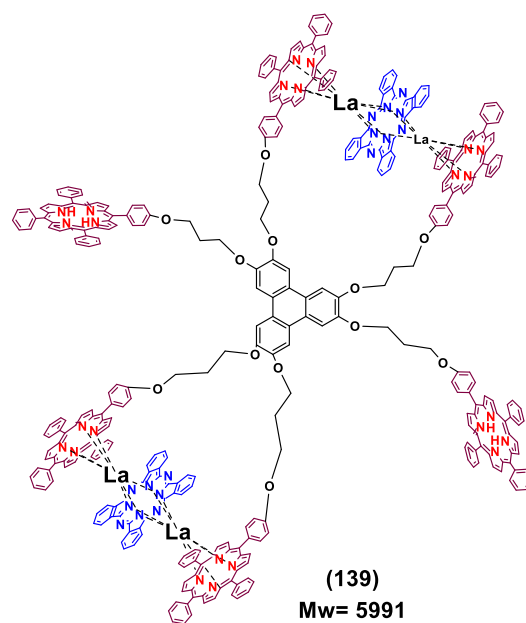
Mw= 4416



Mw= 4624



Mw= 4736



Mw= 5991

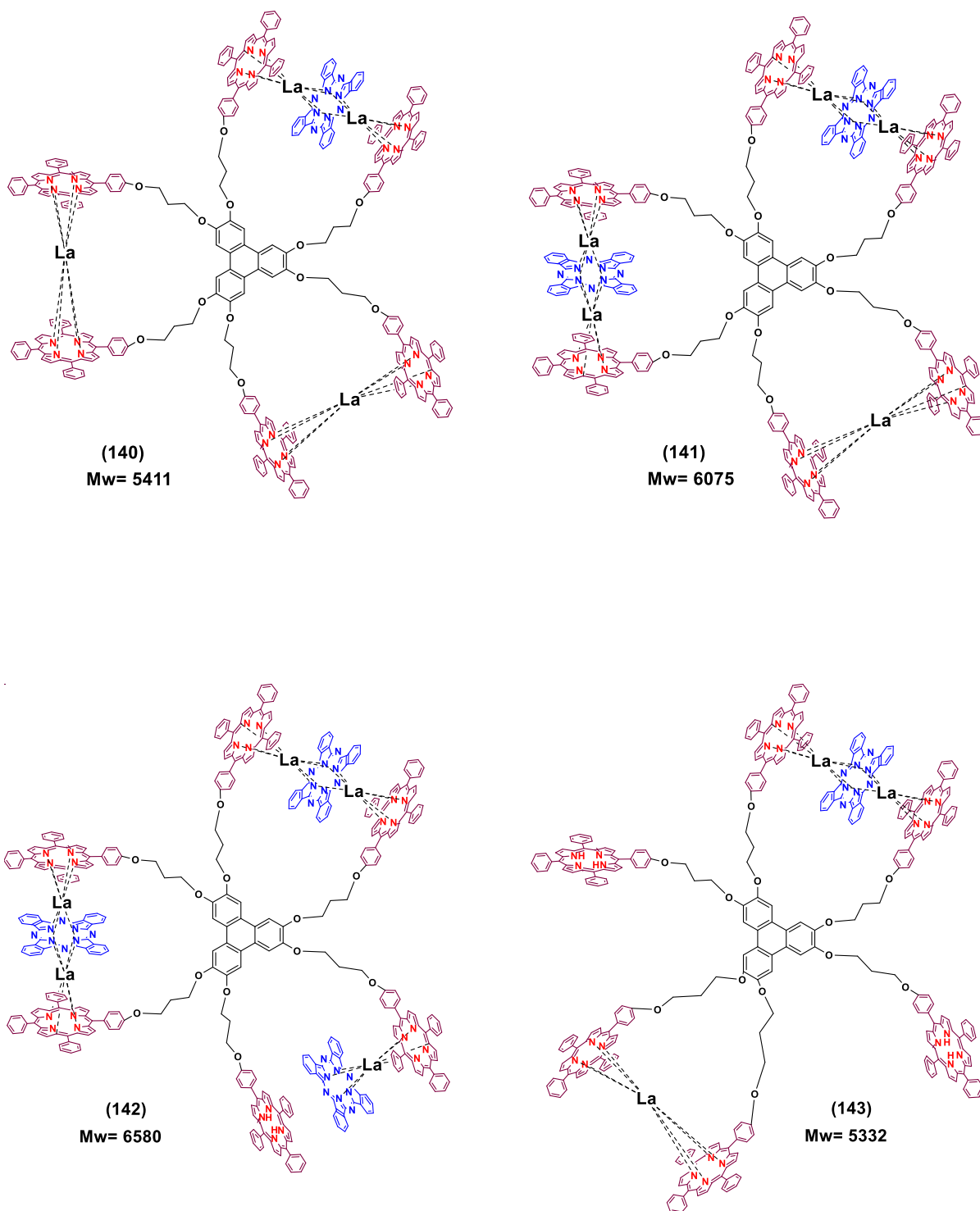


Figure 3.41. MALDI-TOF-MS results for by-products of *tris* triple-decker reaction attempts.

In the first attempt, a mixture of the *hexa*-system **127** and 6 equivalents of Pc **2** were heated in 1-pentanol at 165 °C for 48 hrs. Subsequently, 12 equivalents of $\text{La}(\text{AcAc})_3 \cdot \text{H}_2\text{O}$ were added and refluxed for 3-4 hrs. Analysis via MALDI-TOF-MS revealed the by-products (likely to be **136**, **137**), as well as the formation of a *bis* triple-decker assigned

tentatively as structure **139**. It can be envisaged that this outcome leads to an uncongested system but would halt any further reaction as there are no two adjacent porphyrins to allow formation of a third triple-decker (Fig. 3.42).

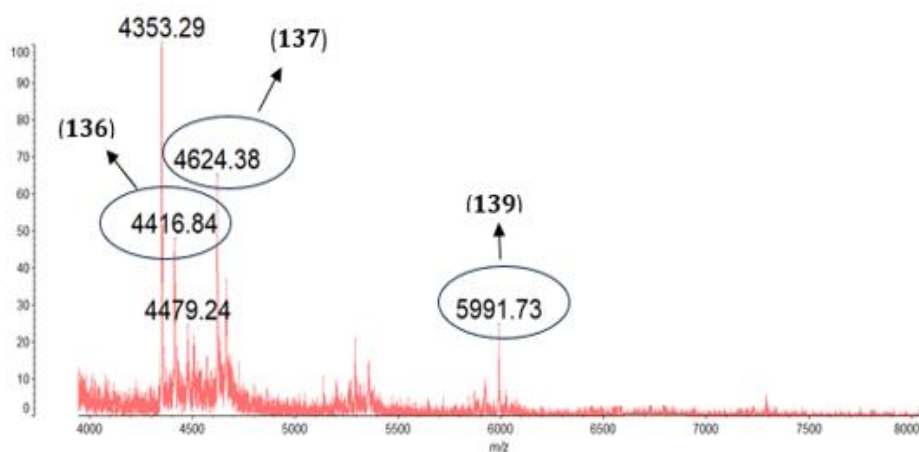


Figure 3.42. MALDI-TOF-MS for first attempt of synthesising *tris* triple-decker system.

Therefore, in the second attempt, the reaction was modified by increasing the quantity of metal added to 18 equivalents while maintaining all other reaction conditions. MALDI-TOF-MS analysis displayed the presence of various by-products, with possible formation of double-decker systems because a prominent observed mass corresponds to **(138)**. Furthermore, masses corresponding to a *single* triple-decker-double-decker (**140**) and a *bis* triple-decker-double-decker (**141**) were observed (Fig. 3.43(A)).

Therefore, the reaction was repeated with a higher excess of both Pc (12 equivalents) and metal (24 equivalents), with the reaction conditions unchanged. However, MALDI-TOF-MS analysis revealed the presence of high-mass complexes with increased Pc insertion (7381 and 8717 m/z), alongside other by-products. However, this attempt showed promise as a peak corresponding to a 3xPc, 5xLa was also observed, (**142**), (Fig. 3.43(B)).

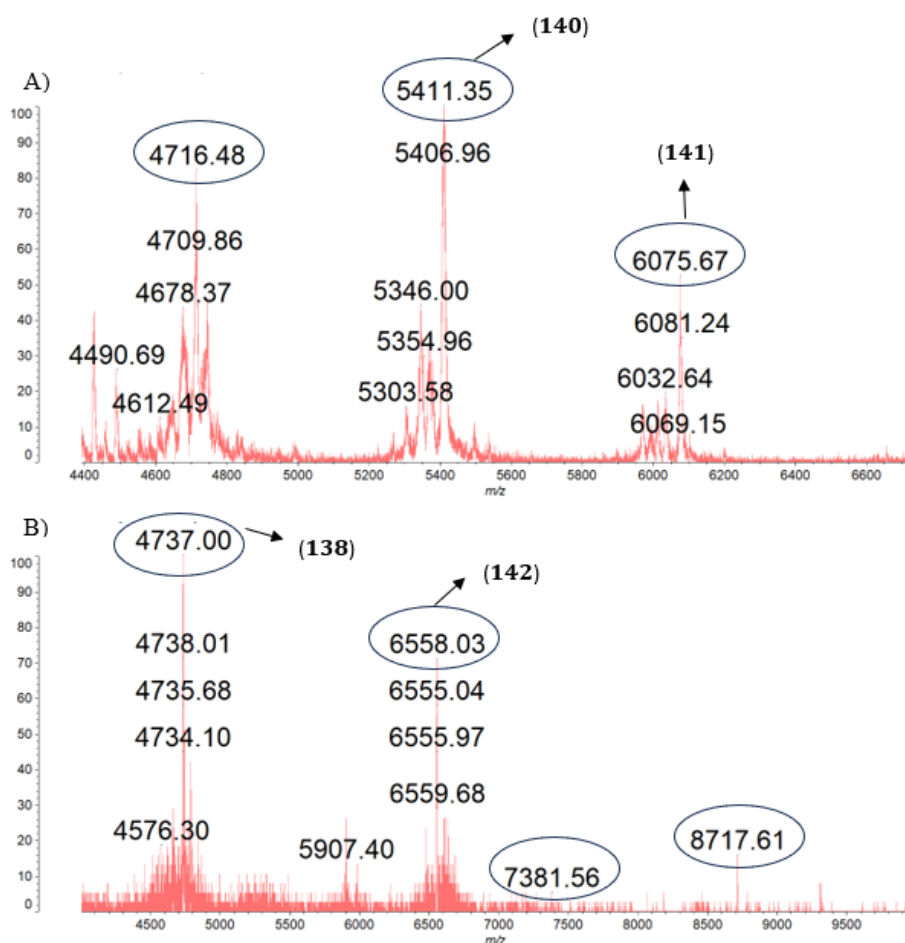


Figure 3.43. MALDI-TOF results.

Based on the previous outcomes, another repetition of the reaction was conducted with an excess amount of only the metal (24 equivalents) and extended the reaction time to 12 hrs instead of the previous 3-4 hrs. As a result, MALDI-TOF-MS analysis revealed two obvious peaks corresponding to metal insertion alone (**138**) and the *tris* triple-decker structure with one missing metal atom (**142**), (Fig. 3.44 (A)). Subsequently, the reaction time was increased to 3 days. MALDI-TOF-MS exhibited similar results, with a higher mass observed for complexes with increased Pc core insertion (8756 m/z), (Fig. 3.44 (B)).

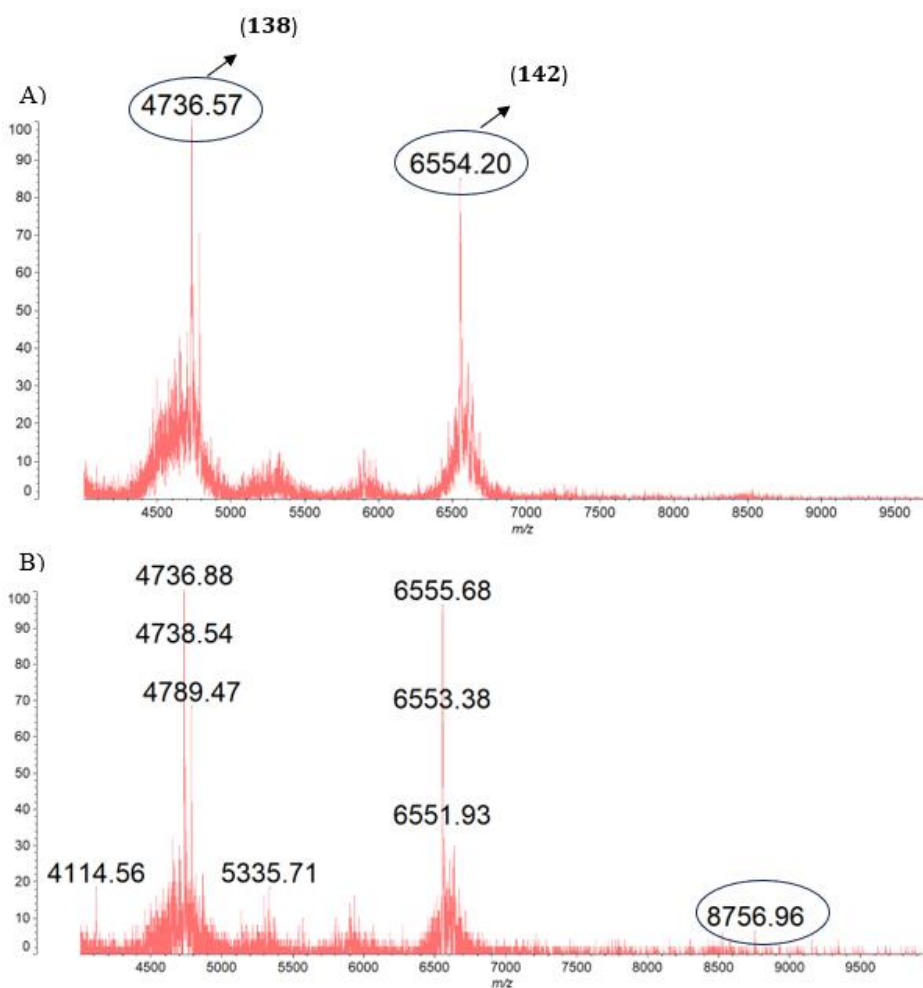


Figure 3.44. illustrating further MALDI-TOF-MS results.

The reaction was repeated using an excess amount of metal (24 equivalents), while this time raising the temperature to 200°C by using a sealed tube setup. MALDI-TOF-MS displayed a major peak corresponding to the *tris* triple-decker structure with one uninserted metal atom (**142**), as previously observed (Fig. 3.45 (A)). Notably, this result indicated that the insertion of the final metal atom proved to be significantly more challenging compared to previous attempts, which was unexpected but consistent with the challenging formation of such a congested system.

To force this insertion, an excess of metals were added, and both the temperature and reaction time were increased. Here, the reaction was maintained at 250°C in a sealed tube for a week. Following this, analysis by MALDI-TOF-MS confirmed the formation of the *tris* triple-decker structure with all 6 metal atoms inserted (**135**), giving a mass of 6713 m/z (Fig. 3.45 (B)).

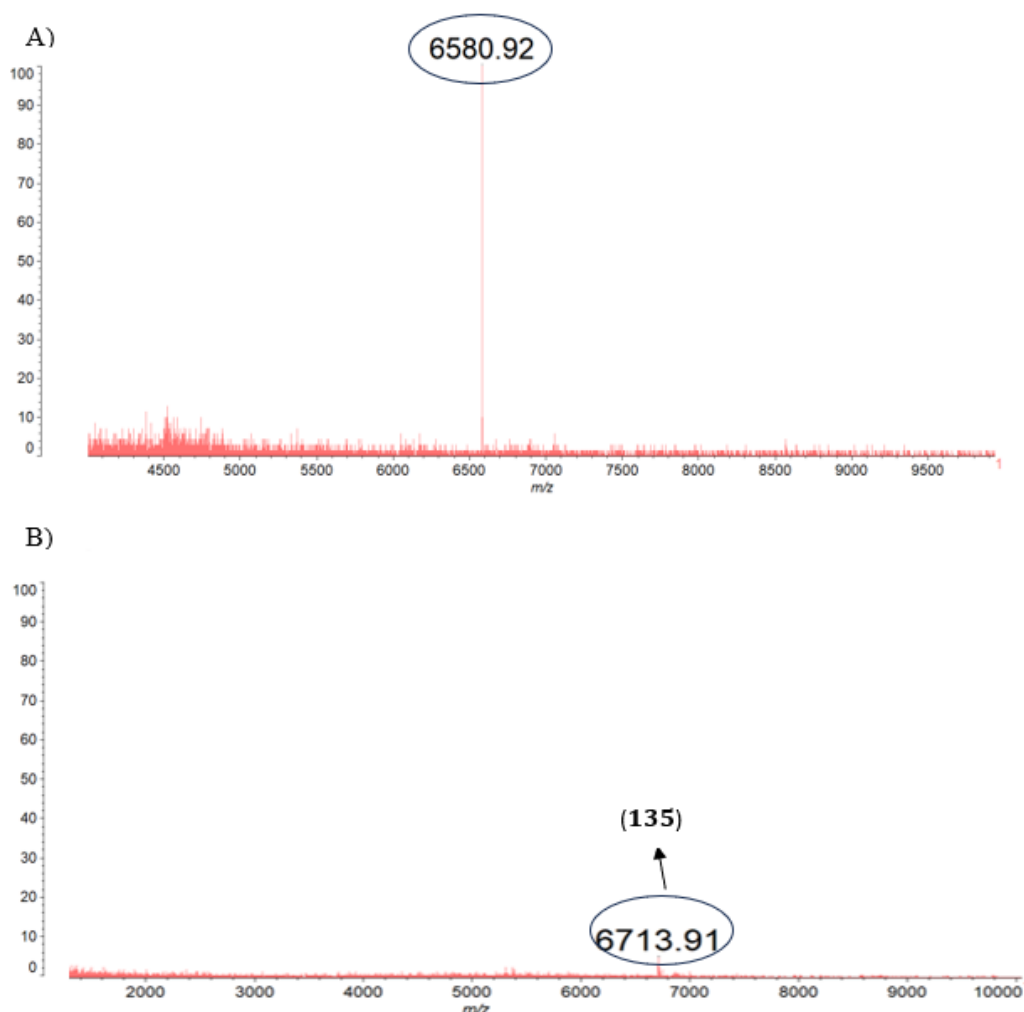


Figure 3.45. MALDI-TOF-MS for final attempt.

The green product was precipitated by adding MeOH followed by filtration to isolate it. It was then subjected to short silica chromatography, washed with (100% DCM) to separate first any excess La-Pc. The resulting product **135** was obtained through a further purification step using column chromatography with a solvent mixture of DCM:PET:TEA in a ratio of (v:v:v 7:10:1). This process yielded ~27% of the desired system **135** in the form of a dark green solid. Many attempts were made to recrystallize **135** using different solvents but were unsuccessful. TLC analysis of the isolated material proved challenging and often irreproducible (a phenomenon often associated with crystallisation and/or decomposition on the plate). Nevertheless, samples did appear to be single product. However, very complex and poor-quality NMR-spectra were produced each time. The ^1H NMR-spectra of *tris* system **135** exhibited distinct peak characteristics that matched the formation of TDs, resulting in a high chemical shift similar to that of *single* TD complex, about 9.95 to 10.0 ppm (Fig. 3.46 (a) and (b)).

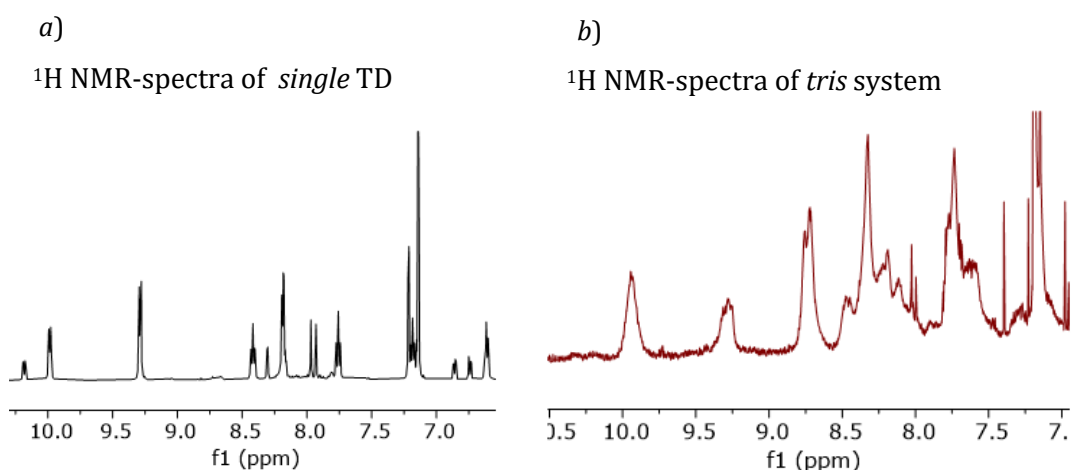


Figure 3.46. Illustrating similar peaks characteristic of both *single* and *tris* system.

A more detailed investigation was conducted using the MALDI-TOF-MS results. There was evidence that the sample was not in fact pure, and closer inspection revealed the presence of additional peaks in the MALDI-TOF-MS-spectra corresponding to *bis* triple-decker (**139**) and (**143**). The presence of these side product impurities make the spectra complex, indicating double-decker units are included. Several further purifications were attempted, and MALDI-TOF-MS confirmed a main peak associated with the *tris*-system **135**, but additional peaks still always were present (Fig. 3.47).

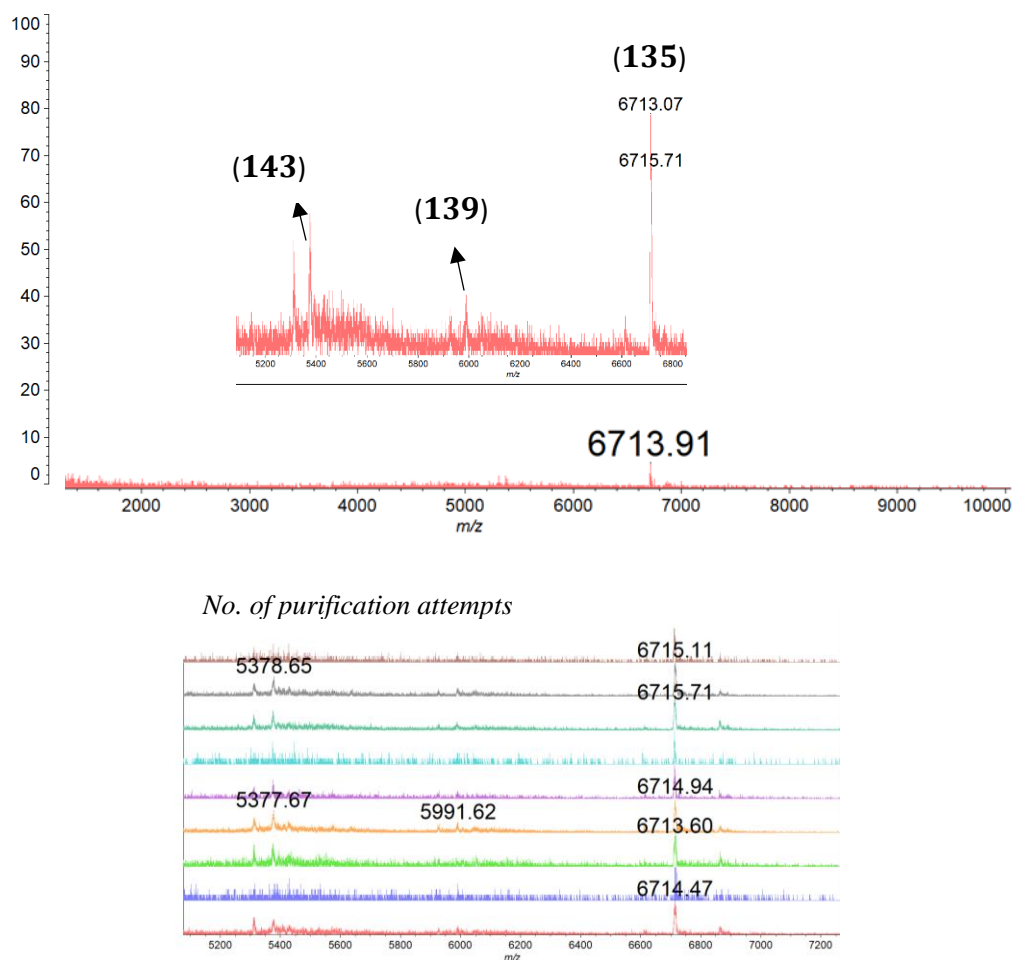


Figure 3.47. Additional MALDI-TOF-MS investigation results.

Upon comparing the UV-vis spectra of **135** (-green trace) with the previously synthesised 3,6-La *single* triple-decker complex, it is apparent that they display comparable signal patterns, confirming the formation of **135**. However, *tris* triple-decker system **135** spectra displayed an extra Q-band signal due to mixing with by-products of (**139**), having metal-free porphyrin units, again consistent with our assumption that a *bis* TD like **139** is favourably formed and inseparable from our target *tris* TD, (Fig. 48).

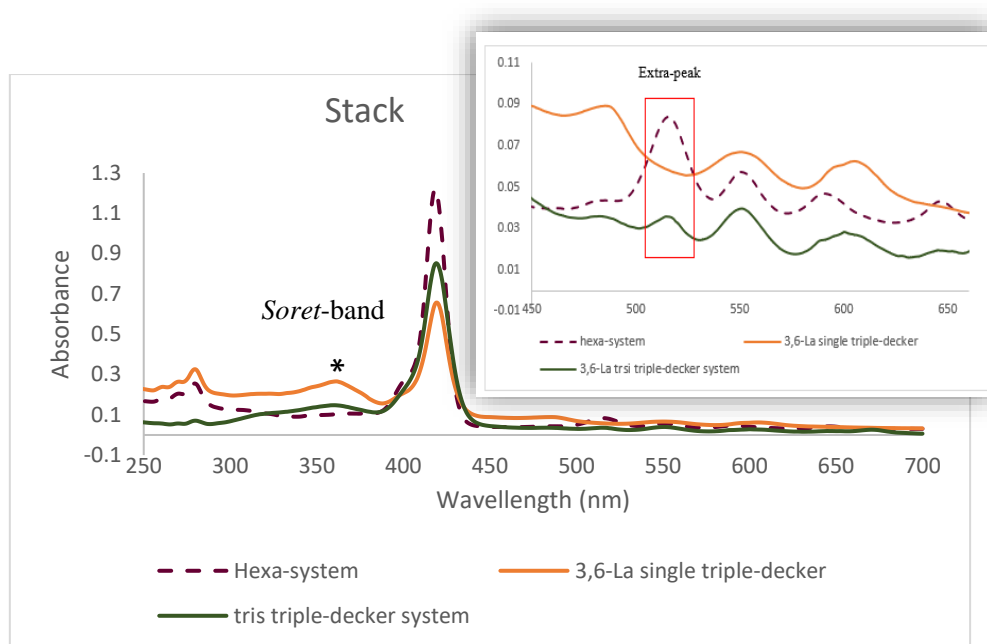
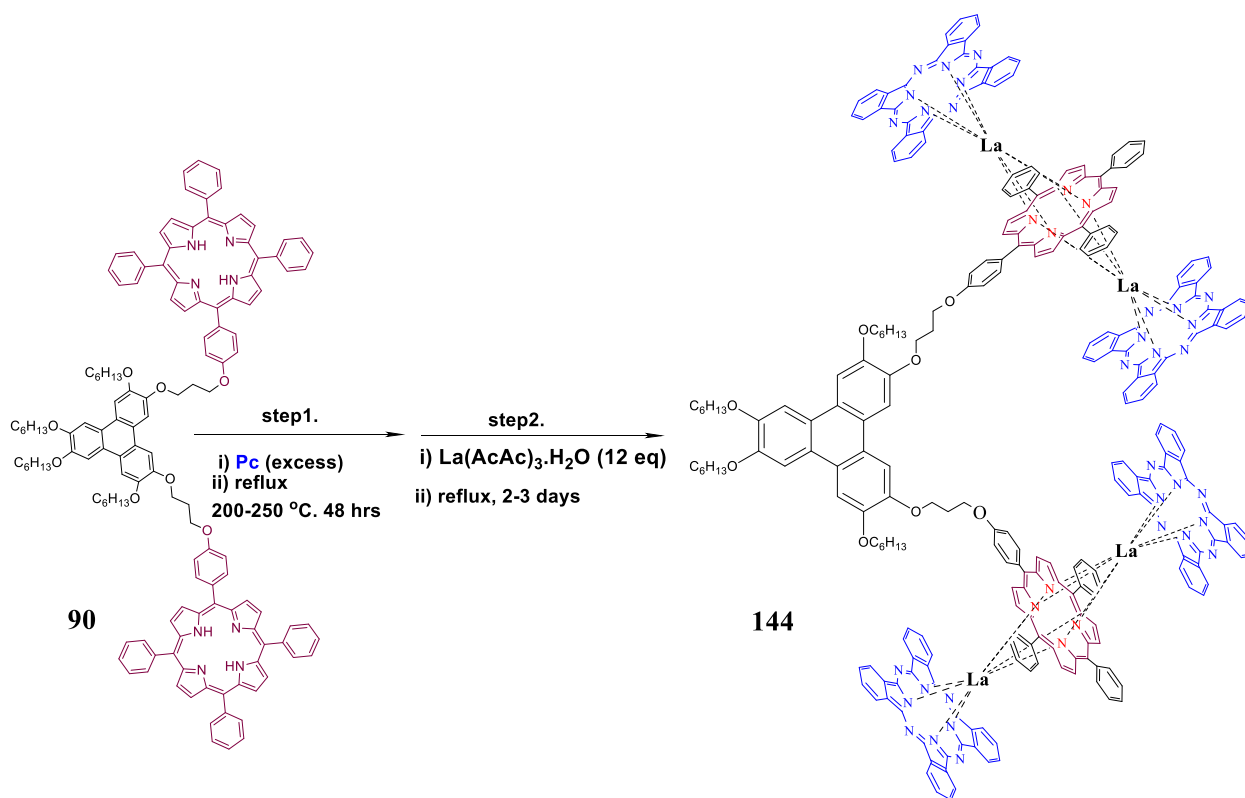


Figure 3.48. UV-vis spectra for *tris* triple-decker system **135** with starting material **127** and 3,6-La *single* triple-decker complex.

3.7 Synthesis of open *bis*-triple decker system **144**

As previously noted, satisfactory NMR-spectroscopy results could not be obtained for the *tris* triple-decker system **135**. Consequently, the decision was made to synthesise the open *bis* triple-decker system instead, with the ultimate goal of fully characterizing an alternative *bis* triple-decker system for this project. The 3,6-isomer **90** was chosen for its more open structure, which spans a bigger distance between porphyrins. This can assist in the production of a multi-decker system by using a modified conditions instituted for *single* TD complex that described before, as illustrated in (Scheme 3.43).



Scheme 3.43. Synthesis of *bis*-triple-decker system **144**.

In order to preferentially synthesise the open *bis*-triple-decker system **144**, 3,6-*bis*(porphyrin)triphenylene **90** and an excess of Pc **2**, were refluxed in 1-pentanol in an inert atmosphere for 48 hrs. 12 equivalents of La(acac)₃·H₂O was added and heated in a sealed tube at (200-250°C) for 3 days. The reaction product was analyzed using MALDI-TOF-MS, which confirmed the molecular ion of m/z 4604.75, [M]⁺ (C₂₆₄H₁₈₈La₄N₄₀O₈), cal.: 4604.21 (Fig. 3.49).

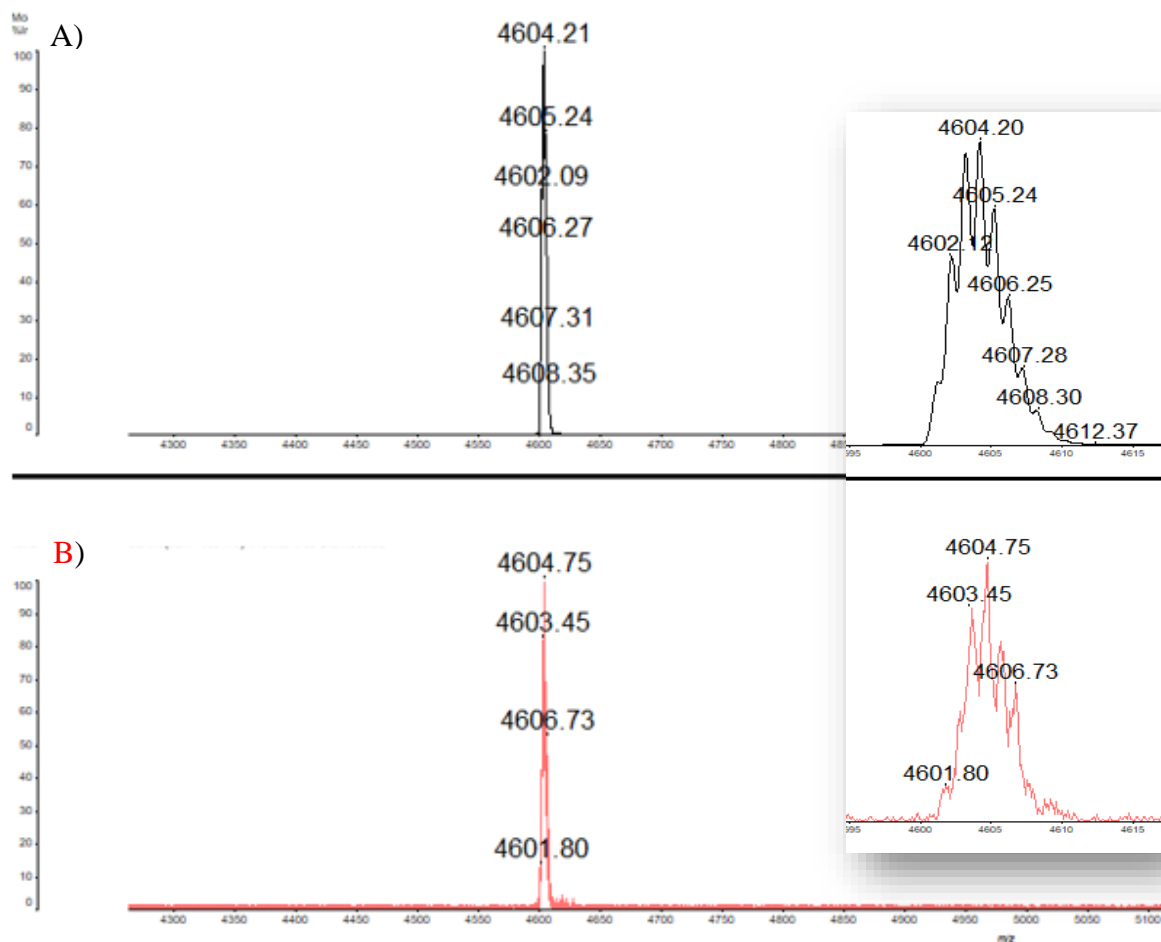


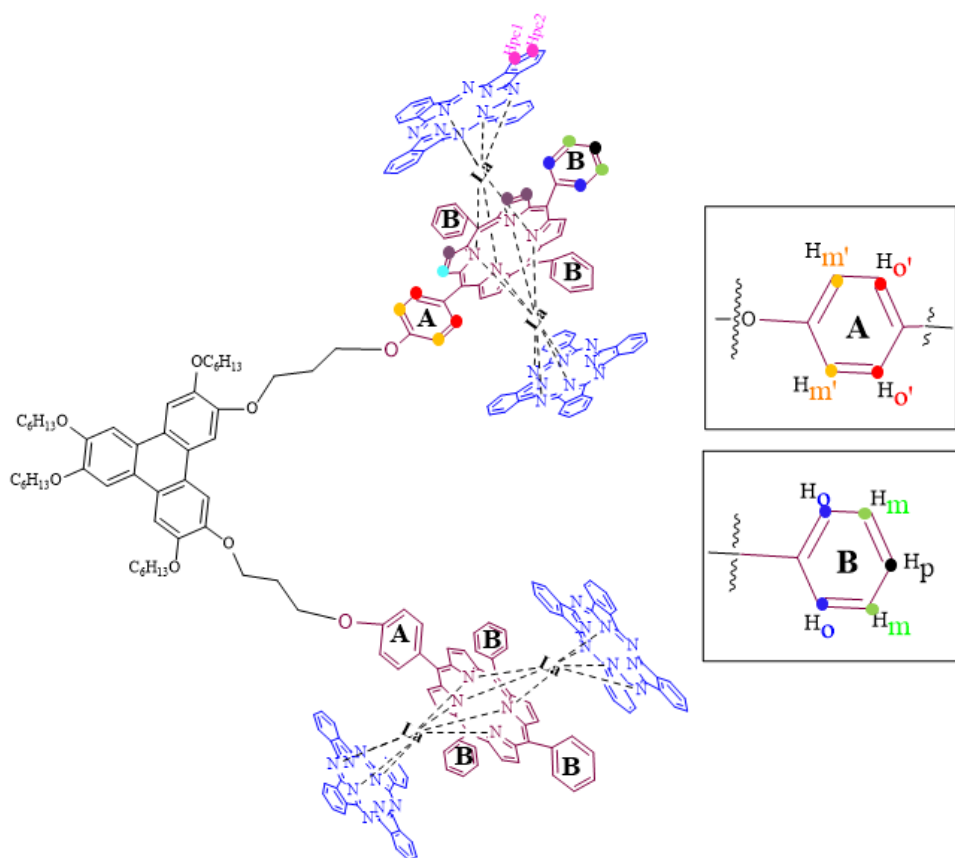
Figure 3.49. MALDI-TOF-MS of compound **144**. The inset shows (B) obtained and (A) theoretical isotopic patterns.

The open *bis* triple-decker **144** was isolated by employing the same sequence for the previous work up. It was precipitated by using MeOH and filtered, was then subjected to short silica, washed with (100% DCM) to separate any excess of Pc. Recrystallization of **144** using DCM:MeOH to obtain 40% yield.

Analysis of NMR spectrum

The NMR spectroscopy absorption indicates the symmetrical assembly of the open *bis*-triple-decker system **144**. Analysis of the ^1H NMR-spectra of **144** revealed very sharp signals of Pc; two doublets of doublets for 32H at 8.72 and 7.75 ppm, referred to as H_{pc1} and H_{pc2} . In Figure 3.50, other distinct signals corresponding to the benzene rings (A), (B), and pyrrole of the di-porphyrin unit and triphenylene core are shown. However, the free rotation of the di-porphyrin units was prevented, as described previously in the 2,3 and 3,6-isomeric TD complex. This is attributed to the open *bis*-TD complex of four

phthalocyanine cores, which makes the system robust and blocks the bridge chain from undergoing free rotation. Consequently, this open system exhibits a significant difference in characterization in the NMR-spectra, with no observed inner or outer rotation.



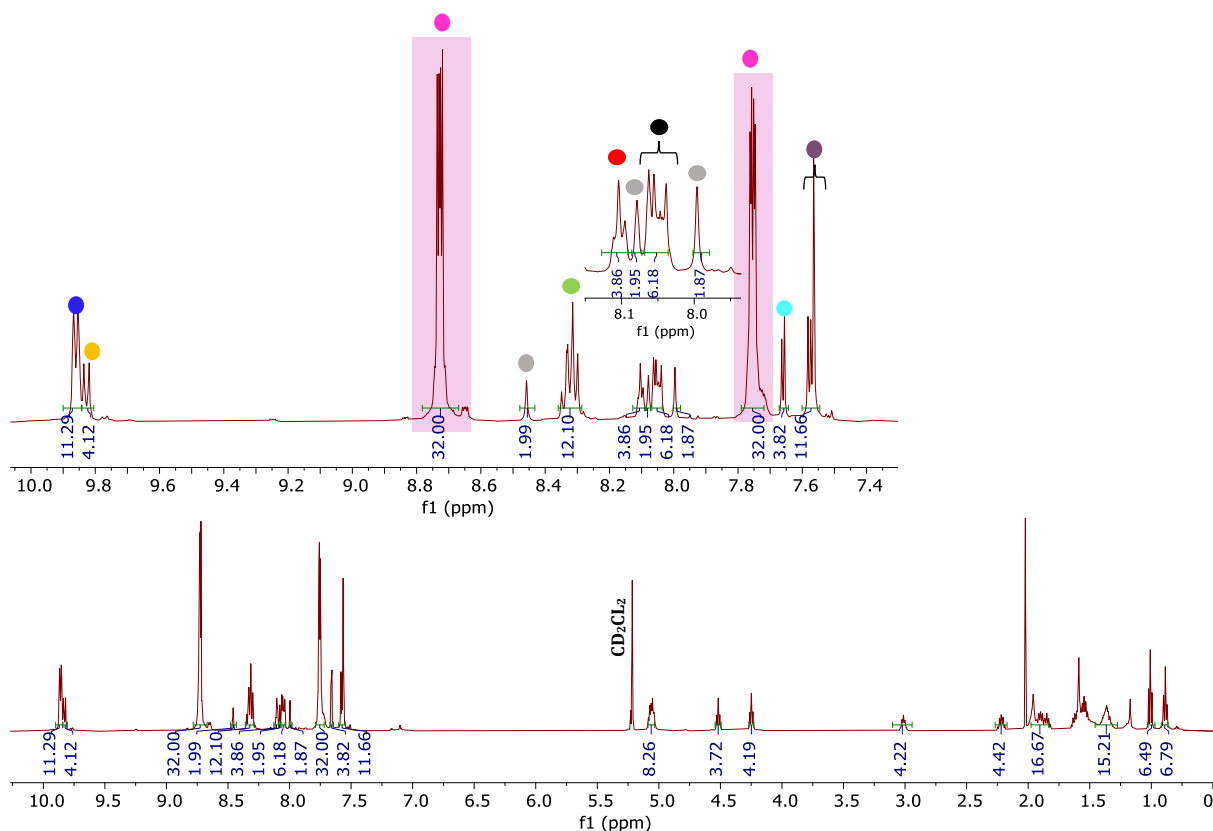


Figure 3.50. ^1H NMR of *bis*-triple-decker system **144** (500 MHz, CD_2Cl_2), expansion of 10.0-7.51 ppm aromatic area.

3.7.1 Comparing between open *bis* triple-decker **144** with open *bis* triple-decker for Cammidge's group

The spectra for the corresponding **144** was depicted as stacks with simple C_{10} bridged open *bis* triple-decker in (Fig. 3.51 (a) and (b)). The spectra of the two open *bis* TD derivatives show considerable similarities, as highlighted below. Particularly, porphyrins and Pc peaks are essentially identical in both derivatives; ($\text{H}_{\text{Pc}1,2}$) signals appearing at 8.83 and 7.83 ppm and hydrogen peaks of *ortho*-position for *meso*-porphyrins units showing chemical shift at 8.99 ppm for both are also similar. However, in the **144** system (a), the corresponding protons of the triphenylene singlets Ar-H*; overlapped with porphyrins signals appearing around 8.56 – 8.10 ppm.

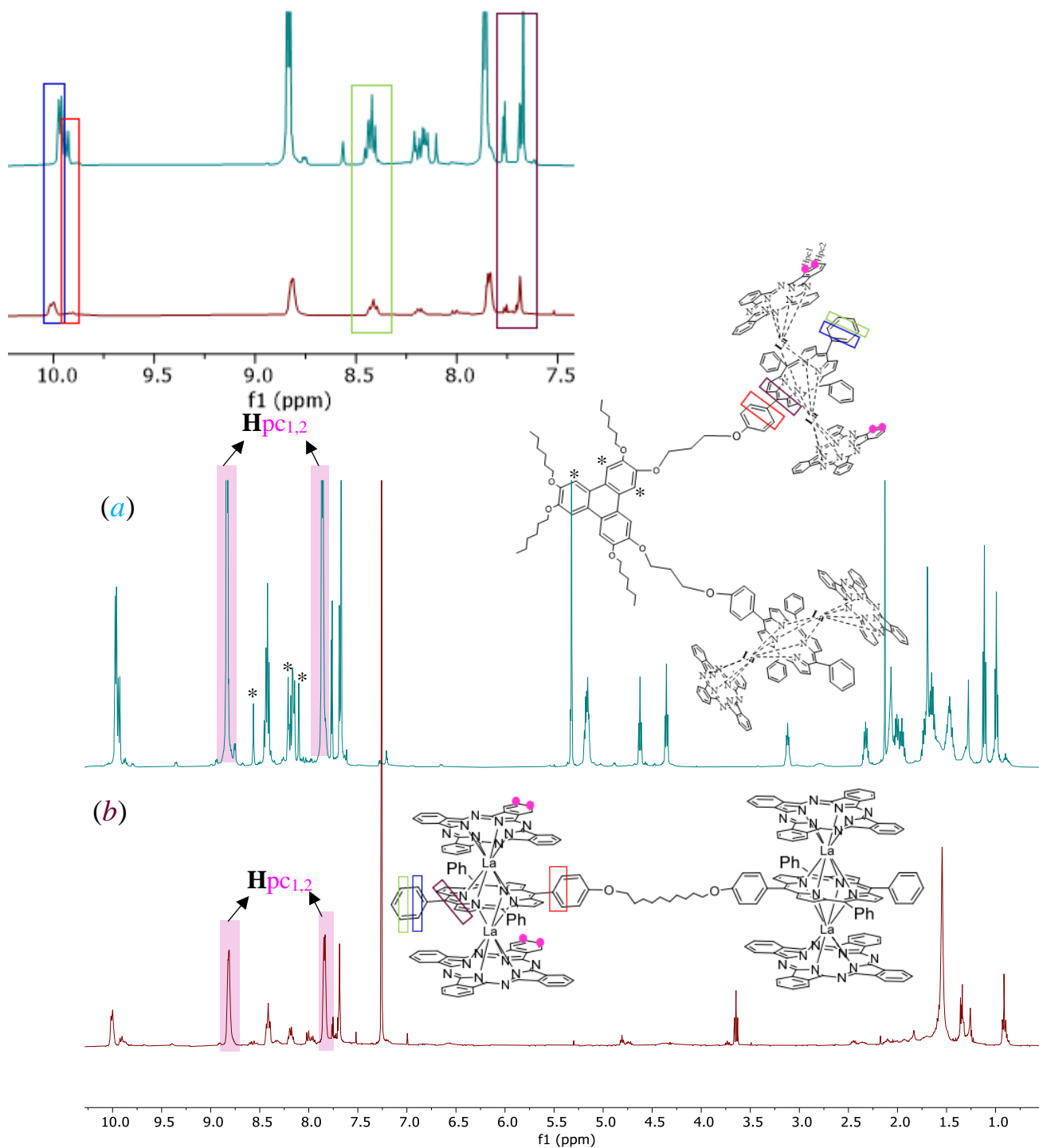


Figure 3.51. ^1H NMR-spectroscopy comparison between **144** system open bis complex of Cammidge's group.

To further support the assignment of observed signals to the appropriate aromatic protons, 2D COSY-NMR was conducted. The COSY spectrum of **144** reveals that the doublet of doublets for H_{Pc1} at 9.35 ppm correlates with the doublet of doublets for H_{Pc2} at 8.29 ppm, both associated with the four Pc cores. Furthermore, there is a clear and regular pattern of hydrogen coupling observed in both benzene rings (A) and (B), as indicated in (Fig. 3.52).

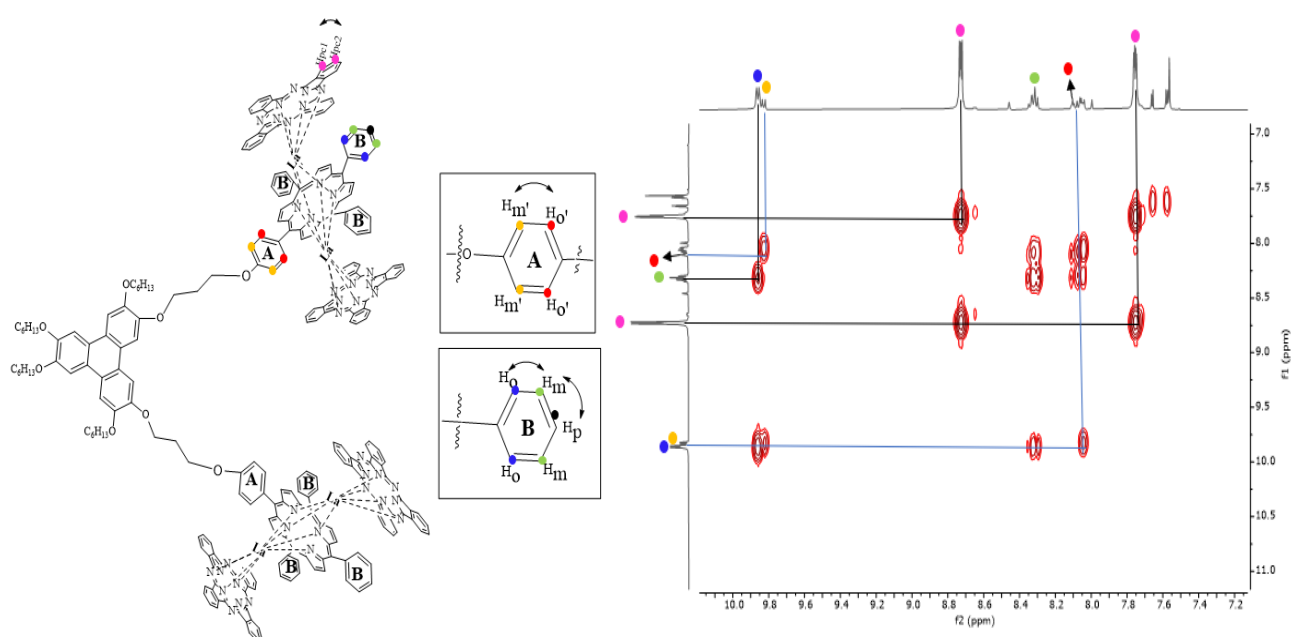


Figure 3.52. 2D COSY NMR-spectroscopy for *bis*-triple-decker system **144**.

UV-vis spectroscopy was conducted to confirm the formation of an open *bis* triple-decker system **144**, as depicted in Figure 3.48 (-green trace). The figure illustrates stacked signals for both *single* and *bis* triple-decker substitutes, indicating a reduction in Q-band peaks from 4 to 3 signals due to the formation of TD in comparison to signals observed for the starting material of metal-free porphyrin (3,6-model), (Fig. 3.53).

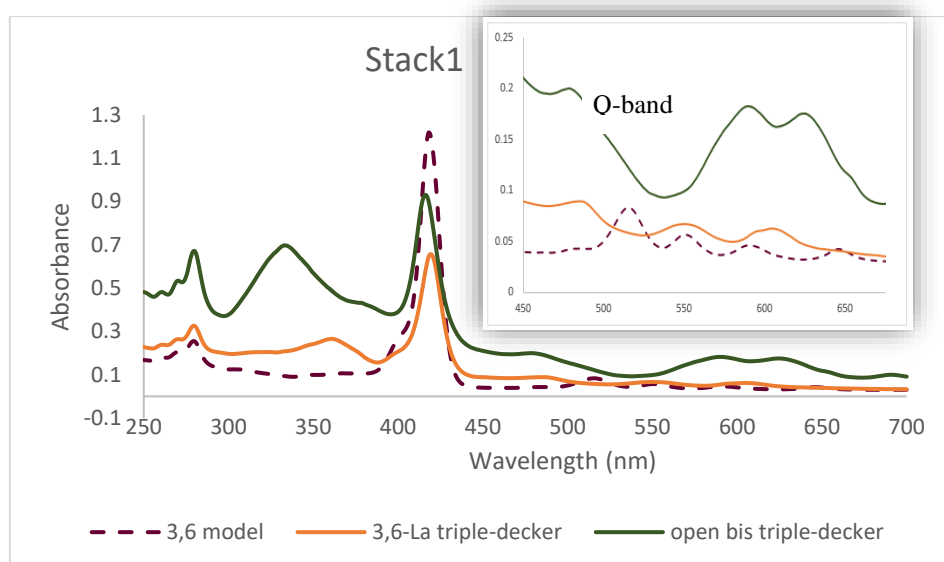


Figure 3.53. UV-vis spectroscopy for *bis* triple-decker system **144**, *single* triple-decker and 3,6-model.

In conclusion, an intensive investigation into a multistep synthetic approach for porphyrin–phthalocyanine multi-decker systems has been conducted. This strategy successfully led to the smooth synthesis of model systems, specifically the (2,3LnTD) and (3,6LnTD) assemblies, using lanthanide (III) salts with different ionic radii (La^{3+} =103 pm, Pr^{3+} =99 pm, Nd^{3+} =98 pm, Sm^{3+} =96 pm, Eu^{3+} =95 pm). Importantly, the assembly and isolation of these *single* TD systems exhibits a more balance of isomeric TD, resulting in spectroscopic similarities and no obvious difference in stability between two different isomeric TD complexes. The ion of smaller size as Dy failed to easily generate TD complex. The investigation into the selectivity of the lanthanide series was also performed, including the combination of two isomers with a lanthanide ion. This indicated that the *tris* triple-decker system does indeed offer excellent controlled formation for the selectivity of (3,6LnTD). The assembly of *tris* triple-decker systems did not result in a completely pure compound, and no significant spectroscopic analysis was obtained; however, MALDI-MS-TOF evidence suggests their formation. As part of our project to assemble high-order systems from porphyrin and phthalocyanine, an open multi-decker system design was also investigated successfully.

The study so far has uncovered a promising approach to complex multidecker systems. While specific problems have been identified in the molecular design, there are clear

indications for how future work could deliver efficient synthesis of related assemblies. In particular, future work should focus on the replacement of the investigated flexible propyl linker chain with a more rigid, potentially longer unit (e.g. incorporating an alkyne) in order to increase the selectivity between 2,3- and 3,6- assembly modes. At the same time this is expected to solve the identified issue of steric crowding in the multidecker's final assembly step.

Chapter 4: Experimental

4. Experimental

4.1 General methods

4.1.1 Physical methods

A Bruker Ascend™ 500 spectrometer was used, with deuterated solvents were used deuteriochloroform (CDCl₃) or deuterated methylene chloride (CDCl₂), to record the ¹H NMR spectra. A measurement of 500 MHz was observed. The recording of signals was in ppm, as δ. The residual solvent was used as a reference. Hertz (Hz) were used to give the coupling constant, *J*. ¹³C{¹H}-NMR spectra of 126 MHz were recorded. The same spectrometer and solvent were used. Unless otherwise indicated, all spectra were recorded at room temperature, (Some compounds had assignments for 1D NMR signals due to their simplicity and distinct proton environments, others had assignments for 2D NMR techniques to achieve accurate signal assignments, ensuring more structural clarification).

A Perkin-Elmer UV-vis spectrometer Lambda XLS was used to check the UV- vis spectra in the solvent stated.

Direct sample deposition was used to record mass spectra, by means of a MALDI-TOF-MS Performance instrument, Shimadzu Axima-CFR spectrometer. Isotopic distribution patterns were used to confirm the assigned molecular formulae by comparison to theory.

IR spectra were recorded using a Perkin-Elmer Spectrum BX FT-IR spectrometer.

Thin layer chromatography (TLC) was conducted using a Merck aluminium backed silica gel 60 F254 coated plates. Visualisation was achieved using a UV light at 254 nm.

Column chromatography was mainly achieved at ambient pressure and temperature. However, for the occasional application of moderate pressure, silica gel was utilized Davisil LC 60A, 40-63 micron of 70-230 mesh (Grace GM BH & Co). The ratio of solvent was v:v.

A Reichert Thermovar microscope, which included a Thermopar based temperature control, was employed to measure, and record melting points.

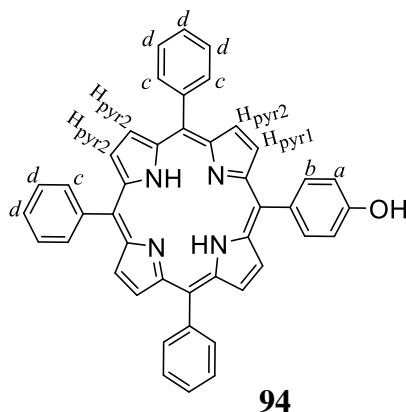
Microwave reactor model: Biotage Initiator+ system (1-point support), serial number; 014242, radio frequency emission level; 0.0 mw/ cm² at 5 cm; nature of any reactor sealed vessels was used.

4.1.2 Reagents, solvents, and reaction conditions

The solvents and reagents, used in this study, were all bought from commercial suppliers, and were of analytical grade. The solvents used were SLR- grade (standard Laboratory Reagent) and did not require drying. It was therefore considered unnecessary to purify them. Petroleum ether is light petroleum, 40-60 °C boiling point. Magnesium sulphate (MgSO₄) was used to dry the organic layers, and solvent evaporation was conducted at reduced pressure, by means of a Büchi rotator evaporator (*vacuo*). Reactions sensitive to water and air were carried out under an inert environment, typically under nitrogen or argon gas, (argon was preferred).

4.2 Synthesis

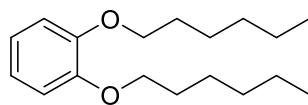
4.2.1 Synthesis unsymmetrical tetraphenyl-porphyrin ((10,15,20-triphenylporphyrin-5-yl)phenol) TPP-OH **94**



Following the procedure reported by Adler¹⁶², benzaldehyde (3.8 ml, 3.97 g, 37.40 mmol) and *p*-hydroxybenzaldehyde (1.52 g, 12.50 mmol) were mixed in propionic acid (200 ml), and then the mixture was heated to reflux. Freshly distilled pyrrole (3.25 ml, 3.14 g, 50.0 mmol) was then added dropwise. After the addition was finished, the resulting mixture was refluxed for another 30 min. The mixture was cooled down to room temperature. MeOH (200 ml) was added, then left overnight in the fridge to precipitate. The resulting product was a purple solid, which was filtered and washed with MeOH. The crude compound was purified by chromatography on a silica gel column using DCM:PET (1:1 v:v) as eluent. The first fraction was the symmetrical porphyrin TPP (0.2 g, 11%). After collecting all the TPP, the polarity of the eluent was increased to (DCM) to collect the TPP-OH product, which was separated out as a dark purple fraction. Then the compound was recrystallized using a mixture of DCM and MeOH to give hydroxyphenylporphyrin **94** as a purple solid (420 mg, 5.4%). “data consistent with previously reported”

¹H NMR (500 MHz, chloroform-*d*) δ 8.81 (d, J = 4.8 Hz, 2H, H_{pyr1}), 8.79 – 8.75 (m, 6H, H_{pyr2}), 8.18 – 8.12 (m, 6H, H_c), 8.04 – 7.98 (m, 2H, H_b), 7.75 – 7.64 (m, 9H, H_d), 7.15 (d, 2H, H_a), -2.85 (s, 2H, NH).; **MS (MALDI-TOF):** m/z [M^+] calc, for (C₄₄H₃₀N₄O)⁺: 630.24, found = 630.44 [M^+].

4.2.2 Synthesis of 1,2-Dihexyloxybenzene DBU 96

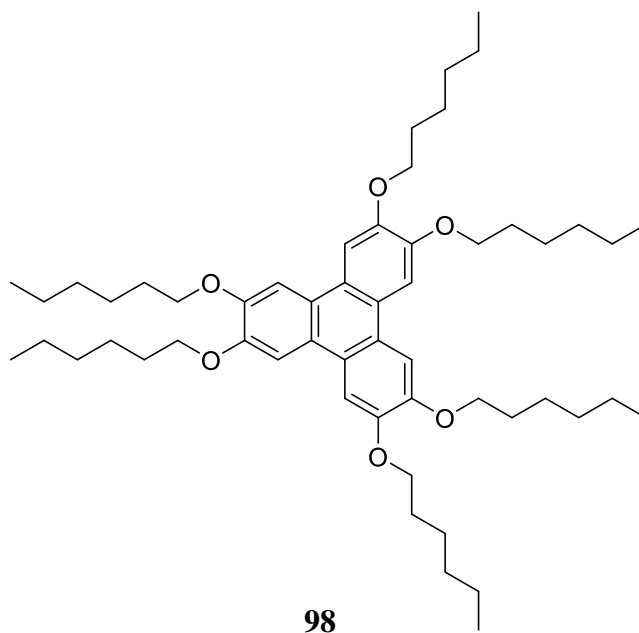


96

Following a modification to the procedure described by Howard et al,¹⁶⁹ and Cammidge group¹⁹⁴ catechol **95** (50.0 g, 0.454 mol), 1-bromohexane (180.0 g, 1.090 mol) and potassium carbonate (150.0 g, 1.090 mol) were suspended in EtOH (300 ml) with potassium iodide (0.01 g) and the reaction mixture was refluxed for 3 days. The mixture was then cooled to room temperature, filtered, and the solvent was removed under reduced pressure. The crude product was purified by distillation to give 1,2-dihexyloxy benzene **96** as a pale brown oil. (83.55 g, 66%).“data consistent with previously reported”

¹H NMR (500 MHz, Chloroform-*d*) δ 6.92 – 6.88 (m, 4H), 4.01 (t, $J = 6.7$ Hz, 4H), 1.88 – 1.78 (m, 4H), 1.53 – 1.45 (m, 4H), 1.42 – 1.33 (m, 8H), 0.97 – 0.89 (m, 6H).

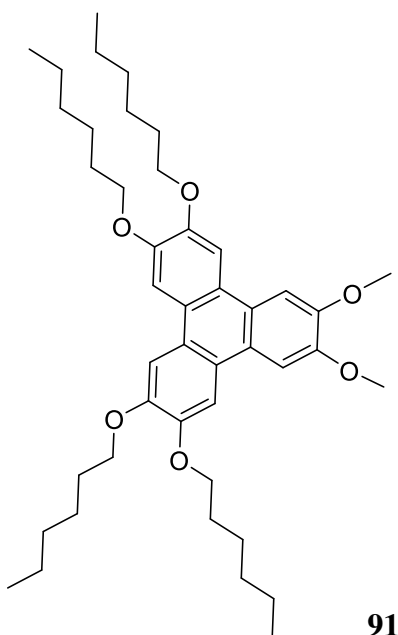
4.2.3 Synthesis of 2,3,6,7,10,11-Hexahexyloxytriphenylene [HAT6] **98** (iron(III) chloride route)



Following the method that was reported by the Cammidge group,^{172, 194} 1,2-dihexyloxybenzene **96** (1.0 g, 3.590 mmol) was added to a vigorously stirred suspension of iron(III) chloride (1.74 g, 10.770 mmol) in dichloromethane (25 ml) with concentrated sulfuric acid (2 drops). The reaction mixture was stirred in ice bath for 2 hrs then was quenched with methanol (60 ml). The reaction mixture was filtered off, and the solvent was removed in vacuo. Then, the black solid was purified by column chromatography, eluting with DCM: PET (1:1 v:v) to give the product of 2,3,6,7,10,11-hexahexyloxytriphenylene **98** as a plate yellow solid, which was recrystallized from ethanol (0.36 g, 36%). “data consistent with previously reported”

¹H NMR (500 MHz, chloroform-*d*) δ 7.84 (s, 6H), 4.23 (t, $J = 6.6$ Hz, 12H), 1.97 – 1.91 (m, 12H), 1.61 – 1.55 (m, 12H), 1.43 – 1.36 (m, 24H), 0.93 (t, $J = 6.8$ Hz, 18H).

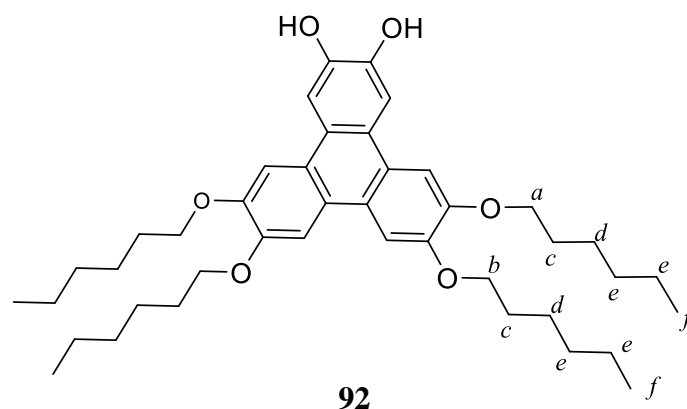
4.2.4 Synthesis of 2,3-dimethoxy-6,7,10,11-tetrahexyloxytriphenylene **91**



Following the reported method¹⁷² a mixture of 1,2-dihexyloxybenzene **96** (2.0 g, 7.20 mmol) and veratrole **97** (1.0 g, 7.20 mmol) was added dropwise to a stirred mixture of iron(III) chloride (7.0 g, 43.2 mmol) and dichloromethane (50 ml). The reaction mixture was maintained stirred in ice bath. The mixture was stirred for a further 2 hrs, then quenched with methanol (100 ml). The resulting product was filtered. The solid was purified by column chromatography on silica, eluting with DCM: PET (1:1 v:v). The white solid was recrystallized by using a mixture of DCM: MeOH to give the product of 2,3-dimethoxy-6,7,10,11-tetrahexyloxytriphenylene **91** (0.45 g, 21%). “data consistent with previously reported”

M.P. 125 °C., lit.¹⁷² 116 °C.; **¹H NMR (500 MHz, chloroform-*d*)** δ 7.86 (s, 2H), 7.86 (s, 2H), 7.82 (s, 2H), 4.28 – 4.20 (m, 8H), 4.13 (s, 6H), 2.00 – 1.90 (m, 8H), 1.54 – 1.36 (m, 24H), 0.98 – 0.91 (m, 12H).; **MS (MALDI-TOF):** m/z [M^+] calc, for (C₄₄H₆₄O₆)⁺: 688, found = 688 [M^+].

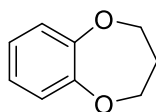
4.2.5 Deprotection of 2,3- bis(hydroxy)triphenylene **92**



Using our new method of employing microwave reaction, a mixture of 2,3-dimethoxytriphenylene **91** (1.0 g, 1.50 mmol), potassium carbonate (1.3 g, 9.44 mmol) and thiophenol (0.81 g, 7.26 mmol) were placed in a microwave vessel and sealed with magnetic bar. It was filled with argon after being purged for five minutes. To this was added dry DMF (6 ml) and stirring continued under argon for a further 10 min. Then the combination was irradiated via microwave at 120 °C for 3 hrs. Finally, the solution was allowed to cool down, then poured onto concentrated HCl (10 ml) and ice (50 ml), filtered, and the residue dissolved in a minimum of DCM. This was then purified by using column chromatography, eluting with DCM: PET (2: 1 v: v). The solvent was removed under reduced pressure to give 2,3-bis(hydroxy)triphenylene **92**, which was recrystallized using a mixture of DCM: MeOH to give the product as a white solid, (0.71 g, 74%).

¹H NMR (500 MHz, chloroform-*d*) δ 7.89 (s, 2H, Ar-*H*), 7.80 (s, 2H, Ar-*H*), 7.77 (s, 2H, Ar-*H*), 4.21 (t, $J = 6.6$ Hz, 4H, H_a), 4.16 (t, $J = 6.6$ Hz, 4H, H_b), 1.94 – 1.86 (m, 8H, H_c), 1.59 – 1.47 (m, 8H, H_d), 1.39 – 1.35 (m, 16H, H_e), 0.92 (t, $J = 12.6$ Hz, 12H, H_f). **MS (MALDI-TOF):** m/z [M^+] calc, for (C₄₂H₆₀O₆)⁺: 660.43, found = 660.38 [M^+].

4.2.6 3,4-dihydro-2H-[b][1,4]dioxepine **101** (side Product)

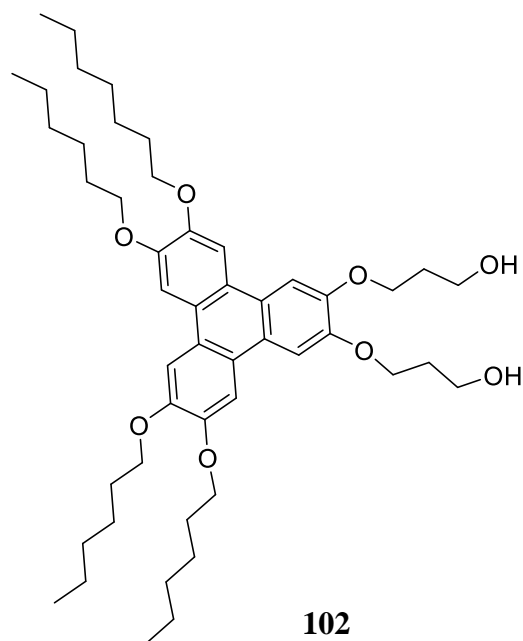


101

Following a modification to the procedure described by Howard et al,¹⁶⁹ Catechol **95** (10.0 g, 90.910 mmol), 1,3-dibromopropane (184.0 g, 909.00 mmol) and potassium carbonate (38.0 g, 272.70 mmol) were suspended in EtOH (100 ml) and refluxed for 3 days. The mixture was then cooled to room temperature, filtered, and the solvent was removed under reduced pressure. The crude product was purified by column chromatography to give 3,4-dihydro-2H-[b][1,4]dioxepine **101** as brown oil , (2.6 g, 20%). “data consistent with previously reported”

¹H NMR (500 MHz, chloroform-*d*) δ 6.96 – 6.87 (m, 4H), 4.29 – 4.23 (m, 4H), 2.32 – 2.24 (m, 2H).

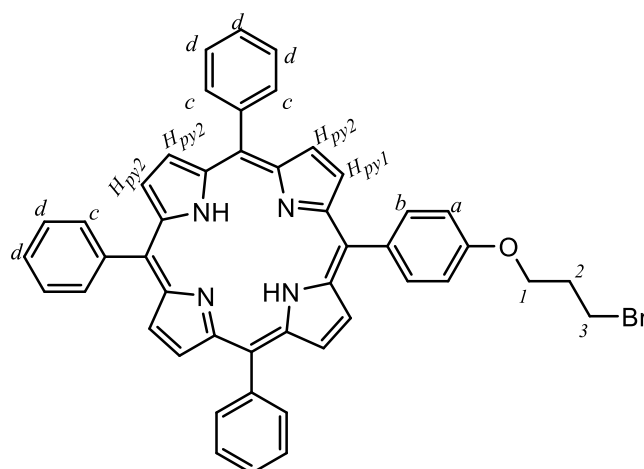
4.2.7 Synthesis of 2,3-bis(hydroxypropoxy)triphenylene **102**



2,3-Bis(hydroxy)triphenylene **92** (0.44 g, 0.605 mmol), 1-bromo-3-propanol (0.25 g, 1.815 mmol) and potassium carbonate (0.28 g, 1.990 mmol) were suspended in EtOH (15 ml) and refluxed for 2 days. The mixture was then cooled to room temperature, water (100 ml) was added, and the mixture was extracted by using DCM (3 x 50 ml) and dried with anhydrous (MgSO_4), filtered off, then the solvent removed under reduced pressure. The crude product was purified by column chromatography. Then the compound was recrystallized with EtOH to give the product 2,3-bis(hydroxypropoxy)triphenylene **102** as a white semi-solid. (29 mg, 6%).

$^1\text{H NMR}$ (500 MHz, Chloroform-*d*) δ 7.83 (s, 6H), 4.43 (t, $J = 5.6$ Hz, 4H), 4.25 – 4.21 (m, 8H), 3.96 (t, $J = 5.5$ Hz, 4H), 3.75 – 3.72 (m, 16H), 2.22 – 2.15 (m, 4H), 1.98 – 1.89 (m, 16H), 1.58 (t, $J = 7.4$ Hz, 12H).

4.2.8 Synthesis of bromoalkoxy porphyrin **93**

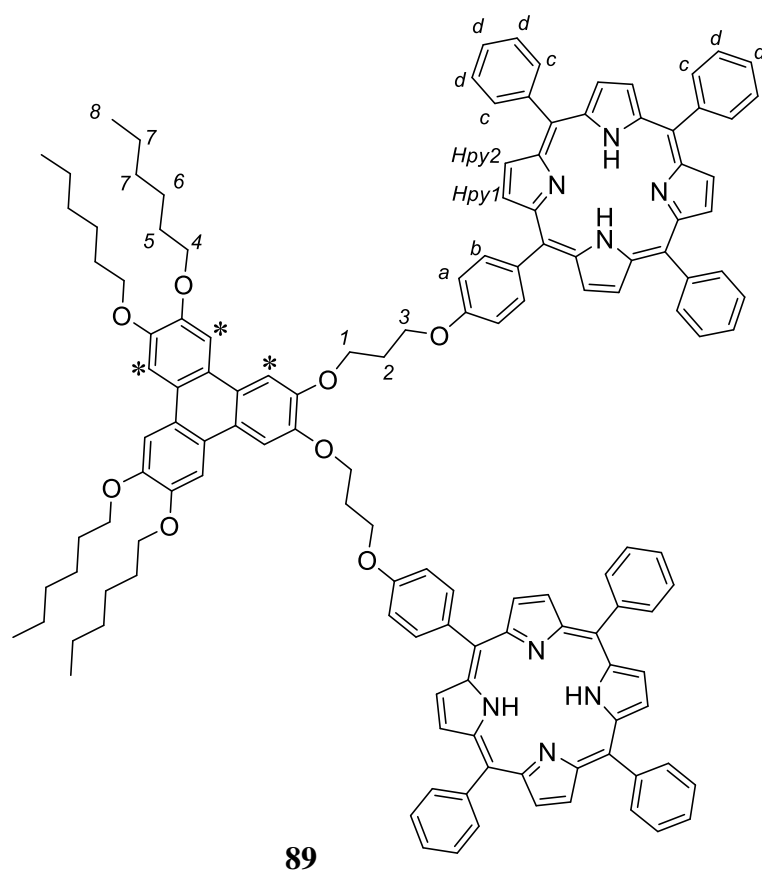


93

TPPOH **94** (2 g, 3.172 mmol), 1,3-dibromopropane (16.0 g, 8.03 ml, 79.20 mmol) and potassium carbonate (4.4 g, 31.67 mmol) were added to EtOH (20 ml) and the mixture was heated at 80°C for 24 hrs in normal refluxing. The mixture dissolved in DCM (50 ml). This was washed with water (100 ml) and the organic layer was extracted by using DCM (3 x 50 ml) and dried with anhydrous magnesium sulphate. The solvent was removed under reduced pressure. The product was recrystallized by using a mixture of DCM: MeOH to produce bromoalkoxy porphyrin **93** as a purple solid. (2.35 g, 98 %).

M.P. 293°C.; **¹H NMR (500 MHz, chloroform-*d*)** δ 8.88 (s, 2H, H_{py1}), 8.84 (s, 6H, H_{py2}), 8.22 (d, $J = 9.2$ Hz, 6H, H_c), 8.13 (d, $J = 6.5$ Hz, 2H, H_b), 7.82 – 7.71 (m, 9H, H_d), 7.29 (d, $J = 8.6$ Hz, 2H, H_a), 4.41 (t, $J = 5.7$ Hz, 2H, H_1), 3.79 (t, $J = 6.4$ Hz, 2H, H_3), 2.57 – 2.48 (m, 2H, H_2), -2.77 (s, 2H, NH).; **¹³C NMR (126 MHz, CDCl₃)** δ 158.5, 142.2, 142.2, 135.6, 135.6, 134.8, 134.5, 133.3, 127.7, 126.6, 120.1, 120.0, 119.9, 118.0, 112.9, 112.7, 69.1, 65.6, 32.6, 30.9, 30.1.; **MS (MALDI-TOF):** m/z [M^+] calc, for (C₄₇H₃₅BrN₄O)⁺: 752.19, found = 752.00 [M^+].; **UV-vis, λ_{max} (DCM)/nm** 415, $\epsilon=2 \times 10^5$; 515, $\epsilon=1.42 \times 10^3$; 556, $\epsilon=5.14 \times 10^3$; 595, $\epsilon=3.57 \times 10^3$; 645, $\epsilon=2.15 \times 10^3$.; **IR (KBr, cm⁻¹):** 3317, 2704, 2599, 2356, 1595, 1504, 1469, 1346, 1220, 1172, 1152, 979, 963, 844, 780, 699, 656.

4.2.9 Synthesis of 2,3-bis(porphyrin)triphenylene first model **89**

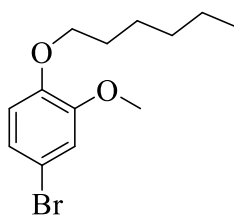


Bromoalkoxy porphyrin **93** (1.7 g, 2.270 mmol), 2,3-bis(hydroxy)triphenylene **92** (0.6 g, 0.911 mmol) and potassium carbonate (0.4 g, 2.723 mmol) were added to dry DMF (20 ml). This was placed under nitrogen and heated at 80°C for 2 days. The mixture was cooled to room temperature and DCM (50 ml) was added, washed with water (50 ml) and the organic layer was extracted with DCM (3 x 50 ml). The crude product was purified by using column chromatography, eluting with DCM:PET (1:1 v:v) to produce 2,3-bis(porphyrin)triphenylene **89** which was recrystallized using a mixture of DCM: MeOH to give the compound as a dark purple solid. (0.77 g, 43 %).

M.P. 210°C.; **¹H NMR (500 MHz, chloroform-*d*)** δ 8.77 (d, 4H, *H_{py1}*), 8.74-8.65 (m, 12H, *H_{py2}*), 8.12 (d, 4H, *H_b*), 8.06 – 8.00 (m, 12H, *H_c*), 7.98 (s, 2H, *Ar-H**), 7.89 (s, 2H, *Ar-H**), 7.81 (s, 2H, *Ar-H**), 7.69 – 7.53 (m, 18H, *H_d*), 7.30 (d, 4H, *H_a*), 4.64 – 4.55 (m, 8H, *H₄*), 4.22 (t, 4H, *H₁*), 4.18 (t, 4H, *H₃*), 2.61 (p, 4H, *H₂*), 1.92 – 1.83 (m, 8H, *H₅*), 1.35 – 1.26 (m, 8H, *H₆*), 1.11 – 1.02 (m, 16H, *H₇*), 0.86 (t, 6H, *H₈*), 8.80 (t, 6H, *H₈*), -2.87 (s, 4H, *NH*).; **¹³C NMR (126 MHz, chloroform-*d*)** δ 158.8, 149.2, 149.1, 148.7, 142.1, 142.1, 135.7, 134.7, 134.56, 134.4, 127.6, 126.6, 126.5, 124.0, 123.8, 123.5, 120.0, 119.9, 119.9, 112.8, 107.6, 107.5, 107.4, 69.8,

69.7, 66.4, 65.0, 31.7, 31.7, 29.8, 29.5, 29.4, 25.8, 22.6, 22.6, 14.0, 14.0.; **MS (MALDI-TOF):** m/z $[M^+]$ calc, for $(C_{136}H_{128}N_8O_8)^+$: 2001.98, found 2001.88 $[M^+]$.; **UV-vis, λ_{max} (DCM)/nm** 275, $\epsilon=3 \times 10^5$; 418, $\epsilon=2.02 \times 10^4$; 516, $\epsilon=1.28 \times 10^4$; 545, $\epsilon=3.17 \times 10^4$; 595, $\epsilon=2.01 \times 10^4$; 650, $\epsilon=1 \times 10^4$.; **IR (KBr, cm^{-1}):** 3312, 2945, 2909, 2850, 1598, 1504, 1470, 1250, 1161, 1033, 1005, 979, 964, 873, 842, 797, 723, 700.

4.2.10 Synthesis 4-bromo-1-hexoxo-2-methoxybenzene **108**

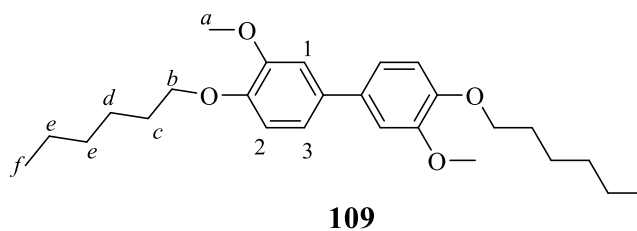


108

4-Bromo-2-methoxyphenol **107** (10.0 g, 49.250 mmol) was mixed with 1-bromohexane (102.0 g, 615.620 mmol), potassium carbonate (34.0 g, 246.250 mmol) and potassium iodide (16.60 mg) and suspended in ethanol (200 ml) and it was refluxed for 3 days. Then, it was washed with water (3 x 50 ml) and extracted with DCM (3 x 50 ml). The organic extracts were combined and dried using anhydrous magnesium sulphate. The solvent was evaporated under vacuo and distillation took place to obtain 4-bromo-1-hexoxo-2-methoxybenzene **108** as a clear oil (13.46 g, 95%)

1H NMR (500 MHz, chloroform-*d*) δ 7.28 (d, $J = 2.3$ Hz, 1H), 7.26 (d, $J = 1.9$ Hz, 1H), 7.00 (d, $J = 8.3$ Hz, 1H), 4.24 (t, $J = 6.8$ Hz, 2H), 4.11 (s, 3H), 2.15 – 2.05 (m, 2H), 1.79 – 1.69 (m, 2H), 1.68 – 1.57 (m, 4H), 1.25 – 1.16 (m, 3H).

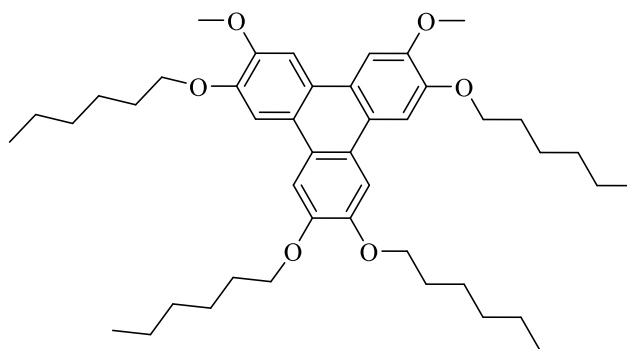
4.2.11 Synthesis di(hexyloxy)di(methoxy)biphenyl **109**



Following a modification to the method outlined by Lin *et al.*,¹⁸³ 4-bromo-1-hexyloxy-2-methoxybenzene **108** (9.0 g, 31.330 mmol), NiCl₂ (0.2 g, 1.565 mmol), PPh₃ (3 g, 9.4022 mmol) and Zn powder (3.07g, 47.00 mmol) were added to dry pyridine (20-25ml). It was refluxed for 3-4 hrs under argon. Then, it was stirred overnight to cool. DCM (50 ml) was added, and the Zinc powder filtered off. The solution then was washed with water (3 x 50 ml) and the aqueous washings extracted with DCM (3 x 50 ml). Then it was dried with MgSO₄. The solvent was removed under reduced pressure and cold MeOH was then added, and the product filtered off. This gave the di(hexyloxy)di(methoxy)biphenyl **109** as a white solid (5.62 g, 44%)

¹H NMR (500 MHz, Chloroform-*d*) δ 7.09 (d, 2H, *Ar-H*₂), 7.07 (s, 2H, *Ar-H*₁), 6.93 (d, 2H, *Ar-H*₃), 4.05 (t, *J* = 6.9 Hz, 4H, *H*_a), 3.93 (s, 6H, *H*_b), 1.91 – 1.83 (m, 4H, *H*_c), 1.52 – 1.45 (m, 4H, *H*_d), 1.38 – 1.31 (m, 8H, *H*_e), 0.91 (t, 6H, *H*_f).

4.2.12 Synthesis of 3,6-bis(methoxy)triphenylene **105**

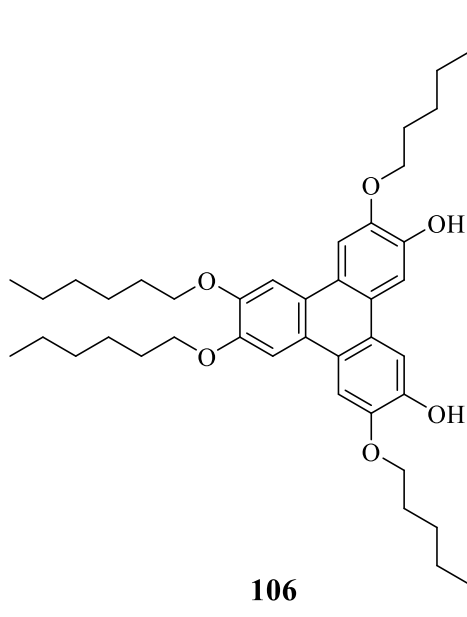


105

Following the procedure reported by Cammidge group,¹⁸⁵ di(hexyloxy)di(methoxy)biphenyl **109** (1.0 g, 2.412 mmol) was mixed with 1,2-bis(hexyloxy)benzene **96** (1.34 g, 4.820 mmol) and added dropwise to a stirred mixture of iron(III) chloride (2.34 g, 14.470 mmol) in DCM (50 ml). The reaction mixture was maintained in an ice bath for 5 hrs. Then, the reaction crude was quenched with cold MeOH (100 ml) and filtered. The product was then purified by column chromatography eluting with DCM: PET (1:1 v:v), then recrystallized by using DCM:MeOH to gain 3,6-bis(methoxy)triphenylene **105** as white solid (0.8 g, 49%).

M.P. 114.5 °C; **¹H NMR (500 MHz, Chloroform-*d*)** δ 7.86 (s, 2H), 7.80 (s, 2H), 7.82 (s, 2H), 4.29 – 4.21 (m, 8H), 4.10 (s, 6H), 2.03 – 1.90 (m, 8H), 1.64 – 1.56 (m, 8H), 1.47 – 1.34 (m, 16H), 0.94 (t, $J = 6.9$ Hz, 12H).

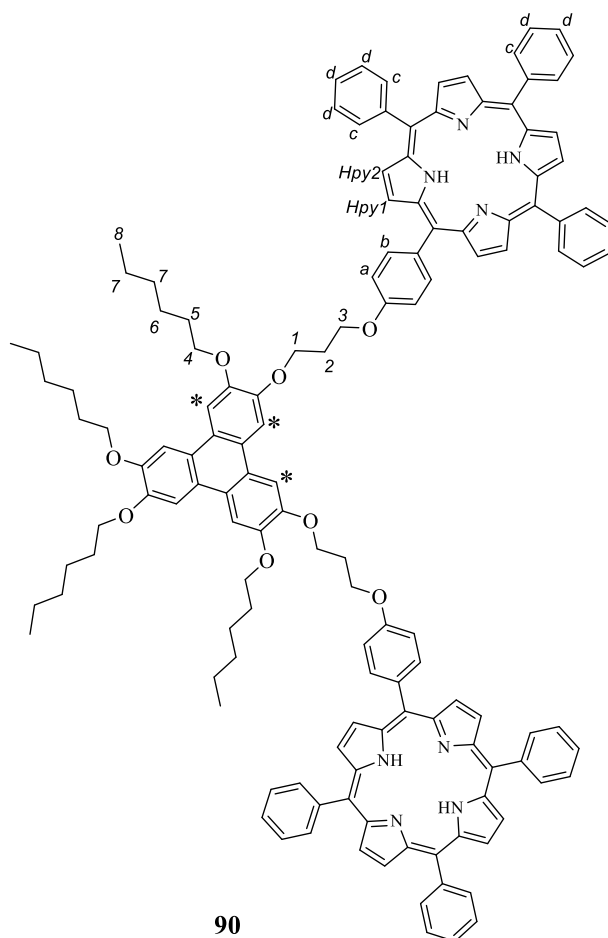
4.2.13 Deprotection of 3,6-*bis*(hydroxy)triphenylene **106**



Applying our modified conditions described above, 3,6-dimethoxytriphenylene **105** (1.5 g, 2.20 mmol), potassium carbonate (2 g, 14.30 mmol) and thiophenol (1.2 g, 11.00 mmol) were sealed in microwave vessel and (6 ml) of dry DMF was then added. The mixture was microwave-irradiated for 4 hrs at 120°C, then allowed to cool down. The solution was poured onto concentrated HCl (10 ml) and ice (50 ml) and filtered. The crude solid was then purified by using column chromatography, eluting with DCM: PET (2:1 v:v). Recrystallisation from DCM: MeOH gave 2,3-*bis*(hydroxy)triphenylene **106** as a white solid, (1 g, 72%).

M.P. 95.8 °C.; **¹H NMR (500 MHz, chloroform-*d*)** δ 7.94 (s, 2H), 7.81 (s, 2H), 7.76 (s, 2H), 4.26 (t, 4H), 4.23 (t, 4H) 1.99 – 1.89 (m, 8H), 1.61 – 1.53 (m, 8H), 1.46 – 1.35 (m, 16H), 0.97 – 0.90 (m, 12H).

4.2.14 Synthesis of 3,6-bis(porphyrin)triphenylene second model **90**

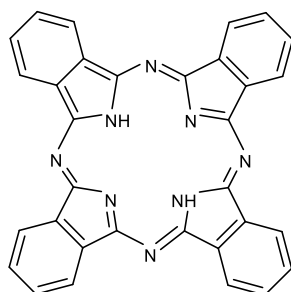


Bromoalkoxy porphyrin **93** (1.42 g, 1.890 mmol), 3,6-bis(hydroxy)triphenylene **106** (0.5 g, 0.750 mmol) and potassium carbonate (0.52 g, 3.790 mmol) were added to dry DMF (20 ml). This was placed under nitrogen and heated at 80 °C for 2 days. The mixture was cooled to room temperature, DCM (50 ml) was added, washed with water (50 ml) and the organic layer was extracted with DCM (3 x 50 ml). The crude product was purified by using column chromatography, eluting with DCM:PET (1:1 v:v) to give 3,6-bis(porphyrin)triphenylene **90** which was recrystallized using a mixture of DCM: MeOH to give the compound as a purple solid. (0.75 g, 50%).

M.P. 212°C.; **¹H NMR (500 MHz, chloroform-*d*)** δ 8.78 (d, 4H, H_{pyr1}), 8.75 – 8.69 (m, 12H, H_{pyr2}), 8.16 – 8.06 (m, 12H, H_c), 8.03 (s, 2H, $Ar-H^*$), 8.01 (d, 4H, H_b), 7.83 (s, 2H, $Ar-H^*$), 7.81 (s, 2H, $Ar-H^*$), 7.72 – 7.56 (m, 18H, H_d), 7.24 (d, 4H, H_a), 4.58 (t, $J = 6.0$ Hz, 4H, H_l),

4.50 (t, $J = 6.0$ Hz, 4H, H_3), 4.23 (t, $J = 6.6$ Hz, 4H, H_4), 4.18 (t, $J = 6.6$ Hz, 4H, H_4), 2.55 (p, $J = 6.1$ Hz, 4H, H_3), 1.98 – 1.79 (m, 8H, H_5), 1.61 – 1.47 (m, 8H, H_6), 1.41 – 1.25 (m, 16H, H_7), 0.86 (t, $J = 7.1$ Hz, 6H, H_8), 0.80 (t, $J = 7.2$ Hz, 6H, H_8), -2.85 (s, 4H, NH).; ^{13}C NMR (126 MHz, chloroform- d) δ 158.8, 149.1, 149.1, 148.8, 142.2, 135.6, 134.6, 134.5, 134.5, 127.6, 126.6, 126.6, 124.0, 123.7, 123.6, 120.0, 119.9, 112.8, 107.7, 107.4, 107.2, 69.7, 69.6, 66.4, 64.9, 53.4, 31.7, 29.8, 29.5, 29.4, 25.9, 25.8, 22.7, 22.6, 14.0.; MS (MALDI-TOF): m/z [M^+] calc, for $(C_{136}H_{128}N_8O_8)^+$: 2001.98, found 2001.77 [M^+].; UV-vis, λ_{max} (DCM)/nm 282, $\epsilon=2.3 \times 10^2$; 419, $\epsilon=1.2 \times 10^3$; 518, $\epsilon=8.1 \times 10^4$; 554, $\epsilon=5.5 \times 10^4$; 591, $\epsilon=4.6 \times 10^4$; 698, $\epsilon=4.2 \times 10^4$; 607, $\epsilon=2.9 \times 10^5$.; IR (KBr, cm^{-1}): 2950, 2914, 2847, 1599, 1553, 1504, 1465, 1426, 1380, 1349, 1258, 1238, 1161, 1031, 997, 979, 964, 876, 842, 797, 729, 700.

4.2.15 Metal-free phthalocyanine 2

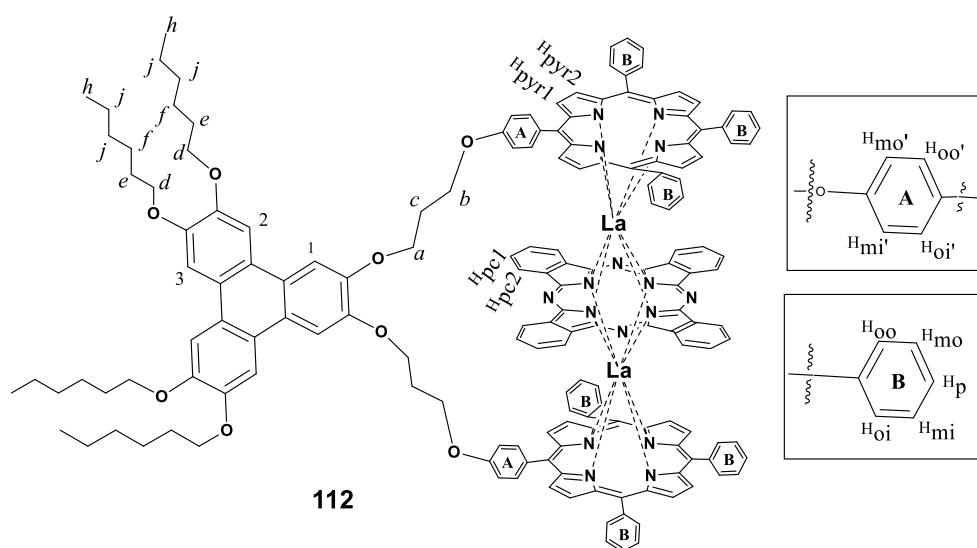


2

Following the method reported in the literature,¹⁴⁹ phthalonitrile (0.5 g, 4.00 mmol) was dissolved in 1-pentanol (6 ml), then the mixture was heated at reflux. An excess of lithium (50.0 mg, 7.20 mmol) was added to the reaction mixture, which then continued to reflux for another 1 hr. Then, acetic acid (10 ml) was added to the mixture which was refluxed for a further hour. The resulting mixture was cooled to room temperature. Finally, methanol (100 ml) was poured into the mixture to precipitate the product. A dark blue solid of phthalocyanine **2** was filtered off, to give (250 mg, 50 %). “data consistent with previously reported”

M.P.>300°C.; **MS (MALDI-TOF):** m/z [M^+] calc, for $(C_{32}H_{18}N_8)^+$: 514.17, found 514.41 [M^+].; **UV-vis, λ_{max} (THF)/nm** 326, $\epsilon=2.8 \times 10^2$; 663, $\epsilon=2.5 \times 10^3$; 692, $\epsilon=3.1 \times 10^3$.

4.2.16 Lanthanum triple-decker from 2,3-bis(porphyrin)triphenylene 112



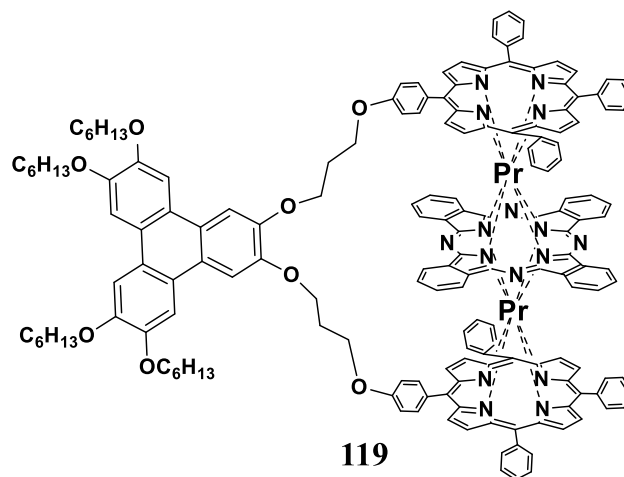
Protocol A:

2,3-bis(porphyrin)triphenylene model **89** (50.0 mg, 0.025 mmol) and metal-free phthalocyanine **2** (25.0 mg, 0.050 mmol) were heated in 1-pentanol (8 ml), reflux overnight. Then, an excess of lanthanum(III) acetylacetonate hydrate (43.5 mg, 0.100 mmol) was added and the reaction was then left refluxing for 2-4 hrs. The mixture was allowed to cool to room temperature, methanol was then added, and the mixture was left to precipitate overnight. The crude compound was filtered off then purified by column chromatography using DCM:PET:TEA (3:10:1 v:v:v) as eluent. The fraction containing the product was then recrystallised from DCM to give the La triple-decker **112** as green solid (33 mg, 47 %)

M.P >349.5°C; **¹H NMR (500 MHz, methylene chloride-*d*₂)** δ 10.32 (d, $J = 8.0$ Hz, 2H, Hoi'ph), 10.06 (d, $J = 7.3$ Hz, 6H, Hoiph), 9.35 (dd, $J = 5.6, 2.5$ Hz, 8H, Hpc₁), 8.50 (t, 6H, Hmiph), 8.29 (dd, $J = 5.6, 2.5$ Hz, 8H, Hpc₂), 8.26 (d, $J = 8.0$ Hz, 2H, Hmi'ph), 8.17 (s, 2H, H₁), 8.08 (s, 2H, H₂), 8.00 (s, 2H, H₃), 8.00, 7.85 (t, 6H, Hpph), 7.38 (d, $J = 4.2$ Hz, 4H, Hpyrr₁), 7.27 (t, $J = 7.4$ Hz, 6H, Hmoph), 7.25 – 7.21 (m, 12H, Hpyrr₂), 7.04 (d, 2H, Hoo'ph), 7.03 (d, 2H, Hmo'ph), 6.73 – 6.67 (m, 6H, Hooph), 5.09 (t, $J = 6.2$ Hz, 4H, H_a), 4.86 (bt, $J = 4.8$ Hz, 4H, H_b), 4.38 (t, $J = 6.7$ Hz, 4H, H_d), 4.34 (t, $J = 6.7$ Hz, 4H, H_d), 2.97 – 2.88 (bm, 4H, H_c), 2.03 – 2.00 (m, 8H, H_e), 1.73 – 1.62 (m, 8H, H_f), 1.52 – 1.41 (m, 16H, H_j), 0.99 (t, $J = 9.8, 7.1$ Hz, 12H, H_h); **¹³C NMR (126 MHz, methylene chloride-*d*₂)** δ 141.4, 141.2, 140.5, 140.3, 134.9, 134.9, 134.7, 134.2, 130.7, 125.4, 125.2, 125.2, 124.7, 123.0, 113.7, 106.7, 106.5, 104, 69.3, 69.3, 64.5, 64.5, 36.3, 31.5, 29.2, 25.6, 22.9, 22.5, 22.5, 22.3, 13.7, 13.7, 13.7, 13.7; **MS (MALDI-TOF):** m/z [M⁺] calc, for (C₁₆₈H₁₄₀La₂N₁₆O₈)⁺: 2787.90, found 2787.23 [M⁺]; **UV-vis, λ_{max} (DCM)/nm** 282, $\epsilon=3.36 \times 10^5$; 365, $\epsilon=2.30 \times 10^5$; 421, $\epsilon=6.13 \times 10^5$; 487, $\epsilon=5.7 \times 10^5$;

553, $\epsilon=3.32 \times 10^5$; 607, $\epsilon=2.9 \times 10^5$; **IR (KBr, cm^{-1}):** 3062, 2919, 2852, 1607, 1504, 1429, 1255, 1161, 1060, 983, 796, 729, 702.

4.2.17 Praseodymium triple-decker from 2,3-bis(porphyrin)triphenylene model **119**

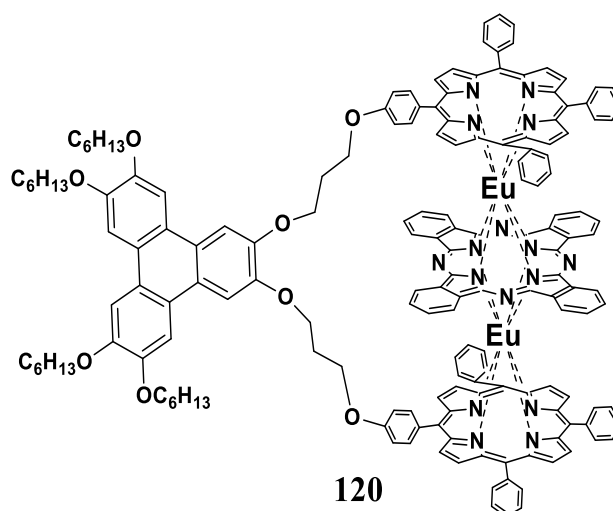


Protocol B:

2,3-Bis(porphyrin)triphenylene **89** (50.0 mg, 0.025 mmol) and metal-free phthalocyanine **2** (25.0 mg, 0.049 mmol) were heated in 1-pentanol (8 ml), reflux for 48 hrs. Then, an excess of praseodymium(III) acetylacetonate hydrate (43.71mg, 0.099 mmol) was added and the reaction was then left refluxing for 2-4 hrs. The mixture was allowed to cool to room temperature, methanol was then added, and the mixture was left to precipitate overnight. The crude compound was filtered off then purified by column chromatography using 100% DCM. The fraction containing the product was then recrystallised from DCM:MeOH to give the Pr triple-decker **119** as green solid (35 mg, 50 %)

^1H NMR (500 MHz, methylene- d_2) δ 9.47 (d, $J = 8.2$ Hz, 2H), 9.27 (d, 4H), 8.25 (d, $J = 8.9$ Hz, 2H), 7.51 (d, $J = 3.7$ Hz, 2H), 7.38 (s, 2H), 7.33 – 7.21 (m, 8H), 6.47 (d, $J = 8.9$ Hz, 4H), 6.34 – 6.26 (m, 6H), 5.68 – 5.65 (m, 8H), 5.43 (d, $J = 4.9$ Hz, 4H), 5.37 (d, 4H), 4.99 – 4.94 (m, 4H), 4.89 (s, 2H), 4.39 (s, 2H), 3.94 (t, $J = 6.4$ Hz, 4H), 3.89 (t, $J = 6.3$ Hz, 4H), 3.80 – 3.66 (m, 8H), 3.07 (t, $J = 6.5$ Hz, 4H), 1.78 – 1.73 (m, 4H), 1.72 – 1.61 (m, 4H), 1.48 – 1.45 (m, 8H), 1.38 – 1.31 (m, 4H), 1.26 – 1.16 (m, 16H), 0.77 (t, 12H); .); **^{13}C NMR (126 MHz, methylene- d_2)** δ 165.9, 158.1, 148.4, 141.3, 136.4, 132.3, 127.0, 126.8, 123.0, 116.2, 100.0, 68.2, 64.5, 31.5, 29.7, 26.7, 22.5, 21.2, 16.6.; **MS (MALDI-TOF):** m/z [M^+] calc, for $(\text{C}_{168}\text{H}_{140}\text{Pr}_2\text{N}_{16}\text{O}_8)^+$: 2791.89, found 2791.24 [M^+].; **UV-vis, λ_{max} (DCM)/nm** 282, $\epsilon=7.1 \times 10^5$; 363, $\epsilon=5.9 \times 10^5$; 420, $\epsilon=1.4 \times 10^5$; 491, $\epsilon=1.7 \times 10^5$; 549, $\epsilon=9.1 \times 10^4$; 607, $\epsilon=1.1 \times 10^4$; **IR (KBr, cm^{-1}):** 2904, 2847, 15599, 1571, 1504, 1465, 1426, 1325, 1240, 1157, 1111, 1057, 982, 852, 728.

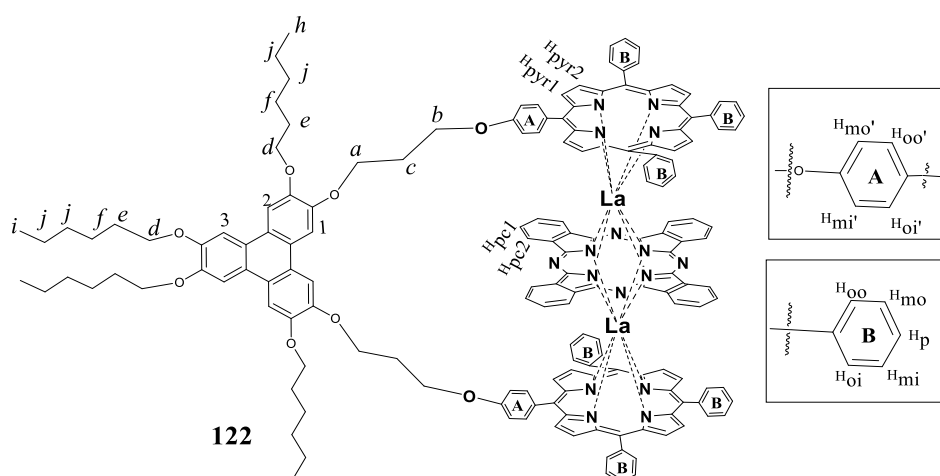
4.2.18 Europium triple-decker from 2,3-bis(porphyrin)triphenylene 120



2,3-Bis(porphyrin)triphenylene **89** (50.0 mg, 0.025 mmol) and metal-free phthalocyanine **2** (25.0 mg, 0.049 mmol) were heated in 1-pentanol (8 ml), reflux for 48 hrs. Then, an excess of europium(III) acetylacetonate hydrate (44.81 mg, 0.099 mmol) was added and the reaction was then left refluxing for 2-4 hrs. Following **protocol B** to give the Eu triple-decker **120** which was recrystallized using a mixture of DCM:MeOH to obtain the TD as green solid (36 mg, 52 %)

¹H NMR (500 MHz, methylene chloride-*d*₂) δ 14.43 (s, 2H), 14.23 (s, 2H), 14.03 (s, 4H), 12.98 – 12.94 (m, 8H), 10.74 – 10.70 (m, 8H), 10.01 (d, $J = 8.4$ Hz, 2H), 9.90 (d, $J = 8.6$ Hz, 2H), 9.76 (s, 2H), 8.54 (s, 2H), 8.53 – 8.43 (m, 6H), 8.36 (s, 2H), 8.19 (d, $J = 5.0$ Hz, 2H), 7.20 (s, 2H), 7.12 – 7.02 (m, 4H), 6.58 (s, 2H), 5.89 (t, $J = 6.1$ Hz, 4H), 4.57 (t, $J = 6.8$ Hz, 4H), 4.48 (t, $J = 6.5$ Hz, 4H), 4.01 – 3.89 (m, 8H), 3.41 – 3.35 (m, 4H), 2.12 – 2.11 (m, 4H), 1.82 – 1.74 (m, 4H), 1.60 – 1.56 (m, 16H), 1.08 (t, $J = 7.1$ Hz, 6H), 1.04 (t, $J = 7.3$ Hz, 6H).; **¹³C NMR (126 MHz, methylene chloride-*d*₂)** δ 153.1, 149.5, 149.4, 149.0, 130.1, 129.2, 127.7, 126.7, 126.3, 126.2, 125.8, 125.6, 123.8, 123.7, 123.6, 107.4, 107.3, 105.5, 73.1, 73.0, 72.5, 72.5, 69.8, 69.8, 66.9, 66.1, 66.1, 36.1, 31.8, 30.9, 30.6, 29.7, 29.6, 26.0, 26.0, 22.8, 22.8, 13.9, 13.9.; **MS (MALDI-TOF):** m/z [M^+] calc, for (C₁₆₈H₁₄₀Eu₂N₁₆O₈)⁺: 2814.96, found 2814.98[M^+].; **UV-vis, λ_{max} (DCM)/nm** 280, $\epsilon=4.8 \times 10^5$; 359, $\epsilon=4.2 \times 10^5$; 418, $\epsilon=7.7 \times 10^5$; 487, $\epsilon=1.02 \times 10^5$; 550, $\epsilon=1.1 \times 10^4$; 610, $\epsilon=2.9 \times 10^4$; **IR (KBr, cm⁻¹):** 2914, 2854, 1736, 1606, 1504, 1428, 1255, 1160, 1059, 983, 881, 835, 795, 729.

4.2.19 Lanthanum triple-decker from 3,6-bis(porphyrin)triphenylene **122**

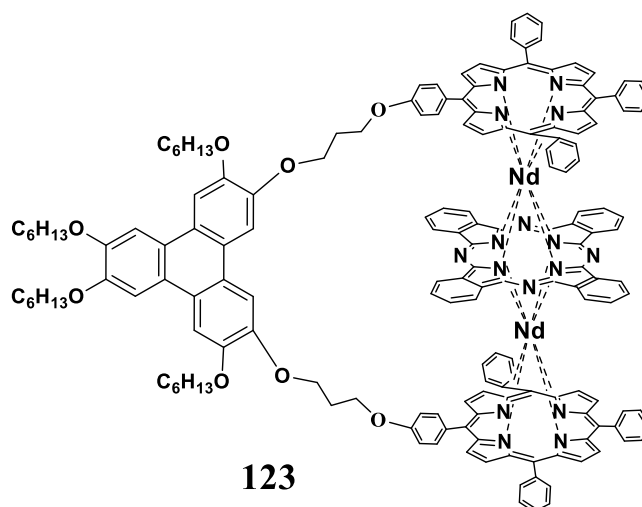


Protocol C:

3,6-Bis(porphyrin)triphenylene **90** (50.0 mg, 0.025 mmol) and metal-free phthalocyanine **2** (50.0 mg, 0.099 mmol) were heated in 1-pentanol (8 ml), reflux for 48 hrs. Then, an excess of lanthanum(III) acetylacetonate hydrate (86.89 mg, 0.199 mmol) was added. The reaction mixture was then left refluxing for 2-6 hrs, then allowed to cool down, methanol was then added, and the mixture was left to precipitate overnight. The crude solid was purified by column chromatography using 100% DCM to give the La triple-decker **122** as green solid, which was recrystallized from DCM:MeOH (35 mg, 50.72 %)

M.P >344⁰C; **¹H NMR (500 MHz, methylene chloride-*d*₂)** δ 10.18 (dd, $J = 8.1, 2.4$ Hz, 2H) $H_{oi\cdot ph}$, 10.01 – 9.96 (m, 6H) $H_{oi\cdot ph}$, 9.29 (dd, $J = 5.3, 2.9$ Hz, 8H) H_{pc1} , 8.45 – 8.38 (m, 6H) $H_{mi\cdot ph}$, 8.30 (d, $J = 2.8$ Hz, 2H) H_l , 8.18 (dd, 8H) H_{pc2} , 8.16 (d, $J = 2.9$ Hz, 2H) $H_{mi\cdot ph}$, 7.97 (s, 2H) H_2 , 7.93 (s, 2H) H_3 , 7.79 – 7.72 (m, 6H) $H_{p\cdot ph}$, 7.22 (d, $J = 4.2$ Hz, 4H) H_{pyrr} , 7.20 – 7.16 (m, 6H) $H_{mo\cdot ph}$, 7.16 – 7.13 (m, 12H) H_{pyrr} , 6.86 (dd, $J = 8.0, 2.8$ Hz, 2H) $H_{oo\cdot ph}$, 6.74 (dd, $J = 7.9, 2.4$ Hz, 2H) $H_{mo\cdot ph}$, 6.61 (t, $J = 6.7$ Hz, 6H) H_a , 4.82 (t, $J = 6.1$ Hz, 4H) H_b , 4.33 – 4.23 (m, 8H) H_d , 2.69 (p, $J = 6.1$ Hz, 4H) H_c , 1.99 – 1.89 (m, 8H) H_e , 1.64 – 1.55 (m, 8H) H_f , 1.45 – 1.34 (m, 16H) H_j , 0.92 (t, $J = 7.0$ Hz, 6H) H_h , 0.86 (t, $J = 7.2$ Hz, 6H) H_i ; **¹³C NMR (126 MHz, methylene chloride-*d*₂)** δ 133.8, 128.5, 123.6, 123.4, 121.7, 121.5, 121.5, 121.4, 121.3, 117.3, 117.1, 114.9, 114.7, 114.6, 114.3, 114.2, 70.8, 70.0, 67.6, 67.1, 66.9, 66.2, 65.89, 32.7, 32.1, 32.0, 31.8, 30.5, 30.0, 29.8, 29.6, 29.6, 26.0, 22.8, 15.1, 14.0, 14.0, 14.0, 13.9; **MS (MALDI-TOF):** m/z [M^+] calc, for (C₁₆₈H₁₄₀La₂N₁₆O₈)⁺: 2787.90, found 2787.23[M^+]. **UV-vis, λ_{max} (DCM)/nm** 229, $\epsilon=1.32\times 10^6$; 279, $\epsilon=7.54\times 10^5$; 361, $\epsilon=3.09\times 10^5$; 421, $\epsilon=7.10\times 10^5$; 490, $\epsilon=7.47\times 10^4$; 554, $\epsilon=3.40\times 10^4$; 608, $\epsilon=2.84\times 10^4$; **IR (KBr, cm⁻¹):** 2919, 2888, 1842, 1607, 1506, 1470, 1426, 1328, 1240, 1160, 1114, 1060, 982, 878, 835, 746, 729, 698.

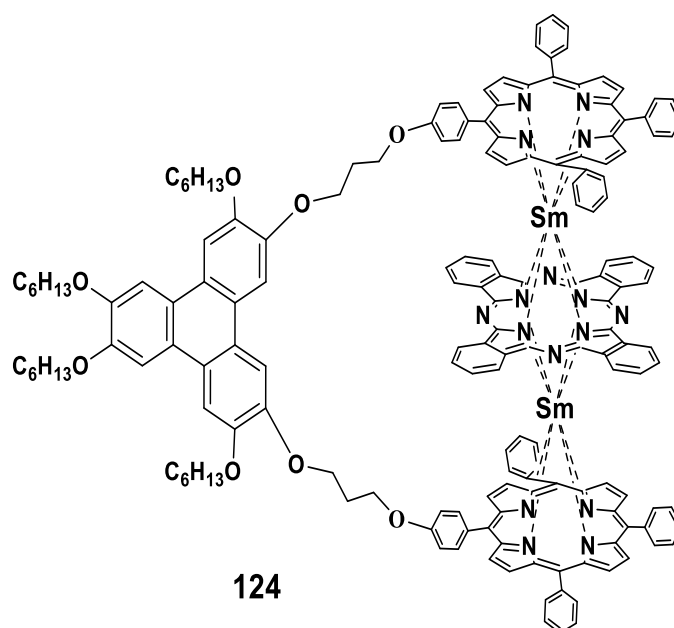
4.2.20 Neodymium triple-decker from 3,6-bis(porphyrin)triphenylene 123



3,6-bis(porphyrin)triphenylene **90** (50.0 mg, 0.025 mmol) and metal-free phthalocyanine **2** (50.0 mg, 0.099 mmol) were heated in 1-pentanol (8 ml), reflux for 48 hrs. then, an excess of neodymium(III) acetylacetonate hydrate (86.16 mg, 0.199 mmol) was added. Following **protocol C** gave the TD of Nd triple-decker **123** as green solid (42 mg, 60 %)

¹H NMR (500 MHz, methylene chloride-*d*₂) δ 8.37 (d, $J = 7.8$ Hz, 2H), 8.27 (d, $J = 7.7$ Hz, 4H), 7.63 (s, 4H), 7.60 (s, 2H), 7.35 – 7.31 (m, 8H), 7.30 – 7.21 (m, 15H), 6.82 (t, $J = 7.1$ Hz, 6H), 6.75 (d, 2H), 6.23 (d, $J = 6.5$ Hz, 4H), 6.20 – 6.16 (m, 2H), 5.88 (s, 2H), 5.20 – 5.16 (m, 8H), 4.49 – 4.45 (m, 2H), 4.39 – 4.35 (m, 4H), 4.21 – 4.17 (m, 9H), 4.10 (t, $J = 6.1$ Hz, 4H), 4.07 – 4.00 (m, 8H), 3.89 (t, $J = 6.3$ Hz, 4H), 2.17 – 2.09 (m, 4H), 1.80 – 1.71 (m, 8H), 1.51 – 1.47 (m, 16H), 1.47 – 1.37 (m, 8H), 1.34 – 1.21 (m, 14H), 0.81 (t, 12H).; **¹³C NMR (126 MHz, methylene chloride-*d*₂)** δ 157.3, 151.8, 151.7, 151.2, 149.0, 148.8, 148.6, 139.9, 136.2, 135.9, 135.7, 134.0, 127.6, 126.1, 125.5, 124.4, 123.5, 123.2, 123.1, 116.9, 107.3, 107.1, 106.9, 106.8, 69.4, 65.8, 63.9, 63.8, 31.6, 31.5, 29.6, 29.3, 29.3, 25.7, 22.6, 22.6, 13.7, 13.7.; **MS (MALDI-TOF):** m/z [M^+] calc, for $(C_{168}H_{140}Nd_2N_{16}O_8)^+$: 2797.93, found 2797.65 [M^+].; **UV-vis, λ_{max} (DCM)/nm** 281, $\epsilon=4.1 \times 10^5$; 358, $\epsilon=3.8 \times 10^5$; 421, $\epsilon=7.5 \times 10^5$; 489, $\epsilon=9.2 \times 10^4$; 554, $\epsilon=4.7 \times 10^4$; 617, $\epsilon=4.7 \times 10^4$; **IR (KBr, cm^{-1}):** 2950, 2928, 2852, 1604, 1510, 1470, 1434, 1328, 1260, 1166, 1114, 1067, 984, 881, 797, 731, 698.

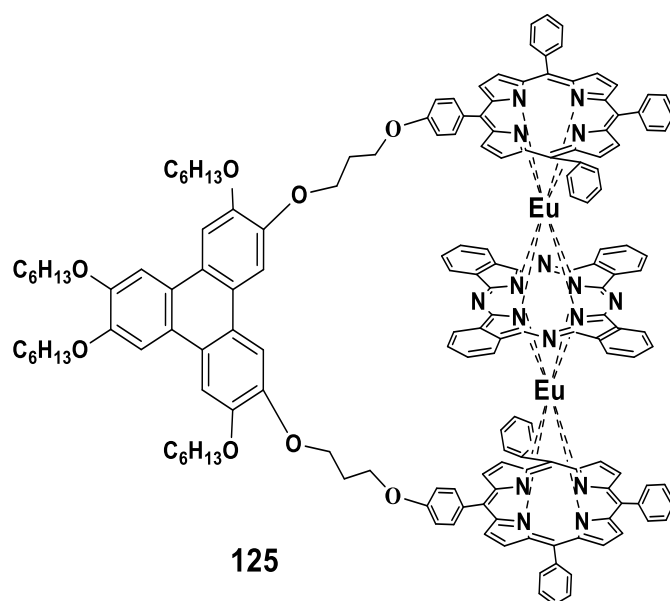
4.2.21 Samarium triple-decker from 3,6-bis(porphyrin)triphenylene 124



3,6-bis(porphyrin)triphenylene **90** (50.0 mg, 0.025 mmol) and metal-free phthalocyanine **2** (50.0 mg, 0.099 mmol) were heated in 1-pentanol (8 ml), reflux for 48 hrs. Then, an excess of samarium(III) acetylacetonate hydrate (93.37 mg, 0.199 mmol) was added. **Protocol C** was followed to produce the Sm triple-decker **124** as green solid (44 mg, 64 %)

¹H NMR (500 MHz, methylene chloride-*d*₂) δ 8.66 (dd, $J = 8.2, 2.3$ Hz, 2H), 8.57 (d, $J = 8.9$ Hz, 6H), 8.10 (s, 2H), 7.96 (dd, $J = 5.5, 3.0$ Hz, 8H), 7.87 (s, 2H), 7.84 (s, 2H), 7.83 – 7.77 (m, 6H), 7.61 – 7.57 (m, 2H), 7.50 (s, 2H), 7.50 – 7.48 (m, 4H), 7.46 (dd, 8H), 7.18 – 7.11 (m, 6H), 6.98 (dd, $J = 8.1, 2.2$ Hz, 2H), 6.97 – 6.93 (m, 6H), 6.78 (dd, $J = 8.1, 2.8$ Hz, 2H), 6.48 – 6.43 (m, 2H), 6.33 (d, $J = 4.5$ Hz, 4H), 6.30 – 6.24 (m, 10H), 4.59 (t, $J = 6.2$ Hz, 4H), 4.42 (t, $J = 6.1$ Hz, 4H), 4.26 – 4.13 (m, 8H), 2.57 – 2.48 (m, 8H), 1.94 – 1.83 (m, 8H), 1.59 – 1.49 (m, 8H), 1.46 – 1.43 (m, 8H), 1.42 – 1.27 (m, 16H), 0.87 (t, $J = 14.4, 6.9$ Hz, 12H).; **¹³C NMR (126 MHz, methylene chloride-*d*₂)** δ 158.1, 156.5, 150.2, 150.1, 150.1, 150.0, 149.2, 149.2, 149.0, 142.7, 142.6, 134.9, 133.3, 132.8, 132.6, 131.5, 128.4, 126.8, 125.7, 125.3, 123.9, 123.8, 123.83, 123.4, 122.1, 117.4, 117.1, 107.1, 69.6, 66.5, 31.7, 31.6, 30.0, 29.5, 29.4, 25.8, 25.1, 22.7, 13.8, 13.8.; **MS (MALDI-TOF):** m/z [M^+] calc, for (C₁₆₈H₁₄₀Sm₂N₁₆O₈)⁺: 2811.96, found 2811.06 [M^+].; **UV-vis, λ_{max} (DCM)/nm** 281, $\epsilon=6.7 \times 10^5$; 358, $\epsilon=6.2 \times 10^5$; 421, $\epsilon=1.1 \times 10^6$; 490, $\epsilon=2.0 \times 10^5$; 552, $\epsilon=8.2 \times 10^4$; 611, $\epsilon=6.1 \times 10^4$.; **IR (KBr, cm⁻¹):** 2919, 2888, 2842, 1607, 1506, 1470, 1426, 1328, 1240, 1160, 1114, 1060, 982, 878, 835, 786, 729, 699.

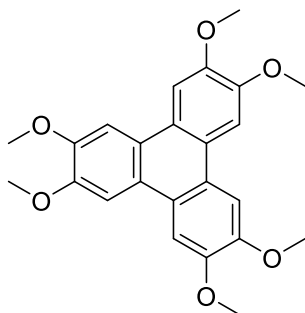
4.2.22 Europium triple-decker from 3,6-bis(porphyrin)triphenylene 125



3,6-bis(porphyrin)triphenylene model **90** (50.0 mg, 0.0249 mmol) and metal-free phthalocyanine **2** (50.0 mg, 0.0996 mmol) were heated in 1-pentanol (8 ml), reflux for 48 hrs. Then, an excess of europium(III) acetylacetonate hydrate (89.5 mg, 0.1992 mmol) was added. Following **protocol C** gave the Eu triple-decker **125** as green solid (38 mg, 55 %).

¹H NMR (500 MHz, methylene chloride-*d*₂) δ 14.01 (d, 4H), 13.83 (d, 4H), 12.96 (dd, 8H), 10.72 (s, 2H), 9.92 (d, *J* = 8.9 Hz, 2H), 9.86 (d, 2H), 9.66 (s, 2H), 8.91 (d, *J* = 5.8 Hz, 3H), 8.53 – 8.43 (m, 7H), 8.31 (s, 2H), 8.24 (s, 2H), 7.13 – 7.04 (m, 6H), 6.94 (d, *J* = 6.7 Hz, 2H), 5.91 (d, *J* = 7.0 Hz, 3H), 5.45 – 5.37 (m, 6H), 5.31 (d, 2H), 5.26 (t, *J* = 5.9 Hz, 4H), 4.62 (t, *J* = 7.0 Hz, 4H), 4.52 (t, *J* = 6.1 Hz, 4H), 4.34 – 4.25 (m, 3H), 4.15 – 4.09 (m, 4H), 4.04 – 3.98 (m, 8H), 3.24 – 3.15 (m, 4H), 2.26 – 2.12 (m, 8H), 1.89 – 1.77 (m, 8H), 1.68 – 1.58 (m, 8H), 1.57 – 1.50 (m, 16H), 1.13 (t, *J* = 6.9 Hz, 6H), 1.03 (t, *J* = 7.3 Hz, 6H).; **¹³C NMR (126 MHz, methylene chloride-*d*₂)** δ 31.8, 30.6, 29.7, 29.6, 26.0, 26.0, 22.8, 13.9, 13.9, 130.1, 130.1, 129.2, 128.6, 127.7, 126.7, 126.3, 126.2, 125.7, 109.9, 107.3, 107.3, 105.5, 73.1, 73.0, 72.5, 72.3, 69.8, 69.8, 66.9.; **MS (MALDI-TOF):** *m/z* [*M*⁺] calc, for (C₁₆₈H₁₄₀Eu₂N₁₆O₈)⁺: 2814.96, found 2814.92 [*M*⁺].; **UV-vis, λ_{max} (DCM)/nm** 280, ϵ =5.1x10⁵; 360, ϵ =4.4x10⁵; 417, ϵ =9.3x10⁵; 488, ϵ =8.5x10⁴; 551, ϵ =1.3x10⁴; 606, ϵ =2.1x10⁴; **IR (KBr, cm⁻¹):** 2915, 2914, 2848, 1738, 1604, 1501, 1469, 1426, 1369, 1328, 1238, 1160, 1104, 1059, 984, 878, 796, 719.

4.1.23 Synthesis of *hexa*-(methoxy)triphenylene **128**

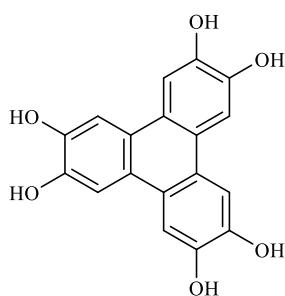


128

Following the method initially outlined by Krebs *et al*,¹⁸⁹ 1,2dimethoxybenzene **97** (5.0 g, 36.190 mmol) was dissolved in DCM (500 ml). FeCl₃ (35.0 g, 217.130 mmol) was added and stirred for 2 hrs. This was then poured onto cold methanol (100 ml) and filtered to produce the *hexa*-(methoxy)triphenylene **128** (4.46 g, 30%).

M.P. 296 °C.; **¹H NMR (500 MHz, chloroform-*d*)** δ 87.81 (s, 6H) 4.13 (s, 18H).

4.1.24 Attempted deprotection of *hexa*-(methoxy)triphenylene **129**

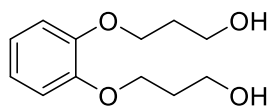


129

Hexa-(methoxy)triphenylene **128** (2.0 g, 4.90 mmol) was added to a mixture of HBr (100 ml) and acetic acid (100 ml) and refluxed overnight. Water (250 ml) was added, and the resulting product was filtered. Then, the black solid **129** was collected (1.35 g, 84 %).

Decomposed.; **¹H NMR (500 MHz, chloroform-*d*)** δ 8.26 (s, 6H).

4.1.25 Synthesis of *o*-bis((3-hydroxypropyl)oxy)benzene **131**

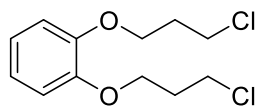


131

Catechol **95** (10 g, 90.9 mmol), 3-bromo-1-propanol (26 g, 181.80 mmol) and potassium carbonate (50 g, 364 mmol) were suspended in EtOH (200 ml) with potassium iodide (0.1 g) and the reaction mixture was refluxed for 2 days. The mixture was then cooled to room temperature, filtered and the solvents were evaporated under pressure. The crude product was purified by distillation and recrystallized by using (DCM:PET) to give *o*-bis((3-hydroxypropyl)oxy)benzene **131** as a white solid. (16.5 g, 80%).

M.P. 49.2 °C.; **¹H NMR (400 MHz, chloroform-*d*)** δ 6.98 – 6.85 (m, 4H), 4.17 (t, *J* = 5.7 Hz, 4H), 3.86 (t, 4H), 2.13 – 1.98 (m, 4H).; **¹³C NMR (126 MHz, chloroform-*d*)** δ 148.3, 121.3, 113.0, 67.7, 61.1, 31.6.

4.1.26 Synthesis of 1,2-bis(3-chloropropoxy)benzene **132**

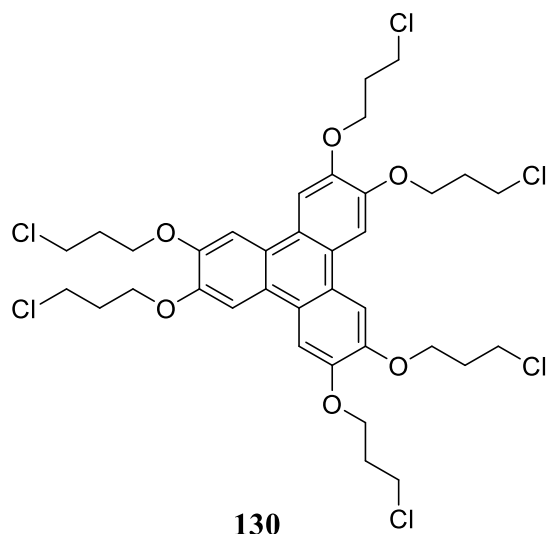


132

o-Bis((3-hydroxypropyl)oxy)benzene **131** (5.0 g, 22.09 mmol) was stirred in dry DCM with thionyl chloride (16 ml) under N₂. One to two drops of DMF were added. The solution was stirred for 48 h under anhydrous conditions at room temperature. The solvent was removed under reduced pressure and the compound was passed through a pad of silica. A colourless oil **132** was collected (4.49 g, 77%).

¹H NMR (500 MHz, chloroform-*d*) δ 6.93 (s, 4H), 4.15 (t, 4H), 3.78 (t, *J* = 6.3 Hz, 4H), 2.30 – 2.22 (m, 4H).; **¹³C NMR (126 MHz, chloroform-*d*)** δ 148.8, 121.7, 114.6, 65.7, 41.6, 32.4.

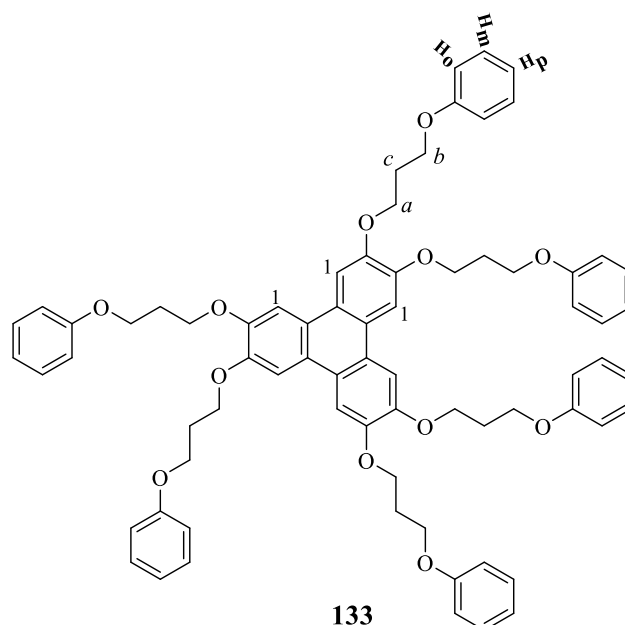
4.1.27 Synthesis of 2,3,6,7,10,11-hexa-(6-chloropropoxy)triphenylene 130



1,2-Bis(3-chloropropoxy)benzene **132** (4.5 g, 17.10 mmol) was added to a vigorously stirred suspension of iron(III) chloride (16 g, 1.102 mmol) in dichloromethane (150 ml) and in ice bath. The mixture was stirred for a further 2 hrs, then was quenched with methanol (100 ml). The resulting product was filtered off. Then, the black solid was purified by column chromatography, eluting with DCM:PET (1:1 v:v) to give the product as a pale solid **130** which was recrystallized from ethanol (9.5 g, 70 %).

M.P. 158.2°C; **¹H NMR (500 MHz, chloroform-*d*)** δ 7.83 (s, 6H), 4.34 (t, $J = 5.9$ Hz, 12H), 3.80 (t, $J = 6.2$ Hz, 12H), 2.38 – 2.28 (m, 12H).; **¹³C NMR (126 MHz, chloroform-*d*)** δ 206.9, 148.6, 123.8, 107.5, 77.2, 77.0, 76.7, 66.0, 53.4, 41.7, 32.4, 30.9.; **MS (MALDI-TOF):** m/z [M^+] calc, for $(C_{36}H_{42}Cl_6O_6)^+$: 780.11, found 780.52 [M^+].

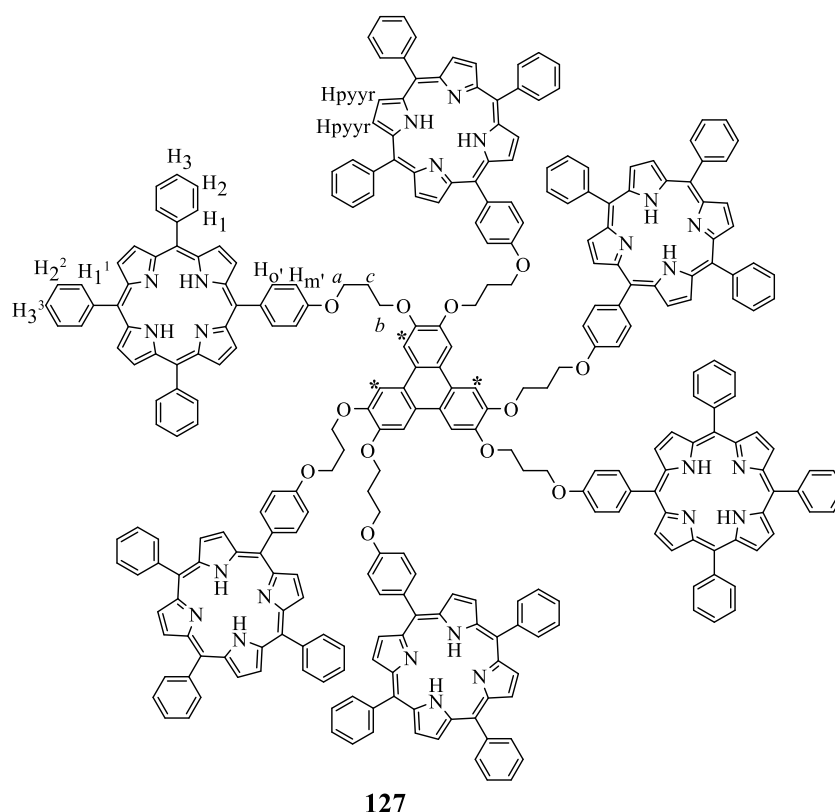
4.1.28 Synthesis test reaction with phenol 133



Phenol **134** (0.06 g, 0.640 mmol) and potassium carbonate (0.2 g, 1.280 mmol) were added to dry DMF (5 ml) with small amount of KI and benzo-15-crown (0.1 g). This was placed under nitrogen and heated at 120 °C for overnight. Then, 2,3,6,7,10,11-hexa-(6-chloropropoxy)triphenylene **130** (0.05 g, 0.064 mmol) was added to the mixture and refluxed for another 5 days. Then mixture was cooled to room temperature and DCM (50 ml) was added, washed with water (50 ml) and the organic layer was extracted with DCM (3 x 50 ml). The crude product was purified by using column chromatography, eluting with DCM: PET (2:1 v:v) to produce **133** which was recrystallized using a mixture of DCM:MeOH to give the compound as a white solid (0.042 g, 70 %).

M.P. 101°C.; **$^1\text{H NMR}$ (500 MHz, methylene chloride- d_2)** δ 7.90 (s, 6H) H_i , 7.31 – 7.22 (m, 12H) H_{oPh} , 6.99 – 6.88 (m, 18H) $H_{m,pPh}$, 4.41 (t, $J = 6.1$ Hz, 12H) H_a , 4.23 (t, $J = 6.1$ Hz, 12H) H_b , 2.36 (p, $J = 6.1$ Hz, 12H) H_c .; **$^{13}\text{C NMR}$ (126 MHz, chloroform- d)** δ 158.9, 148.7, 129.5, 120.7, 114.5, 114.5, 66.1, 64.4, 53.4, 41.3, 41.3, 29.5, 22.6, 20.4, 19.4, 14.3, 11.4.; **MS (MALDI-TOF):** m/z [M^+] calc, for $(C_{72}H_{72}O_6)^+$: 1032.53, found 1032.84 [M^+].; **UV-vis, λ_{max} (DCM)/nm** 281, $\epsilon = 7.8 \times 10^5$.; **IR (KBr, cm^{-1}):** 2925, 2869, 1598, 1495, 1469, 1434, 1390, 1300, 1240, 1168, 1052, 1027, 873, 842, 687.

4.1.29 Synthesis of *hexa*-(porphyrin) triphenylene **127**

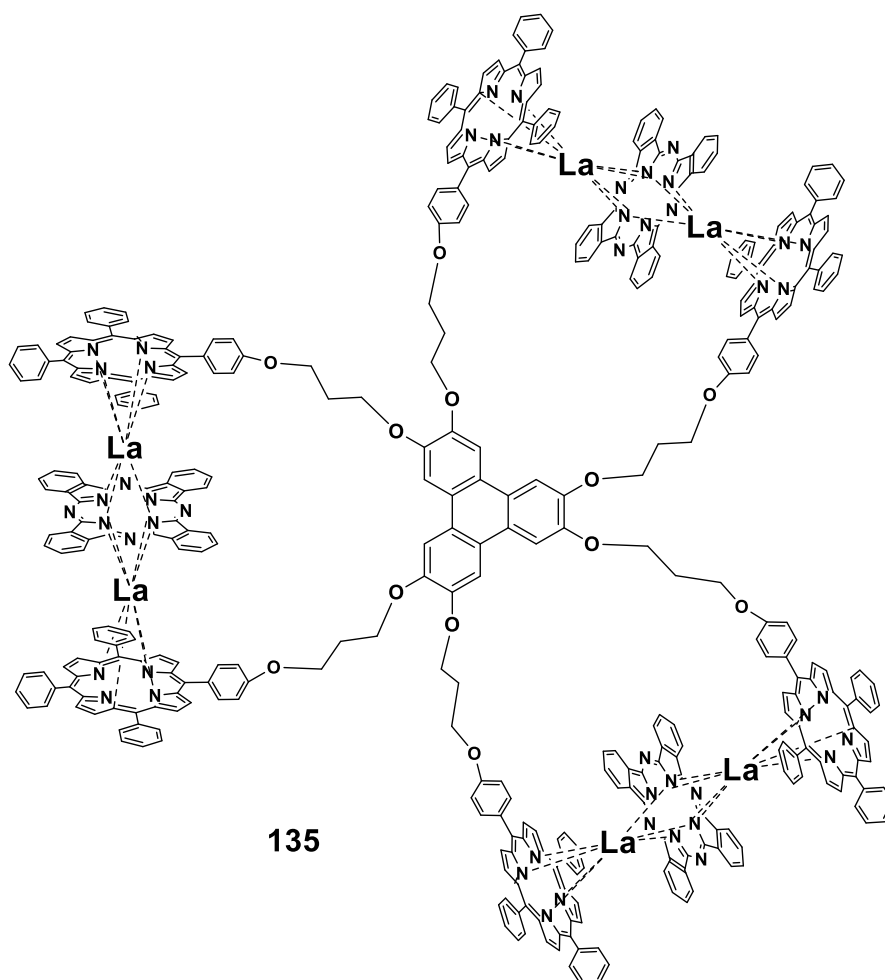


Hydroxyphenylporphyrin **94** (2 g, 2.880 mmol) and potassium carbonate (1 g, 6.730 mmol) as base were added to dry DMF (20 ml) with small amount of KI and benzo-15-crown (0.1 g). This was placed under nitrogen and heated at 120°C for overnight. Then, 2,3,6,7,10,11-*hexa*-(6-chloropropoxy)triphenylene **130** (150mg, 0.192mmol) was added to the mixture and refluxed for another 5 days. Then mixture was cooled to room temperature and DCM (50 ml) was added, washed with water (50 ml) and the organic layer was extracted with DCM (3 x 50 ml). The organic extracts were dried using magnesium anhydrous sulphate, and the solvent was then evaporated under vacuum. The crude product was purified by using column chromatography, eluting with DCM: PET (2:1 v:v) to produce **127** which was recrystallized using a mixture of DCM:MeOH to give the compound as a purple solid (0.46 g, 57.5 %).

M.P >350°C.; **¹H NMR (500 MHz, methylene chloride-*d*₂)** δ 8.68 (dq, 48H) *H*_{pyyr}, 8.11 (s, 6H) *H*^{*}, 8.01 (d, *J* = 6.6, 1.5 Hz, 12H) *H*₁¹*ph*, 7.90 (d, 12H) *H*_m'*ph*, 7.88 – 7.84 (d, 24H) *H*₁*ph*, 7.65 – 7.52 (m, 18H) *H*₃ and ³*ph*, 7.50 – 7.28 (m, 36H) *H*₂ and ²*ph*, 7.17 (d, 12H) *H*_o'*ph*, 4.61 (t, *J* = 5.9 Hz, 12H) *H*_a, 4.45 (t, *J* = 6.0 Hz, 12H) *H*_b, 2.51 (p, *J* = 5.9 Hz, 12H) *H*_c, -2.98 (s, 12H) N-H.; **¹³C NMR (126 MHz, methylene chloride-*d*₂)** δ 158.9, 149.2, 142.0, 141.9, 135.6, 134.4, 134.4, 134.3, 127.6, 127.4, 126.6, 126.4, 123.9, 120.0, 120.0, 119.9, 112.8, 66.4,

64.9, 29.8, 0.7.; **MS (MALDI-TOF):** m/z [M^+] calc, for $(C_{300}H_{216}N_{24}O_{12})^+$: 4348.71, found 4348.69 [M^+].; **UV-vis, λ_{max} (DCM)/nm** 282, $\epsilon=4.1 \times 10^4$; 419, $\epsilon=1.8 \times 10^6$; 518, $\epsilon=7.8 \times 10^4$; 553, $\epsilon=7.8 \times 10^4$; 595, $\epsilon=1.7 \times 10^4$; 650, $\epsilon=1.1 \times 10^4$.; **IR (KBr, cm^{-1}):** 3312, 3049, 2912, 1708, 1568, 1597, 1553, 1503, 1469, 1439, 1398, 1346, 1241, 1154, 1070, 1046, 1026, 979, 964, 878, 795, 699.

4.1.30 Synthesis of *tris* triple-decker system 135

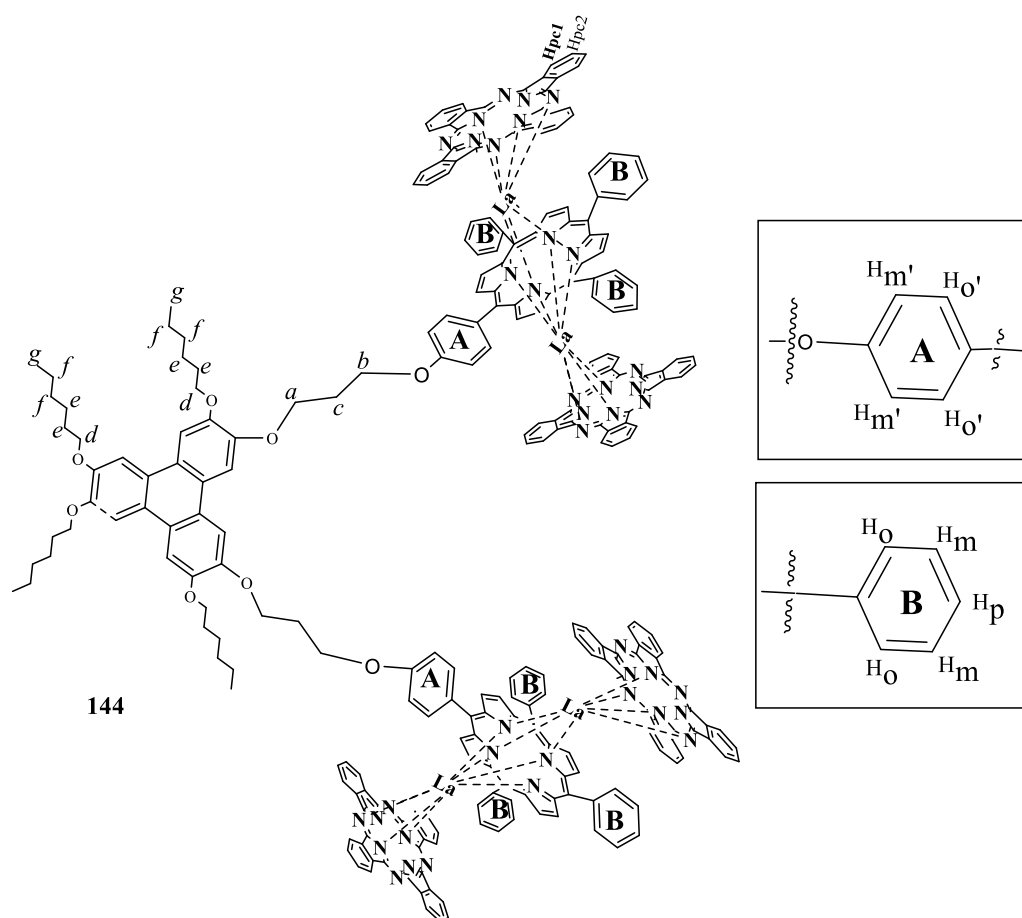


In a sealed tube, *hexa*-system model **127** (50 mg, 0.012 mmol) was mixed with (35 mg, 0.068 mmol) of metal free phthalocyanine **2** in 8 ml of 1-pentanol and was sealed then left overnight at 200 °C. An excess of lanthanum(III) acetylacetonate hydrate (120 mg, 0.280 mmol) was added and the reaction was left for week at 250 °C. The crude was precipitated with methanol (100 ml), and the required compound was filtered through a pad of silica using 100% of DCM. Then it was isolated using column chromatography over

silica gel using DCM: PET: TEA (7:10:1 v:v:v) as eluent. The dark green was collected then recrystallised from DCM:MeOH to give (21 mg, 28 %) of La-*tris* triple-decker system **135**.

R_f 0.06 (7:10:1) DCM:PET:TEA; **M.P**>350°C.; **MS (MALDI-TOF):** *m/z* [M⁺], 6713.91 [M⁺].; **UV-vis, λ_{max} (DCM)/nm** 284, ε=4.5x10⁵ ; 363, ε=6.7x10⁵ ; 419, ε=3.2x10⁶ ; 521, ε=1.4x10⁵ ; 553, ε=1.7x10⁵ ; 603, ε=1.2x10⁵.; **IR (KBr, cm⁻¹):** 3099, 2919.896, 2852.713, 2351.421, 1607.380, 1504.086, 1429.334, 1255.013, 1161.585, 1060.865, 983.996, 796.318, 729.551, 702.127

4.1.31 Synthesis of 3,6-open *bis* triple-decker system 144



In a sealed tube, 3,6-*bis*(porphyrin)triphenylene model **90** (50 mg, 0.025 mmol) and metal-free phthalocyanine **2** (10 mg, 0.190 mmol) were dissolved in 8 ml of 1-pentanol. The mixture was set up to heat at 250 °C overnight. Then, an excess of lanthanum(III) acetylacetonate hydrate (130.5 mg, 0.290 mmol) was added and the reaction was sealed then left for 3 days at 200 °C. The crude was precipitated with methanol (100 ml), and the required compound was isolated using column chromatography over silica gel using DCM:PET (3:10 v:v) as eluent. The green fraction containing the title product was collected then recrystallised from DCM:MeOH to yield the open *bis* triple-decker system **144** as dark green solid (0.046 mg, 40 %).

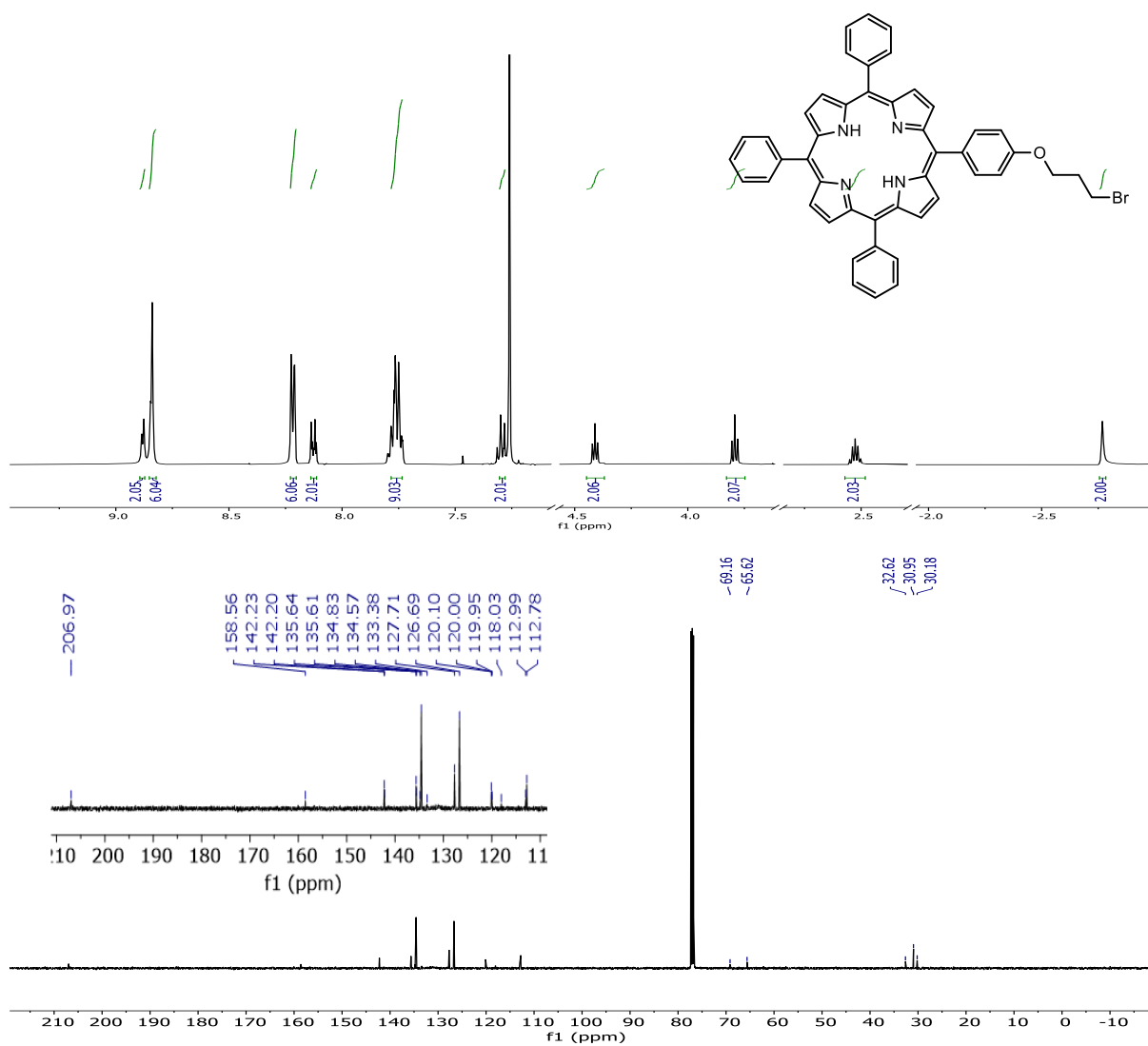
M.P >350°C. $^1\text{H NMR}$ (500 MHz, methylene chloride- d_2) δ 9.86 (d, 12H, *Hoph*), 9.83 (d, $J = 8.2$ Hz, 4H, *Hm'ph*), 8.73 (dd, $J = 5.2, 2.9$ Hz, 32H, *Hpc1*), 8.46 (s, 2H, H_1), 8.35 – 8.29 (m, 12H, *Hmph*), 8.12 – 8.09 (m, 4H, *Ho'ph*), 8.08 (s, 2H, H_2), 8.07 – 8.04 (m, 6H, *Hpph*), 8.00 (s, 2H, H_3), 7.75 (dd, $J = 5.7, 2.5$ Hz, 32H, *Hpc2*), 7.66 (d, $J = 4.2$ Hz, 4H, *Hpyrr1*), 7.59 – 7.56 (m, 12H, *Hpyrr2*), 5.10 – 5.02 (m, 8H, H_d), 4.52 (t, $J = 6.6$ Hz, 4H, H_a), 4.25 (t, $J = 6.5$ Hz, 4H, H_b), 3.01 (q, $J = 6.1$ Hz, 4H, H_c), 2.26 – 2.17 (m, 8H, H_d), 1.98 – 1.94 (m, 16H, H_e), 1.43 –

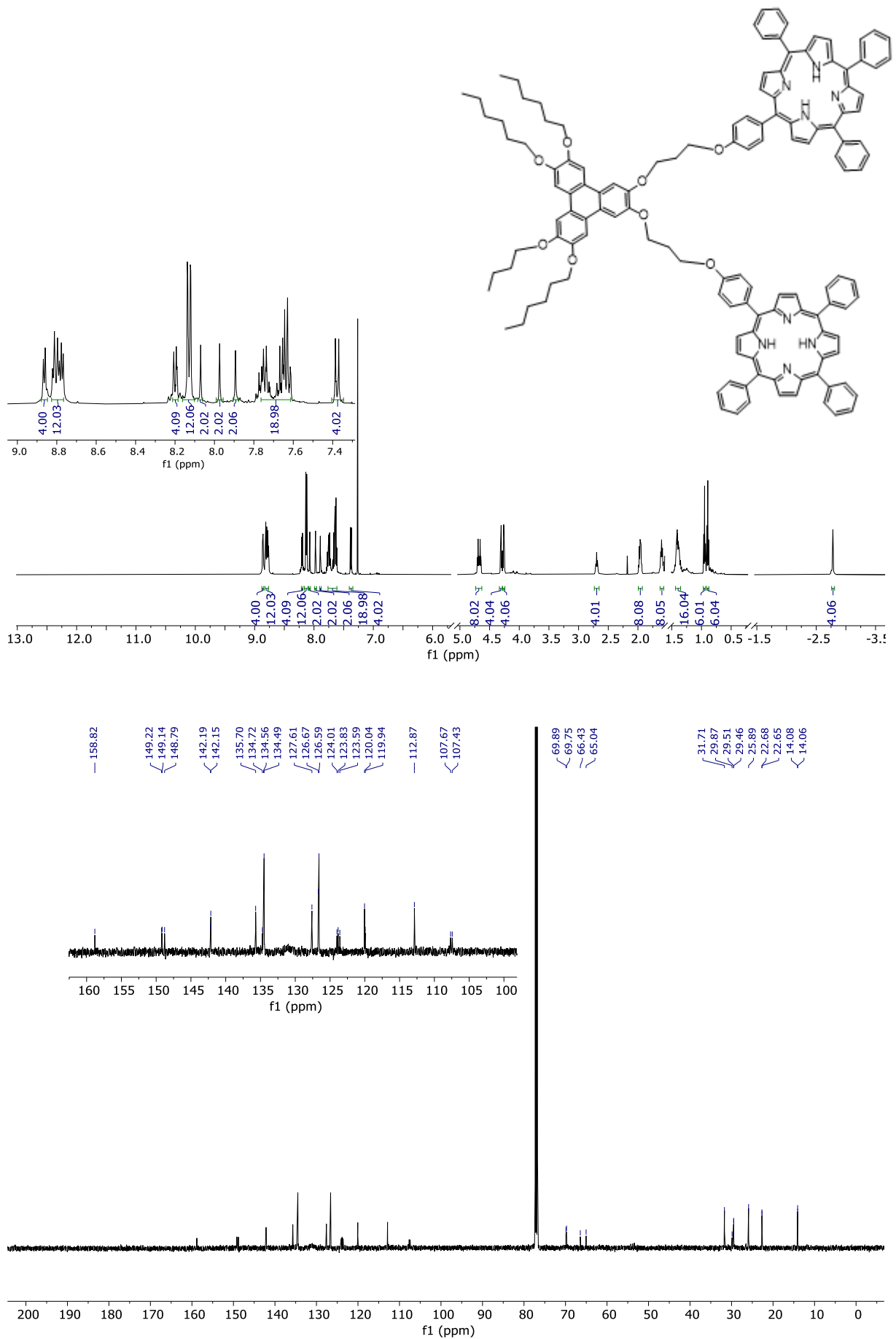
1.29 (m, 16H, H_f), 1.01 (t, $J = 7.2$ Hz, 6H, H_h), 0.89 (t, $J = 7.8, 6.2$ Hz, 6H, H_g); ^{13}C NMR (126 MHz, methylene chloride- d_2) δ 159 152.7, 149.7, 149.5, 149.45, 148.9, 148.6, 148.5, 148.5, 141.1, 136.6, 135.3, 131.7, 131.6, 131.6, 129.1, 128.0, 126.9, 125.1, 123.8, 122.1, 119.4, 119.1, 113.0, 108.1, 107.4, 69.9, 69.8, 67.0, 65.6, 32.2, 32.0, 31.8, 30.7, 30.5, 29.93 29.8, 29.6, 26.5, 26.3, 26.0, 23.3, 23.0, 22.8, 14.2, 14.0, 0.9.; MS (MALDI-TOF): m/z [M^+] calc, for $(\text{C}_{264}\text{H}_{188}\text{La}_4\text{N}_{40}\text{O}_8)^+$: 4604.75, found 4604.21 [M^+]; UV-vis, λ_{max} (DCM)/nm 281, $\epsilon=1.5 \times 10^5$; 336, $\epsilon=1.6 \times 10^5$; 417, $\epsilon=2.1 \times 10^5$; 484, $\epsilon=4.5 \times 10^5$; 590, $\epsilon=4.2 \times 10^5$; 628 $\epsilon=4.0 \times 10^5$. IR (KBr, cm^{-1}): 3364, 2919, 2837, 1604, 1504, 1469, 1434, 1392, 1323, 1240, 1157, 1108, 1056, 974, 842, 796, 729.

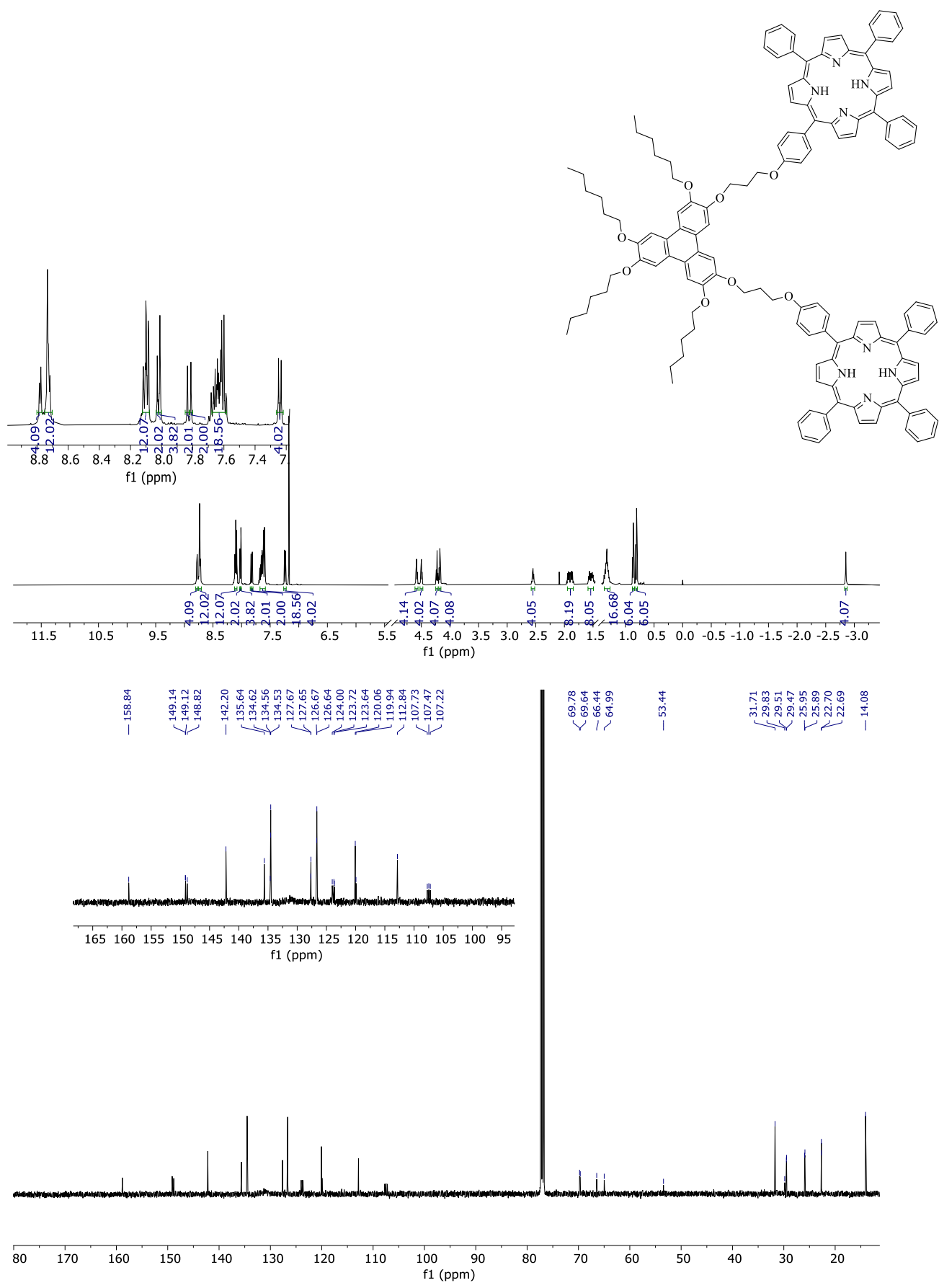
Chapter 5: Appendix

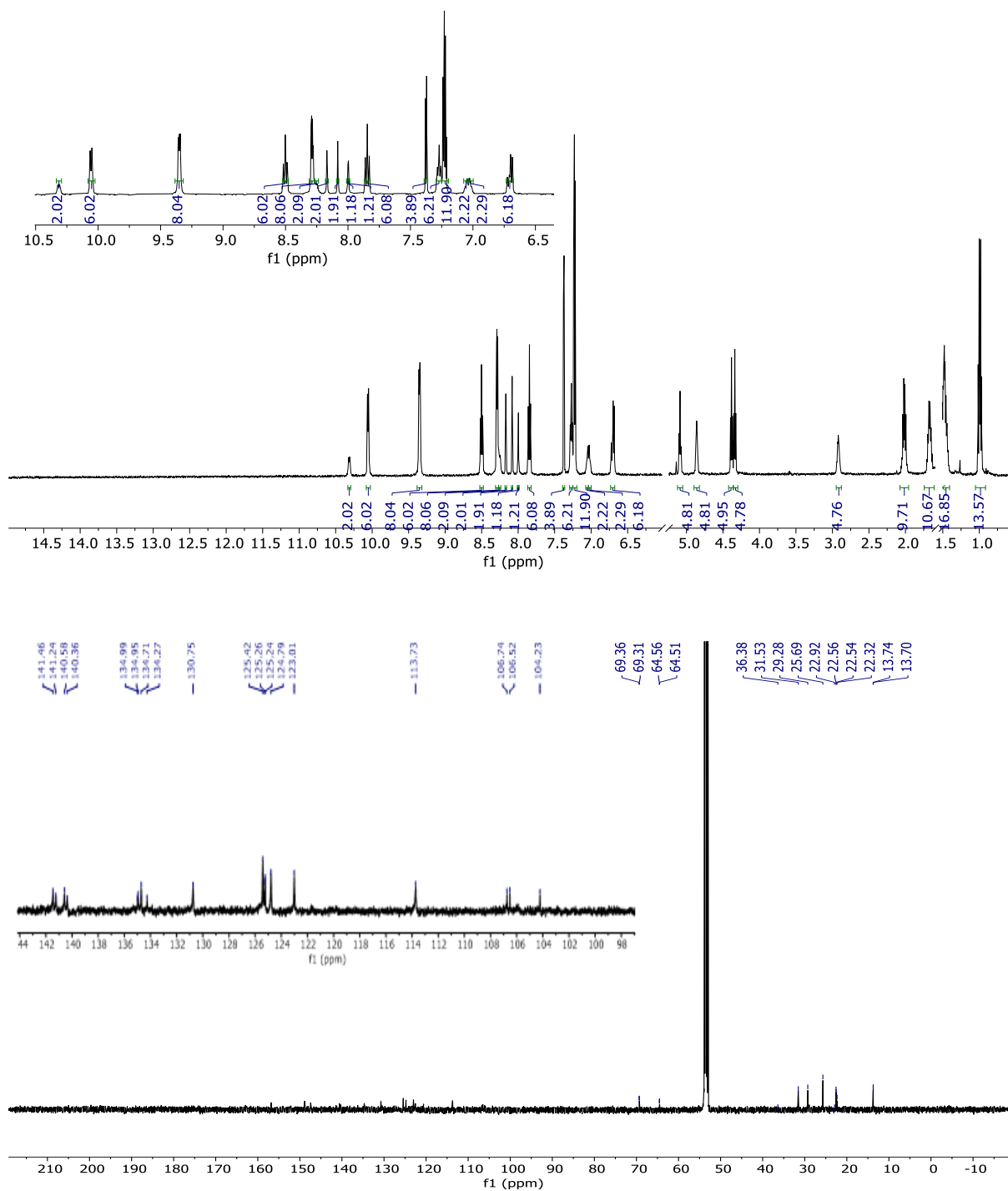
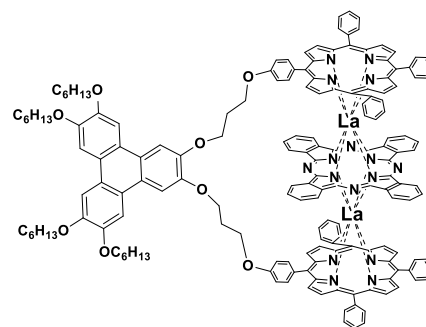
5. Appendix

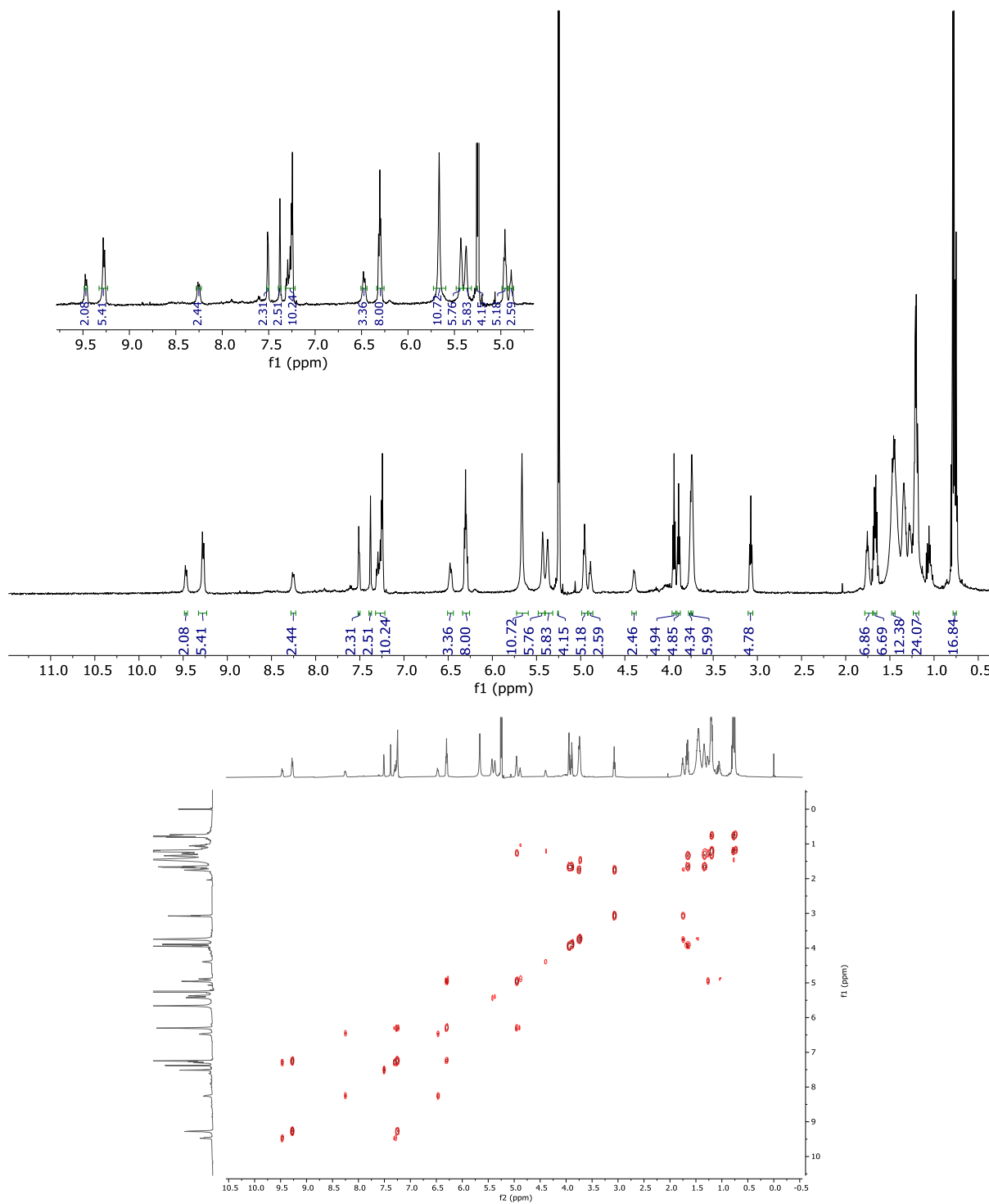
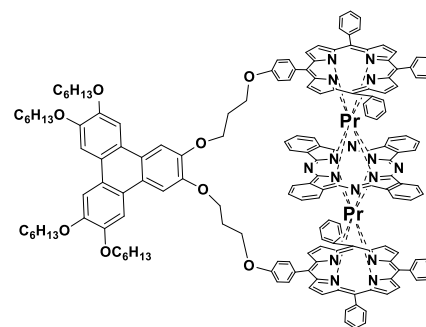
5.1 Selected NMR-spectra

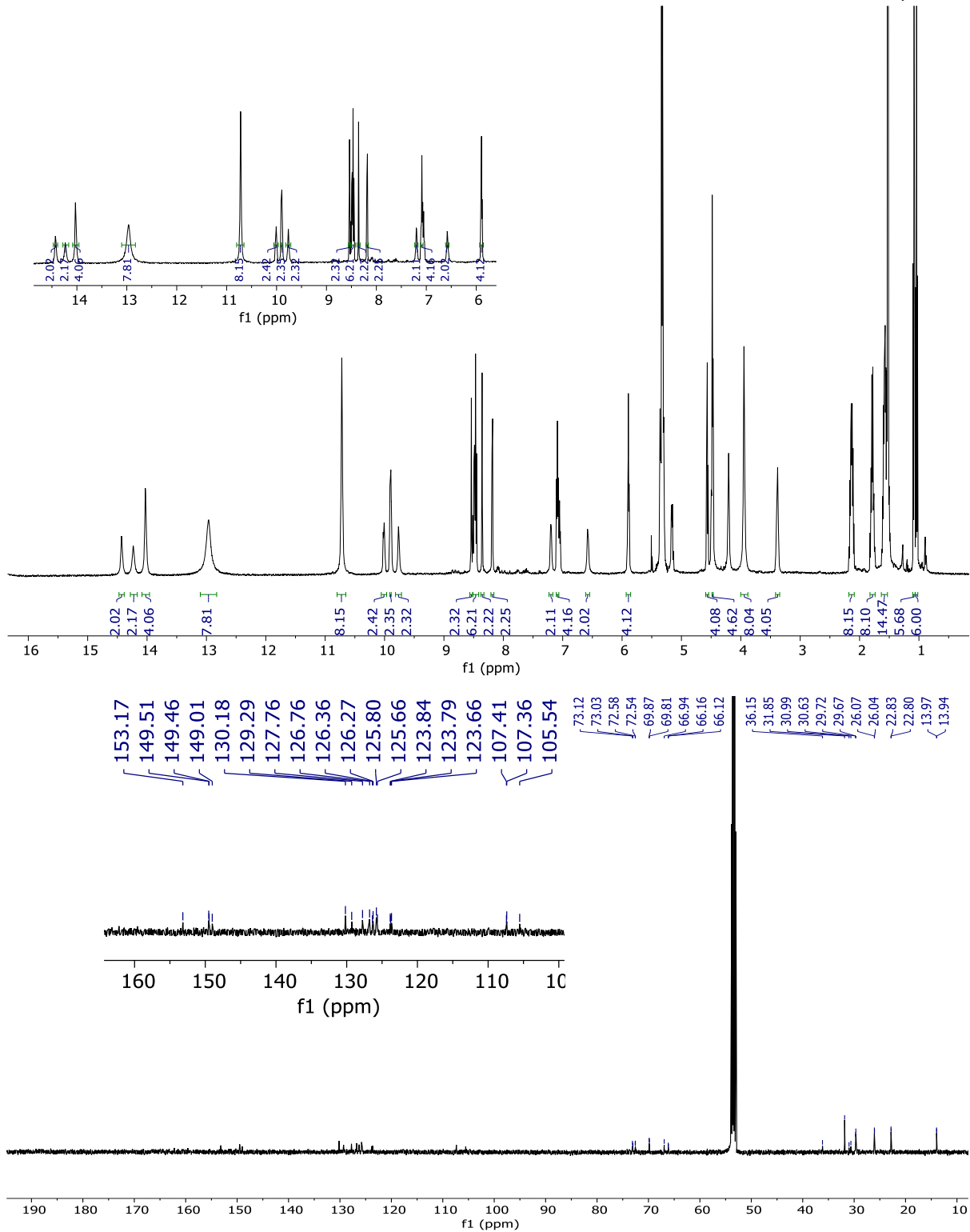
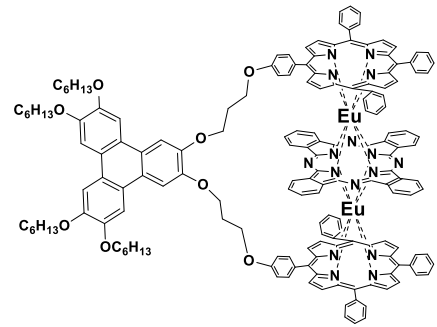


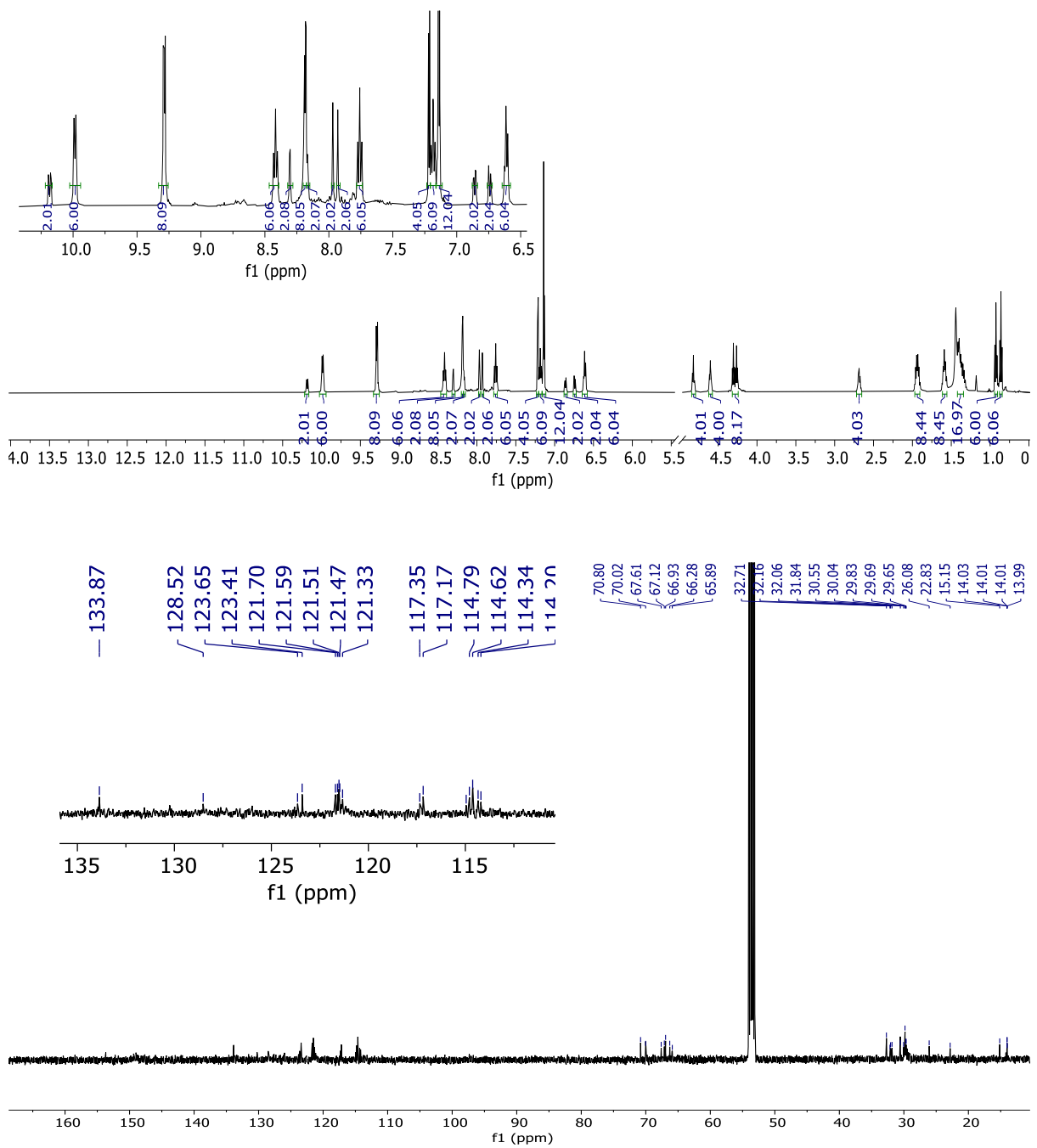
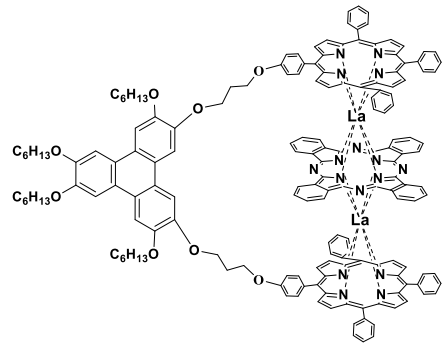


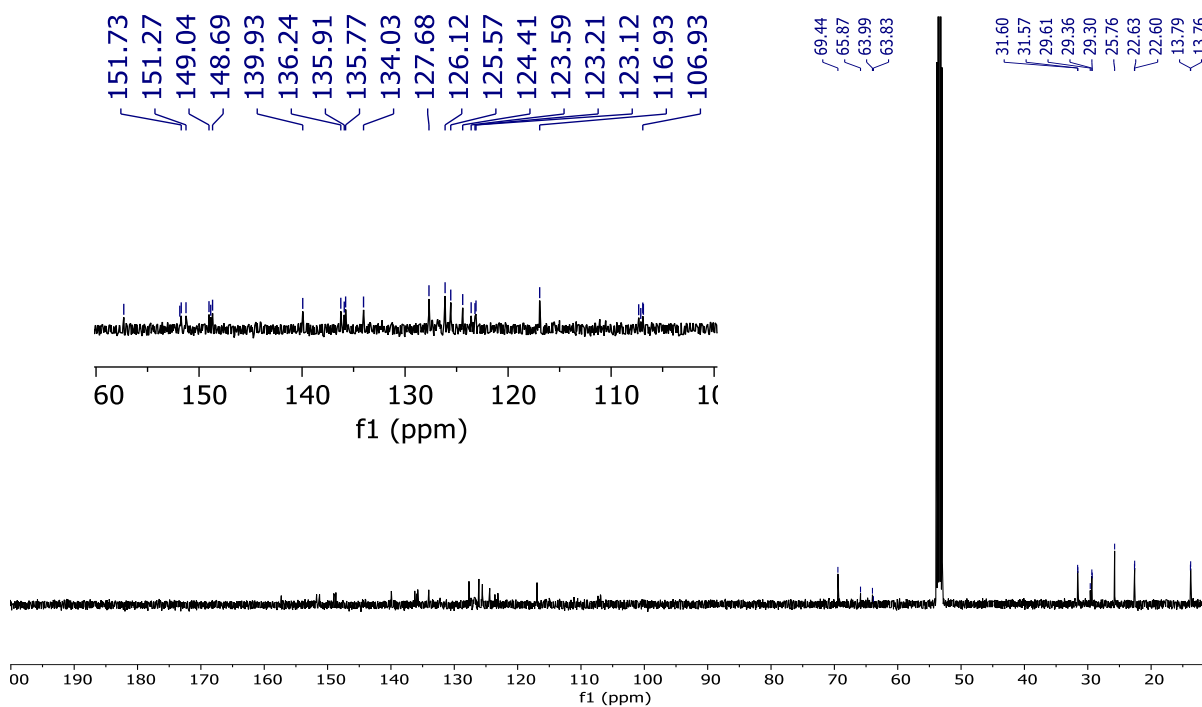
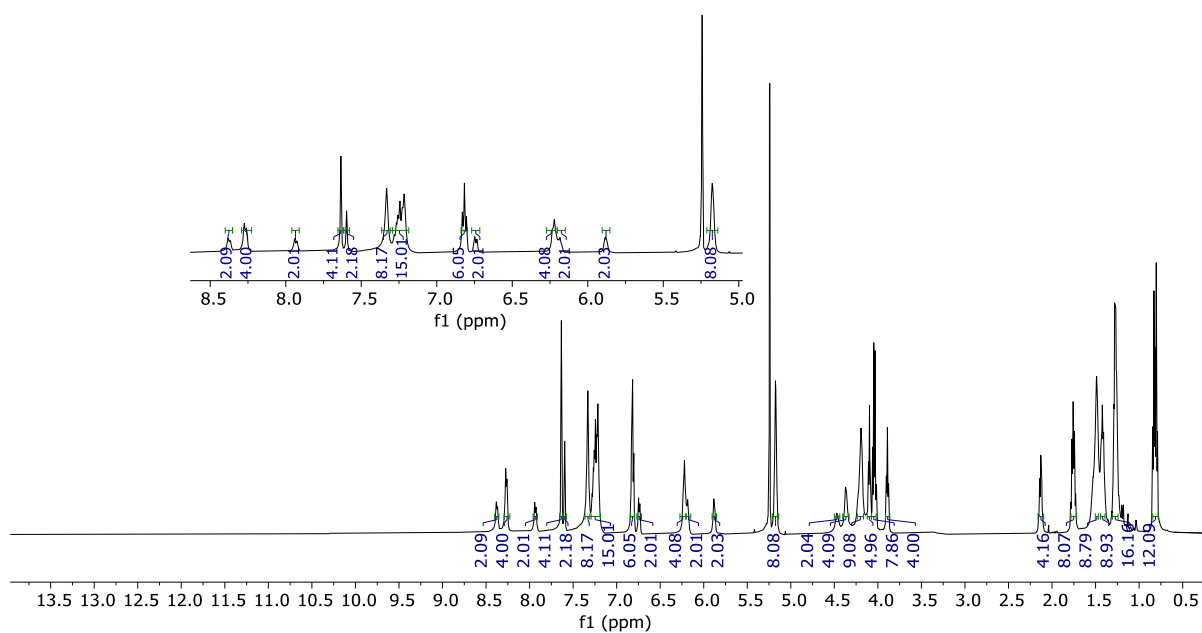
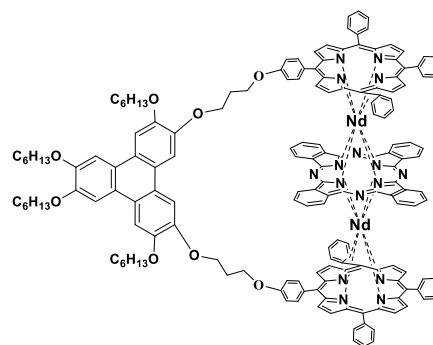


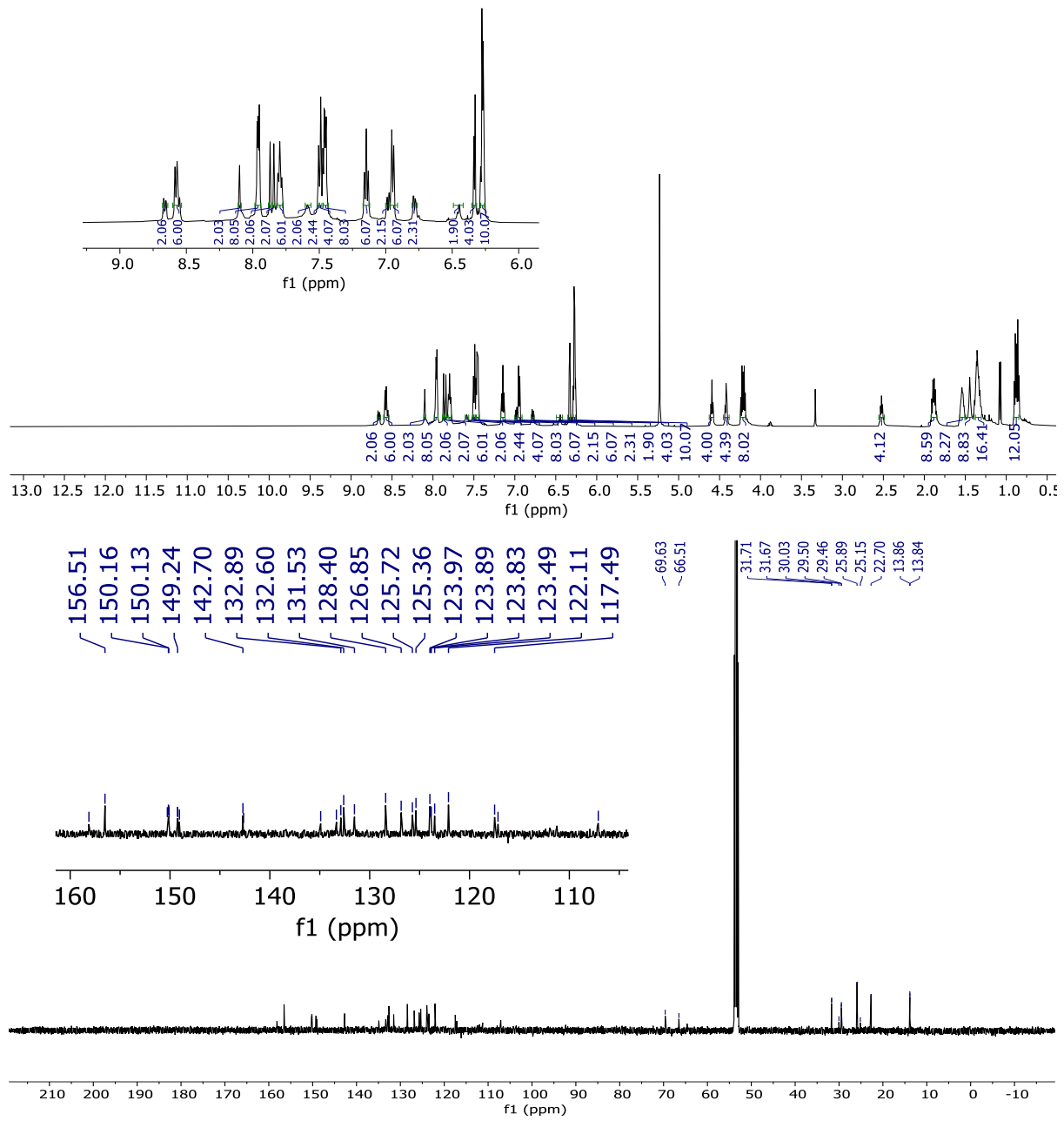
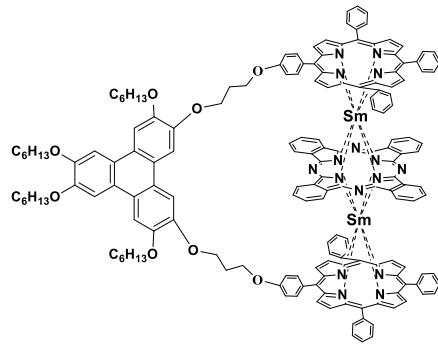


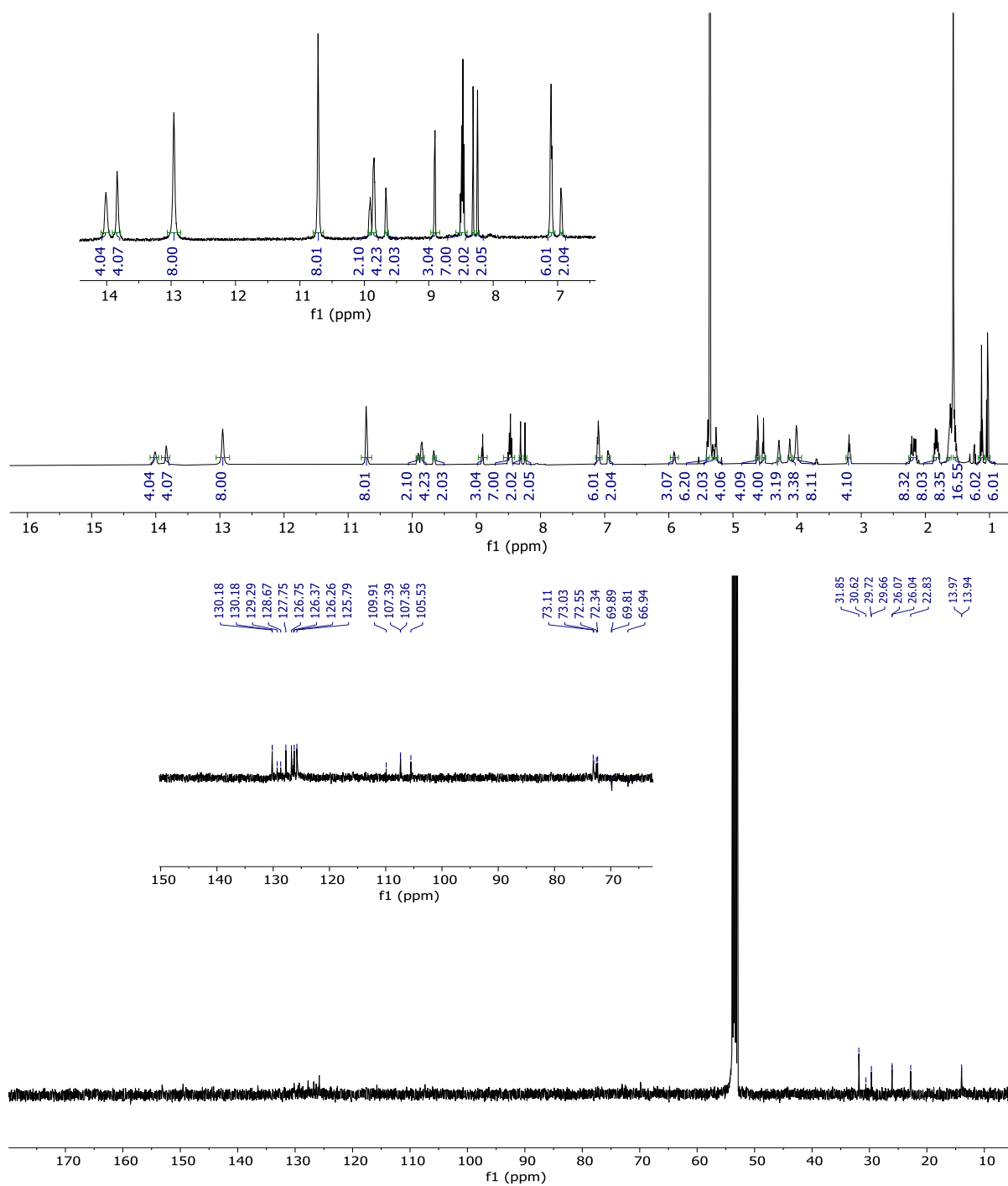
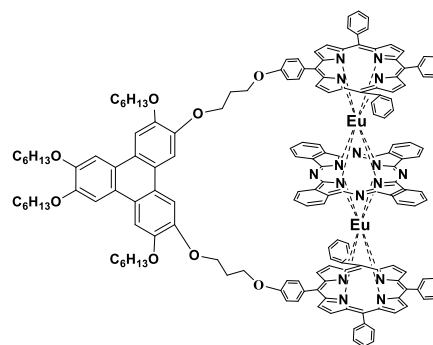


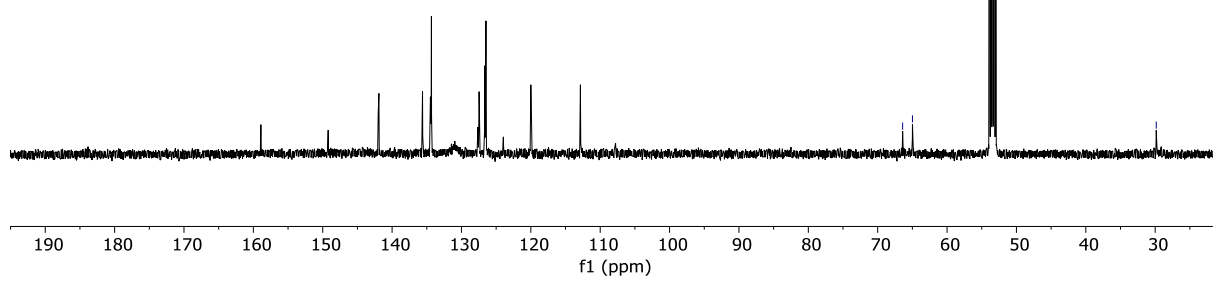
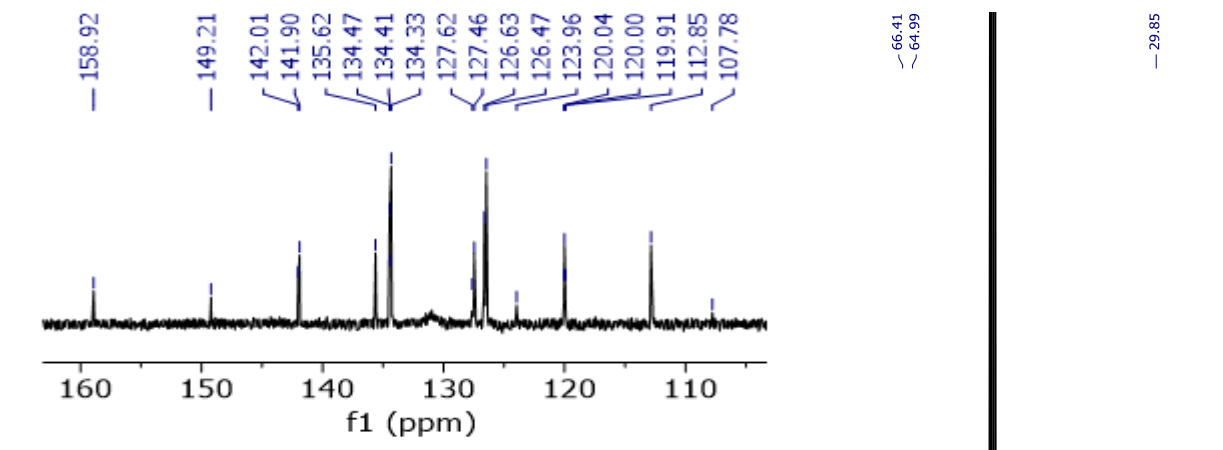
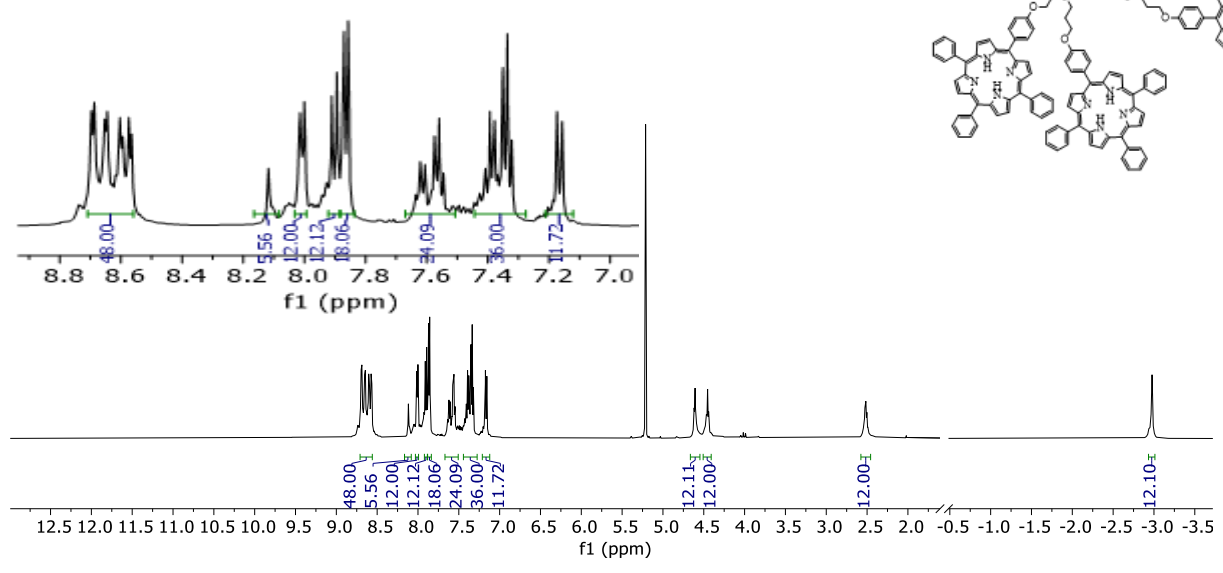
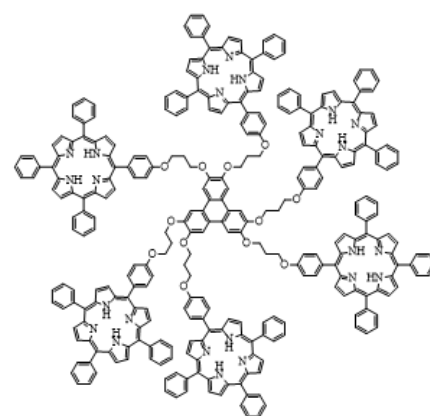


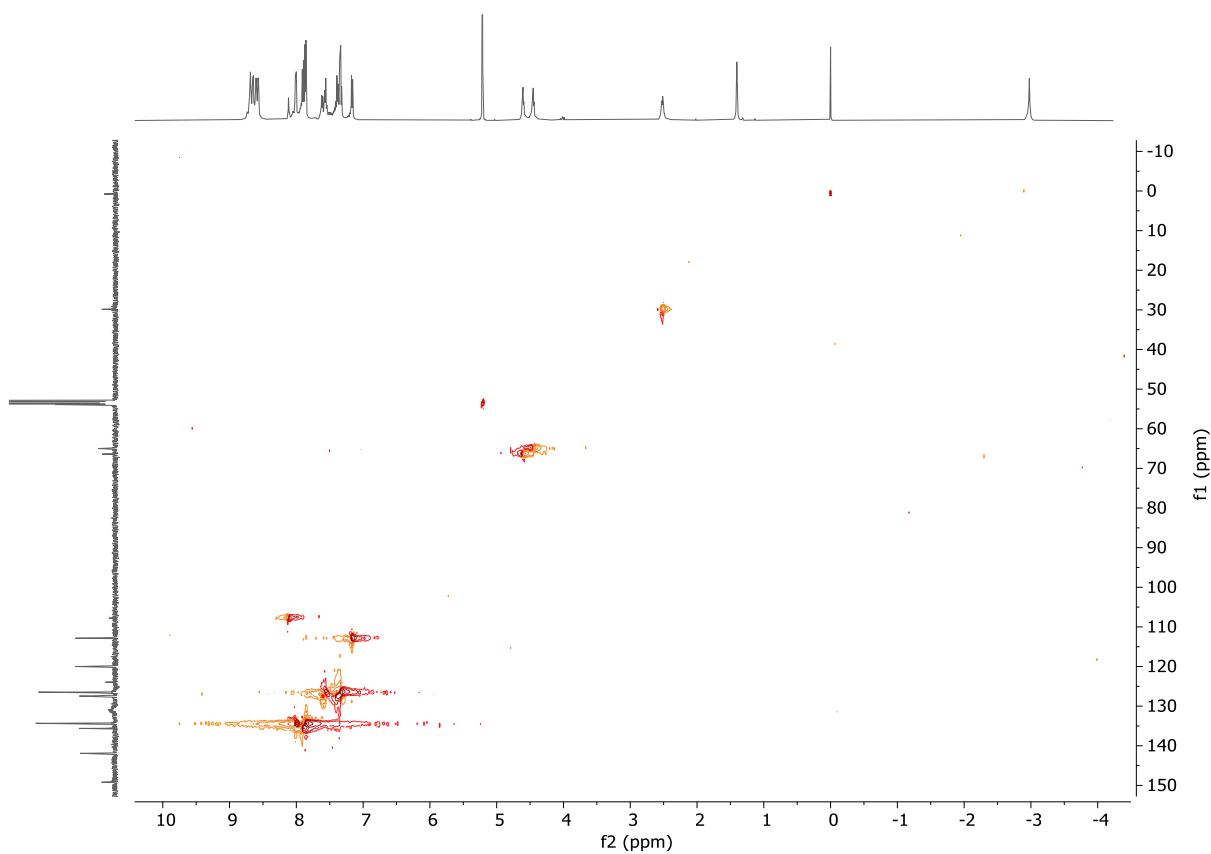
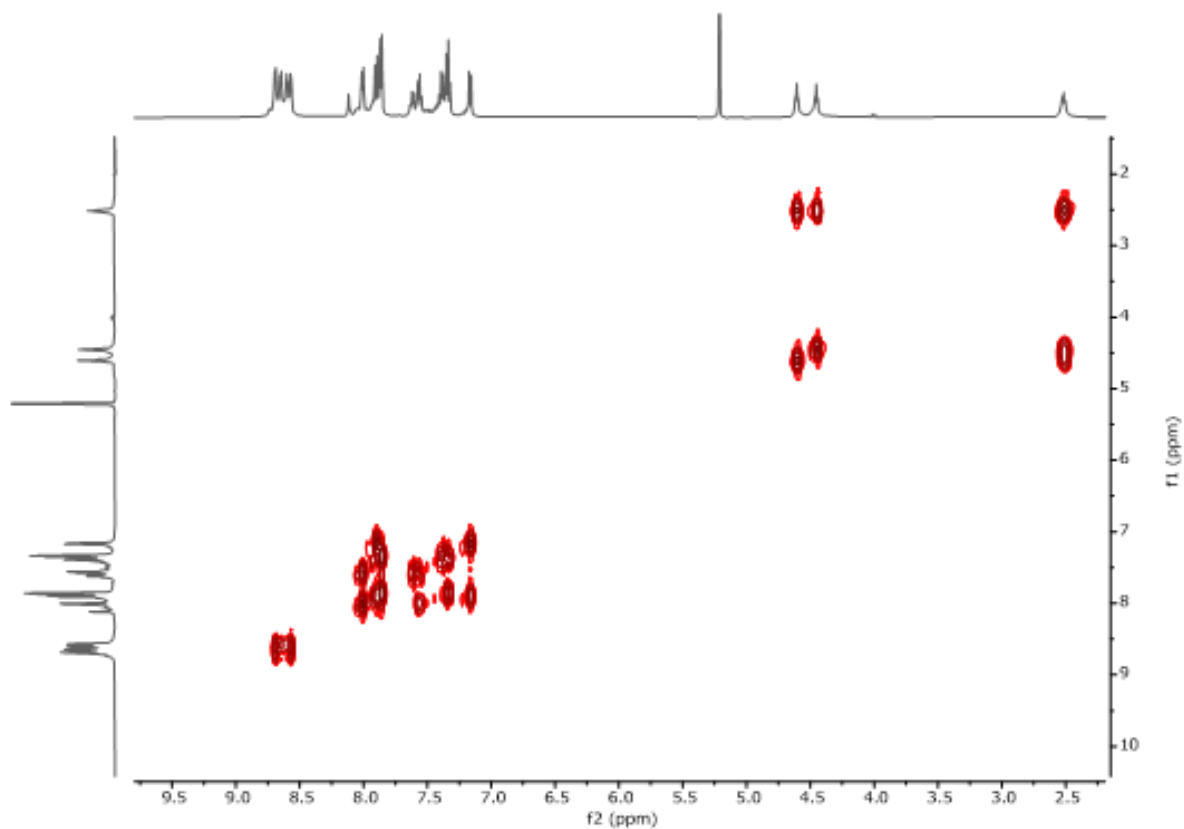


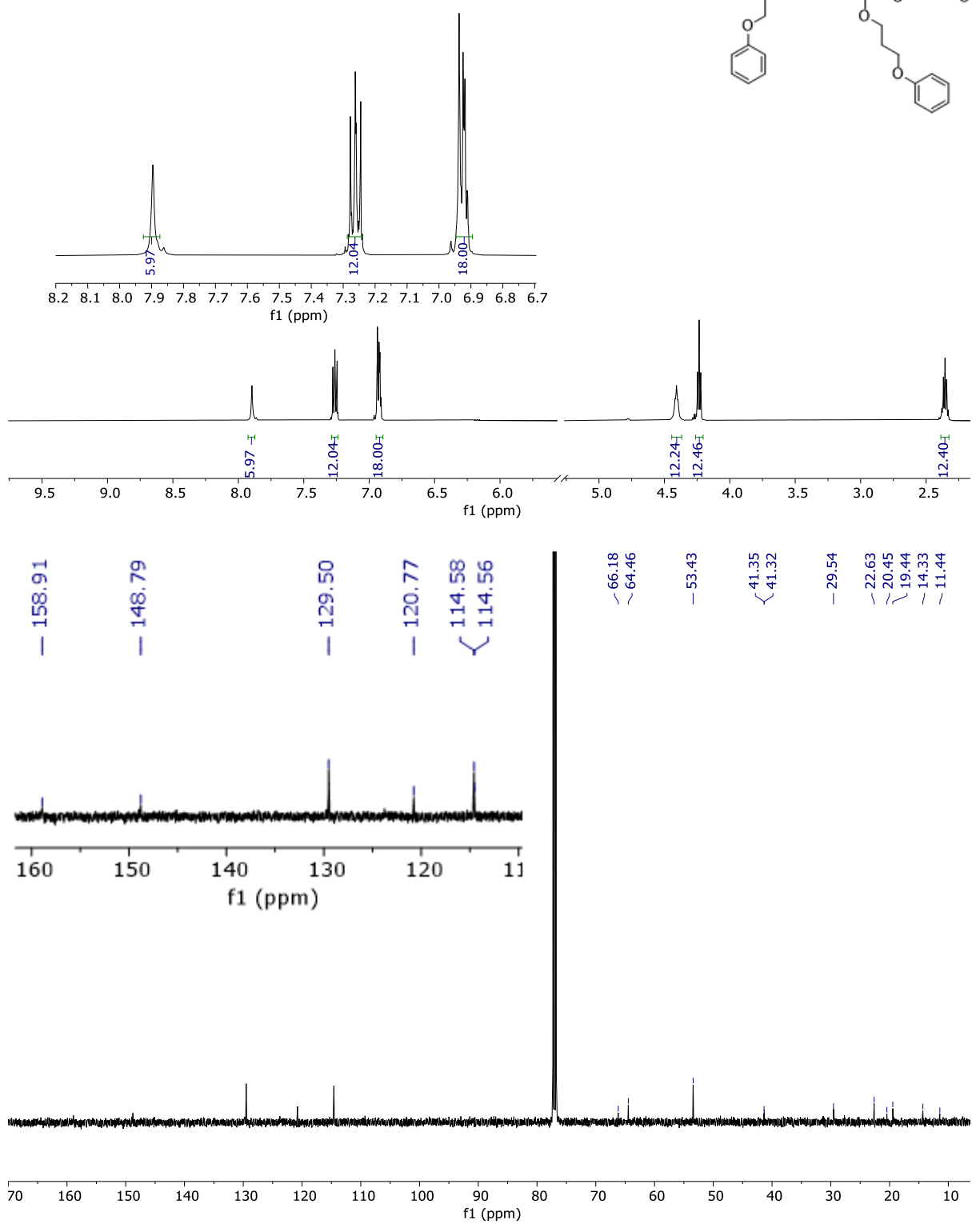
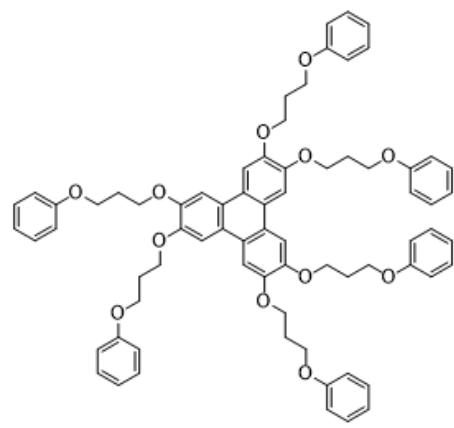


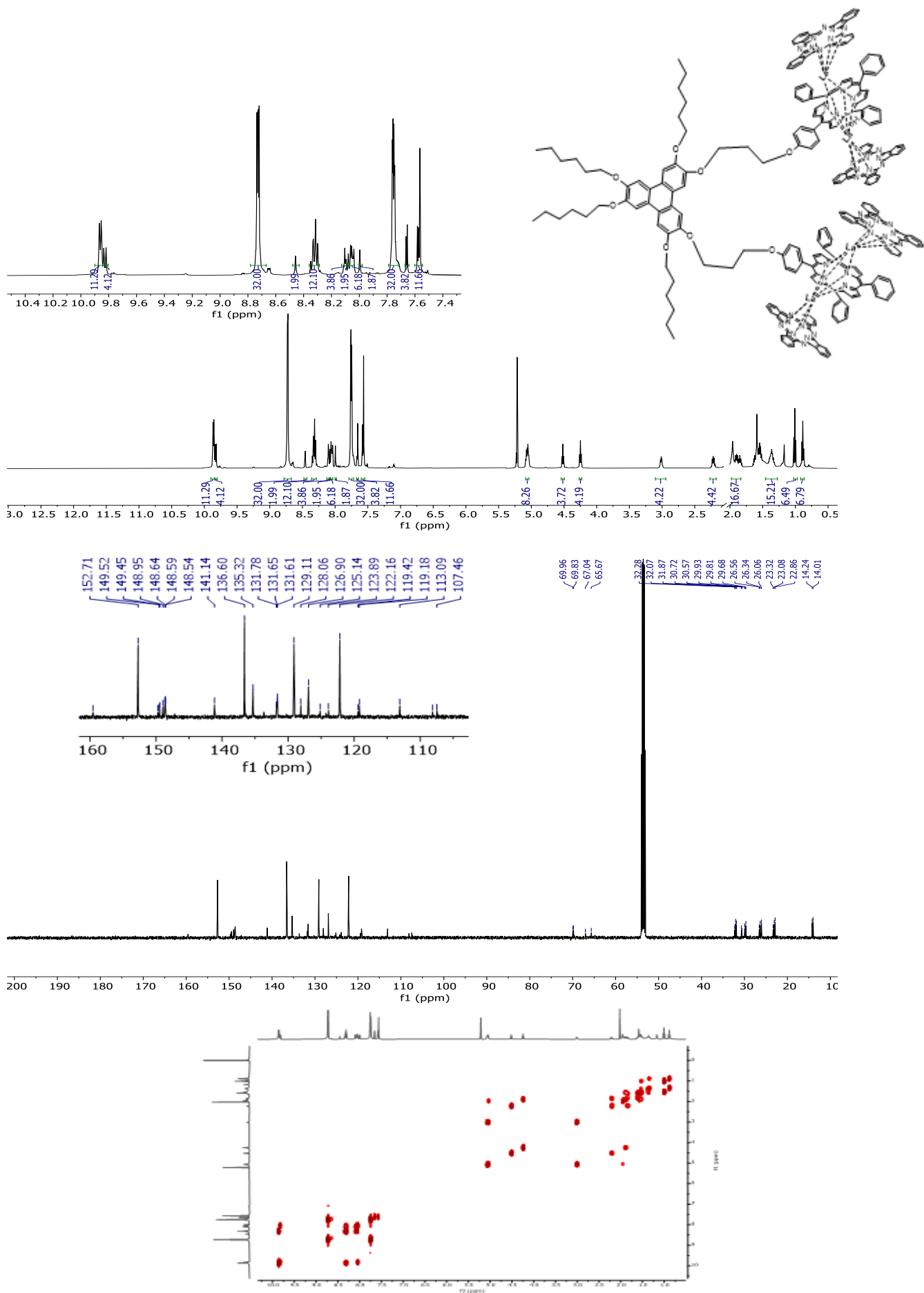












5.2 Publications

5.2.1 Publication No.1

Scramble-Free Synthesis of Unhindered *trans*-A₂B₂-Mesoaryl Porphyrins via Bromophenyl Dipyrromethanes

Muteb H. Alshammari, Sultanah M. N. Alhunayhin, David L. Hughes, Isabelle Chambrier, and Andrew N. Cammidge*

Cite This: <https://doi.org/10.1021/acs.orglett.3c04215>

Read Online

ACCESS |

Metrics & More

Article Recommendations

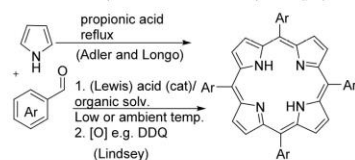
Supporting Information

ABSTRACT: *Trans*-disubstituted porphyrins are highly valuable intermediates across diverse fields, but they pose a significant synthesis challenge in some cases due to scrambling and formation of complex mixtures. Conditions that minimize scrambling also lower yields, but steric hindrance around the meso-aryl substituent can effectively suppress scrambling altogether. Here we report a straightforward approach to valuable *trans*-A₂B₂ porphyrin intermediates that are otherwise very difficult to obtain, through use of removable blocking bromide substituents.



The synthetic chemistry of porphyrins was first revolutionized by Adler and Longo's simple procedure that permitted easy access to *meso*-aryl porphyrins in a single step from pyrrole and aromatic aldehydes by refluxing in propionic acid open to air.¹ The general methodology was subsequently refined and expanded by Lindsey and co-workers who, among many other developments, introduced higher yielding protocols that employed milder acidic conditions in organic solvents to allow the incorporation of more sensitive substrates (Scheme 1).²

Scheme 1. Direct Synthesis of *meso*-Aryl Porphyrins



Unsymmetrically substituted derivatives can be accessed through a mixed condensation of pyrrole with two different aldehydes. As expected, reactions of this type produce a complex mixture with low yields of the individual products isolated after challenging separations. The reactions can be useful for synthesis of A₃B type porphyrins, and we have exploited this in our own work for building symmetrical diporphyrins as precursors to multidecker systems,³ and unsymmetrical chromophore dyads.⁴ The strategy is rarely useful for A₂B₂ derivatives where both AABB (*cis*) and ABAB (*trans*) isomers are formed. The *trans* isomers are highly valued intermediates and have been widely employed across diverse

fields including supra-/supermolecule construction and catalysis.^{5–7} A rational approach to the synthesis of *trans*-ABAB porphyrins exists⁶ whereby a preformed dipyrromethane is condensed with a different aldehyde. The synthesis, which follows from MacDonald's original use of a dipyrromethane dialdehyde + dipyrromethane,⁸ is widely employed and is highly successful in selected cases. However, a major problem that is inevitably encountered in these syntheses is that of scrambling, whereby acidolysis of dipyrromethane and/or higher oligomers (essentially reverse condensation) leads to a set of products identical to that expected from a simple mixed condensation with two aldehydes. The reaction has been carefully and systematically investigated, and conditions have been developed to minimize scrambling. Typically, conditions that minimize scrambling have a negative impact on yield, but a key observation is that significant steric hindrance around the *meso*-aryl substituent can effectively suppress scrambling altogether (Scheme 2).⁶ In many cases this is a benefit because the same bulky substituents aid the porphyrin solubility (useful in supra- and supermolecule construction and characterization) and can affect the environment above and below the porphyrin plane around the axial position of any incorporated metal ion, a feature that can be exploited in catalysis.⁹

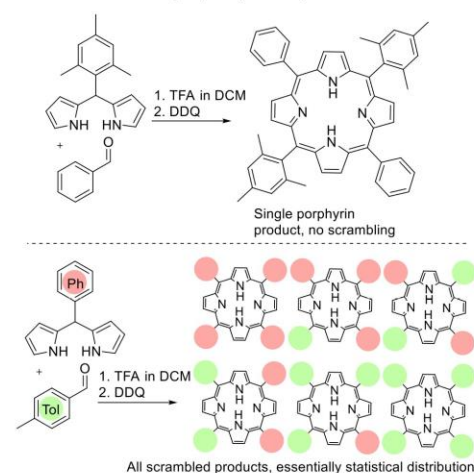
In our ongoing work on heteroleptic triple-decker porphyrin–phthalocyanine complexes³ we required efficient

Received: December 15, 2023

Revised: January 24, 2024

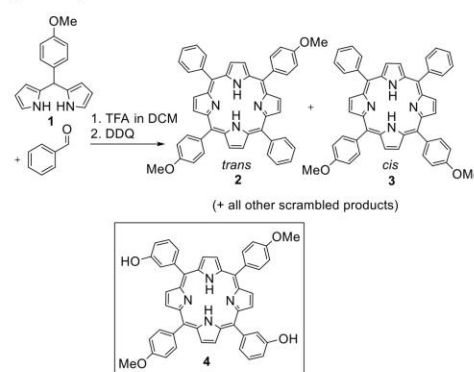
Accepted: February 14, 2024

Scheme 2. Efficient Rational Synthesis of *trans*A₂B₂-*meso*-Aryl Porphyrins Using a Dipyromethane Bearing a Sterically Hindered Aryl (e.g., Mesityl, Top) and Inefficient Synthesis Due to Scrambling When Unhindered Aryl Substituents Are Employed (Bottom)^{6b}



syntheses of differentially substituted *trans* ABAB-*meso*-aryl porphyrins suitable for further elaboration at either of the 5,15-positions only, or separately at the 5,15- and then 10,20-positions. The planned chemistry is one example where the use of sterically hindered aryl substituents cannot be used, because the hindrance required for efficient *trans*-porphyrin synthesis prevents the subsequent face-to-face assembly of multidecker complexes. Here even fluorine substituents on the 2,6-positions prevent face-to-face assembly and essentially only hydrogen can be accommodated. However, porphyrins bearing only remote functionality (3- and 4-positions) are valuable for elaboration in many other areas also, for example to build oligomers and polymers, and for attachment to complementary organic and inorganic species and surfaces.¹⁰ We particularly targeted *trans*-porphyrins bearing opposite pairs of hydroxyl and/or methoxy groups, knowing the latter can be selectively hydrolyzed to reveal phenolic residues following alkylation of the first pair of phenols and therefore provide valuable versatility for further stepwise elaboration. *trans*-Bis(4-methoxyphenyl)porphyrin **2** can be prepared using the dipyromethane route, but the outcome is similar to the standard mixed porphyrin synthesis from aldehyde precursors. The reactions yielded the full mixture of scrambled products from which the dimethoxy isomeric mixture can be isolated in low (5–12%) yield (Scheme 3). The isomers cannot be separated, but NMR analysis of the mixture shows that the ratio of isomers is between 2:1 and 1:1 (Supporting Information). Hydrolysis allows careful separation of the isomeric diols and reveals the major isomer to be *cis* (5,10-). The presence of the activating methoxy substituent no doubt accelerates acidolysis. The reason for domination of the *cis*-isomer over *trans* is less clear, but the result is consistent with reported direct synthesis of di(4-hydroxyphenyl)porphyrins where the *cis*-isomer is also formed preferentially.¹¹ The differentially substituted *trans* di(4-methoxyphenyl)-di(3-

Scheme 3. Attempted Synthesis of *trans*-Dimethoxyphenyl Porphyrin **2 Is Inefficient Due to Scrambling and Favors *cis*-Isomer Production (Top); Lightly Functionalized Opposite-*trans*-Substituted Porphyrins Like the Target **4** (Bottom) Are Not Accessible**



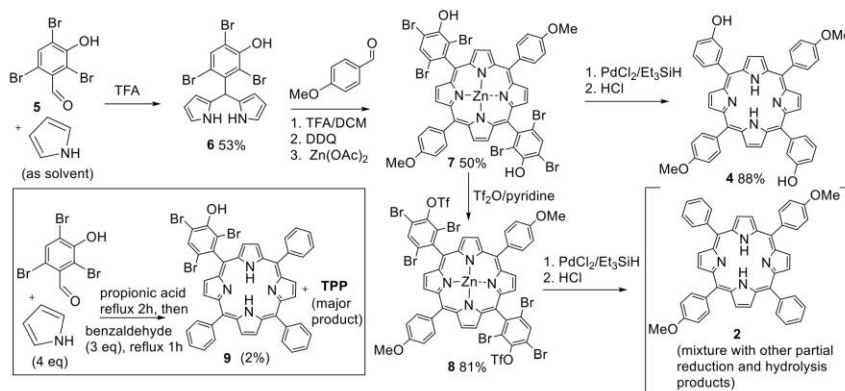
hydroxyphenyl)porphyrin **4** is unknown, and there is no obvious direct synthesis possible. Our brief investigation of mixed cyclizations confirmed that separation of the porphyrin mixture, and particularly the isomers, would be impractical.

While multistep synthesis via cross-coupling strategies is possible,¹² we reasoned that the most pragmatic solution to overcoming the scrambling issue would be to employ steric blocking groups that could later be removed after guiding efficient dipyromethane + aldehyde porphyrin synthesis without scrambling. The success of the sequence would rely on the ready availability of suitable precursors, so that the overall effectiveness of the sequence outweighed the inherent low atom economy of protecting group strategies. A survey of suitably designed benzaldehyde derivatives highlighted the potential of 3-hydroxy-2,4,6-tribromobenzaldehyde **5** which is readily available both commercially and from bromination of 3-hydroxybenzaldehyde.¹³ We recognized that aldehyde **5** could act as a precursor for both the complex, differentially substituted porphyrin **4**, and the simple (but difficult to access) *trans*-dimethoxyporphyrin **2** via common intermediate *trans*-porphyrin **7**. The sequence is shown in Scheme 4 along with the simple statistical porphyrin synthesis that was employed to generate a suitable model porphyrin **9** for the initial evaluation of deprotection (reduction) conditions.

Unsurprisingly the hindered aldehyde **5** proved to be less reactive than benzaldehyde itself, resulting in a 2% yield of the 3:1 porphyrin **9** alongside tetraphenylporphyrin (TPP) as the major porphyrin product. Nevertheless, sufficient porphyrin **9** was isolated to allow investigation of known reduction conditions employing triethylsilane and palladium chloride catalyst (Scheme 5).¹⁴ Porphyrin **9** and PdCl₂ (5 mol %) were heated in triethylsilane at 120 °C in a sealed tube, and the reaction was monitored periodically by analysis of aliquots by MALDI-MS. Reduction proceeded slowly, and it was clear that palladium porphyrin derivatives were also formed in the process. While this is not surprising, and the palladium can be easily removed in the acidic workup, the side reaction effectively removes the palladium catalyst from the system

B

<https://doi.org/10.1021/acs.orglett.3c04215>
Org. Lett. XXXX, XXX, XXX–XXX

Scheme 4. Synthesis of Lightly Substituted *Trans* Porphyrins Employing Removable Bromide Substituents To Prevent ScramblingScheme 5. Reductive Debromination of Porphyrin **9** Using Triethyl Silane and Palladium Chloride

and slows the rate. Nevertheless, mono-(3-hydroxyphenyl)-porphyrin **10** was isolated after workup (HCl) in 62% yield.

The main synthesis of *trans*-porphyrin targets began with straightforward synthesis of dipyrrromethane **6** from the reaction of aldehyde **5** with excess pyrrole (used as reactant and solvent). As expected, dipyrrromethane **6** proved to be relatively stable and could be stored for several weeks as a crystalline solid in the dark at 0–5 °C without any noticeable degradation. Pleasingly the synthesis of the corresponding *trans*-porphyrin was also smoothly achieved using 4-methoxybenzaldehyde following conditions developed by Lindsey,² and it is worth noting this electron-rich, unhindered aldehyde represents one of the most challenging reactants in terms of suppressing scrambling during porphyrin synthesis. However, based on the previous observations during reductive debromination of the model porphyrin **9**, we decided to insert zinc at the end of the reaction in order to prevent palladium sequestration during subsequent reduction. Dipyrrromethane **6** and 4-methoxybenzaldehyde were therefore reacted together in DCM (0.85 mM) with TFA catalyst at 0 °C. At the end of the reaction, DDQ was added followed (after 1 h) by addition of Zn(OAc)₂. *Trans* porphyrin **7** was isolated as the only observed porphyrin product in a 50% yield. Porphyrin **7** exists as an equilibrated mixture of atropisomers. They appear as two distinct spots by tlc but are essentially identical in ¹H NMR spectroscopy. Atropisomer interconversion occurs in minutes at room temperature (tlc).

Reductive debromination of zinc porphyrin **7** was achieved smoothly by using triethylsilane and PdCl₂ at 120 °C for 3–5

days. The crude reaction mixture was treated with HCl to remove zinc, neutralized, and separated to give the target differentially substituted *trans* porphyrin **4** in 88% yield. Alternative reduction conditions using formate and palladium, successfully employed by us in other projects for reduction of Ar–X,¹⁵ gave very slow reduction, an observation that likely reflects the effect of the electron-donating hydroxyl group in retarding palladium insertion (oxidative addition) into the Ar–Br bonds.

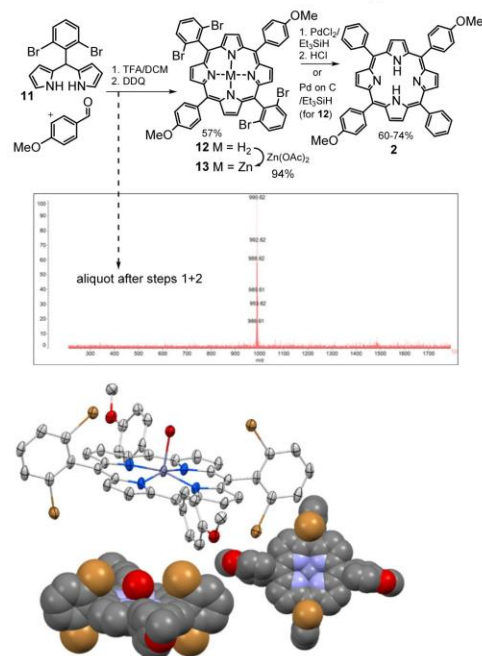
Conversion of intermediate **7** into *trans* di(methoxyphenyl) porphyrin **2** required reductive removal of both the bromide and hydroxyl substituents and was achieved by first converting the free phenols to triflates using triflic anhydride. Reduction of triflate **8** was attempted by using both PdCl₂/Et₃SiH and Pd/formate conditions. In each case the reduction of both triflate and bromide could be achieved, but the reactions were slow and impractical. Each reaction was monitored periodically by MALDI-MS. Under PdCl₂/Et₃SiH conditions, the MALDI-MS spectra clearly demonstrated initial preferential (faster) removal of bromides but very sluggish aryl triflate reduction (incomplete after 7 days at 120 °C). Reductions using Pd/formate conditions were also inefficient and slow, with evidence for competing triflate hydrolysis at long reaction times. Rather than pursue investigation of alternative conditions to achieve this, more simple, target, we elected to instead use the developed blocking strategy with an alternative bromoaryl aldehyde. Fortunately, 2,6-dibromobenzaldehyde is available. Indeed, it has been previously employed for synthesis of *trans* porphyrins, although not with challenging electron-rich partners.⁹ The convenient synthesis of *trans* di(methoxyphenyl) porphyrin **2** is shown in Scheme 6.

Dipyrrromethane **11** was synthesized as reported,⁹ and reaction first with 4-methoxybenzaldehyde, then DDQ, and then zinc acetate gave the corresponding *trans* Zn-porphyrin **13** with no evidence for other scrambled products; Scheme 6 (inset) shows the MALDI-MS taken for an aliquot of the reaction mixture, before addition of zinc acetate, with essentially a single signal (cluster at *m/z* 990.62) corresponding to porphyrin **12**. The zinc porphyrin **13** showed a strong tendency toward crystallization that complicated chromatographic purification. It was found to be more convenient to

C

<https://doi.org/10.1021/acs.orglett.3c04215>
Org. Lett. XXXX, XXX, XXX–XXX

Scheme 6. Convenient Synthesis of *trans* Dimethoxyporphyrin 2 (Inset Shows the Single Mass Observed in MALDI-MS of a Sample before Addition of Zinc Acetate), and the X-ray Crystal Structure for Porphyrin 13 (Shown as Elipsoids at 65% Probability, H-Atoms and Molecule of Chloroform Removed for Clarity)



first isolate the metal-free porphyrin **12** (57%) and then insert zinc in a separate step (94%). Crystals of porphyrin **13** suitable for X-ray diffraction were obtained (CCDC 2313839), and the structure is also shown in Scheme 6. The space-filling representations clearly illustrate the effective steric blocking of *meso*-sites provided by the *o*-bromines. Reduction also proceeded smoothly using PdCl₂/Et₃SiH and gave the desired porphyrin **2** in 74% yield after workup (HCl) and straightforward isolation. Direct reductive debromination of metal-free *trans* porphyrin **12** was also investigated by using palladium on carbon. Pleasingly the reduction works well, again employing triethylsilane, giving porphyrin **2** in 60% yield.

In conclusion, we have developed a straightforward approach to valuable *trans*-A₂B₂ porphyrin intermediates that are otherwise very difficult to obtain by direct methods. Access to such porphyrins, which bear remote functionality but lack excessive steric blocking on the porphyrin core, opens the potential for wide application, particularly in super/supramolecule construction and surface grafting.

■ ASSOCIATED CONTENT

Data Availability Statement

The data underlying this study are available in the published article and its Supporting Information.

■ Supporting Information

The Supporting Information is available free of charge at <https://pubs.acs.org/doi/10.1021/acs.orglett.3c04215>.

Experimental and characterization data for synthesized compounds plus crystallography details for porphyrin **13** (PDF)

■ Accession Codes

CCDC 2313839 contains the supplementary crystallographic data for this paper. These data can be obtained free of charge via www.ccdc.cam.ac.uk/data_request/cif, or by emailing data_request@ccdc.cam.ac.uk, or by contacting The Cambridge Crystallographic Data Centre, 12 Union Road, Cambridge CB2 1EZ, UK; fax: +44 1223 336033.

■ AUTHOR INFORMATION

Corresponding Author

Andrew N. Cammidge – School of Chemistry, University of East Anglia, Norwich NR4 7TJ, U.K.; orcid.org/0000-0001-7912-4310; Email: a.cammidge@uea.ac.uk

Authors

Muteb H. Alshammari – School of Chemistry, University of East Anglia, Norwich NR4 7TJ, U.K.

Sultanah M. N. Alhunyayhin – School of Chemistry, University of East Anglia, Norwich NR4 7TJ, U.K.

David L. Hughes – School of Chemistry, University of East Anglia, Norwich NR4 7TJ, U.K.

Isabelle Chambrier – School of Chemistry, University of East Anglia, Norwich NR4 7TJ, U.K.

Complete contact information is available at: <https://pubs.acs.org/10.1021/acs.orglett.3c04215>

Author Contributions

M.A. and S.A. performed the experimental synthetic work with equal contribution. I.C. and D.L.H. performed X-ray crystallographic analysis. A.C. conceived and led the research and prepared the manuscript draft.

Notes

The authors declare no competing financial interest.

■ ACKNOWLEDGMENTS

Financial support is gratefully acknowledged from Northern Border University (MA) and Almajmaah University (SA).

■ REFERENCES

- (1) Adler, A. D.; Longo, F. R.; Finarelli, J. D.; Goldmacher, J.; Assour, J.; Korsakoff, L. A simplified synthesis of *meso*-tetraphenylporphyrin. *J. Org. Chem.* **1967**, *32*, 476.
- (2) Lindsey, J. S.; Schreiman, I. C.; Hsu, H. C.; Kearney, P. C.; Marguerettaz, A. M. Rothmund and Adler-Longo reactions revisited: synthesis of tetraphenylporphyrins under equilibrium conditions. *J. Org. Chem.* **1987**, *52*, 827–836.
- (3) González-Lucas, D.; Soobrattee, S. C.; Hughes, D. L.; Tizzard, G. J.; Coles, S. J.; Cammidge, A. N. Straightforward and controlled synthesis of porphyrin-phthalocyanine-porphyrin heteroleptic triple-decker assemblies. *Chem.—Eur. J.* **2020**, *26*, 10724–10728.
- (4) Bressan, G.; Cammidge, A. N.; Jones, G. A.; Heisler, I. A.; González-Lucas, D.; Remiro-Buenamañana, S.; Meech, S. R. Electronic Energy Transfer in a subphthalocyanine-Zn porphyrin dimer studied by linear and nonlinear ultrafast spectroscopy. *J. Phys. Chem.* **2019**, *123*, 5724–5733.

D

<https://doi.org/10.1021/acs.orglett.3c04215>
Org. Lett. XXXX, XXX, XXX–XXX

- (5) Marschner, S. M.; Haldar, R.; Fuhr, O.; Wöll, W.; Bräse, S. Modular synthesis of trans-A₂B₂-porphyrins with terminal esters: systematically extending the scope of linear linkers for porphyrin-based MOFs. *Chem.—Eur. J.* **2021**, *27*, 1390–1401 and references therein.
- (6) (a) Littler, B. J.; Ciringh, Y.; Lindsey, J. S. Investigation of conditions giving minimal scrambling in the synthesis of trans-porphyrins from dipyrromethanes and aldehydes. *J. Org. Chem.* **1999**, *64*, 2864–2872 and references therein. (b) Geier, G. R., III; Littler, B. J.; Lindsey, J. S. Investigation of porphyrin-forming reactions. Part 3. The origin of scrambling in dipyrromethane + aldehyde condensations yielding trans-A₂B₂-tetraarylporphyrins. *J. Chem. Soc., Perkin Trans.* **2001**, *2*, 701–711.
- (7) Zwick, P.; Dulić, D.; van der Zant, H. S. J.; Mayor, M. Porphyrins as building blocks for single-molecule devices. *Nanoscale* **2021**, *13*, 15500–15525.
- (8) (a) Arsenaault, G. P.; Bullock, E.; MacDonald, S. F. Pyrromethanes and porphyrins therefrom. *J. Am. Chem. Soc.* **1960**, *82*, 4384–4389. (b) Lash, T. D. What's in a name? The MacDonald condensation. *J. Porphyrins Phthalocyanines* **2016**, *20*, 855–888.
- (9) Lu, H.; Li, C.; Jiang, H.; Lizardi, C. L.; Zhang, X. P. Chemoselective amination of propargylic C(sp³)-H bonds by cobalt(II)-based metalloradical catalysis. *Angew. Chem.Int. Ed.* **2014**, *53*, 7028–7032.
- (10) (a) Walter, M. G.; Rudine, A. B.; Wamser, C. C. Porphyrins and phthalocyanines in solar photovoltaic cells. *J. Porphyrins Phthalocyanines* **2010**, *14*, 759–792. (b) Day, N. U.; Wamser, C. C.; Walter, M. G. Porphyrin polymers and organic frameworks. *Polym. Int.* **2015**, *64*, 833–857.
- (11) Esquivel Guzmán, J. A.; Zhang, H.; Rivera, E.; Lavertu, M.; Zhu, X.-X. Porphyrin-based polyesters synthesized by enzymatic catalysis. *ACS Appl. Polym. Mater.* **2021**, *3*, 3659–3665.
- (12) Shi, B.; Boyle, R. W. Synthesis of unsymmetrically substituted meso-phenylporphyrins by Suzuki cross coupling reactions. *J. Chem. Soc., Perkin Trans.* **2002**, *1*, 1397–1400.
- (13) Osuna, M. R.; Aguirre, G.; Somanathan, R.; Molins, E. Asymmetric synthesis of amathamides A and B: novel alkaloids isolated from *Amathia wilsoni*. *Tetrahedron Asymm.* **2002**, *13*, 2261–2266.
- (14) Villemin, D.; Nechab, B. Rapid and efficient palladium catalysed reduction of aryl halides by triethylsilane under microwave irradiation. *J. Chem. Res. (S)* **2000**, *2000*, 432–434.
- (15) Cammidge, A. N.; Crépy, K. C. Application of the Suzuki reaction as the key step in the synthesis of a novel atropisomeric biphenyl derivative for use as a liquid crystal dopant. *J. Org. Chem.* **2003**, *68*, 6832–6835.

5.2.2 Publication No.2

LIQUID CRYSTALS
<https://doi.org/10.1080/02678292.2023.2259856>

Taylor & Francis
Taylor & Francis Group

INVITED ARTICLE

OPEN ACCESS 

Triphenylene discotic liquid crystals: biphenyls, synthesis, and the search for nematic systems

Sultanah M. N. Alhunayhin^a, Richard J. Bushby^b, Andrew N. Cammidge^a and Saeed S. Samman^a

^aSchool of Chemistry, University of East Anglia, Norwich, UK; ^bSchool of Chemistry, University of Leeds, Leeds, UK

ABSTRACT

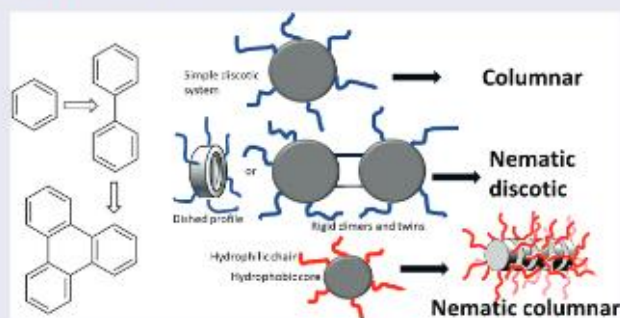
The development of the cyanobiphenyls for display applications was one of the most important technological advances of the 20th century. Here, we present a personal account of how advances in biphenyl science (synthesis and application) influenced the development of discotic liquid crystals. We focus on those based on triphenylene, the most widely studied discotic core. The search for nematic discotics proved to be challenging with relatively few early examples being reported. In examples of symmetrically hexasubstituted triphenylenes, a ring of peripheral aryl ester or alkynylaryl substituents provides effective steric blocking to columnar assembly – the face-to-face molecular arrangement that is observed in the majority of triphenylene discotics. The synthetic challenges associated with early triphenylene synthesis have now been largely overcome. Efficient oxidative trimerisation of dialkoxybenzenes gave direct access to materials with high purity and at scale. The intermediates can be manipulated through deprotection and elaboration, a pathway that allowed synthesis of lyotropic (N_c) systems among others. The combination of modern cross-coupling chemistry with oxidative processes has proved versatile, leading to synthesis of unsymmetrical monomeric and dimeric systems. Dimeric systems linked by rigid bridges have been identified as a separate class of materials that show strong tendency for nematic mesophase formation.

ARTICLE HISTORY

Received 8 August 2023

KEYWORDS

Triphenylenes; discotics; synthesis; nematic; biphenyls



Introduction

The flat-screen display industry was founded upon the ease with which thermotropic nematic phases can be aligned using surface effects and the ease with which that alignment can be switched using electromagnetic fields. In the development of these applications the invention of the cyanobiphenyls was the game-changing step. Cyanobiphenyls became the basis of most displays as well as the main 'workhorse' used by liquid crystal scientists

world-wide. It was this success that led to the belief that, for essentially all liquid crystal devices, electromagnetically switchable phases would be the key to success, and the focus naturally lay with the low viscosity nematics.

As a result, when discotic liquid crystals were discovered, there was immediate interest in finding mesogens that could be switched, and particularly on materials that would give discotic nematic (N_D) phases. Partly, these hopes proved false (discotic nematics

CONTACT Andrew N. Cammidge a.cammidge@uea.ac.uk; Richard J. Bushby R.J.Bushby@leeds.ac.uk

© 2023 The Author(s). Published by Informa UK Limited, trading as Taylor & Francis Group.

This is an Open Access article distributed under the terms of the Creative Commons Attribution License (<http://creativecommons.org/licenses/by/4.0/>), which permits unrestricted use, distribution, and reproduction in any medium, provided the original work is properly cited. The terms on which this article has been published allow the posting of the Accepted Manuscript in a repository by the author(s) or with their consent.

proved difficult to obtain, difficult to align and difficult to switch!), but it was the N_D phases which led to the first commercially important application. The first generation of discotic liquid crystals were all columnar [1] and subsequent development of the field has been dominated by studies of the columnar phase [2,3]. Indeed, some early studies also investigated potential switching of ferroelectric/chiral columnar systems [4]. While biphenyls can be considered the workhorse of calamitic liquid crystal development, the same can be said for triphenylenes within the development of discotic liquid crystals [5]. Unlike calamitic systems, where nematic systems are not uncommon and where it is not unusual to find nematic/smectic phase transitions, N_D phases are relatively rare and N_D /columnar phase transitions are particularly scarce [6]. This is because the molecular features which give rise to columnar and to N_D phases are different (Figure 1).

The tendency of discotic liquid crystals to give columnar phases is often vaguely attributed to 'pi-stacking interactions' with the unspoken implication that 'something' always causes aromatic rings to stack on top of each other giving columns. However, this is not the case. In the absence of significant dipole/dipole interactions, the stacking of aromatic rings is dictated by the competing effects of the van der Waals interaction (favouring coplanar/columnar stacking) and quadrupole/quadrupole interaction (favouring an orthogonal arrangement) [7]. Hence, for benzene and many of its derivatives, the

quadrupole term dominates leading to a preferred orthogonal arrangement of nearest neighbour molecules; often a 'herringbone' packing in the crystalline state. Only for polynuclear aromatics, where there is increased delocalisation, easier polarisation, and stronger van der Waals interactions, is columnar stacking favoured. For discotic mesogens, the significant 'extra factor' which favours columnar stacking is chain/core micro-phase separation. The large enthalpy associated with the Cr/Col transition relates to the melting of the side-chains [8]; it relates to the entropic term associated with the transformation from one to many conformational states. This is maximised when the conformational space available to the side-chains is also maximised. This is the case when discogens are stacked one-on-top of each other (as in the columnar phase, Figure 1(c)) but not when the side-chains are (partly) sandwiched between rigid aromatic cores (as in the N_D phase, Figure 1(e)). The first triphenylene N_D systems to be discovered were those where the core was surrounded by $O_2CC_6H_4R$ [9–12] or $C\equiv CC_6H_4R$ [13,14] substituents (Figure 1(a)). These substituents create a core that has a 'dished surface'; one that is thicker at its rim than it is in its centre (Figure 1(b)). In the case of the $O_2CC_6H_4R$ systems, this arises because, in the most stable conformation, the benzene ring is twisted out of the plane of the triphenylene. In the $C\equiv CC_6H_4R$ systems, the most stable conformation has all the aryl rings coplanar, but the barrier to rotation is so low [15] that there is a significant population of non-coplanar states. This

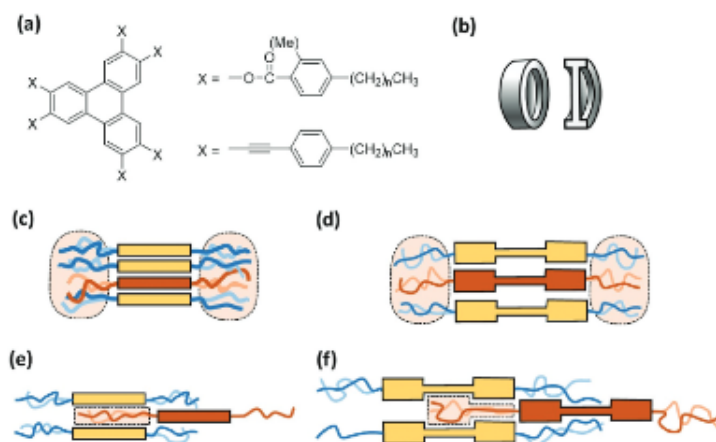


Figure 1. (Colour online) (a) mesogens giving rise to the N_D phase (b) schematic representation of a discogen core with a 'dished' surface. (cross-section right) (c) schematic of the columnar stacking of flat aryl cores. (d) schematic of the columnar stacking of 'dished' aryl cores. (e) schematic of the N_D phase of flat aryl cores. (f) schematic of the N_D phase of 'dished' aryl cores. In (c)-(f) the varying degrees of accessible conformational space (c>f>e) for the (red) side-chains is indicated by the pale red shading (see text).

destabilises the columnar phase. Packing of 'dished' rings is generally difficult and packing in columns (in particular) creates free space [16] (Compare Figure 1(c,d)). However, in the nematic phase, it provides additional conformational space for the side-chains (compare Figure 1(e,f)).

It was the N_D phases of the ester derivatives that were to lead to the first significant (and, so far, only significant) commercial application of discotics. Although they have switching times that are far too slow for them to be useful as display materials, their optical properties provided the ideal solution to the problem of improving the angle of view of liquid crystal display [17,18]. In the early years of liquid crystal displays this was a persistent problem. A clear image with true colours was only seen when the observer was positioned directly in front of the screen. This is a result of the birefringence of the oriented liquid crystal film. In the 'on' state of a twisted nematic display, although the director is perpendicular to the electrodes in the centre of the cell, it remains pinned in a planar orientation next to the surface. This 'hybrid' orientation of the director gives a birefringence profile that can be cancelled by a matching discotic film with the opposite birefringence profile. Fortunately, thin films of N_D discotics provide exactly that with planar alignment of the director at the solid interface and a perpendicular or tilted alignment at the air interface (Figure 2(b)). Furthermore, in the case of the 'reactive mesogen esters' (Figure 2(a)), polymerisation locks this birefringence profile into a stable film that is transparent and cheap to make; a polymer film that solves the 'angle of view' problem.

The success of the nematic phases of the cyanobiphenyls also stimulated interest in the stabilisation of nematic phases of lyotropic liquid crystals and, once again, discotic mesogens provided an answer. It was shown as far back as 1967 [19] that solutions of orientationally ordered disc-shaped (N_D) or rod-shaped (N_C)

micelles [20–22] could give rise to nematic behaviour, but the first lyotropic nematic phases found were only stable over very restricted ranges of temperature and concentration [23,24]. In part, this is a result of the fact that (because hydrophobic alkyl chains are so flexible) a conventional amphiphile can give rise to rod-shaped, spherical or disc-shaped aggregates (Figure 3(b)). However, amphiphiles with a rigid hydrophobic part can only form one type of aggregate. For example, a discoid amphiphile consisting of a rigid hydrophobic core which is surrounded by hydrophilic groups can only give rod-shaped aggregates and N_C nematic phases. The first example of such a discoid amphiphile was 2,3,6,7,10,11-hexa-(1',4',7'-trioxaoctyl)-triphenylene (Figure 3(a)) normally known by the abbreviation TP6EO2M [25]. In water, this amphiphile forms an N_C phase over a wide range of concentrations and temperatures [26]. Although designating these rod-like aggregates as 'micelles' is perhaps useful in making the conceptual link to the N_C phases formed by conventional lyotropic systems, perhaps the term 'aggregate' is preferable. The aggregation of TP6EO2M is pseudo-isodesmic, and there is no critical micelle concentration [26–30]. Since the discovery of TP6EO2M, a range of similar systems with wide nematic ranges have been reported. These include mesogens in which perylenebisimine [31], dibenzophenazine [32], phthalocyanine [33] and tricycloquinazoline [34] hydrophobic cores are surrounded by an annulus of hydrophilic EO_n chains. Like thermotropic nematic systems, the lyotropic N_C systems can be oriented in strong magnetic fields, but unlike the thermotropic nematics, they prove frustratingly difficult to orient using surface effects [35]. What was not realised at the time TP6EO2M was developed was that it is a non-ionic analogue of a 'chromonic' liquid crystal and chromonic liquid crystals systems [36] had been known (if not properly understood) for many years [37,38].

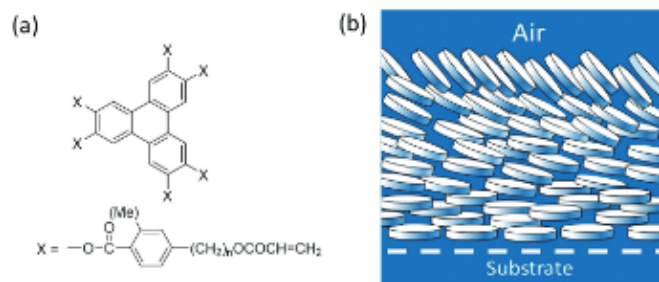


Figure 2. (Colour online) (a) example of a mesogen used in the manufacture of optical compensating film. (b) schematic of a nematic film with a hybrid orientation of the director.

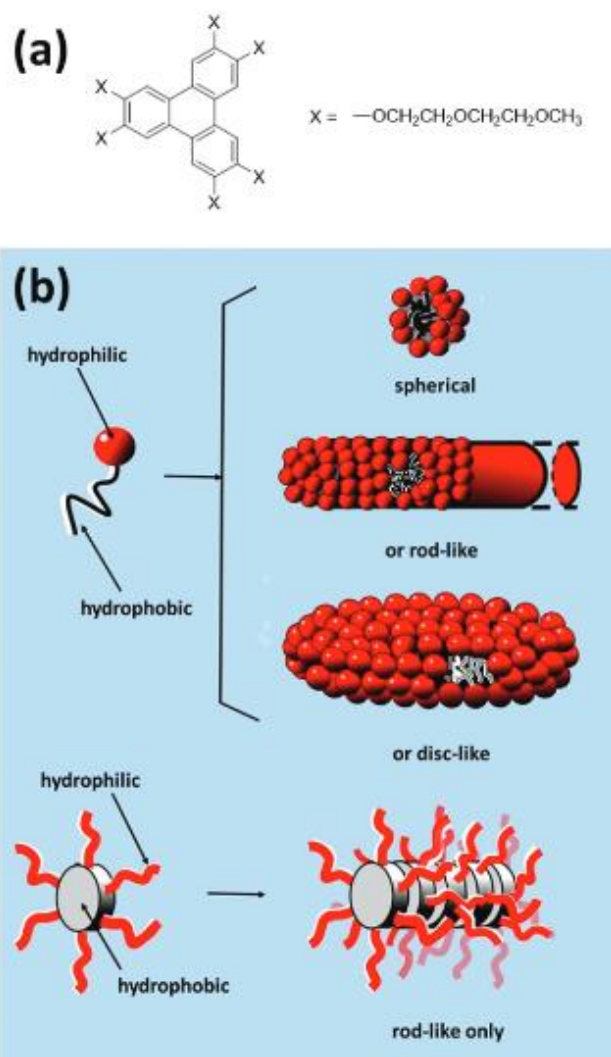
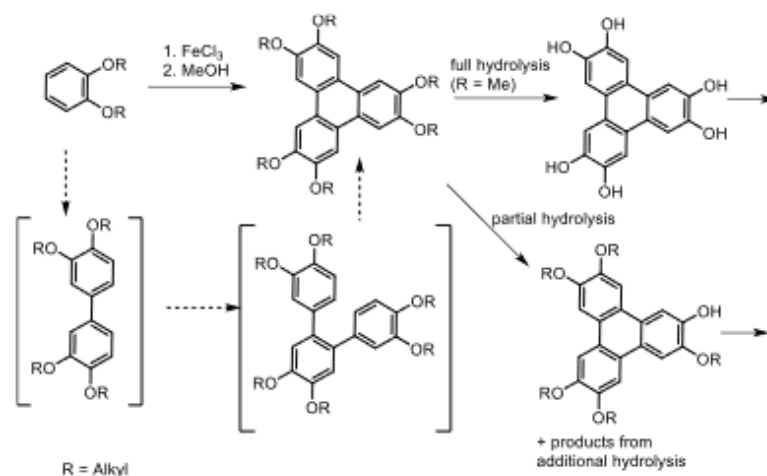


Figure 3. (Colour online) (a) the molecular formula of TP6EO2M (b) the contrast between the types of aggregate that can be formed in water by an amphiphile with a flexible hydrophobic alkyl chain and one (like TP6EO2M) that has a rigid hydrophobic aryl core. For the first three aggregates a few molecules have been removed from part of the surface to reveal the hydrophobic core.

The link between biphenyls and triphenylenes extends beyond their respective status as benchmark cores for calamitic and discotic liquid crystals because biphenyls play an important role in the synthesis and synthetic development of triphenylenes. For the most part, the molecules discussed so far are based on symmetrically hexa-substituted triphenylenes. Structures of this type became readily available when efficient cyclotrimerization of dialkoxybenzenes was achieved [39].

Oxidative trimerisation of dimethoxybenzene (veratrole) followed by exhaustive demethylation provides the starting material for synthesis of hexa-esters, among many other possibilities (Scheme 1).

Unsymmetrically substituted triphenylenes remained difficult to access for some time. Some success has been achieved via reaction of a mixture of substituted benzenes [39] or partial dealkylation/hydrolysis strategies [40–42], followed by separation of the various reaction

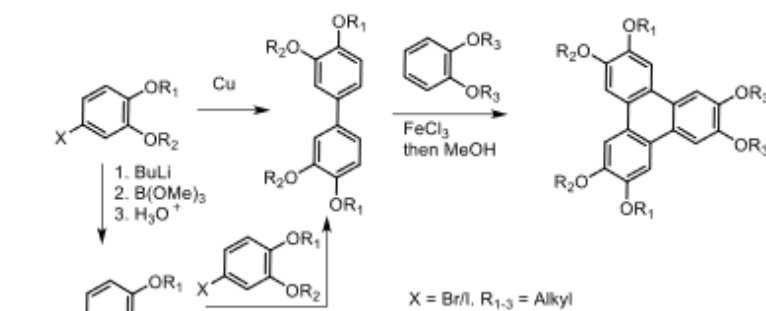


Scheme 1. Straightforward synthesis of hexaalkoxytriphenylenes (HAT), the presumed reaction sequence, and products from full and partial (single) hydrolysis.

products. However, the first breakthrough in this area stemmed from consideration of the mechanistic sequence that converts (substituted) benzenes into triphenylenes. As depicted in Scheme 1, the reaction is presumed to follow the sequence benzene-biphenyl-terphenyl-triphenylene, intermediates with frameworks that had become highly familiar within the LC field. We reasoned that a pre-synthesised suitable biphenyl intermediate could subsequently lead to controlled preparation of a single unsymmetrical triphenylene upon reaction with a complementary benzene partner, so long as the reaction conditions favoured triphenylene formation over the known oxidative dimerisation of biphenyl intermediates [43]. The protocol proved to be successful and convenient [44]. Symmetrical and

unsymmetrical tetraalkoxybiphenyls, prepared by traditional Ullman-type coupling of halobenzenes, were reacted with dialkoxybenzenes again using FeCl_3 as oxidant (Scheme 2). Combinations of long-chain alkoxy (hexyl) and methoxy substituents were chosen to aid separation/isolation, but also to allow further manipulation via selective deprotection of the methyl ethers. The resulting dihydroxytriphenylene derivatives were originally converted to main-chain polymers [45], but the intermediates have since been more widely employed in investigations of differentially substituted unsymmetrical triphenylenes to probe substituent effects and their influence on mesophase behaviour.

At around the same time, the application of transition-metal catalysed cross-coupling chemistry in biaryl



Scheme 2. Synthesis of unsymmetrically substituted hexaalkoxytriphenylenes by reaction of a pre-formed tetraalkoxybiphenyl with dialkoxybenzene.

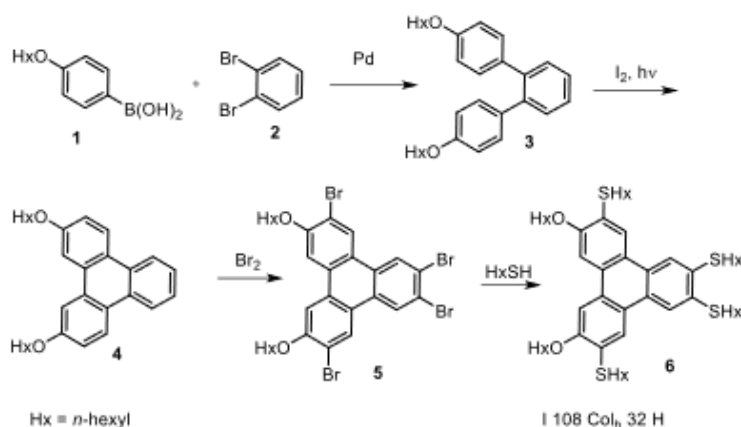
synthesis, and synthesis in general, was gaining significant momentum. Hird and co-workers [46] used Suzuki-Miyaura cross-coupling strategies to efficiently access biphenyl intermediates to deliver unsymmetrical triphenylenes, and the combination of cross-coupling with oxidative approaches has proved highly effective. A significant advantage of the cross-coupling approach is that the electronic character of the reacting components does not need to be matched and electron-rich systems (required for oxidative coupling) are not needed. Triphenylenes can be synthesised with free β -positions (e.g. **4**) through construction of *o*-terphenyl intermediates, and they can be post-functionalised by simple electrophilic aromatic substitution [47]. Bromination, for example, conveniently gives intermediates suitable for nucleophilic aromatic substitution [47] or subsequent cross-coupling [48–51]. Scheme 3 shows one example where this sequence was employed to produce an unsymmetrical triphenylene **6** that exhibits the rare helical columnar mesophase at room temperature [47].

The range of triphenylene materials available for design has therefore been significantly expanded and has particularly opened the way for investigation of new structural motifs to probe factors controlling columnar stability and to encourage nematic mesophase formation. A wide range of differentially (hexa)substituted triphenylenes have now been investigated, sequentially replacing alkoxy substituents on the parent hexaalkoxytriphenylenes. The studies reveal some general trends. Mesophase formation is often supported so long as conjugating substituents are introduced (essentially extending the core) [50]. The reduced symmetry of

the systems also typically results in a suppression of crystallisation leading to glassy columnar phases. Figure 4 shows representative examples that demonstrate how relatively minor changes can impact mesophase formation and stability.

The contrasting mesophase behaviour of the triphenylene hexaethers (columnar) and the hexaarylesters (nematic) has been highlighted earlier. Studies investigating mixed ether-ester linkages in the triphenylene series have been initiated recently. Replacing a single ether of the parent hexaalkoxytriphenylene with aryl ester substituents so far leads only to columnar mesophases. In fact, in the initial study, we find that the mesophase range is remarkably insensitive to the size and character of the aryl ester employed, implying that the single aromatic unit can be easily accommodated in the chain region between columns [52]. This investigation has now been extended to include selected examples of isomeric diesters, reported here for the first time, and again columnar mesophases only are observed (Figure 5).

While columnar packing/assembly is effectively constrained in examples of triphenylene hexaaryl esters, an alternative approach to generating nematic mesophases in triphenylene discotics has emerged whereby columnar packing is disfavoured by the formation of dimeric systems, typically linked by rigid bridges. Some examples are shown in Figure 6 Here the behaviour contrasts with dimeric systems linked by flexible spacer chains of appropriate length, where columnar mesophase formation is preserved [53–55]. The first examples of this motif were the diacetylene-bridged triphenylenes reported by Kumar and Varshney [56]. Twinned



Scheme 3. An example of synthesis of a lightly substituted triphenylene via an *o*-terphenyl, and subsequent functionalisation to give a mesogenic hexasubstituted material [47].

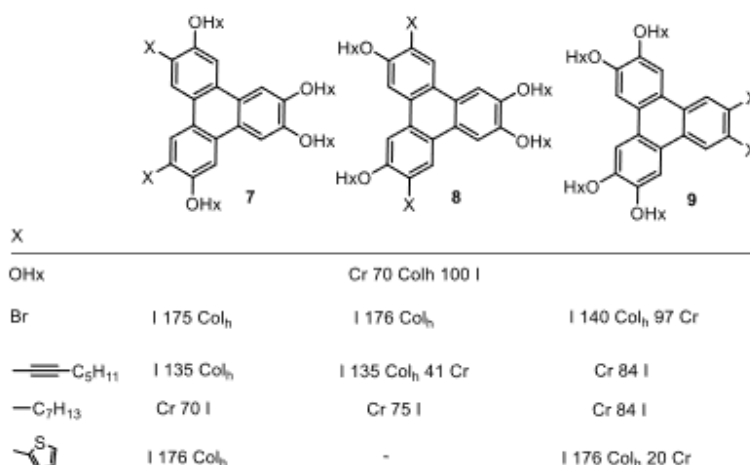


Figure 4. Examples of structural variation in unsymmetrically substituted triphenylenes (Hx = *n*-hexyl) [47–50].

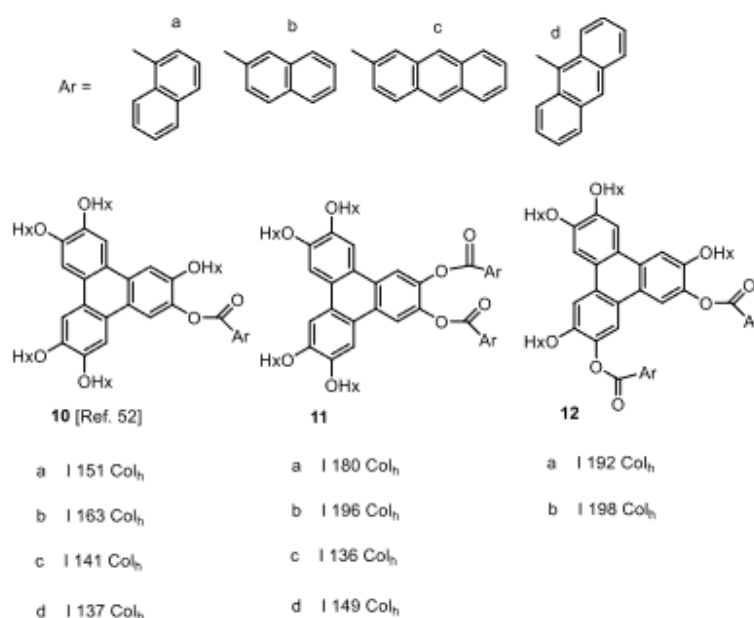


Figure 5. Triphenylenes with mixed ether and ester substituents showing only columnar mesophases (Hx = *n*-hexyl).

systems – two triphenylene cores linked by two rigid bridges to form a macrocycle – show a strong tendency towards nematic behaviour [57–59]. Complementary to the design features that lead to nematic phases in the triphenylene hexaaryl esters, here the formation of columnar assemblies also leads to free space (through

the centre of the column in this case) favouring the slipped (N_D) arrangement [57].

Further examples of dimers where the bridges are systematically engineered to modify core–core separation and conformational freedom have been investigated more recently, focusing on aryl ester [52] and

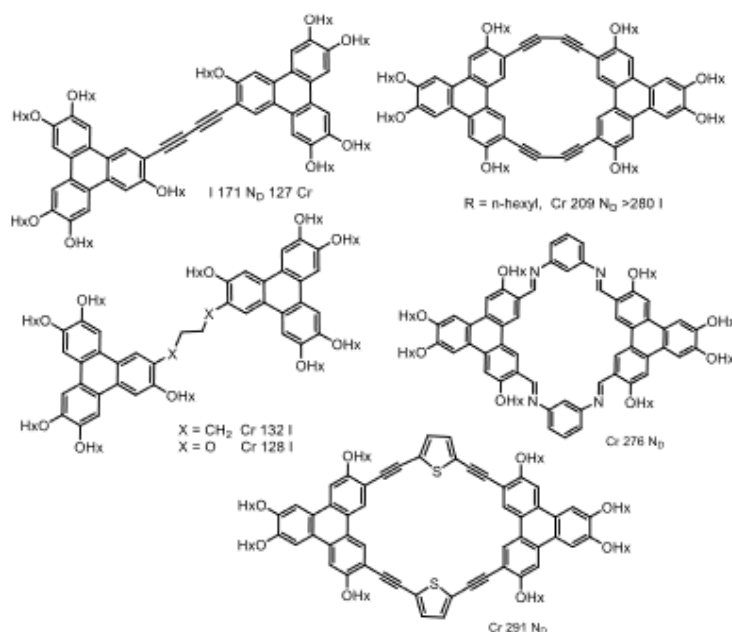


Figure 6. Triphenylene dimers and twins, linked through rigid bridges, showing nematic mesophases [56–59].

aryl alkyne [60] links (Figure 7). In the diester (phthalate) series, mesophase behaviour is completely suppressed when the core–core separation is enforced to be too short (*o*-phthalate where face-to-face packing is difficult to achieve) or too long (the stilbene system). The 2,5-thiophene diester shows an enantiotropic N_D phase, while the similarly bent 2,7-naphthaloate bridge gives a rare example of a material that forms a columnar phase on cooling from the nematic (albeit alongside glass formation).

The alkyne linked dimers [60] are particularly interesting. The single aryl-diacetylene bridge between the triphenylenes provides materials that have intermediate conformational freedom compared to, for example, the complementary aryl diester series and rigid twinned (double bridge) systems. Similar to the *o*-phthalate system [52], the 1,2-phenyl diacetylene bridge does not support any mesophase behaviour. However, opening the linking angle leads to mesophase formation over a wide temperature range. The unique combination of fixed core–core separation alongside limited conformational freedom provides a series of discotic materials that each form both nematic and columnar mesophases (Figure 8) [60].

Experimental

Synthesis of triphenylene-2,3-bis(1-naphthoate) ester 11a (general procedure)

2,3-Dihydroxy-6,7,10,11-tetrakis(hexyloxy)triphenylene (100 mg, 0.15 mmol), and 1-naphthoyl chloride (0.069 g, 0.36 mol) were stirred in dry CH_2Cl_2 (10 ml) at 0°C . Then, dry NEt_3 (2 ml) was added slowly. After 2 h, the solvents were evaporated and the residue precipitated from methanol to give a pale yellow solid (0.055 g, 38%). ^1H NMR (400 MHz, Chloroform-*d*) δ 9.05–9.00 (m, 2 H), 8.47 (s, 2 H), 8.40 (dd, $J = 7.4, 1.3$ Hz, 2 H), 7.94 (dt, $J = 8.3, 1.1$ Hz, 2 H), 7.89 (s, 2 H), 7.83 (s, 2 H), 7.82–7.79 (m, 2 H), 7.53–7.46 (m, 4 H), 7.25 (dd, $J = 8.2, 7.3$ Hz, 2 H), 4.25 (t, $J = 6.6$ Hz, 4 H), 4.21 (t, $J = 6.6$ Hz, 4 H), 1.96–1.86 (m, 8 H), 1.58–1.43 (m, 8 H), 1.39–1.26 (m, 16 H), 0.93 (t, $J = 7.2$ Hz, 6 H), 0.88 (t, $J = 7.2$ Hz, 6 H). ^{13}C NMR (101 MHz, CD_2Cl_2) δ 165.15, 149.92, 149.23, 141.40, 134.39, 133.80, 131.46, 131.38, 128.59, 128.11, 127.86, 126.36, 125.42, 125.00, 124.37, 124.18, 122.54, 117.61, 106.80, 106.59, 69.47, 69.25, 31.69, 31.63, 29.43, 29.37, 25.85, 25.78, 22.67, 22.62, 13.82, 13.78.

Diesters **11** and **12** were prepared following the same procedure using the 2,3-dihydroxytriphenylene (for **11**)

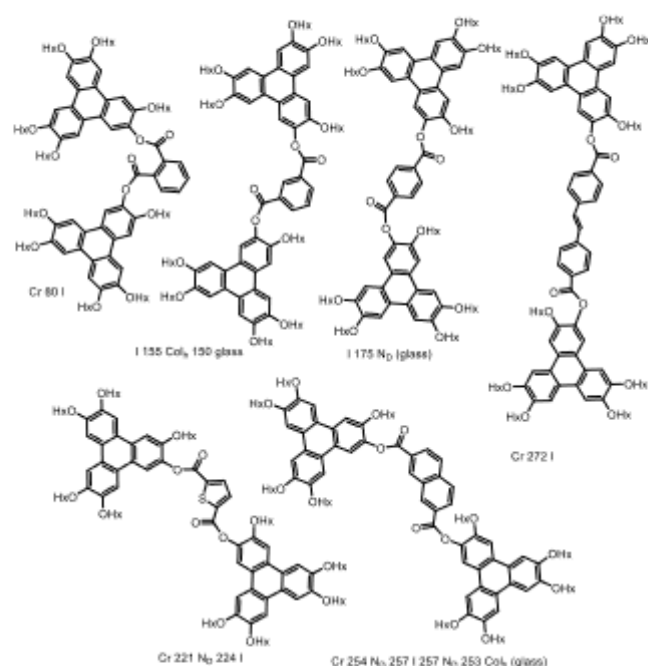


Figure 7. The influence of linker on mesophase behaviour in ester-linked triphenylene dimers [52].

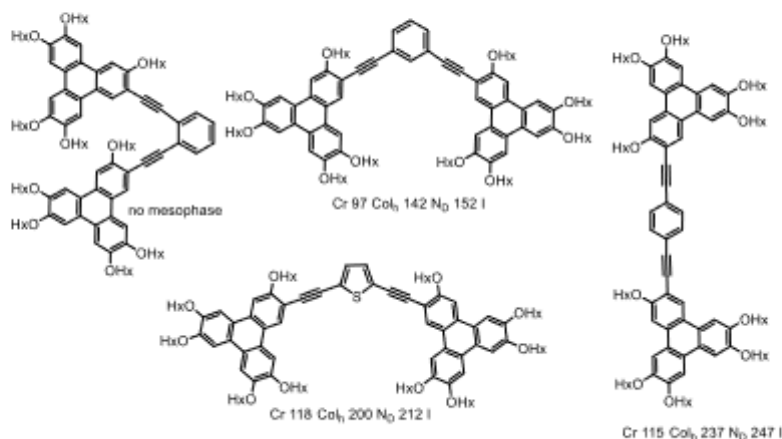


Figure 8. Aryl diacetylene linked triphenylene dimers showing both columnar and nematic mesophases [60].

or the 3,6-dihydroxytriphenylene (for **12**) and the appropriate acid chloride.

2,3-bis(2-naphthoate) ester **11b**

(0.05 g, 34%). $^1\text{H NMR}$ (400 MHz, Chloroform-*d*) δ 8.71 (br s, 2 H), 8.50 (s, 2 H), 8.13 (dd, $J = 7.4, 1.3$ Hz,

2 H), 7.88 (s, 2 H), 7.84 (s, 2 H), 7.78 (d, $J = 8.3$ Hz, 2 H), 7.77 (d, $J = 8.2$ Hz, 2 H), 7.72 (d, $J = 8.5$ Hz, 2 H), 7.54 (dt, $J = 8.0, 1.0$ Hz, 2 H), 7.43 (dt, $J = 8.0, 1.0$ Hz, 2 H), 4.26 (t, $J = 6.6$ Hz, 4 H), 4.22 (t, $J = 6.6$ Hz, 4 H), 1.99–1.88 (m, 8 H), 1.63–1.51 (m, 8 H), 1.46–1.29 (m, 16 H), 0.93 (t, $J = 7.2$ Hz, 6 H), 0.89 (t, $J = 7.2$ Hz, 6 H). $^{13}\text{C NMR}$ (101 MHz, CD_2Cl_2) δ 165.15, 149.92, 149.23,

141.40, 134.39, 133.80, 131.46, 131.38, 128.59, 128.11, 127.86, 126.36, 125.42, 125.00, 124.37, 124.18, 122.54, 117.61, 106.80, 106.59, 69.47, 69.25, 31.69, 31.63, 29.43, 29.37, 25.85, 25.78, 22.67, 22.62, 13.82, 13.78.

2,3-bis(2-anthracenoate) ester 11c

(0.051 g, 32%). ¹H NMR (400 MHz, Chloroform-*d*) 8.89 (s, 2 H), 8.59 (s, 2 H), 8.24 (s, 2 H), 8.16 (s, 2 H), 8.06 (dd, *J* = 8.9, 1.7 Hz, 2 H), 7.93 (s, 2 H), 7.90 (s, 2 H), 7.88 (s, 2 H), 7.86 (s, 2 H), 7.68 (d, *J* = 8.5 Hz, 2 H), 7.46 (t, *J* = 7.0 Hz, 2 H), 7.31 (t, *J* = 7.0 Hz, 2 H), 4.27 (t, *J* = 6.6 Hz, 4 H), 4.24 (t, *J* = 6.6 Hz, 4 H), 2.01–1.90 (m, 8 H), 1.65–1.51 (m, 8 H), 1.46–1.32 (m, 16 H), 0.95 (t, *J* = 7.0 Hz, 4 H), 0.90 (t, *J* = 7.0 Hz, 4 H). ¹³C NMR (101 MHz, CDCl₃) δ 164.99, 149.75, 149.19, 141.29, 133.65, 133.18, 132.57, 131.82, 130.01, 128.83, 128.70, 128.33, 128.01, 127.86, 126.69, 126.07, 125.78, 125.59, 124.31, 123.92, 122.93, 117.40, 107.03, 69.66, 69.31, 31.72, 31.66, 29.43, 29.35, 25.87, 25.83, 22.68, 22.64, 14.07, 14.03 (2 signals unresolved).

2,3-bis(9-anthracenoate) ester 11d

(0.03 g, 19%). ¹H NMR (400 MHz, CD₂Cl₂) δ 8.82 (s, 2 H), 8.47 (s, 2 H), 8.18 (d, *J* = 9.0 Hz, 4 H), 8.07 (s, 2 H), 7.94 (d, *J* = 9.0 Hz, 4 H), 7.92 (s, 2 H), 7.34 (t, *J* = 8.3 Hz, 4 H), 7.0 (t, *J* = 8.3, 4 H), 4.33 (t, *J* = 6.7 Hz, 4 H), 4.32 (t, *J* = 6.7 Hz, 4 H), 2.05–1.96 (m, 8 H), 1.70–1.38 (m, 24 H), 0.98 (t, *J* = 7.2 Hz, 4 H), 0.94 (t, *J* = 7.2 Hz, 4 H). ¹³C NMR (101 MHz, CDCl₃) δ 167.38, 150.10, 149.24, 141.06, 130.68, 130.37, 128.81, 128.27, 128.10, 126.91, 125.79, 125.32, 124.87, 124.63, 122.85, 117.40, 107.75, 106.98, 69.73, 69.64, 31.94, 31.72, 29.67, 29.42, 29.37, 25.89, 25.87, 22.69, 22.66, 14.13, 14.08.

3,6-bis(1-naphthoate) ester 12a

(0.043 g, 61%). ¹H NMR (500 MHz, Chloroform-*d*) 9.03 (d, *J* = 8.7 Hz, 2 H), 8.46 (dd, *J* = 7.3, 1.3 Hz, 2 H), 8.00 (d, *J* = 8.0 Hz, 2 H), 7.95 (d, *J* = 8.0 Hz, 2 H), 7.92 (s, 2 H), 7.91 (d, *J* = 7.5 Hz, 2 H), 7.80 (s, 2 H), 7.58–7.46 (m, 6 H), 4.20 (t, *J* = 6.4 Hz, 4 H), 4.15 (t, *J* = 6.5 Hz, 4 H), 1.84–1.75 (m, 4 H), 1.74–1.67 (m, 4 H), 1.46–1.38 (m, 4 H), 1.36–1.30 (m, 4 H), 1.29–1.25 (m, 8 H), 1.13–0.98 (m, 8 H), 0.84 (t, *J* = 7.0 Hz, 6 H), 0.64 (t, *J* = 7.2 Hz, 6 H). ¹³C NMR (126 MHz, CDCl₃) 165.81, 149.76, 149.48, 140.12, 133.91, 133.88, 131.69, 131.15, 128.54, 127.89, 127.84, 126.46, 126.31, 126.08, 124.58, 124.10, 122.95, 117.07, 107.63, 105.98, 69.61, 68.87, 31.72, 31.55, 29.41, 29.40, 25.84, 25.74, 22.65, 22.44, 14.07, 13.86.

3,6-bis(2-naphthoate) ester 12b

(0.04 g, 54%). ¹H NMR (500 MHz, Chloroform-*d*) 8.86 (br s, 2 H), 8.26–8.23 (m, 6 H), 8.00 (d, *J* = 8.0 Hz, 2 H), 7.95 (d, *J* = 8.0 Hz, 2 H), 7.92 (s, 2 H), 7.91 (d, *J* = 7.5 Hz, 2 H), 7.90 (s, 2 H), 7.62 (t, *J* = 8.5 Hz, 2 H), 7.57 (t, *J* = 8.5 Hz, 2 H), 4.27 (t, *J* = 6.4 Hz, 4 H), 4.24 (t, *J* = 6.5 Hz, 4 H), 1.99–1.92 (m, 4 H), 1.79–1.71 (m, 4 H), 1.63–1.55 (m, 4 H), 1.46–1.38 (m, 12 H), 1.22–1.09 (m, 8 H), 0.94 (t, *J* = 7.2 Hz, 6 H), 0.71 (t, *J* = 7.2 Hz, 6 H). ¹³C NMR (126 MHz, CDCl₃) 163.89, 148.65, 148.41, 139.15, 132.31, 129.24, 128.64, 127.44, 126.73, 122.99, 121.88, 115.83, 106.56, 105.23, 68.56, 67.91, 30.69, 30.49, 28.40, 28.23, 24.84, 24.63, 21.64, 21.48, 13.03, 12.89.

Conclusions

The development and commercial application of the (cyano) biphenyls can be seen to have influenced the later development of discotic materials where the triphenylene nucleus has become the most widely studied core. The search for discotic nematic materials was originally driven by interest in the potential of discotics to be active, switchable components in displays, but they proved both difficult to design and synthesise, and their properties did not compete. Nevertheless, nematic discotics have played vital role in display devices as a passive, thin-film optical compensating layers to widen viewing angles. Nematic discotics have remained intriguing within liquid crystal science. They are relatively rare and studies now indicate that columnar packing needs to be disfavoured by molecular design. This can be achieved by construction of systems where the side-chains themselves prevent columnar packing by providing a thick ring around the core (the aryl esters and phenyl acetylenes) or by rigidly linking cores such that they cannot achieve face-to-face assembly (rigid dimers and twins). Some examples are now known that show both columnar and nematic mesophases. The later development of more intricate molecular designs has been made possible by advances in synthetic chemistry that can deliver unsymmetrical systems. The chemistry here also sees a parallel with bi- (and ter-)phenyl development, not least because their pre-synthesis has been key to developing versatile new routes to triphenylene discotics. In this regard, the combination of transition metal catalysed cross-coupling and oxidative cyclisation has been proved the most powerful.

Acknowledgments

We thank Almajmaah University (SA) and Taibah University (SS) for their financial support.

Disclosure statement

No potential conflict of interest was reported by the author(s).

Funding

The work was supported by Majmaah University and Taibah University.

References

- Chandrasekhar S, Sadashiva BK, Suresh KA. Liquid crystals of disc-like molecules. *Pramana J Phys*. 1977;9(5):471–480. doi: 10.1007/BF02846252
- Cammidge AN, Bushby RJ. Discotic liquid crystals: synthesis and structural features. In: Demus D, Goodby J, Gray G, Spiess H Vill V, editors. *Handbook of liquid crystals*. Vol. 2. Weinheim: Wiley-VCH; 1998. p. 693–748. doi: 10.1002/9783527620623.ch4
- Kumar S. *Chemistry of discotic liquid crystals*. Florida: CRC Press; 2010.
- Bock II, Helfrich W. Two ferroelectric phases of a columnar dibenzopyrene. *Liq Cryst*. 1995;18(3):387–399. doi: 10.1080/02678299508036636
- Kumar S. Recent developments in the chemistry of triphenylene-based discotic liquid crystals. *Liq Cryst*. 2004;31(8):1037–1059. doi: 10.1080/02678290410001724746
- Cammidge AN, Gopee H. Design and synthesis of nematic phases formed by disk-like molecules. In: Goodby J, Collings P, Kato T, Tschierske C, Gleeson H, Raynes P, editors. *Handbook of liquid crystals*. 2nd ed. Vol. 3. Weinheim: Wiley-VCH; 2014. p. 293–334. doi: 10.1002/9783527671403.hlc047
- Hunter CA, Sanders JKM. The nature of pi-pi interactions. *J Am Chem Soc*. 1990;112:5525–5534. doi: 10.1021/ja00170a016
- Dirand M, Bouroukba M, Briard AJ, et al. Temperatures and enthalpies of (solid+solid) and (solid+liquid) transitions of n-alkanes. *J Chem Thermodyn*. 2002;34(8):1255–1277. doi: 10.1006/jcht.2002.0978
- Destradre C, Tinh NH, Gasparoux H, et al. Disc-like mesogens: a classification. *Mol Cryst Liq Cryst*. 1981;71(1–2):111–135. doi: 10.1080/00268948108072721
- Tinh NH, Destradre C, Gasparoux H. Nematic disc-like liquid crystals. *Phys Lett A*. 1979;72(3):251–254. doi: 10.1016/0375-9601(79)90019-7
- Phillips TJ, Jones JC, McDonnell DG. On the influence of short range order upon the physical properties of triphenylene nematic discogens. *Liq Cryst*. 1993;15(2):203–215. doi: 10.1080/02678299308031951
- Hindmarsh P, Hird M, Styring P, et al. Lateral substitution in the peripheral moieties of triphenylene-2,3,6,7,10,11-hexyl hexakis(4-alkoxybenzoate)s: dimethyl-substituted systems. *J Mater Chem*. 1993;3:1117–1128. doi: 10.1039/jm9930301117
- Praefcke K, Kohne B, Singer D. Hexaalkynyltriphenylene: a new type of nematic-discotic hydrocarbon. *Angew Chem Int Ed Engl*. 1990;29:177–179. doi: 10.1002/anie.199001771
- Kohne B, Praefcke K. Liquid-crystalline compounds. 43. Hexaalkynylbenzene derivatives, the 1st hydrocarbon columnar-discotic or nematic-discotic liquid crystals. *Chimia*. 1987;41:196–198. doi: 10.1002/chin.198750161
- Toyota S. Rotational isomerism involving acetylene carbon. *Chem Rev*. 2010;110(9):5398–5424. doi: 10.1021/cr1000628
- Lozman OR, Bushby RJ, Vinter JG. Complementary polytopic interactions (CPI) as revealed by molecular modelling using the XED force field. *J Chem Soc Perkin Trans*. 2001;2(9):1446–1452. doi: 10.1039/b103390p
- Bushby RJ, Kawata K. Liquid crystals that affected the world: discotic liquid crystals. *Liq Cryst*. 2011;38(11–12):1415–1426. doi: 10.1080/02678292.2011.603262
- Mori H, Itoh Y, Nishiura Y, et al. Performance of a novel optical compensation film based on negative birefringence of discotic compound for wide-viewing-angle twisted-nematic liquid-crystal displays. *Jpn J Appl Phys*. 1997;36:143–147. Part 1. doi: 10.1143/JJAP.36.143
- Lawson KD, Flaunt TJ. Magnetically oriented lyotropic liquid crystalline phases. *J Am Chem Soc*. 1967;89:5489–5491. doi: 10.1021/ja00997a054
- Charvolin J, Levelut AM, Samulski ET. Lyotropic nematics: molecular aggregation and susceptibilities. *J De Phys Lett*. 1979;40:L587–L592. doi: 10.1051/jphyslet:019790040022058700
- Holmes MC, Charvolin J. Smectic-nematic transition in a lyotropic liquid crystal. *J Phys Chem*. 1984;88(4):810–818. doi: 10.1021/j150648a039
- Boden N, Jackson PH, McMullen K, et al. Are “nematic” amphiphilic liquid crystalline mesophases thermodynamically stable? *Chem Phys Lett*. 1979;65(3):476–479. doi: 10.1016/0009-2614(79)80275-4
- Forrest BJ, Reeves LW. New lyotropic liquid crystals composed of finite nonspherical micelles. *Chem Rev*. 1981;81:1–14. doi: 10.1021/cr00041a001
- Saupe A. On the structure and the physical properties of micellar nematics. II. *Nuovo Cimento D*. 1984;3(1):16–29. doi: 10.1007/BF02452199
- Boden N, Bushby RJ, Hardy C. New mesophases formed by water soluble discoidal amphiphiles. *J De Phys Lett*. 1985;46:L325–L328. doi: 10.1051/jphyslet:01985004607032500
- Boden N, Bushby RJ, Ferris I, et al. Designing new lyotropic amphiphilic mesogens to optimize the stability of nematic phases. *Liq Cryst*. 1986;1(2):109–125. doi: 10.1080/02678298608086498
- Akinshina A, Walker M, Wilson MR, et al. Thermodynamics of the self-assembly of non-ionic chromonic molecules using atomistic simulations. The case of TP6EO2M in aqueous solution. *Soft Matter*. 2015;11:680–691. doi: 10.1039/C4SM02275K
- Henderson JR. Linear aggregation beyond isodesmic symmetry. *J Chem Phys*. 2009;130(4):045101. doi: 10.1063/1.3063099
- Boden N, Bushby RJ, Hardy C, et al. Phase behaviour and structure of a non-ionic discoidal amphiphile in water. *Chem Phys Lett*. 1986;123(5):359–364. doi: 10.1016/0009-2614(86)80021-5
- Potter TD, Walker M, Wilson MR. Self-assembly and mesophase formation in a non-ionic chromonic liquid crystal: insights from bottom-up and top-down

- coarse-grained simulation models. *Soft Matter*. 2020;16(41):9488–9498. doi: 10.1039/D0SM01157F
- [31] Perez-Calm A, Esquena J, Salonen IM, et al. Pegylated perylene bisimides: chromonic building blocks for the aqueous synthesis of nanostructured silica materials. *J Mol Liq*. 2021;325:114657. doi: 10.1016/j.molliq.2020.114657
- [32] Masters A. Chromonic liquid crystals: more questions than answers. *Liq Cryst Today*. 2016;25(2):30–37. doi: 10.1080/1358314X.2016.1149925
- [33] McKeown NB, Painter J. Lyotropic and thermotropic mesophase formation of novel tetra-[oligo(ethyleneoxy)]-substituted Phthalocyanines. *J Mater Chem*. 1994;4:1153–1156. doi: 10.1039/jm9940401153
- [34] Boden N, Bushby RJ, Donovan K, et al. 2,3,7,8,12,13-Hexakis[2-(2-methoxyethoxy)ethoxy]tricycloquinazoline: a discogen which allows enhanced levels of n-doping. *Liq Cryst*. 2001;28:1739–1748. doi: 10.1080/02678290110082383
- [35] Al-Lawati ZH, Alkhairalla B, Bramble JP, et al. Alignment of discotic lyotropic liquid crystals at hydrophobic and hydrophilic self-assembled monolayers. *J Phys Chem C*. 2012;116(23):12627–12635. doi: 10.1021/jp302634r
- [36] Lydon J. Chromonic review. *J Mater Chem*. 2010;20(45):10071–10099. doi: 10.1039/b926374h
- [37] Hartshorne NH, Woodard GD. Mesomorphism in the System disodium chromoglycate-water. *Mol Cryst Liq Cryst*. 1973;23(3–4):343–368. doi: 10.1080/15421407308083381
- [38] Attwood TK, Lydon JE, Jones F. The chromonic phases of dyes. *Liq Cryst*. 1986;1(6):499–507. doi: 10.1080/02678298608086274
- [39] Boden N, Borner RC, Bushby RJ, et al. The synthesis of triphenylene-based discotic mesogens New and improved routes. *Liq Cryst*. 1993;15:851–858. doi: 10.1080/02678299308036504
- [40] Kumar S, Lakshmi B. A convenient and economic method for the synthesis of monohydroxy-pentaalkoxy- and hexaalkoxytriphenylene discotics. *Tetrahedron Lett*. 2005;46(15):2603–2605. doi: 10.1016/j.tetlet.2005.02.099
- [41] Ban J, Chen S, Zhang H. Synthesis and phase behaviour of mesogen jacketed liquid crystalline polymer with triphenylene discotic liquid crystal mesogen unit in side chains. *RSC Adv*. 2014;4:54158–54167. doi: 10.1039/C4RA07824A
- [42] Kong X, He Z, Gopee H, et al. Improved synthesis of monohydroxytriphenylenes (MHTs) – important precursors to discotic liquid crystals. *Tetrahedron Lett*. 2011;52:77–79. doi: 10.1016/j.tetlet.2010.10.152
- [43] Musgrave OC, Webster CJ. Formation of polycyclic quinones in oxidations of 3,3',4,4'-tetramethoxybiphenyl and veratrole. *J Chem Soc Chem Commun*. 1969;712–713. doi: 10.1039/C29690000712
- [44] Boden N, Bushby RJ, Cammidge AN. A quick-and-easy route to unsymmetrically substituted derivatives of triphenylene: preparation of polymeric discotic liquid crystals. *J Chem Soc Chem Commun*. 1994;4:465–466. doi: 10.1039/c39940000465
- [45] Boden N, Bushby RJ, Cammidge AN. Triphenylene-based discotic-liquid-crystalline polymers: a universal, rational synthesis. *J Am Chem Soc*. 1995;117(3):924–927. doi: 10.1021/ja00108a009
- [46] Goodby JW, Hird M, Toyne KJ, et al. A novel, efficient and general synthetic route to unsymmetrical triphenylene mesogens using palladium-catalysed cross-coupling reactions. *J Chem Soc Chem Commun*. 1994;14:1701–1702. doi: 10.1039/c39940001701
- [47] Cammidge AN, Gopee H. Structural factors controlling the transition between columnar-hexagonal and helical mesophase in triphenylene liquid crystals. *J Mater Chem*. 2001;11(11):2773–2783. doi: 10.1039/b103450m
- [48] Cammidge AN, Gopee H. Mixed alkyl-alkoxy triphenylenes. *Mol Cryst Liq Cryst*. 2003;397:417–428. doi: 10.1080/0714965603
- [49] Cammidge AN, Gopee H. Synthesis and liquid crystal properties of mixed alkynyl-alkoxy-triphenylenes. *Liq Cryst*. 2009;36:809–819. doi: 10.1080/02678290903063000
- [50] Cammidge AN, Chausson C, Gopee H, et al. Probing the structural factors influencing columnar mesophase formation and stability in triphenylene discotics. *Chem Commun*. 2009;47:7375–7377. doi: 10.1039/b913678a
- [51] Cammidge AN. The effect of size and shape variation in discotic liquid crystals based on triphenylene cores. *Philos Trans R Soc A* 2006;364(1847):2697–2708. doi: 10.1098/rsta.2006.1847
- [52] Alanazi BN, Alruwaili AM, Beskeni RD, et al. Pentalkoxytriphenylene monoester and their dyads; structural factors influencing columnar and nematic mesophase behaviour. *Liq Cryst*. 2022;49:1174–1183. doi: 10.1080/02678292.2021.1993456
- [53] Kumar S. Triphenylene-based discotic liquid crystal dimers, oligomers and polymers. *Liq Cryst*. 2005;32(9):1089–1113. doi: 10.1080/02678290500117415
- [54] Boden N, Bushby RJ, Cammidge AN, et al. The creation of long-lasting glassy columnar discotic liquid crystals using “dimeric” discogens. *J Mater Chem*. 1999;9:1391–1402. doi: 10.1039/a810045d
- [55] Wang Y, Zhang C, Wu H, et al. Synthesis and mesomorphism of triphenylene-based dimers with a highly ordered columnar plastic phase. *J Mater Chem C*. 2014;2(9):1667–1674. doi: 10.1039/c3tc31986e
- [56] Kumar S, Varshney SK. Design and synthesis of discotic nematic liquid crystals. *Org Lett*. 2002;4(2):157–159. doi: 10.1021/ol010200v
- [57] Zhang L, Gopee H, Hughes DL, et al. Antiaromatic twinned triphenylene discotics showing nematic phases and 2-dimensional π -overlap in the solid state. *Chem Commun*. 2010;46:4255–4257.
- [58] Zhang L, Hughes DL, Cammidge AN. Discotic triphenylene twins linked through thiophene bridges: controlling nematic behavior in an intriguing class of functional organic materials. *J Org Chem*. 2012;77(9):4288–4297. doi: 10.1021/jo3002886
- [59] Cammidge AN, Turner RJ, Beskeni RD, et al. A modified route to unsymmetrically substituted triphenylenes, new functionalised derivatives and twins, and the smallest reported triphenylene mesogen. *Liq Cryst*. 2017;44:2018–2028. doi: 10.1080/02678292.2017.1346210
- [60] Alsahli AO, Cammidge AN. Synthesis and mesophase properties of triphenylene dimers linked through linear and bent alkyne-aryl-alkyne bridges. *Eur J Org Chem*. 2022;2022:e202200990. doi: 10.1002/ejoc.202200990

6. References:

- (1) (a) Stillman, M.; Nyokong, T.; Leznoff, C.; Lever, A. Phthalocyanines: properties and applications. *by CC Leznoff and ABP Lever, VCH, New York* **1989**, *1*, 133. (b) Wende, H.; Bernien, M.; Luo, J.; Sorg, C.; Ponpandian, N.; Kurde, J.; Miguel, J.; Piantek, M.; Xu, X.; Eckhold, P. Substrate-induced magnetic ordering and switching of iron porphyrin molecules. *Nature materials* **2007**, *6* (7), 516-520. (c) Lee, C. H.; Kwon, Y. W.; Choi, D. H.; Geerts, Y. H.; Koh, E.; Jin, J. I. High-Temperature Ferromagnetism of a Discotic Liquid Crystal Dilutely Intercalated with Iron (III) Phthalocyanine. *Advanced materials* **2010**, *22* (39), 4405-4409. (d) Gauyacq, J.-P.; Novaes, F. D.; Lorente, N. Magnetic transitions induced by tunneling electrons in individual adsorbed M-phthalocyanine molecules (M= Fe and Co). *Physical Review B* **2010**, *81* (16), 165423. (e) Chen, X.; Alouani, M. Effect of metallic surfaces on the electronic structure, magnetism, and transport properties of Co-phthalocyanine molecules. *Physical Review B* **2010**, *82* (9), 094443.
- (2) Tang, Z.-k.; Wang, L.-L.; Zhang, D.-Y.; Xu, L.; Li, X.-F.; Huang, W.-Q. Enhanced ferromagnetism by adding electrons in triple-decker Gd-phthalocyanine. *Physica Scripta* **2013**, *87* (4), 045701.
- (3) Yuan, Y.; Bang, K. T.; Wang, R.; Kim, Y. Macrocyclic-Based Covalent Organic Frameworks. *Advanced Materials* **2023**, *35* (16), 2210952.
- (4) Milgrom, L. R. *The Colours of Life: An introduction to the Chemistry of Porphyrins and Related Compounds*; Oxford university press, 1997.
- (5) Wohrle, D. The colours of life. An introduction to the chemistry of porphyrins and related compounds. By LR Milgrom, Oxford university press, Oxford 1997, vi, 225 pp., softcover, £ 49.50, ISBN 019-855380-3. Wiley Online Library: 1997.
- (6) Hohnholz, D.; Steinbrecher, S.; Hanack, M. Applications of phthalocyanines in organic light emitting devices. *Journal of Molecular Structure* **2000**, *521* (1-3), 231-237.
- (7) Küster, W. Beiträge zur Kenntnis des Bilirubins und Hämins. **1912**.
- (8) Lash, T. D.; Jones, S. A.; Ferrence, G. M. Synthesis and characterization of tetraphenyl-21, 23-dideazaporphyrin: The best evidence yet that porphyrins really are the [18] annulenes of nature. *Journal of the American Chemical Society* **2010**, *132* (37), 12786-12787.
- (9) Steiner, E.; Soncini, A.; Fowler, P. W. Ring currents in the porphyrins: π shielding, delocalisation pathways and the central cation. *Organic & biomolecular chemistry* **2005**, *3* (22), 4053-4059.
- (10) Schmidt, A. M.; Calvete, M. J. Phthalocyanines: an old dog can still have new (photo) tricks! *Molecules* **2021**, *26* (9), 2823.
- (11) Dini, D.; Hanack, M. Physical Properties of 107 Phthalocyanine-Based Materials. *The porphyrin handbook* **2003**, *11*, 1. Nyokong, T.; Antunes, E.; Kadish, K.; Smith, R.; Guillard, R. Handbook of porphyrin science. *World Scientific Press* **2010**, *7*, 247.
- (12) Fischer, H.; Orth, H. *Die Chemie des pyrrols*; Akademische Verlagsgesellschaft M. B. H., 1934.
- (13) Moss, G. P. Nomenclature of tetrapyrroles: recommendations 1986. *European journal of biochemistry* **1988**, *178* (2), 277-328.
- (14) Moss, G. Nomenclature of tetrapyrroles (Recommendations 1986). *Pure and Applied Chemistry* **1987**, *59* (6), 779-832.
- (15) Karlson, P. The nomenclature of tetrapyrroles. A report. **1981**.
- (16) Kadish, K.; Guillard, R.; Smith, K. M. *The porphyrin handbook: phthalocyanines: spectroscopic and electrochemical characterization*; Academic Press, 2012. Calvete, M. J. *Future Trends for Top Materials*; Bentham Science Publishers, 2016.

- (17) Popanda, B.; Środa, M. Porphyrin and phthalocyanine as materials for glass coating—structure and properties. In *Advances in Glass Research*, Springer, 2023; pp 241-317.
- (18) Yahya, M.; Nural, Y.; Seferoğlu, Z. Recent advances in the nonlinear optical (NLO) properties of phthalocyanines: A review. *Dyes and Pigments* **2022**, *198*, 109960. Pişkin, M. Phthalocyanine photosensitizers with bathochromic shift, of suitable brightness, capable of producing singlet oxygen with effective efficiency. *Journal of Photochemistry and Photobiology A: Chemistry* **2023**, *435*, 114325.
- Lukyanets, E. A.; Nemykin, V. N. The key role of peripheral substituents in the chemistry of phthalocyanines and their analogs. *Journal of Porphyrins and Phthalocyanines* **2010**, *14* (01), 1-40.
- (19) Milgrom, L. *The Colours of Life*, Oxford University Press. 1997.
- (20) Barrett, P.; Dent, C.; Linstead, R. 382. Phthalocyanines. Part VII. Phthalocyanine as a co-ordinating group. A general investigation of the metallic derivatives. *Journal of the Chemical Society (Resumed)* **1936**, 1719-1736.
- (21) Rothmund, P.; Menotti, A. R. Porphyrin Studies. IV. 1 The Synthesis of α , β , γ , δ -Tetraphenylporphine. *Journal of the American Chemical Society* **1941**, *63* (1), 267-270.
- (22) Heyes, D. J.; Heathcote, P.; Rigby, S. E.; Palacios, M. A.; van Grondelle, R.; Hunter, C. N. The first catalytic step of the light-driven enzyme protochlorophyllide oxidoreductase proceeds via a charge transfer complex. *Journal of Biological Chemistry* **2006**, *281* (37), 26847-26853. Heyes, D. J.; Ruban, A. V.; Wilks, H. M.; Hunter, C. N. Enzymology below 200 K: the kinetics and thermodynamics of the photochemistry catalyzed by protochlorophyllide oxidoreductase. *Proceedings of the National Academy of Sciences* **2002**, *99* (17), 11145-11150.
- (23) Poulos, T. L. Heme enzyme structure and function. *Chemical reviews* **2014**, *114* (7), 3919-3962. Dolphin, D. *The Porphyrins V7: Biochemistry, Part B*; Elsevier, 2012.
- (24) Lesage, S.; Xu, H.; Durham, L. The occurrence and roles of porphyrins in the environment: possible implications for bioremediation. *Hydrological sciences journal* **1993**, *38* (4), 343-354.
- (25) Beems, E. M.; Dubbelman, T. M.; Lugtenburg, J.; Van Best, J. A.; Smeets, M. F.; Boegheim, J. P. J. Photosensitizing properties of bacteriochlorophyllin a and bacteriochlorin a, two derivatives of bacteriochlorophyll a. *Photochemistry and Photobiology* **1987**, *46* (5), 639-643.
- (26) Sauer, K. Photosynthesis-the light reactions. *Annual Review of Physical Chemistry* **1979**, *30* (1), 155-178.
- (27) Shao, S.; Rajendiran, V.; Lovell, J. F. Metalloporphyrin nanoparticles: Coordinating diverse theranostic functions. *Coordination chemistry reviews* **2019**, *379*, 99-120.
- (28) Färber, G.; Keller, W.; Kratky, C.; Jaun, B.; Pfaltz, A.; Spinner, C.; Kobelt, A.; Eschenmoser, A. Coenzyme F430 from methanogenic bacteria: Complete assignment of configuration based on an X-ray analysis of 12, 13-diepi-F430 pentamethyl ester and on NMR spectroscopy. *Helvetica chimica acta* **1991**, *74* (4), 697-716. Duin, E. C.; McKee, M. L. A new mechanism for methane production from methyl-coenzyme M reductase as derived from density functional calculations. *The Journal of Physical Chemistry B* **2008**, *112* (8), 2466-2482.
- (29) Amos-Tautua, B. M.; Songca, S. P.; Oluwafemi, O. S. Application of porphyrins in antibacterial photodynamic therapy. *Molecules* **2019**, *24* (13), 2456.
- (30) de la Torre, G.; Bottari, G.; Sekita, M.; Hausmann, A.; Guldi, D. M.; Torres, T. A voyage into the synthesis and photophysics of homo- and heterobinuclear ensembles of phthalocyanines and porphyrins. *Chemical Society Reviews* **2013**, *42* (20), 8049-8105. Li, L.-L.; Diao, E. W.-G. Porphyrin-sensitized solar cells. *Chemical society reviews* **2013**, *42* (1), 291-304.
- (31) Koifman, O.; Ageeva, T. Main Strategies for the Synthesis of meso-Arylporphyrins. *Russian Journal of Organic Chemistry* **2022**, *58* (4), 443-479.

- (32) Rothemund, P. A new porphyrin synthesis. The synthesis of porphin. *Journal of the American Chemical Society* **1936**, *58* (4), 625-627.
- (33) Senge, M. O.; Runge, S.; Speck, M.; Ruhlandt-Senge, K. Identification of stable porphomethenes and porphodimethenes from the reaction of sterically hindered aldehydes with pyrrole. *Tetrahedron* **2000**, *56* (45), 8927-8932.
- (34) Rothemund, P. Formation of porphyrins from pyrrole and aldehydes. *Journal of the American Chemical Society* **1935**, *57* (10), 2010-2011.
- (35) Adler, A. D.; Longo, F. R.; Shergalis, W. Mechanistic investigations of porphyrin syntheses. I. Preliminary studies on meso-tetraphenylporphin. *Journal of the American Chemical Society* **1964**, *86* (15), 3145-3149.
- (36) Adler, A. D.; Longo, F. R.; Finarelli, J. D.; Goldmacher, J.; Assour, J.; Korsakoff, L. A simplified synthesis for meso-tetraphenylporphine. *The Journal of Organic Chemistry* **1967**, *32* (2), 476-476.
- (37) Dolphin, D. Porphyrinogens and porphodimethenes, intermediates in the synthesis of meso-tetraphenylporphins from pyrroles and benzaldehyde. *Journal of Heterocyclic Chemistry* **1970**, *7* (2), 275-283.
- (38) Calvin, M.; Ball, R.; Aronoff, S. α , β , γ , δ -Tetraphenylchlorin. *Journal of the American Chemical Society* **1943**, *65* (11), 2259-2259. Drain, C. Synthesis of meso substituted porphyrins in air without solvents or catalysts. *Chemical Communications* **1997**, (21), 2117-2118.
- (39) Semeikin, A.; Koifman, O.; Berezin, B. Synthesis of tetraphenylporphins with active groups in the phenyl rings. 1. Preparation of tetrakis (4-aminophenyl) porphin. *Chemistry of heterocyclic compounds* **1982**, *18* (10), 1046-1047. Semeikin, A.; Koifman, O.; Berezin, B.; Syrbu, S. Synthesis of tetraphenylporphins with active groups in the phenyl rings. 2. Preparation of tetrakis (hydroxyphenyl) porphins. *Chemistry of Heterocyclic Compounds* **1983**, *19*, 1082-1083. Semeikin, A.; Koifman, O.; Berezin, B. Improved method for synthesis of substituted tetraphenylporphins. *Chemistry of Heterocyclic Compounds* **1986**, *22* (6), 629-632.
- (40) Semeikin, A.; Kuzmin, N.; Koifman, O. Appl. Chem. of the. *USSR* **1988**, (61), 1426.
- (41) Gonsalves, A. d. A. R.; Varejão, J. M.; Pereira, M. M. Some new aspects related to the synthesis of meso-substituted porphyrins. *Journal of heterocyclic chemistry* **1991**, *28* (3), 635-640. Gonsalves, A. d. A. R.; Pereira, M. M. A new look into the rothemund meso-tetraalkyl and tetraarylporphyrin synthesis. *Journal of heterocyclic chemistry* **1985**, *22* (3), 931-933.
- (42) Johnstone, R. A.; Nunes, M. L. P.; Pereira, M. M.; Gonsalves, A. M. d. A. R.; Serra, A. C. Improved syntheses of 5, 10, 15, 20-tetrakisaryl- and tetrakisalkylporphyrins. *Heterocycles* **1996**, *7* (43), 1423-1437.
- (43) Pinto, S. M.; Vinagreiro, C. S.; Tomé, V. A.; Piccirillo, G.; Damas, L.; Pereira, M. M. Nitrobenzene method: A keystone in meso-substituted halogenated porphyrin synthesis and applications. *Journal of Porphyrins and Phthalocyanines* **2019**, *23* (04n05), 329-346.
- (44) Lindsey, J. S.; MacCrum, K. A.; Tyhonas, J. S.; Chuang, Y. Y. Investigation of a synthesis of meso-porphyrins employing high concentration conditions and an electron transport chain for aerobic oxidation. *The Journal of organic chemistry* **1994**, *59* (3), 579-587.
- (45) Lindsey, J. S.; Schreiman, I. C.; Hsu, H. C.; Kearney, P. C.; Marguerettaz, A. M. Rothemund and Adler-Longo reactions revisited: synthesis of tetraphenylporphyrins under equilibrium conditions. *The Journal of Organic Chemistry* **1987**, *52* (5), 827-836.
- (46) Lindsey, J. S. Synthetic routes to meso-patterned porphyrins. *Accounts of chemical research* **2010**, *43* (2), 300-311.

- (47) Lindsey, J. S.; Hsu, H. C.; Schreiman, I. C. Synthesis of tetraphenylporphyrins under very mild conditions. *Tetrahedron letters* **1986**, *27* (41), 4969-4970.
- (48) Senge, M. O. Stirring the porphyrin alphabet soup—functionalization reactions for porphyrins. *Chemical Communications* **2011**, *47* (7), 1943-1960.
- (49) Senge, M. O.; Shaker, Y. M.; Pintea, M.; Ryppa, C.; Hatscher, S. S.; Ryan, A.; Sergeeva, Y. Synthesis of meso-Substituted ABCD-Type Porphyrins by Functionalization Reactions. Wiley Online Library: 2010.
- (50) Laha, J. K.; Dhanalekshmi, S.; Taniguchi, M.; Ambroise, A.; Lindsey, J. S. A scalable synthesis of meso-substituted dipyrromethanes. *Organic process research & development* **2003**, *7* (6), 799-812.
- (51) Zaidi, S. H. H.; Loewe, R. S.; Clark, B. A.; Jacob, M. J.; Lindsey, J. S. Nearly chromatography-free synthesis of the A3B-porphyrin 5-(4-hydroxymethylphenyl)-10, 15, 20-tri-p-tolylporphyrinatozinc (II). *Organic process research & development* **2006**, *10* (2), 304-314.
- (52) Arsenault, G.; Bullock, E.; MacDonald, S. Pyrromethanes and porphyrins therefrom¹. *Journal of the American Chemical Society* **1960**, *82* (16), 4384-4389.
- (53) Smith, K. M. Development of porphyrin syntheses. *New Journal of Chemistry* **2016**, *40* (7), 5644-5649.
- (54) Rao, P. D.; Dhanalekshmi, S.; Littler, B. J.; Lindsey, J. S. Rational syntheses of porphyrins bearing up to four different meso substituents. *The Journal of organic chemistry* **2000**, *65* (22), 7323-7344.
- (55) Littler, B. J.; Ciringh, Y.; Lindsey, J. S. Investigation of conditions giving minimal scrambling in the synthesis of trans-porphyrins from dipyrromethanes and aldehydes. *The Journal of Organic Chemistry* **1999**, *64* (8), 2864-2872.
- (56) Lee, C.-H.; Li, F.; Iwamoto, K.; Dadok, J.; Bothner-By, A. A.; Lindsey, J. S. Synthetic approaches to regioisomerically pure porphyrins bearing four different meso-substituents. *Tetrahedron* **1995**, *51* (43), 11645-11672.
- (57) Kooriyaden, F. R.; Sujatha, S.; Arunkumar, C. Study of scrambling in porphyrin forming reactions: Synthesis, structure, photophysical, electrochemical and antimicrobial studies. *Polyhedron* **2017**, *128*, 85-94.
- (58) Cammidge, A. N.; Öztürk, O. Controlled scrambling in porphyrin synthesis—selective synthesis of 5, 10-disubstituted porphyrins. *Tetrahedron Letters* **2001**, *42* (2), 355-358.
- (59) Hölzel, H.; Muth, M.; Lungerich, D.; Jux, N. Addressing Environmental Challenges of Porphyrin Mixtures Obtained from Statistical Syntheses. *Chemistry-Methods* **2021**, *1* (3), 142-147.
- (60) Tu, B.; Ghosh, B.; Lightner, D. A. Novel linear tetrapyrroles: hydrogen bonding in diacetylenic bilirubins. *Monatshefte für Chemie/Chemical Monthly* **2004**, *135*, 519-541.
- (61) Sessler, J. L.; Johnson, M. R.; Lynch, V. Synthesis and crystal structure of a novel tripyrrane-containing porphyrinogen-like macrocycle. *The Journal of Organic Chemistry* **1987**, *52* (19), 4394-4397.
- Grössl, D. M.; Hafner, A. V.; Fischer, R. C.; Saf, R.; Torvisco, A.; Uhlig, F. Bis (chlorido) tin (IV) meso-substituted Porphyrins-Characterization and Solubility. *European Journal of Inorganic Chemistry* **2023**, *26* (28), e202300286.
- Boëns, B.; Faugeras, P.-A.; Vergnaud, J.; Lucas, R.; Teste, K.; Zerrouki, R. Iodine-catalyzed one-pot synthesis of unsymmetrical meso-substituted porphyrins. *Tetrahedron* **2010**, *66* (11), 1994-1996.
- Mondal, S.; Sahu, K.; Patra, B.; Jena, S.; Biswal, H. S.; Kar, S. A new synthesis of porphyrins via a putative trans-manganese (iv)-dihydroxide intermediate. *Dalton Transactions* **2020**, *49* (5), 1424-1432.
- Mondal, S.; Pain, T.; Sahu, K.; Kar, S. Large-scale green synthesis of porphyrins. *ACS omega* **2021**, *6* (35), 22922-22936.
- (62) Linstead, R. 212. Phthalocyanines. Part I. A new type of synthetic colouring matters. *Journal of the Chemical Society (Resumed)* **1934**, 1016-1017.

- (63) Linstead, R.; Lowe, A. 216. Phthalocyanines. Part V. The molecular weight of magnesium phthalocyanine. *Journal of the Chemical Society (Resumed)* **1934**, 1031-1033.
- (64) Nemykin, V.; Dudkin, S.; Dumoulin, F.; Hirel, C.; Gurek, A.; Ahsen, V. Synthetic approaches to asymmetric phthalocyanines and their analogues. *Arkivoc* **2014**.
- (65) TAŞKIRAN, D. T.; ŞAHİN, Z.; İŞÇİ, Ü.; İŞÇİ, F. D. Phthalocyanines prepared from 4, 5-dihexylthiophthalonitrile, a popular building block. *Turkish Journal of Chemistry* **2023**, 47 (5), 814-836.
- (66) Dumoulin, F.; Zorlu, Y.; Menaf Ayhan, M.; Hirel, C.; Isci, Ü.; Ahsen, V. A first ABAC phthalocyanine. *Journal of Porphyrins and Phthalocyanines* **2009**, 13 (01), 161-165.
- (67) Chow, S. Y.; Ng, D. K. Synthesis of an ABCD-type phthalocyanine by intramolecular cyclization reaction. *Organic letters* **2016**, 18 (13), 3234-3237.
- (68) Zhang, L.; Zhao, Y.-Y.; Chen, Z.-X.; Cheng, Y.-T.; Zheng, B.-Y.; Ke, M.-R.; Li, X.; Huang, J.-D. Synthesis, characterization and photodynamic antitumor activity of amine-modified zinc (II) phthalocyanines. *Dyes and Pigments* **2023**, 111490.
- (69) Güzel, E.; Medina, D.-P.; Medel, M.; Kandaz, M.; Torres, T.; Rodríguez-Morgade, M. S. A versatile, divergent route for the synthesis of ABAC tetraazaporphyrins: molecularly engineered, push-pull phthalocyanine-type dyes. *Journal of Materials Chemistry C* **2021**, 9 (33), 10802-10810.
- (70) Urbani, M.; Ragoussi, M.-E.; Nazeeruddin, M. K.; Torres, T. Phthalocyanines for dye-sensitized solar cells. *Coordination Chemistry Reviews* **2019**, 381, 1-64.
- (71) Seikel, E.; Oelkers, B.; Sundermeyer, J. r. Axial functionalization of sterically hindered titanium phthalocyanines. *Inorganic chemistry* **2012**, 51 (4), 2709-2717.
- (72) Liebold, M.; Sharikow, E.; Seikel, E.; Trombach, L.; Harms, K.; Zimčík, P.; Nováková, V.; Tonner, R.; Sundermeyer, J. Experimental and Computational Study of Isomerically Pure Soluble Azaphthalocyanines and Azasubphthalocyanines of Varying Number of Aza Units. *arXiv preprint arXiv:1612.01332* **2016**.
- (73) McKeown, N. B. *Phthalocyanine materials: synthesis, structure and function*; Cambridge university press, 1998. Leznoff, C.; Lever, A. Properties and Applications. *VCH New York* **1989**. Louati, A.; El Meray, M.; Andre, J.; Simon, J.; Kadish, K. M.; Gross, M.; Giraudeau, A. Electrochemical reduction of new, good electron acceptors: the metalloctacyanophthalocyanines. *Inorganic Chemistry* **1985**, 24 (8), 1175-1179.
- (74) Kharisov, B.; Ortiz Mendez, U.; Rivera de la Rosa, J. Low-temperature synthesis of phthalocyanine and its metal complexes. *Russian Journal of Coordination Chemistry* **2006**, 32, 617-631.
- (75) Sakamoto, K.; Ohno-Okumura, E. Syntheses and functional properties of phthalocyanines. *Materials* **2009**, 2 (3), 1127-1179.
- (76) Barrett, P.; Linstead, R.; Tuey, G.; Robertson, J. 371. Phthalocyanines and related compounds. Part XV. Tetrabenztriazaporphin: its preparation from phthalonitrile and a proof of its structure. With a note on a preliminary X-ray investigation. *Journal of the Chemical Society (Resumed)* **1939**, 1809-1820.
- (77) Braun, A.; Tcherniac, J. The products of the action of acetic-anhydride on phthalamide. *Ber. Dtsch. Chem. Ges* **1907**, 40 (2), 2709-2714.
- (78) Byrne, G.; Linstead, R.; Lowe, A. 213. Phthalocyanines. Part II. The preparation of phthalocyanine and some metallic derivatives from o-cyanobenzamide and phthalimide. *Journal of the Chemical Society (Resumed)* **1934**, 1017-1022.
- (79) Watt, G.; Dawes, J. Copper (0) phthalocyanine. *Journal of Inorganic and Nuclear Chemistry* **1960**, 14 (1-2), 32-34.

- (80) Alessio, P.; Rodríguez-Méndez, M. L.; Saez, J. A. D. S.; Constantino, C. J. L. Iron phthalocyanine in non-aqueous medium forming layer-by-layer films: growth mechanism, molecular architecture and applications. *Physical Chemistry Chemical Physics* **2010**, *12* (16), 3972-3983.
- (81) Garland, A. D.; Chambrier, I.; Cammidge, A. N.; Cook, M. J. Design and synthesis of liquid crystalline phthalocyanines: combinations of substituents that promote the discotic nematic mesophase. *Tetrahedron* **2015**, *71* (39), 7310-7314. Cammidge, A. N.; Cook, M. J.; Harrison, K. J.; McKeown, N. B. Synthesis and characterisation of some 1, 4, 8, 11, 15, 18, 22, 25-octa (alkoxymethyl) phthalocyanines; a new series of discotic liquid crystals. *Journal of the Chemical Society, Perkin Transactions 1* **1991**, (12), 3053-3058.
- (82) Lu, H.; Kobayashi, N. Optically active porphyrin and phthalocyanine systems. *Chemical reviews* **2016**, *116* (10), 6184-6261.
- (83) Nemykin, V. N.; Lukyanets, E. A. Synthesis of substituted phthalocyanines. *ARKIVOC: Online Journal of Organic Chemistry* **2010**.
- (84) Demirbaş, Ü.; Pişkin, M.; Durmuş, M.; Kantekin, H. Metal or metal-free phthalocyanines containing morpholine substituents: synthesis, spectroscopic and photophysical properties. *Journal of Coordination Chemistry* **2022**, *75* (9-10), 1243-1255. Pekbelgin Karaoğlu, H.; Kalkan Burat, A. α - and β -substituted metal-free phthalocyanines: synthesis, photophysical and electrochemical properties. *Molecules* **2020**, *25* (2), 363. Barard, S.; Mukherjee, D.; Sarkar, S.; Kreouzis, T.; Chambrier, I.; Cammidge, A. N.; Ray, A. K. Channel length-dependent characterisations of organic thin-film transistors with solution processable gadolinium phthalocyanine derivatives. *Journal of Materials Science: Materials in Electronics* **2020**, *31* (1), 265-273. García-Iglesias, M.; Torres, T.; González-Rodríguez, D. Well-defined, persistent, chiral phthalocyanine nanoclusters via G-quadruplex assembly. *Chemical Communications* **2016**, *52* (60), 9446-9449.
- (85) Rio, Y.; Rodríguez-Morgade, M. S.; Torres, T. Modulating the electronic properties of porphyrinoids: a voyage from the violet to the infrared regions of the electromagnetic spectrum. *Organic & biomolecular chemistry* **2008**, *6* (11), 1877-1894.
- (86) Knör, G.; Strasser, A. Enhanced photoreactivity of zirconium (IV) and hafnium (IV) porphyrin complexes promoted by water molecules. *Inorganic Chemistry Communications* **2005**, *8* (5), 471-473.
- (87) Josefsen, L. B.; Boyle, R. W. Unique diagnostic and therapeutic roles of porphyrins and phthalocyanines in photodynamic therapy, imaging and theranostics. *Theranostics* **2012**, *2* (9), 916.
- (88) Yaraşır, M. N.; Kandaz, M.; Koca, A.; Salih, B. Functional alcohol-soluble double-decker phthalocyanines: synthesis, characterization, electrochemistry and peripheral metal ion binding. *Journal of Porphyrins and Phthalocyanines* **2006**, *10* (08), 1022-1033.
- (89) Chen, Y.; Dini, D.; Hanack, M.; Fujitsuka, M.; Ito, O. Excited state properties of monomeric and dimeric axially bridged indium phthalocyanines upon UV-Vis laser irradiation. *Chemical communications* **2004**, (3), 340-341.
- (90) Casiraghi, G.; Cornia, M.; Zanardi, F.; Rassa, G.; Ragg, E.; Bortolini, R. Synthesis and characterization of porphyrin-sugar carbon conjugates. *The Journal of Organic Chemistry* **1994**, *59* (7), 1801-1808.
- (91) Nasri, H. Porphyrins and metalloporphyrins: an overview. In *2020 IEEE International Conference on Design & Test of Integrated Micro & Nano-Systems (DTS)*, 2020; IEEE: pp 1-6.
- (92) Biesaga, M.; Pyrzyńska, K.; Trojanowicz, M. Porphyrins in analytical chemistry. A review. *Talanta* **2000**, *51* (2), 209-224.

- (93) Ahmed, M. S.; Srivishnu, K. S.; Biswas, C.; Banerjee, D.; Chetti, P.; Soma, V. R.; Giribabu, L.; Raavi, S. S. K. Novel metallated imidazole phthalocyanines: synthesis, ultrafast excited-state carrier dynamics and multiphoton absorption properties. *Materials Advances* **2023**, *4* (16), 3532-3550.
- (94) Horváth, O.; Huszánk, R.; Valicsek, Z.; Lendvay, G. Photophysics and photochemistry of kinetically labile, water-soluble porphyrin complexes. *Coordination chemistry reviews* **2006**, *250* (13-14), 1792-1803.
- (95) Tanaka, T.; Osuka, A. Conjugated porphyrin arrays: synthesis, properties and applications for functional materials. *Chemical Society Reviews* **2015**, *44* (4), 943-969.
- (96) Osuka, A.; Shimidzu, H. meso, meso-Linked porphyrin arrays. *Angewandte Chemie International Edition in English* **1997**, *36* (1-2), 135-137.
- (97) Miller, M. A.; Lammi, R. K.; Prathapan, S.; Holten, D.; Lindsey, J. S. A tightly coupled linear array of perylene, bis (porphyrin), and phthalocyanine units that functions as a photoinduced energy-transfer cascade. *The Journal of Organic Chemistry* **2000**, *65* (20), 6634-6649.
- (98) Makarov, S. G.; Suvorova, O. N.; Litwinski, C.; Ermilov, E. A.; Röder, B.; Tsaryova, O.; Dülcks, T.; Wöhrle, D. Linear and rectangular trinuclear phthalocyanines. Wiley Online Library: 2007.
- (99) Okada, S.; Segawa, H. Substituent-control exciton in J-aggregates of protonated water-insoluble porphyrins. *Journal of the American Chemical Society* **2003**, *125* (9), 2792-2796.
- (100) Aratani, N.; Kim, D.; Osuka, A. Discrete cyclic porphyrin arrays as artificial light-harvesting antenna. *Accounts of Chemical Research* **2009**, *42* (12), 1922-1934.
- (101) Li, X.; Nomura, K.; Guedes, A.; Goto, T.; Sekino, T.; Fujitsuka, M.; Osakada, Y. Enhanced photocatalytic activity of porphyrin nanodisks prepared by exfoliation of metalloporphyrin-based covalent organic frameworks. *ACS omega* **2022**, *7* (8), 7172-7178.
- (102) Yang, X.; Li, X.; Liu, M.; Yang, S.; Niu, Q.; Zhai, L.; Jiang, Z.; Xu, Q.; Zeng, G. Modulating Electrochemical CO₂ Reduction Performance via Sulfur-Containing Linkages Engineering in Metallophthalocyanine Based Covalent Organic Frameworks. *ACS Materials Letters* **2023**, *5* (6), 1611-1618.
- (103) Penon, O.; Marín, M. J.; Russell, D. A.; Pérez-García, L. Water soluble, multifunctional antibody-porphyrin gold nanoparticles for targeted photodynamic therapy. *Journal of colloid and interface science* **2017**, *496*, 100-110.
- (104) Han, J.; Liu, Y.; Peng, D.; Liu, J.; Wu, D. Biomedical application of porphyrin-based amphiphiles and their self-assembled nanomaterials. *Bioconjugate Chemistry* **2023**, *34* (12), 2155-2180.
- (105) Goddard, Z. R.; Marín, M. J.; Russell, D. A.; Searcey, M. Active targeting of gold nanoparticles as cancer therapeutics. *Chemical Society Reviews* **2020**, *49* (23), 8774-8789.
- (106) Alea-Reyes, M. E.; Penon, O.; Calavia, P. G.; Marín, M. J.; Russell, D. A.; Pérez-García, L. Synthesis and in vitro phototoxicity of multifunctional Zn (II) meso-tetrakis (4-carboxyphenyl) porphyrin-coated gold nanoparticles assembled via axial coordination with imidazole ligands. *Journal of colloid and interface science* **2018**, *521*, 81-90.
- (107) Camerin, M.; Moreno, M.; Marín, M. J.; Schofield, C. L.; Chambrier, I.; Cook, M. J.; Coppellotti, O.; Jori, G.; Russell, D. A. Delivery of a hydrophobic phthalocyanine photosensitizer using PEGylated gold nanoparticle conjugates for the in vivo photodynamic therapy of amelanotic melanoma. *Photochemical & Photobiological Sciences* **2016**, *15* (5), 618-625.
- (108) Penon, O.; Patiño, T.; Barrios, L.; Nogues, C.; Amabilino, D. B.; Wurst, K.; Pérez-García, L. A New Porphyrin for the Preparation of Functionalized Water-Soluble Gold Nanoparticles with Low Intrinsic Toxicity. *ChemistryOpen* **2015**, *4* (2), 127-136.

- (109) Martynov, A. G.; Horii, Y.; Katoh, K.; Bian, Y.; Jiang, J.; Yamashita, M.; Gorbunova, Y. G. Rare-earth based tetrapyrrolic sandwiches: chemistry, materials and applications. *Chemical Society Reviews* **2022**, *51*, 9262-9339
- (110) Turek, P.; Petit, P.; Andre, J.; Simon, J.; Even, R.; Boudjema, B.; Guillaud, G.; Maitrot, M. A new series of molecular semiconductors: phthalocyanine radicals. *Journal of the American Chemical Society* **1987**, *109* (17), 5119-5122.
- (111) Qi, D.; Jiang, J. Nature of the Intense Second-Order Nonlinear Optical Activity: DFT Studies on the Octupolarization of Sandwich-Type Bis (phthalocyaninato) Yttrium Skeletons. *ChemPhysChem* **2015**, *16* (9), 1889-1897.
- (112) Tang, X.; Liu, Q.; Wei, C.; Lv, X.; Jin, Z.; Chen, Y.; Jiang, J. Advances in gas sensors of tetrapyrrolo-rare earth sandwich-type complexes—Commemorating the 100th anniversary of the birth of Academician Guangxian Xu. *Journal of Rare Earths* **2021**, *39* (2), 113-120.
- (113) Wang, H.; Wang, B.-W.; Bian, Y.; Gao, S.; Jiang, J. Single-molecule magnetism of tetrapyrrole lanthanide compounds with sandwich multiple-decker structures. *Coordination Chemistry Reviews* **2016**, *306*, 195-216.
- (114) Martynov, A. G.; Sinelshchikova, A. A.; Dorovatovskii, P. V.; Polovkova, M. A.; Ovchenkova, A. E.; Birin, K. P.; Kirakosyan, G. A.; Gorbunova, Y. G.; Tsivadze, A. Y. Solvation-Induced Conformational Switching of Trisphthalocyanates for Control of Their Magnetic Properties. *Inorganic Chemistry* **2023**.
- (115) Parreiras, S. O.; Gallego, J. M.; Écija, D. Lanthanide-directed metal–organic coordination networks. *Chemical Communications* **2023**, *59* (58), 8878-8893.
- (116) Sessoli, R.; Gatteschi, D.; Caneschi, A.; Novak, M. Magnetic bistability in a metal-ion cluster. *Nature* **1993**, *365* (6442), 141-143. Ishikawa, N.; Sugita, M.; Ishikawa, T.; Koshihara, S.-y.; Kaizu, Y. Lanthanide double-decker complexes functioning as magnets at the single-molecular level. *Journal of the American Chemical Society* **2003**, *125* (29), 8694-8695.
- (117) Niranjana, R.; Rudraswamy, B.; Dhananjaya, N. Effective atomic number, electron density and kerma of gamma radiation for oxides of lanthanides. *Pramana* **2012**, *78*, 451-458.
- (118) Ishikawa, N.; Iino, T.; Kaizu, Y. Interaction between f-electronic systems in dinuclear lanthanide complexes with phthalocyanines. *Journal of the American Chemical Society* **2002**, *124* (38), 11440-11447.
- (119) Sairenji, S.; Akine, S.; Nabeshima, T. Lanthanide contraction for helicity fine-tuning and helix-winding control of single-helical metal complexes. *Dalton Transactions* **2016**, *45* (38), 14902-14906.
- (120) Cirera, B.; Matarrubia, J.; Kaposi, T.; Giménez-Agulló, N.; Paszkiewicz, M.; Klappenberger, F.; Otero, R.; Gallego, J. M.; Ballester, P.; Barth, J. Preservation of electronic properties of double-decker complexes on metallic supports. *Physical Chemistry Chemical Physics* **2017**, *19* (12), 8282-8287. Guo, F. S.; Day, B. M.; Chen, Y. C.; Tong, M. L.; Mansikkamäki, A.; Layfield, R. A. A dysprosium metallocene single-molecule magnet functioning at the axial limit. *Angewandte Chemie International Edition* **2017**, *56* (38), 11445-11449. Goodwin, C. A.; Ortu, F.; Reta, D.; Chilton, N. F.; Mills, D. P. Molecular magnetic hysteresis at 60 kelvin in dysprosocenium. *Nature* **2017**, *548* (7668), 439-442.
- (121) Zabala-Lekuona, A.; Seco, J. M.; Colacio, E. Single-Molecule Magnets: From Mn₁₂-ac to dysprosium metallocenes, a travel in time. *Coordination Chemistry Reviews* **2021**, *441*, 213984. Frost, J. M.; Harriman, K. L.; Murugesu, M. The rise of 3-d single-ion magnets in molecular magnetism: towards materials from molecules? *Chemical science* **2016**, *7* (4), 2470-2491.
- (122) Gashigullin, R.; Kendin, M.; Martynova, I.; Tsybarenko, D. Diverse Coordination Chemistry of the Whole Series Rare-Earth L-Lactates: Synthetic Features, Crystal Structure, and Application in Chemical Solution Deposition of Ln₂O₃ Thin Films. *Molecules* **2023**, *28* (15), 5896.

- (123) Prashasti. *Spin Magnetic Moment: Dose an Electron Really Spin?* PhysicsForums, 2014. <https://www.physicsforums.com/threads/spin-magnetic-moment-does-an-electron-really-spin.773970/> (accessed 2024).
- (124) Chabach, D.; De Cian, A.; Fischer, J.; Weiss, R.; El Malouli-Bibout, M. Heteronucleare Tripeldeckerkomplexe mit dem Ligandensystem Porphyrin/Phthalocyanin/Porphyrin. *Angewandte Chemie* **1996**, *108* (8), 942-944.
- (125) Chabach, D.; De Cian, A.; Fischer, J.; Weiss, R.; Bibout, M. E. M. Mixed-Metal Triple-Decker Sandwich Complexes with the Porphyrin/Phthalocyanine/Porphyrin Ligand System. *Angewandte Chemie International Edition in English* **1996**, *35* (8), 898-899.
- (126) Zhang, P.; Guo, Y.-N.; Tang, J. Recent advances in dysprosium-based single molecule magnets: Structural overview and synthetic strategies. *Coordination Chemistry Reviews* **2013**, *257* (11-12), 1728-1763.
- (127) Imahori, H. Giant multiporphyrin arrays as artificial light-harvesting antennas. *The Journal of Physical Chemistry B* **2004**, *108* (20), 6130-6143. Lu, G.; Li, J.; Yan, S.; Zhu, W.; Ou, Z.; Kadish, K. M. Synthesis and characterization of rare earth corrole-phthalocyanine heteroleptic triple-decker complexes. *Inorganic Chemistry* **2015**, *54* (12), 5795-5805. Guilard, R.; Barbe, J.-M.; Ibnfassi, A.; Zrineh, A.; Adamian, V. A.; Kadish, K. M. Synthesis, Characterization, and Electrochemistry of Heteroleptic Double-Decker Complexes of the Type Phthalocyaninato-Porphyrinato-Zirconium (IV) or-Hafnium (IV). *Inorganic Chemistry* **1995**, *34* (6), 1472-1481.
- (128) Birin, K. P.; Gorbunova, Y. G.; Tsvadze, A. Y. Efficient scrambling-free synthesis of heteroleptic terbium triple-decker (porphyrinato)(crown-phthalocyaninates). *Dalton Transactions* **2012**, *41* (32), 9672-9681.
- (129) Jiang, J.; Ng, D. K. A decade journey in the chemistry of sandwich-type tetrapyrrolo-rare earth complexes. *Accounts of chemical research* **2009**, *42* (1), 79-88.
- (130) Mironov, A. F. Porphyrin complexes with lanthanides. *Uspekhi Khimii* **2013**, *82* (4), 333-351. Jiang, J.; Liu, R. C.; Mak, T. C.; Chan, T. D.; Ng, D. K. Synthesis, spectroscopic and electrochemical properties of substituted bis (phthalocyaninato) lanthanide (III) complexes. *Polyhedron* **1997**, *16* (3), 515-520.
- (131) Jiang, J.; Bian, Y.; Furuya, F.; Liu, W.; Choi, M. T.; Kobayashi, N.; Li, H. W.; Yang, Q.; Mak, T. C.; Ng, D. K. Synthesis, Structure, Spectroscopic Properties, and Electrochemistry of Rare Earth Sandwich Compounds with Mixed 2, 3-Naphthalocyaninato and Octaethylporphyrinato Ligands. *Chemistry—A European Journal* **2001**, *7* (23), 5059-5069.
- (132) Wang, H.; Wang, K.; Bian, Y.; Jiang, J.; Kobayashi, N. Mixed (phthalocyaninato)(porphyrinato) heterometal complexes with sandwich quadruple-decker molecular structure. *Chemical communications* **2011**, *47* (24), 6879-6881.
- (133) Pushkarev, V. E. e.; Tomilova, L. G.; Tomilov, Y. V. Synthetic approaches to lanthanide complexes with tetrapyrrole type ligands. *Russian Chemical Reviews* **2008**, *77* (10), 875.
- (134) Kirin, I. Formation of unusual phthalocyanines of the rare-earth elements. *Russ. J. Inorg. Chem.* **1965**, *10*, 1065-1066.
- (135) Kirin, I.; Moskalev, P.; Moskashev, Y. A. New complex compounds of phthalocyanine with rare earth elements. *Zhurnal Neorganicheskoi Khimii* **1967**, *12*, 707-712.
- (136) Zhang, J.-X.; Chan, W.-L.; Xie, C.; Zhou, Y.; Chau, H.-F.; Maity, P.; Harrison, G. T.; Amassian, A.; Mohammed, O. F.; Tanner, P. A. Impressive near-infrared brightness and singlet oxygen generation from strategic lanthanide-porphyrin double-decker complexes in aqueous solution. *Light: Science & Applications* **2019**, *8* (1), 46.

- (137) Erzunov, D. A.; Bontar, A. A.; Futerman, N. A.; Vashurin, A. S.; Pukhovskaya, S. G. A simple way to obtain stable mono-decker porphyrin complexes with heavy metal atoms. *Inorganic and Nano-Metal Chemistry* **2022**, *52* (2), 181-184.
- (138) Kuzmina, E. A.; Dubinina, T. V.; Borisova, N. E.; Tarasevich, B. N.; Krasovskii, V. I.; Feofanov, I. N.; Dzuban, A. V.; Tomilova, L. G. Planar and sandwich-type Pr (III) and Nd (III) chlorinated phthalocyaninates: Synthesis, thermal stability and optical properties. *Dyes and Pigments* **2020**, *174*, 108075.
- (139) Wang, H.; Kobayashi, N.; Jiang, J. New Sandwich-Type Phthalocyaninato–Metal Quintuple-Decker Complexes. *Chemistry–A European Journal* **2012**, *18* (4), 1047-1049.
- (140) Chen, X.; Qi, D.; Liu, C.; Wang, H.; Xie, Z.; Chen, T.-W.; Chen, S.-M.; Tseng, T.-W.; Jiang, J. Elucidating π – π interaction-induced extension effect in sandwich phthalocyaninato compounds. *RSC advances* **2020**, *10* (1), 317-322.
- (141) Ng, D. K.; Jiang, J. Sandwich-type heteroleptic phthalocyaninato and porphyrinato metal complexes. *Chemical Society Reviews* **1997**, *26* (6), 433-442.
- (142) Wang, W.; Bao, G.; Mao, Y.; Lu, F. Infrared spectroscopic characteristics of mixed rare earth triple-decker complexes with phthalocyaninato and 5-(4-hydroxyphenyl)-10, 15, 20-tris (4-octyloxy) porphyrinato ligands. *Spectrochimica Acta Part A: Molecular and Biomolecular Spectroscopy* **2013**, *104*, 165-170.
- (143) Abdullah, K.; Chen, Y.; Jiang, J. Synthesis, fabrication of self-assembled film and ambipolar chemical sensing properties of triple-decker (phthalocyaninato)(porphyrinato) europium complex. *Journal of Porphyrins and Phthalocyanines* **2017**, *21* (12), 893-899.
- (144) Moussavi, M.; De Cian, A.; Fischer, J.; Weiss, R. (Porphyrinato) bis (phthalocyaninato) dilanthanide (III) complexes presenting a sandwich triple-decker-like structure. *Inorganic Chemistry* **1986**, *25* (13), 2107-2108.
- (145) Bian, Y.; Wang, R.; Jiang, J.; Lee, C.-H.; Wang, J.; Ng, D. K. Synthesis, spectroscopic characterisation and structure of the first chiral heteroleptic bis (phthalocyaninato) rare earth complexes. *Chemical communications* **2003**, (10), 1194-1195.
- (146) Martynov, A. G.; Birin, K. P.; Kirakosyan, G. A.; Gorbunova, Y. G.; Tsivadze, A. Y. Site-Selective Solvation-Induced Conformational Switching of Heteroleptic Heteronuclear Tb (III) and Y (III) Trisphthalocyaninates for the Control of Their Magnetic Anisotropy. *Molecules* **2023**, *28* (11), 4474.
- (147) Suryadevara, N.; Boudalis, A. K.; Olivares Peña, J. E.; Moreno-Pineda, E.; Fediai, A.; Wenzel, W.; Turek, P.; Ruben, M. Molecular-Engineered Biradicals Based on the YIII-Phthalocyanine Platform. *Journal of the American Chemical Society* **2023**, *145* (4), 2461-2472.
- (148) Birin, K. P.; Gorbunova, Y. G.; Tsivadze, A. Y. Selective one-step synthesis of triple-decker (porphyrinato)(phthalocyaninato) early lanthanides: the balance of concurrent processes. *Dalton Transactions* **2011**, *40* (43), 11539-11549.
- (149) González-Lucas, D.; Soobrattee, S. C.; Hughes, D. L.; Tizzard, G. J.; Coles, S. J.; Cammidge, A. N. Straightforward and Controlled Synthesis of Porphyrin–Phthalocyanine–Porphyrin Heteroleptic Triple-Decker Assemblies. *Chemistry–A European Journal* **2020**, *26* (47), 10724-10728.
- (150) Liu, C.; Yang, W.; Zhang, Y.; Jiang, J. Quintuple-Decker Heteroleptic Phthalocyanine Heterometallic Samarium–Cadmium Complexes. Synthesis, Crystal Structure, Electrochemical Behavior, and Spectroscopic Investigation. *Inorganic Chemistry* **2020**, *59* (23), 17591-17599.
- (151) Beck, V.; O’Hare, D. Triple-decker transition metal complexes bridged by a single carbocyclic ring. *Journal of organometallic chemistry* **2004**, *689* (24), 3920-3938.

- (152) Lu, J.; Deng, Y.; Zhang, X.; Kobayashi, N.; Jiang, J. Optically active mixed (phthalocyaninato)(porphyrinato) rare earth triple-decker complexes. Synthesis, spectroscopy, and effective chiral information transfer. *Inorganic chemistry* **2011**, *50* (6), 2562-2567.
- (153) Zhang, X.; Muranaka, A.; Lv, W.; Zhang, Y.; Bian, Y.; Jiang, J.; Kobayashi, N. Optically Active Mixed Phthalocyaninato–Porphyrinato Rare-Earth Double-Decker Complexes: Synthesis, Spectroscopy, and Solvent-Dependent Molecular Conformations. *Chemistry—A European Journal* **2008**, *14* (15), 4667-4674. Birin, K. P.; Gorbunova, Y. G.; Tsivadze, A. Y. NMR-based analysis of structure of heteroleptic triple-decker (phthalocyaninato)(porphyrinato) lanthanides in solutions. *Magnetic Resonance in Chemistry* **2010**, *48* (7), 505-515.
- (154) Jin, H.-G.; Jiang, X.; Kühne, I. A.; Clair, S.; Monnier, V.; Chendo, C.; Novitchi, G.; Powell, A. K.; Kadish, K. M.; Balaban, T. S. Microwave-mediated synthesis of bulky lanthanide porphyrin–phthalocyanine triple-deckers: Electrochemical and magnetic properties. *Inorganic Chemistry* **2017**, *56* (9), 4864-4873. Wu, S.; Cao, J. Perovskite modifiers with porphyrin/phthalocyanine complexes for efficient photovoltaics. *Journal of Coordination Chemistry* **2022**, *75* (11-14), 1494-1519.
- (155) Rinck, P. A. *Magnetic resonance in medicine: a critical introduction*; BoD—Books on Demand, 2019.
- (156) Padmaja, K.; Youngblood, W. J.; Wei, L.; Bocian, D. F.; Lindsey, J. S. Triple-decker sandwich compounds bearing compact triallyl tripods for molecular information storage applications. *Inorganic chemistry* **2006**, *45* (14), 5479-5492.
- (157) Jiang, T.; Ou, C.; Wang, L.; Chen, J.; Dmytro, S.; Zhang, Q.; Luo, J.; Wang, H. Electrocatalytic performance of CNTs/graphene composited rare earth phthalocyanines (M= La, Y, Yb, Sc). *Journal of Rare Earths* **2022**.
- (158) Matsuo, Y.; Ogumi, K.; Jeon, I.; Wang, H.; Nakagawa, T. Recent progress in porphyrin-and phthalocyanine-containing perovskite solar cells. *RSC advances* **2020**, *10* (54), 32678-32689.
- (159) Molina, D.; Follana-Berná, J.; Sastre-Santos, Á. Phthalocyanines, porphyrins and other porphyrinoids as components of perovskite solar cells. *Journal of Materials Chemistry C* **2023**, *11* (24), 7885-7919.
- (160) Lu, F.; Sun, X.; Li, R.; Liang, D.; Zhu, P.; Choi, C.-F.; Ng, D. K.; Fukuda, T.; Kobayashi, N.; Bai, M. Synthesis, spectroscopic properties, and electrochemistry of heteroleptic rare earth double-decker complexes with phthalocyaninato and meso-tetrakis (4-chlorophenyl) porphyrinato ligands. *New Journal of Chemistry* **2004**, *28* (9), 1116-1122.
- (161) Kadish, K.; Smith, K. M.; Guilard, R. *The Porphyrin Handbook, Volume 3*; Elsevier, 2000. Little, R. G. The mixed-aldehyde synthesis of difunctional tetraarylporphyrins. *Journal of Heterocyclic Chemistry* **1981**, *18* (1), 129-133. Little, R. G.; Anton, J. A.; Loach, P. A.; Ibers, J. A. The synthesis of some substituted tetraarylporphyrins. *Journal of Heterocyclic Chemistry* **1975**, *12* (2), 343-349.
- (162) Adler, A. D.; Sklar, L.; Longo, F. R.; Finarelli, J. D.; Finarelli, M. G. A Mechanistic Study of the Synthesis of meso-Tetraphenylporphin. *Journal of Heterocyclic Chemistry* **1968**, *5* (5), 669-678.
- (163) Rao, P. D.; Littler, B. J.; Geier, G. R.; Lindsey, J. S. Efficient synthesis of monoacyl dipyrromethanes and their use in the preparation of sterically unhindered trans-porphyrins. *The Journal of Organic Chemistry* **2000**, *65* (4), 1084-1092. Strachan, J.-P.; O'Shea, D. F.; Balasubramanian, T.; Lindsey, J. S. Rational synthesis of meso-substituted chlorin building blocks. *The Journal of organic chemistry* **2000**, *65* (10), 3160-3172.
- (164) Pal, S. K.; Setia, S.; Avinash, B.; Kumar, S. Triphenylene-based discotic liquid crystals: recent advances. *Liquid Crystals* **2013**, *40* (12), 1769-1816.
- (165) Chandrasekhar, S. Discotic liquid crystals. A brief review. *Liquid Crystals* **1993**, *14* (1), 3-14.

- (166) Kumar, S. Recent developments in the chemistry of triphenylene-based discotic liquid crystals. *Liquid Crystals* **2004**, *31* (8), 1037-1059.
- (167) Collings, P. J.; Goodby, J. W. *Introduction to liquid crystals: chemistry and physics*; Crc Press, 2019.
- (168) Pérez, D.; Guitián, E. Selected strategies for the synthesis of triphenylenes. *Chemical Society Reviews* **2004**, *33* (5), 274-283. Cammidge, A. N.; Gopee, H. Structural factors controlling the transition between columnar-hexagonal and helical mesophase in triphenylene liquid crystals. Basis of a presentation given at Materials Discussion No. 4, 11–14 September 2001, Grasmere, UK. *Journal of Materials Chemistry* **2001**, *11* (11), 2773-2783. Boden, N.; Bushby, R. J.; Cammidge, A. N.; Headdock, G. Versatile synthesis of unsymmetrically substituted triphenylenes. *Synthesis* **1995**, *1995* (01), 31-32. Cammidge, A. N.; Lifsey, K. M. A simple synthesis of pyridine-tethered porphyrins. *Tetrahedron Letters* **2000**, *41* (34), 6655-6656. Xiao, W.; He, Z.; Xu, M.; Wu, N.; Kong, X.; Jing, X. A convenient one-step reaction leading to a key discotic intermediate: mono-hydroxy-triphenylene at multi-gram scale. *Tetrahedron Letters* **2015**, *56* (5), 700-705. Cammidge, A. N.; Öztürk, O. Selective Synthesis of meso-Naphthylporphyrins. *The Journal of Organic Chemistry* **2002**, *67* (21), 7457-7464.
- (169) Howard, M. J.; Heitzler, F. R.; Dias, S. I. Synthesis and stereochemistry of long-chain quinoxaline metallocyclophanes. *The Journal of Organic Chemistry* **2008**, *73* (7), 2548-2553.
- (170) Boden, N.; Borner, R.; Brown, D.; Bushby, R.; Clements, J. ESR studies of radical cations produced on doping discotic liquid crystals with Lewis acids. *Liquid Crystals* **1992**, *11* (3), 325-334.
- (171) Xiao, W.; He, Z.; Remiro-Buenamañana, S.; Turner, R. J.; Xu, M.; Yang, X.; Jing, X.; Cammidge, A. N. A π -extended donor-acceptor-donor triphenylene twin linked via a pyrazine bridge. *Organic letters* **2015**, *17* (13), 3286-3289.
- (172) Borner, R. C.; Boden, N.; Bushby, R. J.; Borner, R.; Cammidge, A. N.; Bushby, R.; Cammidge, A.; Jesudason, M. The synthesis of triphenylene-based discotic mesogens. New and improved routes. *Liquid Crystals* **2006**, *33* (11-12), 1439-1448.
- (173) Li, J.; He, Z.; Gopee, H.; Cammidge, A. N. Synthesis of crown ether-linked discotic triphenylenes. *Organic letters* **2010**, *12* (3), 472-475.
- (174) Ogasawara, F.; Kasai, H.; Nagashima, Y.; Kawaguchi, T.; Yoshizawa, A. Structure-property correlations of novel S-shaped liquid crystal oligomers. *Ferroelectrics* **2008**, *365* (1), 48-57.
- (175) Huang, W.-B.; Guo, Y.; Jiang, J.-A.; Pan, X.-D.; Liao, D.-H.; Ji, Y.-F. An efficient strategy for protecting dihydroxyl groups of catechols. *Synlett* **2013**, *24* (06), 741-746. Menard, D.; St-Jacques, M. Conformational dynamic investigation of 1, 5-benzodioxepin and its dimethyl derivative by ^1H and ^{13}C nmr. *Canadian Journal of Chemistry* **1981**, *59* (7), 1160-1168.
- (176) Cerichelli, G.; Luchetti, L.; Mancini, G.; Savelli, G. Cyclization of 2-(3-halopropoxy) phenoxide ions in functionalized surfactants. *Tetrahedron* **1995**, *51* (37), 10281-10288.
- (177) Göktaş, M. Synthesis and characterization of various block copolymers using PMMA-Br macroinitiator. *Chemical Papers* **2019**, *73*, 2329-2339. Shahabuddin, S.; Hamime Ismail, F.; Mohamad, S.; Muhamad Sarih, N. Synthesis of well-defined three-arm star-branched polystyrene through arm-first coupling approach by atom transfer radical polymerization. *International Journal of Polymer Science* **2015**, *2015*.
- (178) Kruk, J.; Szymańska, R. Synthesis of natural polyprenols for the production of biological prenylquinones and tocochromanols. *RSC advances* **2023**, *13* (33), 23122-23129.
- (179) Mohanazadeh, F.; A Zolfigol, M.; Sedrpoushan, A.; Veisi, H. Synthesis of silica bromide as heterogeneous reagent and its application to conversion of alcohols to alkyl bromides. *Letters in Organic Chemistry* **2012**, *9* (8), 598-603.

- (180) Organization, W. H. *The International Programme on Chemical Safety (IPCS)*. the United Nations Environment Programme, the International Labour Organization, 2001. <https://inchem.org/documents/ehc/ehc/ehc222.htm> (accessed 09/09/2023).
- (181) Alhunayhin, S. M.; Bushby, R. J.; Cammidge, A. N.; Samman, S. S. Triphenylene discotic liquid crystals: biphenyls, synthesis, and the search for nematic systems. *Liquid Crystals* **2023**, 1-12.
- (182) Sambiagio, C.; Marsden, S. P.; Blacker, A. J.; McGowan, P. C. Copper catalysed Ullmann type chemistry: from mechanistic aspects to modern development. *Chemical Society Reviews* **2014**, *43* (10), 3525-3550.
- (183) Chen, W.-W.; Zhao, Q.; Xu, M.-H.; Lin, G.-Q. Nickel-catalyzed asymmetric Ullmann coupling for the synthesis of axially chiral tetra-ortho-substituted biaryl diols. *Organic Letters* **2010**, *12* (5), 1072-1075.
- (184) Cohen, T.; Cristea, I. Kinetics and mechanism of the copper (I)-induced homogeneous Ullmann coupling of o-bromonitrobenzene. *Journal of the American Chemical Society* **1976**, *98* (3), 748-753.
- (185) Boden, N.; Bushby, R. J.; Cammidge, A. N. Triphenylene-based discotic-liquid-crystalline polymers: a universal, rational synthesis. *Journal of the American Chemical Society* **1995**, *117* (3), 924-927.
- (186) Gao, F.; Wang, L.; Zhu, G.-Z.; Liu, Y.-H.; Yang, H.; Li, X.; Yang, K. Controllable syntheses and magnetic properties of novel homoleptic triple-decker lanthanide complexes. *Dalton Transactions* **2019**, *48* (35), 13360-13368. Zou, Z. Y.; Wang, X. M.; Liang, Z. Q.; Tao, X. T. Sandwich-Type Porphyrin Complexes as Efficient Sensitizers for Triplet-Triplet Annihilation Upconversion. *ChemistrySelect* **2020**, *5* (5), 1713-1717. Korostei, Y. S.; Pushkarev, V. E.; Tolbin, A. Y.; Dzuban, A. V.; Chernyak, A. V.; Konev, D. V.; Medvedeva, T. O.; Talantsev, A. D.; Sanina, N. A.; Tomilova, L. G. Sandwich quadruple-decker binuclear lanthanide (III) complexes based on clamshell-type phthalocyanine ligand: synthesis and physicochemical studies. *Dyes and Pigments* **2019**, *170*, 107648. Birin, K. P.; Abdulaeva, I. A.; Poddubnaya, A. I.; Gorbunova, Y. G.; Tsvadze, A. Y. Heterocycle-appended lanthanum (III) sandwich-type (porphyrinato)(phthalocyaninates). *Dyes and Pigments* **2020**, *181*, 108550.
- (187) Zhang, Y.; Cao, W.; Wang, K.; Jiang, J. Constructing bis (porphyrinato) rare earth double-decker complexes involving N-confused porphyrin. *Dalton Transactions* **2014**, *43* (24), 9152-9157.
- (188) Zhang, J.; Chan, W.; Xie, C.; Zhou, Y.; Chau, H.; Maity, P.; Harrison, G.; Amassian, A.; Mohammed, O.; Tanner, P. Impressive near-infrared brightness and singlet oxygen generation from strategic lanthanide-porphyrin double-decker complexes in aqueous solution. *Light Sci. Appl.* **8**, 46 (2019).
- (189) Krebs, F. C.; Schiødt, N. C.; Batsberg, W.; Bechgaard, K. Purification of 2, 3, 6, 7, 10, 11-Hexamethoxytriphenylene and Preparation of Hexakiscarbonylmethyl and Hexakiscyanomethyl Derivatives of 2, 3, 6, 7, 10, 11-Hexahydroxytriphenylene. *Synthesis* **1997**, *1997* (11), 1285-1290.
- (190) Nosaka, Y.; Nosaka, A. Understanding hydroxyl radical (\bullet OH) generation processes in photocatalysis. *ACS Energy Letters* **2016**, *1* (2), 356-359.
- (191) Montalbetti, C. A.; Falque, V. Amide bond formation and peptide coupling. *Tetrahedron* **2005**, *61* (46), 10827-10852.
- (192) INOUE, M. Functional dyes for molecular recognition: chromogenic and fluorescent receptors. In *Colorants for Non-Textile Applications*, Elsevier, 2000; pp 238-274.
- (193) Choi, C. M.; Heo, J.; Kim, N. J. Binding selectivity of dibenzo-18-crown-6 for alkali metal cations in aqueous solution: A density functional theory study using a continuum solvation model. *Chemistry Central Journal* **2012**, *6* (1), 1-8.

(194) Borner, R. C.; Boden, N.; Bushby, R. J.; Cammidge, A. N.; Jesudason, M. Ferric chloride/methanol in the preparation of triphenylene-based discotic liquid crystals: The synthesis of triphenylene-based discotic mesogens New and improved routes. *Liquid crystals* **2006**, *33* (11-12), 1439-1448.